ANL/GTRI/TM-13/14
Version 1.0

Reversal of OFI and CHF in Research Reactors Operating at 1 to 50 bar

Version 1.0

Nuclear Engineering Division

ANL/GTRI/TM-13/14
Version 1.0

Reversal of OFI and CHF in Research Reactors Operating at 1 to 50 bar

Version 1.0

by
M. Kalimullah, A. P. Olson, B. Dionne, E. E. Feldman, and J. E. Matos
Nuclear Engineering Division, Argonne National Laboratory

September 15, 2013

This work is sponsored by the
U.S. Department of Energy, National Nuclear Safety Administration (NNSA)
Office of Global Threat Reduction (NA-21)

ACKNOWLEDGEMENTS

This work was supported by the Global Threat Reduction Initiative (GTRI) Reactor Conversion Program of the National Nuclear Security Administration (NNSA) and the U.S. Department of Energy (U.S. DOE) under Prime Contract No. DE-AC02-06CH11357 between the U.S. Department of Energy and UChicago Argonne, LLC. The authors are grateful to John Stevens (ANL/NE) for his support. The authors are very thankful to Erik Wilson (ANL/NE) for providing channel geometry and operating data of the five US high performance research reactors. The authors are grateful to Aurelien Bergeron (ANL/NE) for critically reviewing the report.

TABLE OF CONTENTS

LIST OF FIGURES

LIST OF TABLES

REVERSAL OF OFI AND CHF IN RESEARCH REACTORS OPERATING AT 1 TO 50 BAR

M. Kalimullah, A. P. Olson, B. Dionne, E. E. Feldman, and J. E. Matos
Argonne National Laboratory
Argonne, Illinois 60439 USA

ABSTRACT

The conditions at which the critical heat flux (CHF) and the heat flux at the onset of Ledinegg flow instability (OFI) are equal, are determined for a coolant channel with uniform heat flux as a function of five independent parameters: the channel exit pressure (P), heated length (L_h) , heated diameter (D_h), inlet temperature (T_{in}), and mass flux (G). A diagram is made by plotting the mass flux and heat flux at the OFI-CHF intersection (reversal from CHF > OFI to CHF < OFI as G increases) as a function of P (1 to 50 bar), for 36 combinations of the remaining three parameters (L_h , D_h , T_{in}): L_h = 0.28, 0.61, 1.18 m; D_h = 3, 4, 6, 8 mm; T_{in} = 30, 50, 70 °C. The use of the diagram *to scope* whether a research reactor is OFI-limited (below the curve) or CHF-limited based on the five parameters of its coolant channel is described. Justification for application of the diagram to research reactors with axially non-uniform heat flux is provided. Due to its limitations (uncertainties not included), the diagram cannot replace the detailed thermal-hydraulic analysis required for a reactor safety analysis.

In order to make the OFI-CHF intersection diagram, two world-class CHF prediction methods (the Hall-Mudawar correlation and the extended Groeneveld 2006 table) are compared for 216 combinations of the five independent parameters. The two widely used OFI correlations (the Saha-Zuber and the Whittle-Forgan with η = 32.5) are also compared for the same combinations of the five parameters. The extended Groeneveld table and the Whittle-Forgan OFI correlation are selected for use in making the diagram. Using the above five design parameters, a research reactor can be represented by a point on the reversal diagram, and the diagram can be used to scope, without a thermal-hydraulic calculation, whether the OFI will occur before the CHF, or the CHF will occur before the OFI when the reactor power is increased keeping the five parameters fixed.

1. INTRODUCTION

The existing research reactors have coolant channels of different thicknesses with different fueled or heated lengths, coolant velocities, inlet temperatures, and exit pressures. The heat fluxes at the onset of nucleate boiling (ONB), the onset of flow instability (OFI), and the critical heat flux (CHF) were calculated using the state-of-the-art methods, for heated lengths of 0.28, 0.61, and 1.18 m (about 11, 24, 46.5 inches), over the coolant mass flux range of 1000 to 30000 kg/m^2-s (i.e., the coolant velocity range of roughly 1 to 30 m/s), assuming uniform heat flux. Altogether 216 cases (3 heated lengths × 6 exit pressures × 4 heated diameters × 3 inlet temperatures) were calculated for the following values of independent parameters:

3 heated lengths L_h = 0.28, 0.61, 1.18 m
6 exit pressures P = 1, 5, 10, 20, 30, 50 bar
4 heated diameters D_h = 3, 4, 6, 8 mm
3 inlet temperatures T_{in} = 30, 50, 70 º C

By investigating into the relative magnitudes of the calculated heat fluxes, the OFI heat flux and CHF are found to intersect at a certain mass flux which varies depending on the above four parameters (i.e., P, L_h , D_h , T_{in}). This intersection, referred to OFI-CHF reversal by Siman-Tov et al.[1], is studied in detail. For each heated length, a pair of OFI-CHF reversal diagrams (Fig. 6) is made, plotting the mass flux at the OFI-CHF intersection (G_{rev}) as function of exit pressure in one diagram, and plotting the heat flux at the OFI-CHF intersection (q_{rev}) in the accompanying diagram. Any research reactor having a heated length of 11, 24, or 46.5 inches is represented by a point on these diagrams. The location of the point on the reversal mass flux diagram determines whether the maximum allowed power of the reactor is OFI-limited or CHF-limited. A reactor is defined to be OFI-limited if any coolant channel of the reactor is calculated to reach the OFI (before reaching the CHF) when the reactor power is increased slowly at constant flow. A reactor is defined to be CHF-limited if any coolant channel of the reactor is calculated to reach the CHF (before reaching the OFI) when the reactor power is increased slowly at constant flow. For demonstration, some research reactors are also represented on the diagram. The value of the heat flux at the OFI-CHF reversal can also be read from the accompanying diagram.

1.1. Margin between CHF and OFI

The critical heat flux (CHF) is the maximum heat flux that can be transferred from the heated wall to the coolant, with all independent parameters (P, G, L_h , D_h , T_{in}) kept constant. In order to measure the true CHF, the test loop must be stiff so that the coolant mass flux (G) does not decrease due to the increase in flow resistance caused by boiling. According to one mechanism, the subcooled CHF occurs when the liquid sublayer or thin film on the heated wall under an elongated vapor bubble dries up during the time that the bubble takes to pass over the CHF location[2].

The onset of static flow instability (OFI) is defined as the minimum ΔP point on the plot of ΔP versus flow rate of subcooled boiling liquid in a heated channel. OFI is caused by lack of a hydraulic equilibrium point (on the ΔP versus flow plot) between the ΔP demanded by the heated channel and the ΔP supplied by the pump. The onset of significant void (OSV), i.e., onset of

bubble departure from the heated wall, generally occurs prior to OFI at a slightly higher flow than the OFI on the ΔP versus flow plot[3] (when the flow is gradually decreased at constant heat flux). This was also tentatively pointed out earlier by Whittle-Forgan[4]. As a result, an OSV correlation is used to provide a conservative estimate of OFI[3]. The Saha-Zuber correlation[5] has been quite successful in predicting various experimental data for OSV and OFI[3].

The margin between CHF and OFI is important in the safety analysis of research reactors. Siman-Tov et al. (1995)[1] measured this margin in two (CF115B and CF328A) of their 32 flow instability tests. They measured this margin in a stiff constant flow system by reducing the coolant velocity to achieve a true CHF below the velocity at the minimum ΔP point (on the plot of measured ΔP versus coolant velocity) in a constant-heat-flux test. The flow instability did not really occur in the tests at the minimum ΔP point because the system was stiff. The occurrence of CHF was clearly identified in the tests by a rapid burnout and failure of the test channel. The tests CF115B and CF328A were done at a pressure of about 18 bar at heat fluxes of 10.5 and 11.8 MW/m^2. In test CF115B, the CHF occurred at a velocity of 14.5 m/s compared to OFI at 19.8 m/s. In test CF328A, the CHF occurred at a velocity of 14.0 m/s compared to OFI at 19.3 m/s. In each test, the margin between CHF and OFI is that the coolant velocity at CHF is 73% of the coolant velocity at OFI. Of course this is not true in all cases as described below.

Siman-Tov et al.[1] end their discussion of OFI and CHF with the following remarks: "In most cases, flow instability will precede critical heat flux in a parallel channel fuel assembly as shown by Waters (1966)[6]. The margin between flow instability and CHF narrows as certain parameters are changed, and the trend may even be *reversed*".

A stiff test loop uses a constant-flow pump, withour any bypass flow path around the test section, in order to maintain a constant flow through the test section, unaffected by the changes in its flow resistance due to boiling. To have a stiff system, Siman-Tov et al. used a positive-displacement pump with closed bypass line. This is not the case of coolant channels in a research reactor fuel assembly. The coolant channels in a research reactor fuel assembly share common inlet and outlet plena which effectively impose a common pressure drop (ΔP) on all the channels, and therefore the channels are all hydraulically parallel. This makes a constant-ΔP system (soft system). Added hydraulic resistance due to boiling inception in a channel causes flow to be diverted from that channel to other channels. The reduced flow in the boiling channel can lead (if the boiling proceeds to a little beyond bubble detachment) to a rapid flow excursion (OFI). The excursive flow instability is always accompanied by CHF and fuel failure at the *reduced flow* caused by the flow instability.

1.2. Some Cases Where CHF Occurs Before OFI

While developing a CHF correlation using *true* quality (instead of the thermodynamic quality used in most CHF correlations), Shim et al.[7] stated that there was a small number of CHF data (72 out of 8912 CHF data in their database), for highly subcooled flow with high mass flux, in which CHF occurs before OSV. They noted that their CHF model failed for these CHF data and hence they had to exclude the data from the analysis. According to the Saha-Zuber flow instability criterion, OFI occurs at OSV. The existence of these CHF data shows that CHF can occur before OFI for highly subcooled flow with high mass flux.

The order of occurrence of CHF and OFI was studied earlier[8] by calculating the thermodynamic quality at OSV (X_{osv}) for the tabulated values of subcooled CHF in the Groeneveld 2006 look-up table for a tube of 8 mm diameter at 5 bar pressure. X_{osv} was calculated using the Saha- Zuber correlation[5] on Excel spreadsheet for the CHF values in the Groeneveld table. The calculated X_{osv} was compared with the exit quality X_o given in the Groeneveld table corresponding to the CHF. If X_{osv} is less than X_o, then OFI occurs before CHF, and if X_{osv} is greater than X_o, then the reverse occurs (CHF occurs before OFI). It is found that highly subcooled flow with high mass flux leads to CHF occurring before OFI. An example of this calculation follows:

The CHF is 13200 kW/m^2 at X_o = -0.15, G = 8000 kg/m^2-s in the Groeneveld 2006 table at 5 bar for a tube of 8 mm diameter. The heated length calculated by heat balance assuming an inlet temperature of 30 °C is found to be 0.24 m. For this channel, the onset of significant voids by the Saha-Zuber correlation is found to occur at heat flux 14997 kW/m^2 and quality X_{osv} = -0.137. Comparing the qualities, OFI occurs at a higher quality (−0.137) compared to the quality (−0.15) at which CHF occurs, implying that CHF occurs prior to OFI.

1.3 Cinematographic Data for CHF Occurrence before OFI

The high-speed (up to 20000 frames/s) cinematographic observations and measurements made in various basic experiments are recorded by Tong and Tang[9] in illustrative sketches [see Fig. 5.12 and Section 5.2.3 in Ref. 9] summarizing four CHF mechanisms arranged in the order of decreasing coolant subcooling (i.e., increasing quality) at the location of CHF occurrence. The four CHF mechanisms occur under the following thermal-hydraulic conditions, and are briefly described in Table 1:

1. High subcooling with single-phase liquid flowing in the mainstream of coolant channel,
2. Medium or low subcooling with single-phase liquid flowing in the mainstream of coolant channel,
3. Low quality with slug flow or froth flow in the mainstream of coolant channel, and
4. Medium to high quality with annular flow in the channel.

Chang and Baek[10] have also reviewed the basic concepts of 3 of these 4 mechanisms. The four mechanisms are of two kinds depending on the flow pattern present at the axial location of CHF occurrence. This is because flow boiling CHF is closely related to the flow pattern, e.g., bubbly or annular which have distinctly different radial distributions of void fraction. The radial distribution of void fraction in bubbly flow has a double-peaked shape, with a peak close to each wall of the channel, and with zero or nearly zero void fraction in the mainstream. The radial distribution of void fraction in annular flow has a parabolic shape with a single peak in the mainstream, with very small void fraction at the walls. The CHF mechanisms 1 to 3 are related to bubbly flow and are due to a failure of or departure from nucleate boiling (DNB). The fourth mechanism is related to annular flow and is due to the drying out of the liquid film usually present in annular flow.

The first of the four mechanisms leads to CHF before bubble *detachment* from the heated surface, i.e., before the onset of flow instability (OFI) whereas the mechanisms 2 to 4 occur after the OFI. The point of net vapor generation (NVG) calculated by the Saha-Zuber correlation[5] is

the heat flux at which the bubbles *detach* from the heated surface before collapsing. The flow instability occurs after the NVG, i.e., at a heat flux *slightly higher* than that at the NVG if the heat flux is increased at constant flow to approach flow instability, or at a flow *slightly lower* than that at the NVG if the flow is decreased at constant heat flux to approach flow instability. That is why the Saha-Zuber correlation is frequently used as a conservative estimate of the OFI.

In order to provide cinematographic data for the occurrence of CHF before OFI, the first CHF mechanism in *highly* subcooled nucleate boiling is described here in more detail than that given in Table 1. This mechanism is based on Gunther's cinematographic study[11,12] of the mechanism of subcooled nucleate boiling of water and approach to CHF. Gunther conducted tests on subcooled flow boiling of water in two transparent channels (with axially uniform heat flux), and made high-speed (20000 frames/s), high-resolution movies of bubbles, roughly hemispherical in shape, growing and collapsing while remaining attached to the heated surface. The cinematographic results showed that the coolant flow did not detach the bubbles from the heated surface. The attached bubbles slid downstream during growth and collapse, producing turbulence in the *two-phase wall layer* (on-the-wall coolant layer of thickness equal to the maximum bubble radius) by their translational motion in addition to the turbulence caused by their growing and collapsing action. The sliding velocity was approximately 0.8 of the coolant velocity, increasing slightly with bubble size. The effect of an increase in coolant velocity or subcooling was to reduce bubble size and lifetime. An increase of heat flux caused the bubble population to increase up to the point where bubbles coalesced to form vapor clumps. Gunther photographed the bubble coalescence to vapor clumps in a test at ΔT_{sub} = 105.6 ºC and V = 7.6 m/s when the heat flux was increased to 21.3 MW/m^2 which was within 10 % of CHF. This photograph indicates that bubble coalescence signifies *incipient* film boiling that results in CHF.

A recent, more detailed, photographic study (as the heat flux is increased in small steps) of the phenomena in *highly subcooled* flow boiling from ONB to CHF and from CHF to heater melting is provided by Celata et al.[13]. The inlet subcooling in these experiments was 132 to 214 ºC (T_i = 20 ºC, P = 5 to 30 bar, V = 3 to 7.5 m/s). He also observed that CHF occurred before bubble detachment in highly subcooled flow boiling.

Bankoff[14] formulated a refined mechanistic method of calculating subcooled nucleate boiling heat transfer, analyzed Gunther's experiments[11], and found that the CHF occurs due to a relative inability of the turbulent core liquid to remove heat as fast as it is transmitted through the *two-phase wall layer*. Tong (1975)[15] has also developed a CHF analysis in which the subcooled liquid core is the limiting cause.

Gunther reported the measured maximum bubble radius reached before collapsing, bubble lifetime, bubble formation rate (millions/cm^2-s), fraction of heated surface area covered by bubbles, wall surface temperature, and mean bulk liquid temperature, for 16 nucleate boiling heat transfer tests[11] and 35 CHF burnout tests[12] (shown in Tables 2 and 3). He correlated the 35 CHF tests as $q_c = 72\ V^{0.5}\ \Delta T_{sub}$ where q_c is CHF in kW/m^2, V is coolant velocity in m/s, and ΔT_{sub} is subcooling in ºC.

In order to understand the *approach to CHF* in highly subcooled nucleate flow boiling, Bankoff[14] formulated a refined mechanistic method of calculating subcooled nucleate boiling

heat transfer and used it to analyze Gunther's 16 heat transfer tests[11] using or matching all the measured data. These 16 tests[11] included a series of 6 tests (see Fig. 1 and Table 2) in which the heat flux was increased from 2.45 to 10.63 MW/m^2 to approach CHF at fixed values of subcooling (86 ºC), coolant velocity (3.05 m/s or 10 ft/s), and pressure (1.7 bar). Bankoff calculated (1) the heat flux q_1 that can be transferred from the wall surface to the two-phase wall layer, (2) the heat flux q_2 that the two-phase wall layer is able to transfer to its interface with the bulk core, and (3) the heat flux q_3 that the subcooled liquid in the bulk core can transfer from the edge of the two-phase wall layer (out of the channel). He found that the CHF occurs due to q_3 being smaller than q_2, i.e., due to a relative inability of the turbulent core liquid to remove heat as fast as it is transmitted through the *two-phase wall layer*, as described below.

Before CHF, the wall surface temperature is above T_{sat}; adjacent to the wall surface there is a thin liquid layer (thinner than the *two-phase wall layer*) with temperature greater than T_{sat}; and the temperature at the edge of the *two-phase wall layer* is always below T_{sat} , i.e., 56 to 102 ºC as the heat flux increases from 2.45 to 10.63 MW/m^2, as shown in Fig. 1. As the CHF is approached, the bubbles become smaller; the thickness of the *two-phase wall layer* decreases; its full thickness becomes superheated, with a sharp increase in bubble formation rate. Although the bubble size and lifetime decrease about 50 % with the increase of heat flux over this range, the sharp increase in bubble formation rate causes a resultant increase in the fraction of wall surface covered by bubbles, and leads to CHF. The stirring effect of the bubbles plays an important part in the transfer of heat through the *two-phase wall layer*. The bubbles act as roughness to some extent in promoting turbulent diffusion from the outer edge of the *two-phase wall layer* into the bulk liquid.

In conclusion, this CHF mechanism leads to CHF before bubble detachment from the heated surface, i.e., before OFI.

2. STANDALONE PROGRAM FOR CALCULATING ONB, OFI, AND CHF

A standalone FORTRAN computer program (listed in Appendix F) was developed to calculate the following five safety margins assuming axially uniform heat flux in a single coolant channel of a research reactor.

(1) Heat flux at ONB using the Bergles and Rohsenow correlation[16,17]
(2) Heat flux at OFI using $\eta = 32.5$ in the Whittle-Forgan correlation[4]
(3) Heat flux at OFI using the Saha-Zuber correlation[3,5]
(4) Critical heat flux using the extended Groeneveld 2006 Table[8,18]
(5) Critical heat flux using the Hall-Mudawar inlet conditions correlation (ICC)[19]

The iterative methods used in the program for calculating ONB, OFI, and CHF are described in Appendix A. Each of these safety margins depends on five independent parameters of the coolant channel that are input to the computer program. The independent parameters are: (1) coolant exit pressure (P), (2) heated diameter (D_h), (3) heated length (L_h), (4) coolant inlet temperature (T_i), (5) mass flux (G). The heated diameter is defined as 4 times the flow area divided by the heated perimeter of the coolant channel (see the nomenclature). To calculate the required coolant properties, the standalone program uses the coolant property subroutines of the

PLTEMP/ANL code[20,21]. To find the coolant properties at inlet, the program needs the inlet pressure (P_i) which is obtained by calculating the pressure drop in the channel, or by assuming the inlet pressure equal to the exit pressure (depending upon an input option). The program was verified by comparison with earlier Excel spreadsheet calculations[8].

3. CALCULATED ONB, OFI, AND CHF

Using the FORTRAN program described above, the five safety margins (noted in Section 2) were calculated as a function of the coolant mass flux over the range 1000 to 30,000 kg/m^2-s, at coolant channel exit pressures of 1, 5, 10, 20, 30, 50 bar. The exit pressure is an important parameter since the heat flux at ONB, the heat flux at OFI, and the CHF each occur at the channel exit for a coolant channel with axially uniform heat flux. Three values of the heated length, typical of research reactors, were assumed: 0.28, 0.61, or 1.18 m. Four typical values of the heated diameter were assumed: 3, 4, 6, and 8 mm. The heat flux at ONB, the heat flux at OFI, and the CHF were calculated for three values of the coolant inlet temperature: 30, 50, 70 °C. In short, calculations were done for 72 cases listed in Table 4 (6 exit pressures × 4 heated diameters × 3 inlet temperatures) for each of 3 heated lengths, altogether 216 cases. The inlet pressure was found by calculating the pressure drop in the channel assuming upflow.

Effect of Calculating Inlet Pressure**:** To find the effect of assuming $P_i = P$ in evaluating coolant properties at inlet, as assumed in the earlier spreadsheet calculations[8], the same 216 cases were also calculated using the second input option of the program. The ONB heat flux, OFI heat flux and CHF values obtained in this set of calculations (assuming $P_i = P$) were compared with the corresponding values obtained in the first set of calculations (mentioned in Section 3) in which P_i was calculated accounting for the pressure drop in the channel. The comparison was made for 2160 data points (72 cases × 30 mass fluxes over the range 1000 to 30,000 kg/m^2-s) of each heated length. The mean error, maximum absolute error (MAE) and the RMS error for the five safety margins are summarized in Table 5. The RMS error for the Bergles and Rohsenow ONB heat flux is 0.23 % or less. The RMS error for the Whittle-Forgan OFI heat flux is 0.24 % or less. The RMS error for the Saha-Zuber OFI heat flux is 0.22 % or less. The RMS error for the Groeneveld table CHF is 0.07 % or less. The RMS error for the Hall-Mudawar CHF is 0.10 % or less. In conclusion, the error in assuming $P_i = P$ for evaluating coolant properties at inlet is found to be negligible. Except this comparison, the set of calculations assuming $P_i = P$ was never used.

Before using the extended Groeneveld 2006 CHF table in the OFI-CHF reversal study, it was compared with the Hall-Mudawar ICC for all the 216 cases listed in Table 4, as described in Section 3.1. Similarly, before using the Whittle-Forgan OFI correlation in the OFI-CHF reversal study, it was compared with the Saha-Zuber correlation for all the 216 cases, as described in Section 3.2.

3.1. Comparison of CHFs Calculated Using the Groeneveld Table and the Hall-Mudawar ICC

Based on the set of calculations in which P_i was calculated, Fig. 2A shows a comparison between the CHFs by the extended Groeneveld 2006 CHF table and the Hall-Mudawar ICC for all the 72 cases of heated length 0.28 m, consisting of all data points (72 cases × 30 mass fluxes from 1000

to 30000 kg/m^2-s). Figs. 2B and 2C show similar comparisons for the heated lengths of 0.61 m and 1.18 m. The actual number of data points plotted in these figures is less than the total number 2160 (= 72 × 30) because the Hall-Mudawar ICC holds only for exit quality $X_o \leq 0$ (subcooled CHF). The comparison of the two CHF prediction methods for all the 72 cases of each of the 3 heated lengths (216 cases altogether) as a function of mass flux, is plotted and discussed in Appendix C. The difference between the two methods over the 72 cases of each heated length is given in Table 6. The RMS difference is 8.5 %, 8.6 %, and 8.8 % for the heated lengths of 0.28, 0.61, and 1.18 m respectively. In conclusion, there is a close agreement between the two prediction methods. The extended Groeneveld 2006 table is preferred because it is also applicable to saturated CHF ($X_o \geq 0$).

Parametric Variation of CHF: The effect of heated diameter D_h or inlet temperature T_i on the CHF obtained by the extended Groeneveld 2006 table is also plotted and discussed in Appendix C. In these separate-effect plots, only one parameter is changed at a time, holding the other four parameters constant. It is found that, at each heated length, the CHF *increases* with increasing heated diameter at constant P, L_h , T_{in} , and G while the CHF *decreases* with increasing heated diameter at constant P, L_h , T_{in} , and X_o. The CHF decreases with increasing inlet temperature at constant P, L_h , D_h , and G. These are all expected behavior of CHF.

3.2. Comparison of OFIs Calculated Using the Whittle-Forgan and the Saha-Zuber Correlations

Based on the set of calculations in which P_i was calculated, Fig. 3A shows a comparison between OFI heat fluxes by the Whittle-Forgan (η = 32.5) and the Saha-Zuber correlations for all the 72 cases of heated length 0.28 m, consisting of 2160 data points (72 cases × 30 mass fluxes from 1000 to 30000 kg/m^2-s). Figs. 3B and 3C show similar comparisons for the heated lengths of 0.61 m and 1.18 m. The comparison of the two OFI prediction methods for all the 72 cases of each of the 3 heated lengths (216 cases altogether) as a function of mass flux, is plotted and discussed in Appendix D. The difference between the two methods over the 72 cases of each heated length is given in Table 6. The RMS difference is 5.2 %, 3.0 %, and 1.8 % for the heated lengths of 0.28, 0.61, and 1.18 m respectively. In conclusion, there is a close agreement between the two OFI prediction methods. The Whittle-Forgan (η = 32.5) is preferred because it has been routinely used at Argonne.

Parametric Variation of OFI Heat Flux: The effect of exit pressure P, heated diameter D_h or inlet temperature T_i on the OFI obtained by the Whittle-Forgan (η = 32.5) is also plotted and discussed in Appendix D. In these separate-effect plots, only one parameter is changed at a time, holding the other four parameters constant. It is found that, at each heated length, the OFI heat flux increases with increasing exit pressure at constant D_h, L_h, T_{in}, and G. The OFI heat flux increases with increasing heated diameter at constant P, L_h, T_{in}, and G. The OFI heat flux decreases with increasing inlet temperature at constant P, L_h , D_h , and G.

The numerical values of the Bergles-Rohsenow ONB heat flux, the Whittle-Forgan OFI heat flux, the Saha-Zuber OFI heat flux, and the Groeneveld CHF, the exit quality X_o based on the Groeneveld CHF, and the Hall-Mudawar CHF are tabulated for 36 cases in Tables 7 to 12. These 36 cases are: P = the six pressures; D_h = 4 and 8 mm; T_{in} = 30 °C; L_h = 0.28, 0.61, 1.18 m.

3.3. Comparison of Heat Fluxes at ONB, OFI, and CHF

Three of the five safety margins (the Bergles and Rohsenow ONB heat flux, the Whittle-Forgan OFI heat flux, and the CHF by the extended Groeneveld 2006 table) are plotted together in Appendix B to show their relative magnitudes. For brevity, only 6 of the 72 cases for each heated length, altogether 18 cases for the following values of the input parameters, are shown in Appendix B. Figure 4 is one of the 18 plots of Appendix B. In all these plots, the ONB heat flux is colored green, the OFI heat flux is colored blue, and the CHF is colored red.

Three heated lengths L_h = 0.28, 0.61, 1.18 m,
Six exit pressures P = 1, 5, 10, 20, 30, 50 bar,
Heated diameter D_h = 4 mm,
Inlet temperature T_{in} = 30 °C

It is important to note in Fig. 4 and the plots of Appendix B that there is an intersection of the OFI heat flux and CHF at a certain mass flux and heat flux in 13 out of the 18 cases. The point of intersection is referred to as the reversal point. The corresponding mass flux and heat flux are referred to as the reversal mass flux (G_{rev}) and reversal heat flux (q_{rev}).

To reduce clutter, only the Whittle-Forgan OFI heat flux and the extended Groeneveld table CHF are plotted in Fig. 5 (having 6 parts) so that the intersection of the OFI heat flux and CHF for a given exit pressure could be noted. Each part of Fig. 5 shows the OFI heat flux and CHF plotted as a function of mass flux at the selected six pressures (P = 1, 5, 10, 20, 30, and 50 bar), for a different combination of D_h and L_h typical of research reactors (D_h = 4, 8 mm; L_h = 0.28, 0.61, 1.18 m). The intersection of the OFI heat flux and CHF occurs at a different point for each exit pressure. The mass flux G_{rev} and heat flux q_{rev} at the intersection point depend on the channel exit pressure. The points of intersection at exit pressures of 1, 5, 10, 20, 30, and 50 bar are marked in Fig. 5, and the locus of the point of intersection is also shown in Fig. 5.

The point of intersection is here referred to as the reversal because the OFI heat flux is smaller than the CHF for mass fluxes $G < G_{rev}$ whereas for mass fluxes $G > G_{rev}$ the CHF is smaller than the OFI heat flux. In other words, the channel power is OFI-limited for $G < G_{rev}$ and CHF-limited for $G > G_{rev}$, i.e., a reversal in the roles of OFI and CHF occurs at the point of intersection.

Figure 5 shows only six combinations of T_{in} , D_h and L_h. To make an OFI-CHF reversal diagram that is useful, several combinations of T_{in} , D_h and L_h as well as several values of coolant exit pressure need to be plotted in a single figure. One method of doing this is given in the next section.

Parametric Variation of ONB Heat Flux: The effect of exit pressure P, heated diameter D_h or inlet temperature T_i on the ONB obtained by the Bergles-Rohsenow correlation is plotted and discussed in Appendix E. In these separate-effect plots, only one parameter is changed at a time, holding the other four parameters constant. At each heated length, the ONB heat flux increases with increasing exit pressure at constant D_h , L_h , T_{in} , and G. The ONB increases with increasing heated diameter at constant P, L_h , T_{in} , and G. The ONB decreases with increasing inlet

temperature at constant P, L_h , D_h , and G. In short, the variation trend of ONB heat flux is qualitatively similar to that of the OFI heat flux.

4. OFI-CHF REVERSAL DIAGRAMS

Instead of plotting OFI heat flux and CHF (as done in Fig. 5), only the mass flux at their intersection is plotted in Fig. 6 (parts 1, 3, and 5), as a function of the exit pressure (from 1 to 50 bar), for all 36 combinations of T_{in} , D_h and L_h (T_{in} = 30, 50, 70 °C, D_h = 3, 4, 6, 8 mm, and L_h = 0.28, 0.61, 1.18 m). This was done to put more calculated results in a single figure. Figure 6 (parts 1, 3, and 5) has a set of curves showing the mass flux at reversal (G_{rev}) for different combinations of heated diameter (3 to 8 mm) and coolant inlet temperature (30 to 70 °C). The corresponding heat flux at reversal (q_{rev}) is plotted separately in Fig. 6 (parts 2, 4, and 6). All the data plotted in Fig. 6 are given in Table 4. The blank spaces in Table 4 imply that the OFI-CHF intersection did not occur in the mass flux range studied, i.e., 1000 to 30000 kg/m^2-s.

Figure 6 was developed assuming axially uniform heat flux. The justification for its application to reactors with axially non-uniform heat flux is given in Section 5. Figure 6 does not account for hot channel factors. It can be used by reactor designers only *to scope* whether a research reactor is OFI-limited or CHF-limited based on five characteristics of its coolant channel: the heated length, heated diameter, inlet temperature, exit pressure, and mass flux. Figure 6 cannot replace the detailed thermal-hydraulic analysis that is required to design a research reactor.

To explain the meaning and application of Fig. 6, let us consider a research reactor having a fueled height or heated length of 0.61 m (24 inches) and a channel heated diameter of 4 mm, operating at a coolant exit pressure of 40 bar, inlet temperature of 30 °C, and mass flux of 10000 kg/m^2-s. The point *R* (at the operating mass flux of 10000 kg/m^2-s) on the vertical line *AB* drawn at 40 bar represents this research reactor on Fig. 6 (Part 3). The point *B* is the intersection of this vertical line with the OFI-CHF reversal mass flux curve applicable to this reactor, i.e., the curve corresponding to the reactor's heated diameter and inlet temperature (4 mm and 30 °C). The point *B* gives the mass flux at the OFI-CHF reversal.

To determine whether the research reactor in question is OFI-limited or CHF-limited, one checks in Fig. 8a whether the point *R* is below or above the point *B*. If the point *R* representing the reactor lies below (i.e., the operating mass flux is less than the reversal mass flux), the reactor in question is OFI-limited. If the point *R* is above, the reactor is CHF-limited.

If the point *R* in Fig. 8a is below the applicable reversal curve (OFI-limited reactor), then an estimate of the maximum allowed heat flux (averaged over the heated length) is given by Fig. 8b as follows. The reversal mass flux, G_{rev}, at point B of Fig. 8a (upper graph) corresponds to the reversal heat flux, q_{rev}, provided by point C of Fig. 8b (lower graph). Since the heat flux at OFI is approximately proportional to the mass flux at OFI, the OFI heat flux, q_{OFI}, at the operating mass flux, G, is estimated to be $q_{rev}(G/G_{rev})$. The maximum allowed heat flux for this OFI-limited reactor equals q_{OFI}, i.e., be $q_{rev}(G/G_{rev})$. This heat flux times L_hP_h gives the OFI power, or the maximum allowed power of the channel, without accounting for uncertainties. In the other case, if the point *R* in Fig. 8a lies above the reversal mass flux curve applicable to the reactor, the

maximum allowed reactor power is more than the power determined by the reversal heat flux (q_{rev}), and its value will be determined by the CHF at the operating mass flux G.

5. APPLICABILITY OF THE REVERSAL DIAGRAM TO AXIALLY NON-UNIFORM HEAT FLUX

The heat flux was assumed to be axially uniform in the development of the reversal diagrams. However, there is a basis for the applicability of the reversal diagrams to reactors having axially non-uniform heat flux, as discussed below:

(1) According to the frequently used Whittle-Forgan[4] flow instability criterion, the power removed by the coolant from a channel at OFI depends only on the coolant inlet-to-outlet temperature rise, and not on the axial shape of heat flux. Whittle and Forgan[4] included a non-uniformly heated test section in their experiments that was designed to produce a uniform heat flux from the inlet to the middle and taper to about 68% of the uniform value at the exit. This means that the actual heat flux distribution of the channel can be replaced, for OFI power calculation purposes, by a uniform heat flux equal to the axially averaged value of the actual heat flux distribution.

(2) Similarly, the overall CHF power hypothesis of Lee and Obertelli[22,23] suggests that the total power which can be fed to a tube with axially non-uniform heat flux distribution before CHF is initiated, is the same as the CHF power for a uniformly heated tube of the same inner diameter, heated length, and inlet conditions. The CHF location cannot be predicted with this hypothesis. Lee and Obertelli (1963)[23], Lee (1965)[24], and Lee (1966)[25] found that the hypothesis predicted the CHF power for a number of sine wave heat flux profile tubes reasonably well. It has been shown that the hypothesis is not generally valid for different heat flux profiles. Of the two methods of handling axially non-uniform heat flux distribution, the local conditions hypothesis and the overall power hypothesis, it is found that the latter is slightly more accurate for symmetrical heat flux profiles[22]. This means that the actual heat flux distribution of a channel can be replaced, for CHF power calculation purposes, by a uniform heat flux equal to the axially averaged value of the actual heat flux distribution.

Therefore, as long as nothing other than the channel powers at OFI and at CHF needs to be calculated, a reactor coolant channel having an axially non-uniform heat flux distribution may be replaced by an equivalent channel having an axially uniform heat flux equal to the average heat flux (with the limitations noted in the above two discussions). The reversal diagrams are applicable to the equivalent channel with the average heat flux uniformly distributed over the heated length. This is especially true for symmetrical heat flux profiles as noted above[22]. However, for unsymmetrical heat flux profiles, the CHF power hypothesis is less accurate than the local conditions hypothesis as noted above, and therefore the reversal diagram remains only a *scoping method* in general.

6. APPLICATION OF OFI-CHF REVERSAL DIAGRAM TO RESEARCH REACTORS

A reactor is defined to be OFI-limited if any coolant channel of the reactor is calculated to reach the OFI (before reaching the CHF) when the reactor power is increased slowly at constant flow.

A reactor is defined to be CHF-limited if any coolant channel of the reactor is calculated to reach the CHF (before reaching the OFI) when the reactor power is increased slowly at constant flow. The purpose here is to illustrate the application of the OFI-CHF reversal diagrams of Fig. 6 to some research reactors, to show how a reactor analyst may scope (find without any thermal-hydraulic calculation) whether a reactor is OFI-limited or CHF-limited.

Three limitations of this scoping should be noted:

(1) The development of reversal diagrams used best-estimate values of CHF and OFI heat flux. It does not allow for regulatory requirements like CHF ratio ≥ 2.0. Such a requirement practically reduces the best-estimate of CHF in the reactor analysis. Its effect is significant and is included in a complete thermal-hydraulic analysis.

(2) The effect of uncertainties in coolant mass flux and channel exit pressure, if available, may be accounted for by plotting a rectangle (rather than a point) to represent a coolant channel. However, these uncertainties require a complete thermal-hydraulic analysis, and therefore are not available for scoping without any calculation.

(3) The development of reversal diagrams assumes that the OFI and CHF occur in the same coolant channel. The scoping is not valid for a reactor in which the OFI and CHF first occur in different channels as the reactor power is increased at constant flow.

The five key parameters used in this scoping method are: (1) fueled/heated length, (2) coolant pressure at the outlet of the heated length, (3) coolant mass flux, (4) heated diameter of the coolant channel in the reactor core, and (5) coolant temperature at the inlet to the heated length.

These parameters for some research reactors (operating or designed) are shown in Table 13. A single coolant channel is assumed here to model the thermal-hydraulic conditions in each reactor. For a research reactor having coolant channels of different heated diameters or mass flux, each significantly different channel may by plotted on the reversal diagram, obtaining a point representing each coolant channel. The effect of uncertainties in coolant mass flux and channel exit pressure, if available, may be accounted for by plotting a rectangle (rather than a point) to represent a coolant channel. The reactors are listed in Table 13 in the order of increasing heated (fueled) length, in order to plot them on the OFI-CHF reversal diagrams shown in Parts 1, 3, and 5 of Fig. 6, respectively for heated lengths, 0.28, 0.0.61, and 1.18 m (about 11, 24, and 46.5 inches). Four reactors (the ANS Design, the HIFR, the MITR, and the MURR) are plotted on the OFI-CHF diagram in Part 3 of Fig. 6 that was developed for a heated length of 0.61 m. The Advanced Test Reactor (ATR) is plotted on the OFI-CHF diagram in Part 5 of Fig. 6 that was developed for a heated length of 1.28 m.

If a research reactor's heated diameter and inlet temperature do not match those of one of the reversal lines plotted on the OFI-CHF diagram, then one needs to interpolate between a suitable pair of reversal lines. During the interpolation, one should keep the following trends in mind: The reversal line shifts down if the heated diameter increases, or if the inlet temperature decreases, or if the heated length decreases. The scoping results for the reactors in Table 13 are given in Table 14, with the reasoning used in the application of the reversal diagrams of Fig. 6 to determine whether a reactor is OFI-limited or CHF-limited. The points representing all these reactors are below the OFI-CHF reversal mass flux curve applicable to the reactor (i.e., the curve

corresponding to the reactor's heated diameter and inlet temperature), indicating that all these reactors are OFI-limited.

The point plotted for the ANS Design (D_h=3.1 mm, T_i = 45 ºC) on the reversal diagram for heated length 0.61 m (Part 3 of Fig. 6) is closely below the interpolated reversal line applicable to ANS. So the scoping result is that ANS is OFI-limited and borderline. This agrees with the detailed thermal-hydraulic analysis done by the ORNL staff [Table 5-2 of Ref. 26]. The ORNL staff found that the CHF-limited and OFI-limited powers for ANS are nearly equal, i.e., 448 and 439 MW at the 95% confidence level, or 396 and 414 MW at the 99.9% confidence level.

The scoping result of the reversal diagram for the HEU core of the Advanced Test Reactor (ATR) is that it is OFI-limited. This agrees with the result reported by Atkinson[27] of the Aerojet Nuclear Company that all ATR test data has proved that flow instability will occur before the occurrence of departure from nucleate boiling (DNB).

The scoping result of the reversal diagram for the High Flux Isotope Reactor (HFIR) is that it is OFI-limited which agrees with the 1967 revised assessment by McLain[28] of ORNL. He reported two issues [pp. 3-5 of Ref. 28] for not calculating the maximum safe steady-state power based on burnout by CHF: the possible significant *decrease in burnout heat flux due to flow instability* and narrowing of coolant channels at full power. Due to difficulties in resolving these issues, he chose to calculate the maximum safe power based on ONB, and then reduced the calculated maximum safe power by 30% to arrive at the nominal design power of 100 MW.

The scoping result of the reversal diagram for the Missouri University Research Reactor (MURR) is that it is OFI-limited. This agrees with the detailed thermal-hydraulic analysis, with hot channel factors included, done by ANL[29].

The scoping result of the reversal diagram for the Massachusetts Institute of Technology Reactor (MITR) HEU Core is that it is OFI-limited. This agrees with the detailed thermal-hydraulic analysis done by MIT [p. 140 of Ref. 30]. The MIT analysis finds that the OFI will occur at a mean reactor power of 12.4 MW (mean − 3σ power of 10.7 MW) whereas the CHF will occur at 70 MW (mean − 3σ power of 47 MW) [Table 6-5 of Ref. 30].

In short, these five research reactors are all OFI-limited.

7. CONCLUSIONS

Cinematographic experimental evidence is provided for CHF occurring before bubble detachment from the heated wall (i.e., before OFI) in highly subcooled (ΔT_{sub} > ~85 ºC) flow boiling. The ONB heat flux, OFI heat flux and CHF are calculated using the state-of-the-art prediction methods in the coolant mass flux range of 1000 to 30000 kg.m^2-s, for 216 cases covering the typical parametric range of research reactors: channel exit pressure 1 to 50 bar, heated diameter 3 to 8 mm, heated length 0.28 to 1.18 m, inlet temperature 30 to 70 °C. It is found that the safety limits imposed by OFI and CHF cross over in a consistent manner, in the parametric range studied.

A diagram (Fig. 6) showing the mass flux at the intersection of OFI heat flux and CHF (called the reversal mass flux) is plotted as a function of exit pressure (with heated diameter, inlet temperature, and heated length as parameters). The diagram can be used *to scope* whether a coolant channel of a research reactor is OFI-limited or CHF-limited based on five key characteristics of the channel: the heated length, heated diameter, inlet temperature, exit pressure, and mass flux. A reactor is represented by a point on the reversal diagram, using the values of the exit pressure and mass flux of a single coolant channel to model the thermal-hydraulic conditions in the reactor. If the plotted point is below the *applicable* reversal line corresponding to the channel heated diameter and inlet temperature, the channel is OFI-limited. If the plotted point is above the applicable reversal line, the channel is CHF-limited.

For a reactor having coolant channels of different exit pressures, mass fluxes, or heated diameters, etc., each significantly different channel may by plotted on the reversal diagram, obtaining a point representing each coolant channel.

There is a basis (see Section 5) for the applicability of the reversal diagram to reactors with axially non-uniform (especially symmetrical) axial power shapes although the diagram was developed for coolant channels with axially uniform heat flux. The applicability of the reversal diagram to channels with highly skewed axial power shape is doubtful.

The following conclusions are made based on the comparison of the ONB flux, OFI heat flux and CHF:

(1) The error in calculated heat flux at ONB, heat flux at OFI and CHF due to assuming $P_i = P$ for evaluating coolant properties at inlet is found to be negligible.

(2) There is a close agreement between CHFs predicted by the extended Groeneveld 2006 table and the Hall-Mudawar ICC.

(3) At each heated length, the Groeneveld CHF *increases* with increasing heated diameter at constant P, L_h , T_{in}, and G whereas the CHF *decreases* with increasing heated diameter at constant P, L_h , T_{in}, and X_o. The CHF decreases with increasing inlet temperature at constant P, L_h , D_h , and G.

(4) There is a close agreement between the Whittle-Forgan (using $\eta = 32.5$) and the Saha-Zuber OFI prediction methods.

(5) At each heated length, the OFI heat flux increases with increasing exit pressure at constant D_h , L_h , T_{in}, and G. The OFI heat flux increases with increasing heated diameter at constant P, L_h, T_{in}, and G. The OFI heat flux decreases with increasing inlet temperature at constant P, L_h , D_h , and G.

(6) The parametric variation trend of ONB heat flux is qualitatively similar to that of the OFI heat flux given in item 5 above.

NOMENCLATURE

A_f = Flow area of channel, m^2
A_h = $L_h P_h$ = Area of heated wall in channel, m^2
C_p = Liquid coolant specific heat, kW/kg-ºC
D_e = $4A_f/P_w$ = Hydraulic diameter of coolant channel, m
D_h = $4A_f/P_h$ = Heated diameter of coolant channel, m
G = Mass flux, kg/m^2-s
G_{rev} = Mass flux at the intersection of OFI heat flux and CHF, kg/m^2-s
h = Coolant enthalpy, kJ/kg
H = Convective heat transfer coefficient, kW/m^2-°C
L_h = Heated length of channel, m
Nu = Nusselt number
ONB = Onset of nucleate boiling
OFI = Onset of static flow instability, or flow excursion
P = Coolant pressure at the heated length exit, bar
ΔP = Pressure drop from the channel inlet to exit
Pe = GDC_{pf}/K_f = Peclet number
P_i = Coolant inlet pressure, bar
P_w = Wetted perimeter of coolant channel, m
P_h = Heated perimeter of coolant channel, m
q_c = Critical heat flux, kW/m^2
q_{ONB} = ONB heat flux, kW/m^2
q_{OFI} = OFI heat flux, kW/m^2
q_{rev} = Heat flux at the intersection of OFI heat flux and CHF, kW/m^2
Re = GD_e/μ = Reynolds number, dimensionless
St = $q_{OFI}/(GC_p\Delta T_{sub,o})$ = Stanton number, dimensionless
T_c = Local bulk coolant temperature, °C
T_i = T_{in} = Bulk coolant inlet temperature, °C
T_o = Bulk coolant exit temperature, °C
T_{sat} = Coolant saturation temperature, °C
$\Delta T_{sub,o}$ = $T_{sat} - T_o$ = Outlet coolant subcooling at OFI, °C
V = Coolant velocity, m/s
X_i^* = Pseudo thermodynamic quality at the inlet of heated length
X_o = Thermodynamic equilibrium quality at the outlet of heated length
X_{osv} = Thermodynamic equilibrium quality at onset of significant void
μ = Viscosity of coolant, $N\text{-}s/m^2$
σ = Surface tension, N/m

Subscripts

e = equivalent hydraulic
f = saturated liquid
fe = flow excursion
fg = liquid-to-vapor phase change
g = saturated vapor
h = heated
i or in = channel inlet
o = channel outlet
p = constant pressure
rev = OFI-CHF intersection or reversal
sat = saturation
w = heated wall

REFERENCES

1. M. Siman-Tov, D. K. Felde, J. L. McDuffee, and G. L. Yoder, "Experimental Study of Static Flow Instability in Subcooled Flow Boiling in Parallel Channels," 4th. ASME/JSME Thermal Engineers Joint Conference, Maui, Hawaii (January 1995).
2. W. Liu, H. Nariai, and F. Inasaka, "Prediction of Critical Heat Flux for Subcooled Flow Boiling," Intern. J. Heat and Mass Transfer, Vol. 43, pp. 3371-3390 (2000).
3. J. E. Kennedy, G. M. Roach, Jr., M. F. Dowling, S. I. Abdel-Khalik, S. M. Ghiaasiaan, S. M. Jeter, and Z. H. Qureshi, "The Onset of Flow Instability in Uniformly Heated Horizontal Microchannels," Transactions of the ASME, Vol. 122, pp. 118-125 (2000).
4. R. H. Whittle and R. Forgan, "A Correlation for the Minima in the Pressure Drop vs. Flow Rate Curves for Subcooled Water Flow in Narrow Heated Channels," Nuclear Eng. and Design, Vol. 6, pp. 89-99 (1967).
5. P. Saha and N. Zuber, "Point of Net Vapor Generation and Vapor Void Fraction in Subcooled Boiling," Proc. of 5th Intern. Heat Transfer Conf., Vol. 4, Tokyo, pp. 175-179 (1974).
6. E. D. Waters, "Heat Transfer Experiments for Advanced Test Reactor," Battelle Northwest Laboratory Report, BNWL-216, UC-80 (TID-4500), (1966).
7. W. J. Shim and J. Park, "Analysis of a Generalized CHF Model in Vertical Round Tubes with Uniform Heat Flux," J. Ind. Eng. Chem., Vol. 9, pp. 607-613 (2003).
8. M. Kalimullah, E. E. Feldman, A. P. Olson, B. Dionne, J. G. Stevens, and J. E. Matos, "An Evaluation of Subcooled CHF Correlations and Databases for Research Reactors Operating at 1 to 50 bar Pressure," RERTR 2012, 34th Intern. Meeting on Reduced Enrichment for Research and Test Reactors, Warsaw, Poland (October 14-17, 2012).
9. L. S. Tong and Y. S. Tang, "Boiling Heat Transfer and Two-Phase Flow," 2nd. Edition, Taylor and Francis, Washington, D. C., USA (1997).
10. S. H. Chang and W. Baek, "Understanding, Predicting, and Enhancing Critical Heat Flux," 10th. Intern. Topical Mtg. on Nuclear Reactor Thermal Hydraulics (NURETH-10), Seoul, Korea, pp. 1-20, (October 5-9, 2003).
11. F. C. Gunther, "Photographic Study of Surface-Boiling Heat Transfer to Water with Forced Convection," Progress Report No. 4-75, Jet Propulsion Laboratory, California Institute of Technology, Pasadena, California, USA (1950).
12. F. C. Gunther, "Photographic Study of Surface-Boiling Heat Transfer to Water with Forced Convection," Transactions of ASME, Vol. 73, pp. 11 5-123 (February 1951).
13. G. P. Celata, M. Cumo, A. Mariani, and G. Zummo, "Burnout in Subcooled Flow Boiling of Water, A Visual Experimental Study," Intern. Journal of Thermal Sciences, Vol. 39, pp. 896-908 (2000).
14. S. G. Bankoff, "On the Mechanism of Subcooled Nucleate Boiling, Parts I and II," Chem. Eng. Progress Symposium Series, Vol. 57, No. 32, pp. 156-172 (1961).
15. L. S. Tong, "A Phenomenological Study of Critical Heat Flux," ASME Paper 75-HT-68, National Heat Transfer Conf., San Francisco, California, USA (1975).
16. A.E. Bergles and W.M. Rohsenow, "The Determination of Forced-Convection Surface-Boiling Heat Transfer," J. Heat of Transfer, Vol. 86, pp. 365–372 (1964).
17. N. Basu, G. R. Warrier, and V. K. Dhir, "Onset of Nucleate Boling and Active Nucleation Site Density During Subcooled Flow Boling," J. Heat of Transfer, Vol. 124, pp. 717-728 (2002).

18. D. C. Groeneveld, J. Q. Shan, A. Z. Vasic, L. K. H. Leung, A. Durmayaz, J. Yang, S. C. Cheng, and A. Tanase, "The 2006 CHF Look-up Table," Nucl. Eng. and Design, Vol. 237, pp. 1909-1922 (2007).
19. D. D. Hall and I. Mudawar, "Critical Heat Flux for Water Flow in Tubes – II. Subcooled CHF Correlations," Intern. J. Heat and Mass Transfer, Vol. 43, pp. 2605-2640 (2000).
20. "International Association for the Properties of Steam (IAPS)," H. J. White, Secretary, National Bureau of Standards, Washington, D.C., 1977 (revised 1983).
21. A. P. Olson and M. Kalimullah, "A User's Guide to the PLTEMP/ANL Code," ANL/RERTR/TM-11-22, Version 4.11, Nuclear Engineering Division, Argonne National Laboratory, Argonne, IL, USA (November 15, 2011).
22. J. G. Collier and J. R. Thome, "Convective Boiling and Condensation," 3rd Edition, Clarendon Press, Oxford, Section 9.2.1.2 (1994).
23. D. H. Lee and J. D. Obertelli, "An Experimental Investigation of Forced Convection Burnout in High Pressure Water – Part II," Report UK AERE-R-309, Atomic Energy Research Establishment, Harwell, England (1963).
24. D. H. Lee, "An Experimental Investigation of Forced Convection Burnout in High Pressure Water – Part III," Report UK AERE-R-355, Atomic Energy Research Establishment, Harwell, England (1965).
25. D. H. Lee, "An Experimental Investigation of Forced Convection Burnout in High Pressure Water – Part IV," Report UK AERE-R-479, Atomic Energy Research Establishment, Harwell, England (1966).
26. G. L. Yoder, Jr., et al., "Steady-State Thermal-Hydraulic Analysis of the Advanced Neutron Source Reactor," ORNL/TM-12398, Oak Ridge National Laboratory, Tennessee May 1994).
27. S. A. Atkinson, "A Forced Convection DNB Correlation for Stainless Steel or Aluminum Heaters for Low Subcooling Based on Savannah River Laboratory Data," TR-813, Aerojet Nuclear Company, Idaho Falls, ID (March 25, 1976).
28. H. A. McLain, "HFIR Fuel Element Steady-State Heat Transfer Analysis, Revised Version," ORNL-TM-1904, Oak Ridge National Laboratory, Oak Ridge, Tennessee, USA (December 1967).
29. Feldman, E. E., et al., Technical Basis in Support of the Conversion of the University of Missouri Research Reactor (MURR) Core from Highly-Enriched to Low-Enriched Uranium – Steady-State Thermal-Hydraulic Analysis, ANL/RERTR/TM-12-37, Argonne National Laboratory, Argonne, IL (August 2012).
30. K. Y. Chiang, "Thermal Hydraulic Limits Analysis for the MIT Research Reactor Low Enrichment Uranium Core Conversion Using Statistical Propagation of Parametric Uncertainties," Thesis for Master of Science Degree, Certified and Accepted by L. W. Hu, B. Forget, T, Newton, and M. S. Kazimi, Department of Nuclear Science and Engineering, Massachusetts Institute of Technology, Cambridge, MA, USA (June 2012).
31. G. J. Kirby, R. Staniforth, and J. H. Kinneir, "A Visual Study of Forced Convection Boiling, Part 2: Flow Patterns and Burnout for a Round Test Section," AEEW-R506, Atomic Energy Establishment, Winfrith, Dorchester, Dorset (March 1967).
32. M. P. Fiori and A. E. Bergles, "Model of Critical Heat Flux in Subcooled Flow Boiling," DSR 70281-56, Massachusetts Institute of Technology, Cambridge, Massachusetts, USA (September 1968).

33. J. Weisman and B. S. Pei, "Prediction of Critical Heat Flux in Flow Boiling at Low Qualities," Intern. J. Heat and Mass Transfer, Vol. 26, pp. 1463-1477 (1983).
34. H. Kinoshita, H. Nariai, and F. Inasaka, "Study of Critical Heat Flux Mechanism in Flow Boiling Using Bubble Crowding Model – Application to CHF in Short Tube and in Tube with Twisted Tape under Non-Uniform Heating Conditions," JSME International Journal, Series B, Vol. 44, No. 1, pp. 81-89 (2001).
35. C. H. Lee and I. Mudawar, "A Mechanistic Critical Heat Flux Model for Subcooled Flow Boiling Based on Local Bulk Flow Conditions," Intern. Journal of Multiphase Flow, Vol. 14, No. 6, pp. 711-728 (1988).
36. G. P. Celata, M. Cumo, A. Mariani, M. Simoncini, and G. Zummo, "Rationalization of Existing Mechanistic Models for the Prediction of Water Subcooled Flow Boiling Critical Heat Flux," Intern. J. of Heat and Mass Transfer, Vol. 37, Supplement 1, pp. 347-360 (1994).
37. H. Zhang, I. Mudawar, and M. M. Hasan, "Photographic Study of High-Flux Subcooled Flow Boiling and Critical Heat Flux," Intern. Communication in Heat and Mass Transfer, Vol. 34, pp. 653-660 (2007).
38. G. F. Hewitt and N. S. Hall Taylor, "Annular Two-Phase Flow," Pergamon Press, Oxford (1970).
39. P. B. Whalley, "The Calculation of Dryout in a Rod Bundle," Report UK AERE-R-8319, Atomic Energy Research Establishment, Harwell, England (1976).
40. G. F. Hewitt, "Experimental Studies of the Mechanism of Burnout in Heat Transfer to Steam Water Mixtures," Proc. 4th. International Heat Transfer Conf., Versailles, France, Paper B6.6 (1970).
41. G. P. Celata, "On the Application Method of Critical Heat Flux Correlations," Letter to the Editor, Nuclear Eng. Design, Vol. 163, pp. 241-242 (1996).
42. P. Hejzlar and N. E. Todreas, "Consideration of Critical Heat Flux Margin Prediction by Subcooled or Low Quality Critical Heat Flux Correlations," Nucl. Eng. Design, Vol. 163, pp. 215-223 (1996).

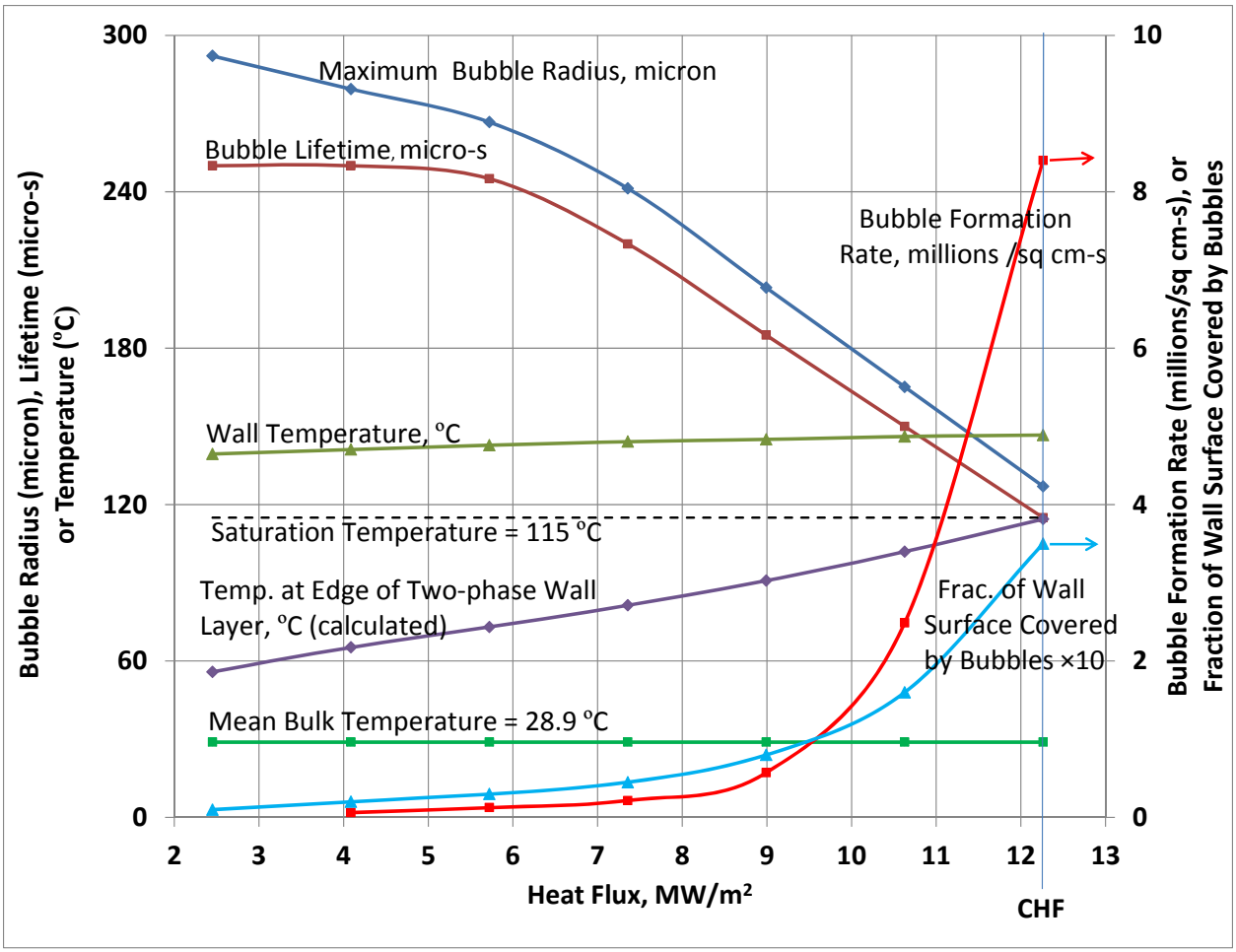

Fig. 1. Bankoff's Analysis of Gunther's Data for Approach to CHF in Highly Subcooled Boiling of Water (6 Tests at P = 1.7 bar, ΔT_{sub} = 86 °C, Velocity = 3.05 m/s)

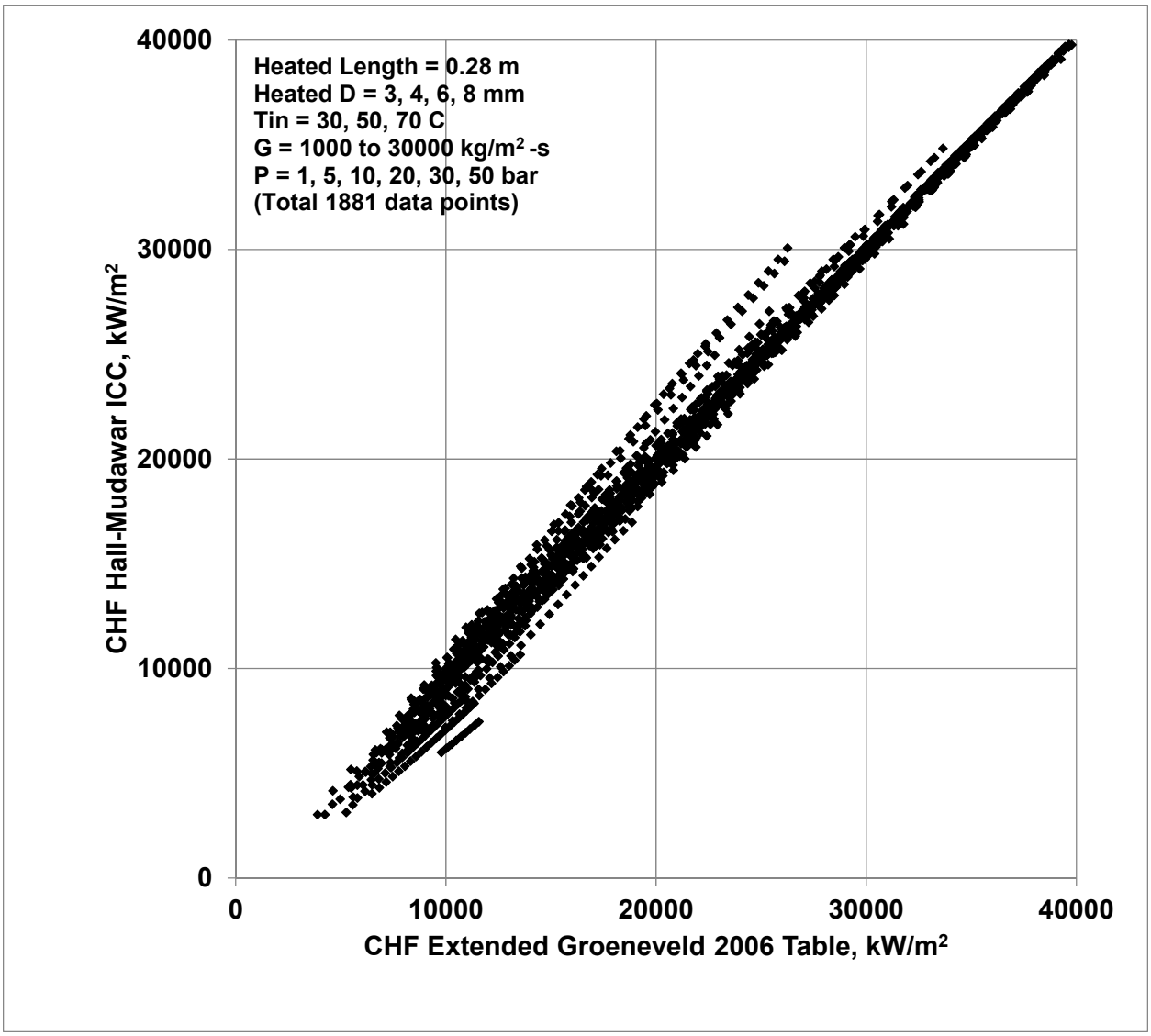

Fig. 2A. Comparison between CHFs by the Extended Groeneveld 2006 Table and the Hall-Mudawar ICC for 72 Cases of Heated Length 0.28 m

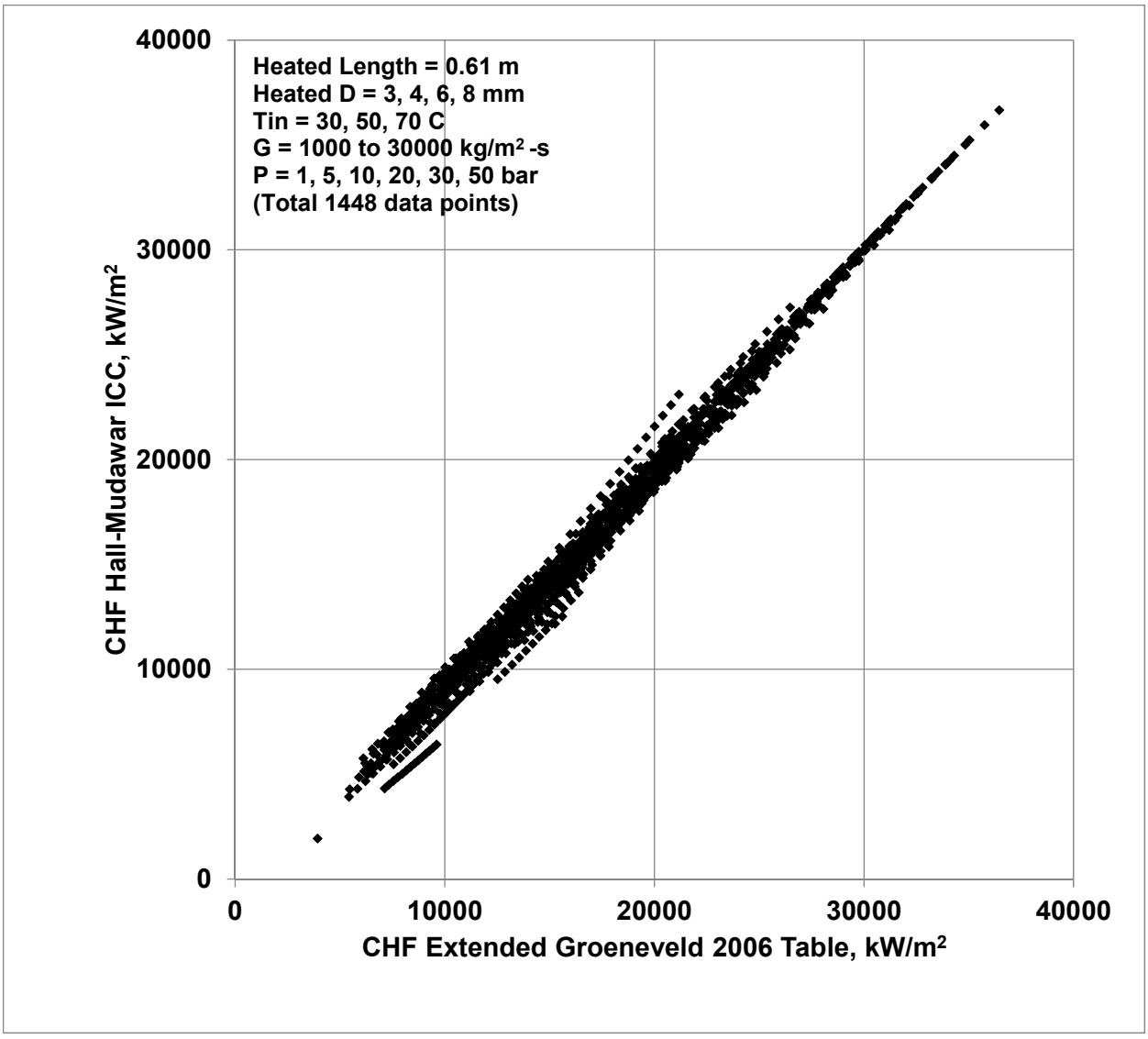

Fig. 2B. Comparison between CHFs by the Extended Groeneveld 2006 Table and the Hall-Mudawar ICC for 72 Cases of Heated Length 0.61 m

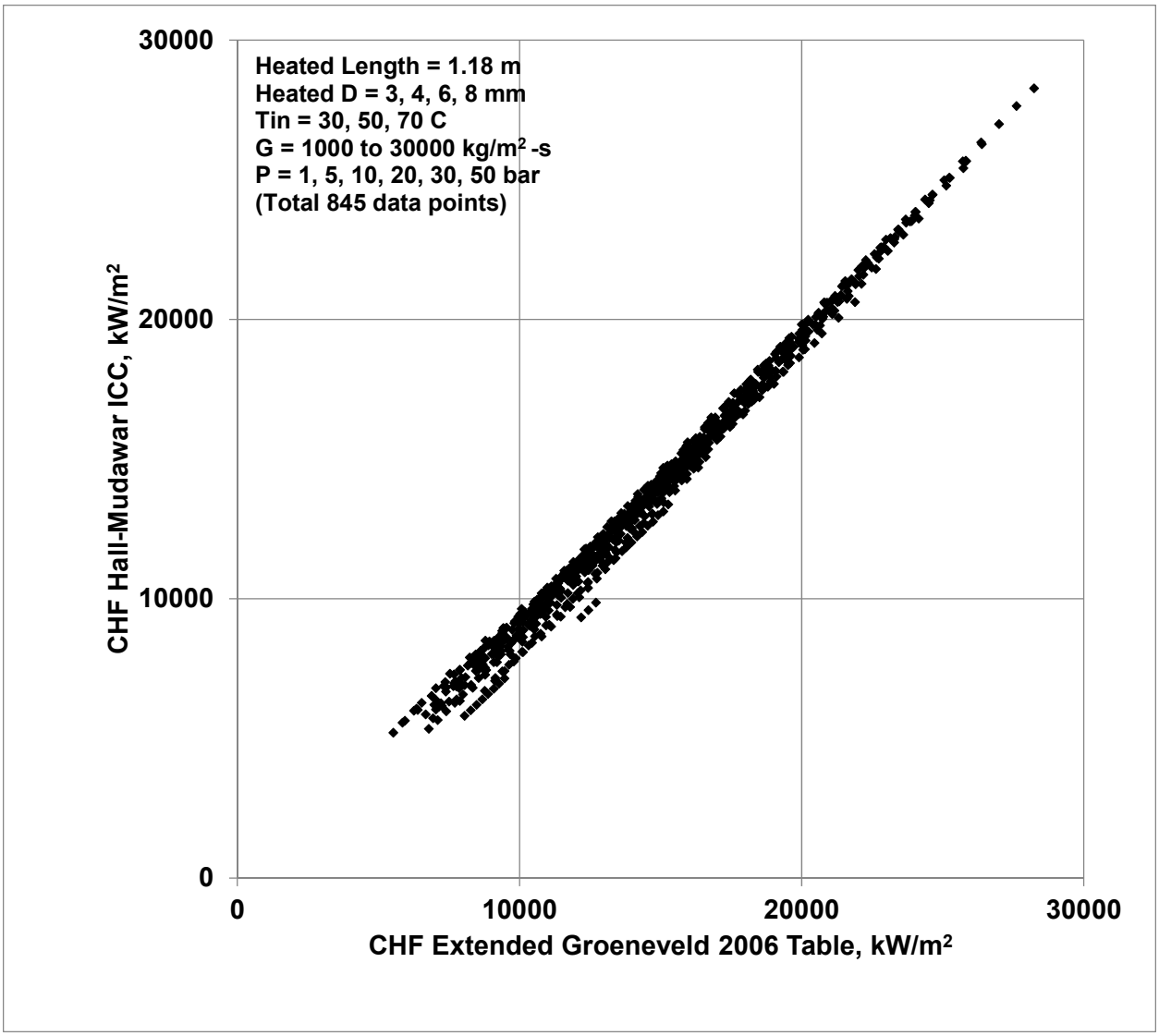

Fig. 2C. Comparison between CHFs by the Extended Groeneveld 2006 Table and the Hall-Mudawar ICC for 72 Cases of Heated Length 1.18 m

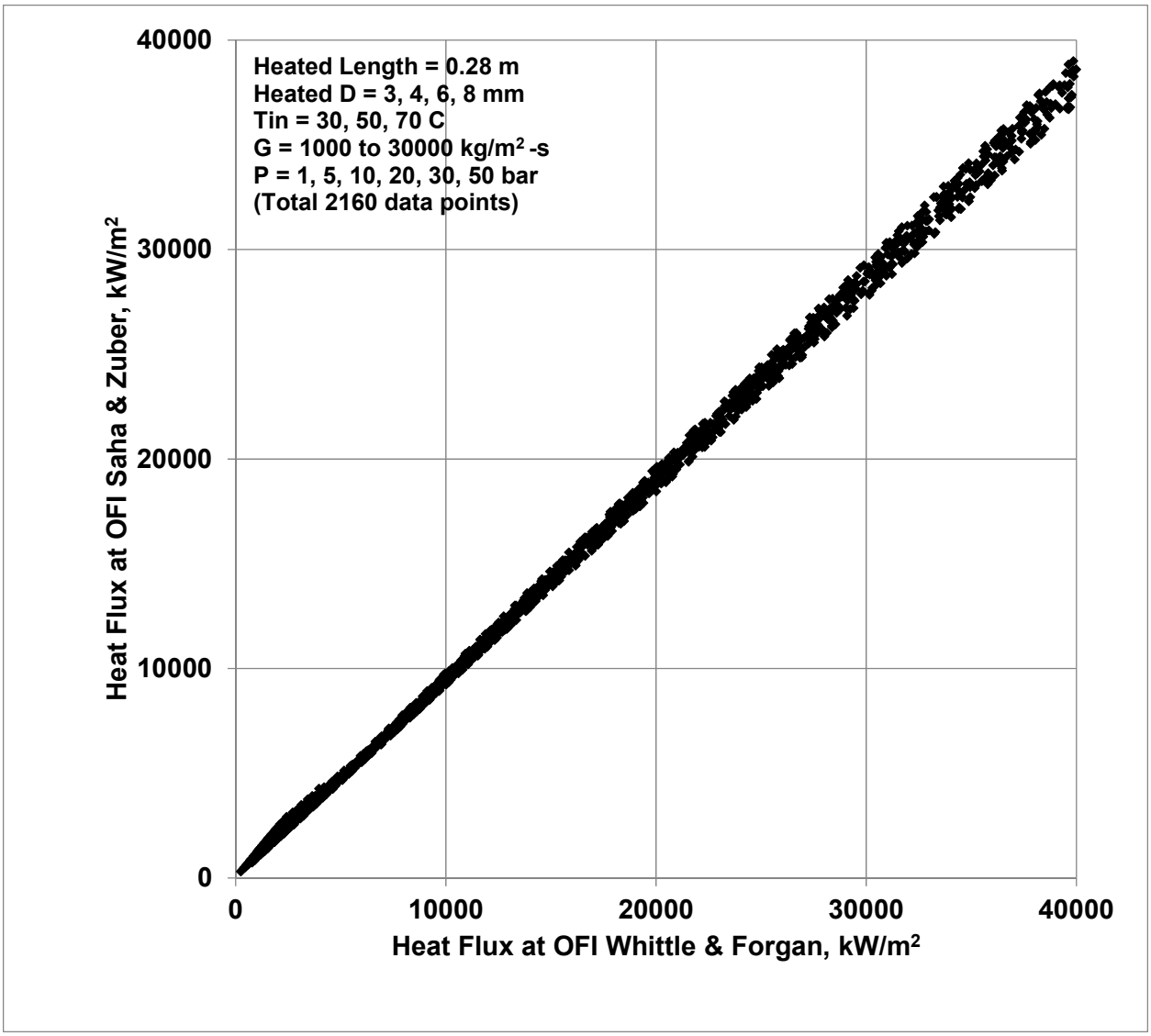

Fig. 3A. Comparison between OFI Heat Fluxes by the Whittle-Forgan (η = 32.5) and the Saha-Zuber Correlations for 72 Cases of Heated Length 0.28 m

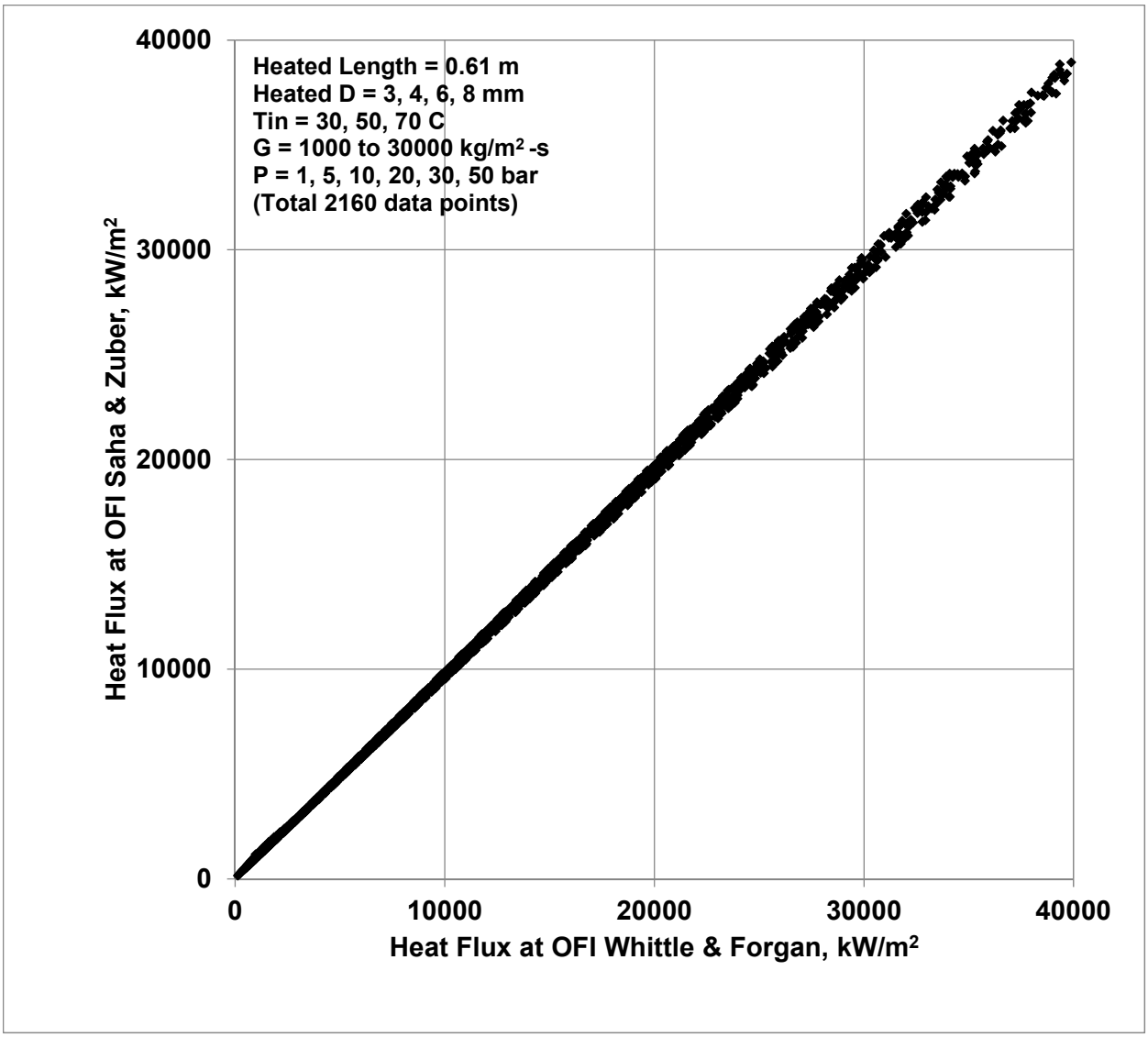

Fig. 3B. Comparison between OFI Heat Fluxes by the Whittle-Forgan (η = 32.5) and the Saha-Zuber Correlations for 72 Cases of Heated Length 0.61 m

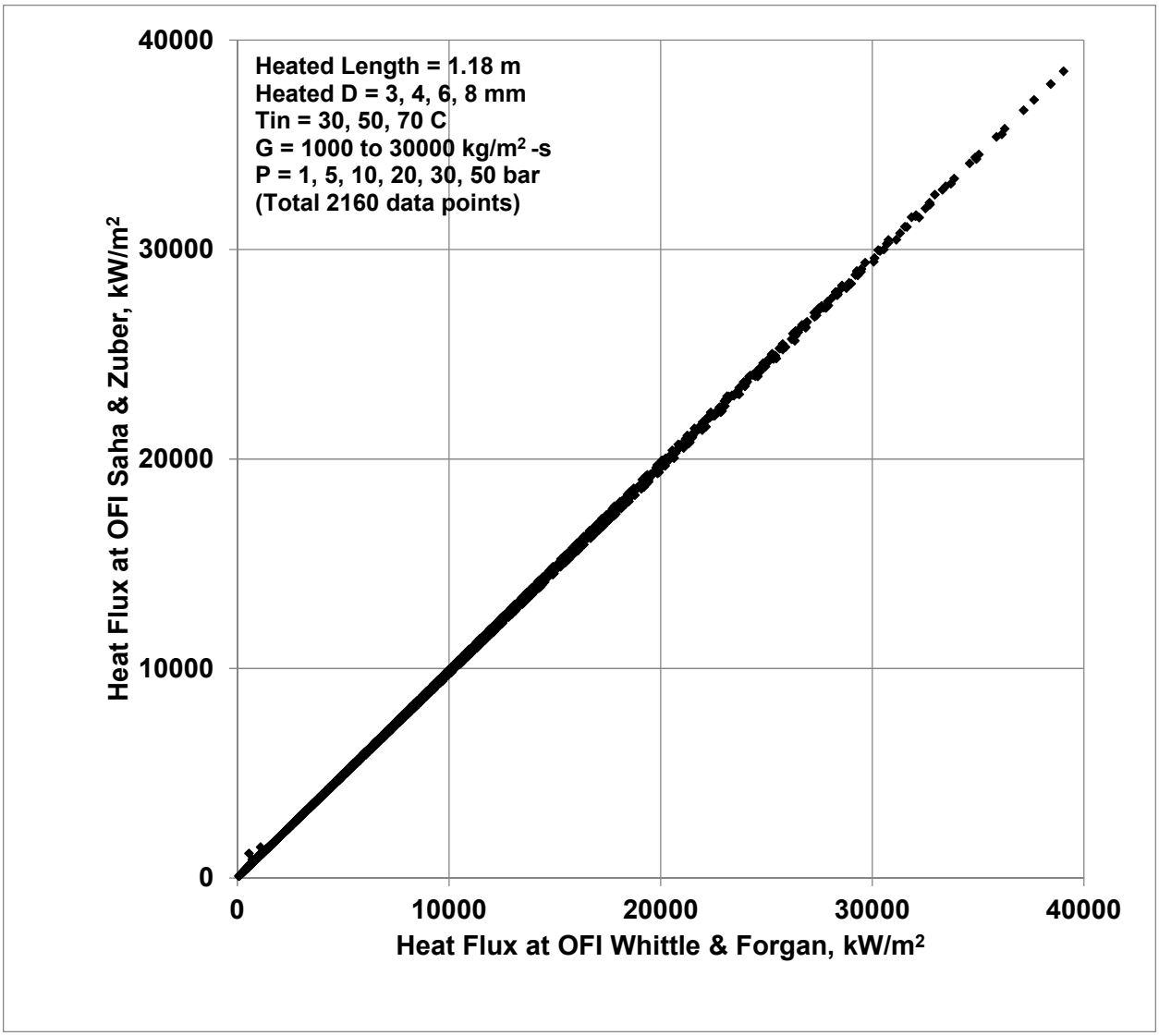

Fig. 3C. Comparison between OFI Heat Fluxes by the Whittle-Forgan (η = 32.5) and the Saha-Zuber Correlations for 72 Cases of Heated Length 1.18 m

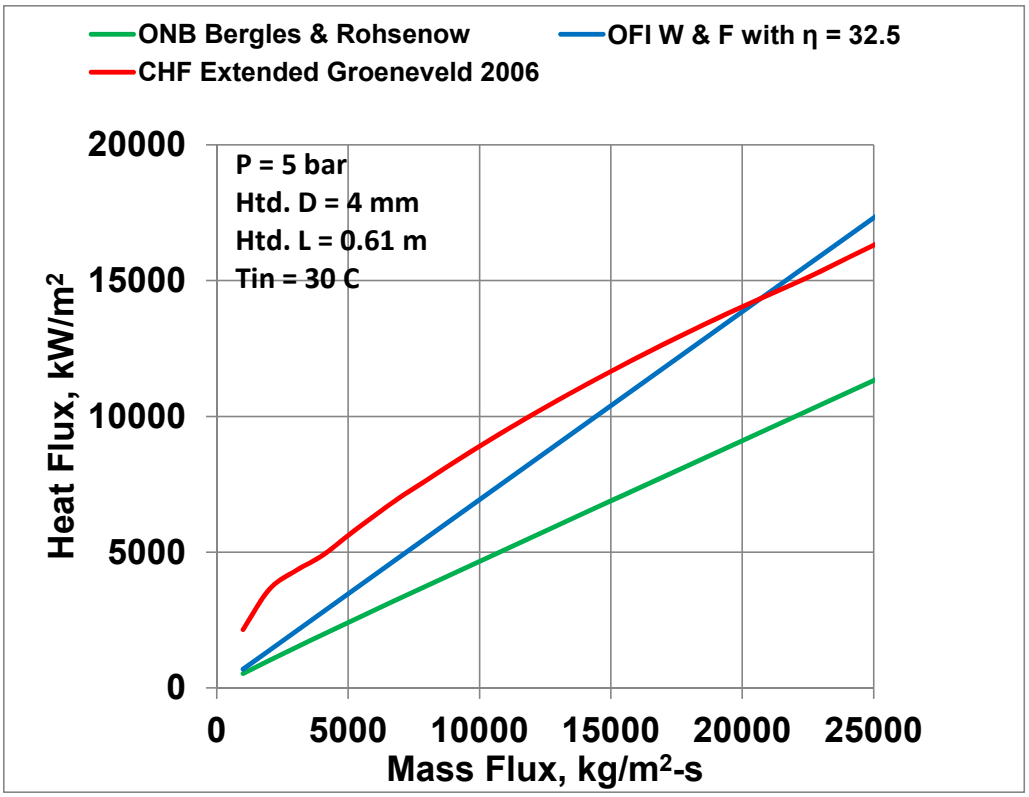

Fig. 4. Heat Fluxes at ONB, OFI, and CHF as a Function of Coolant Mass Flux (It is one of 18 plots in Appendix B)

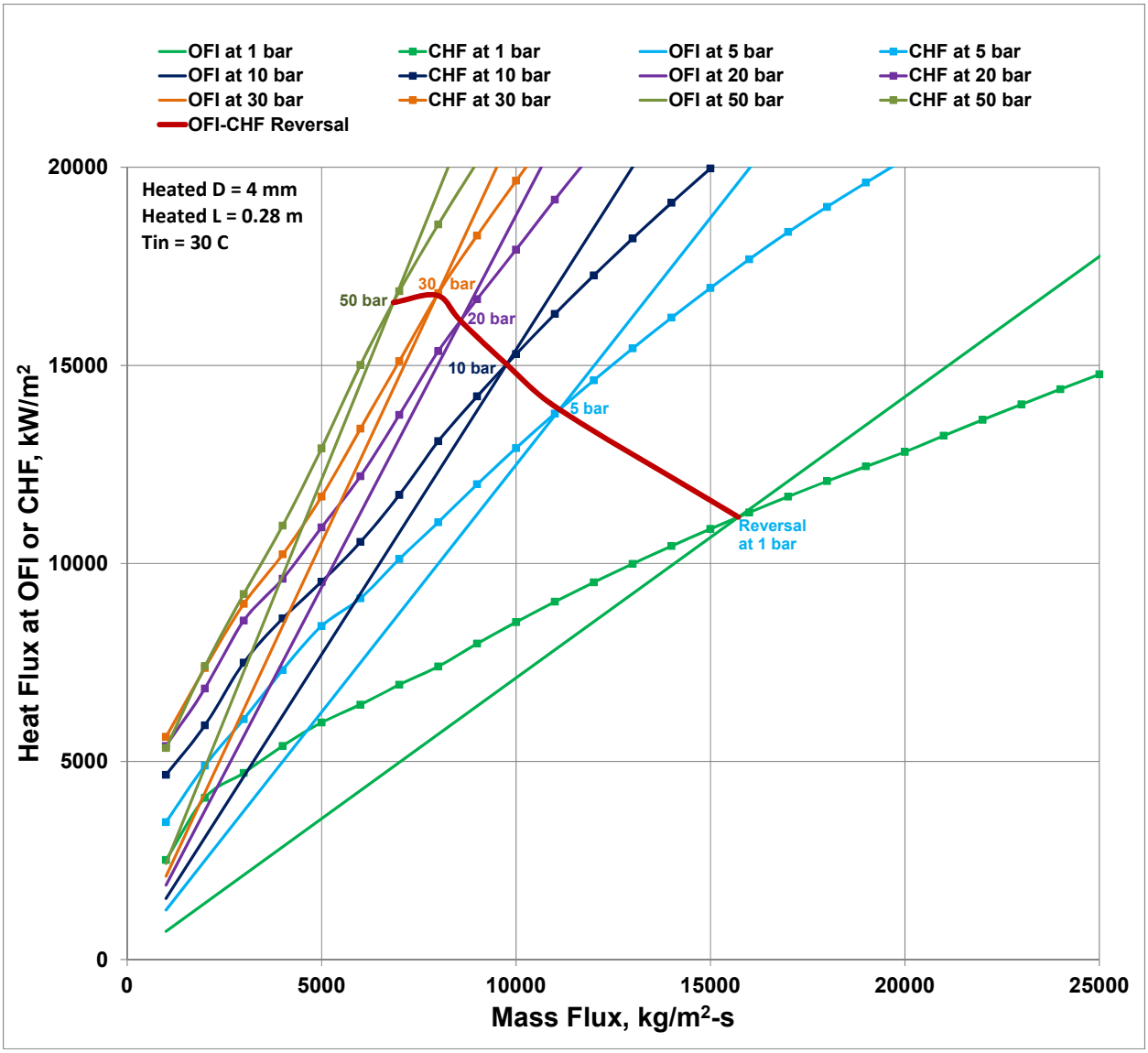

Part 1 of 6

Fig. 5. Intersection of OFI Heat Flux and CHF at Exit Pressures of 1 to 50 bar

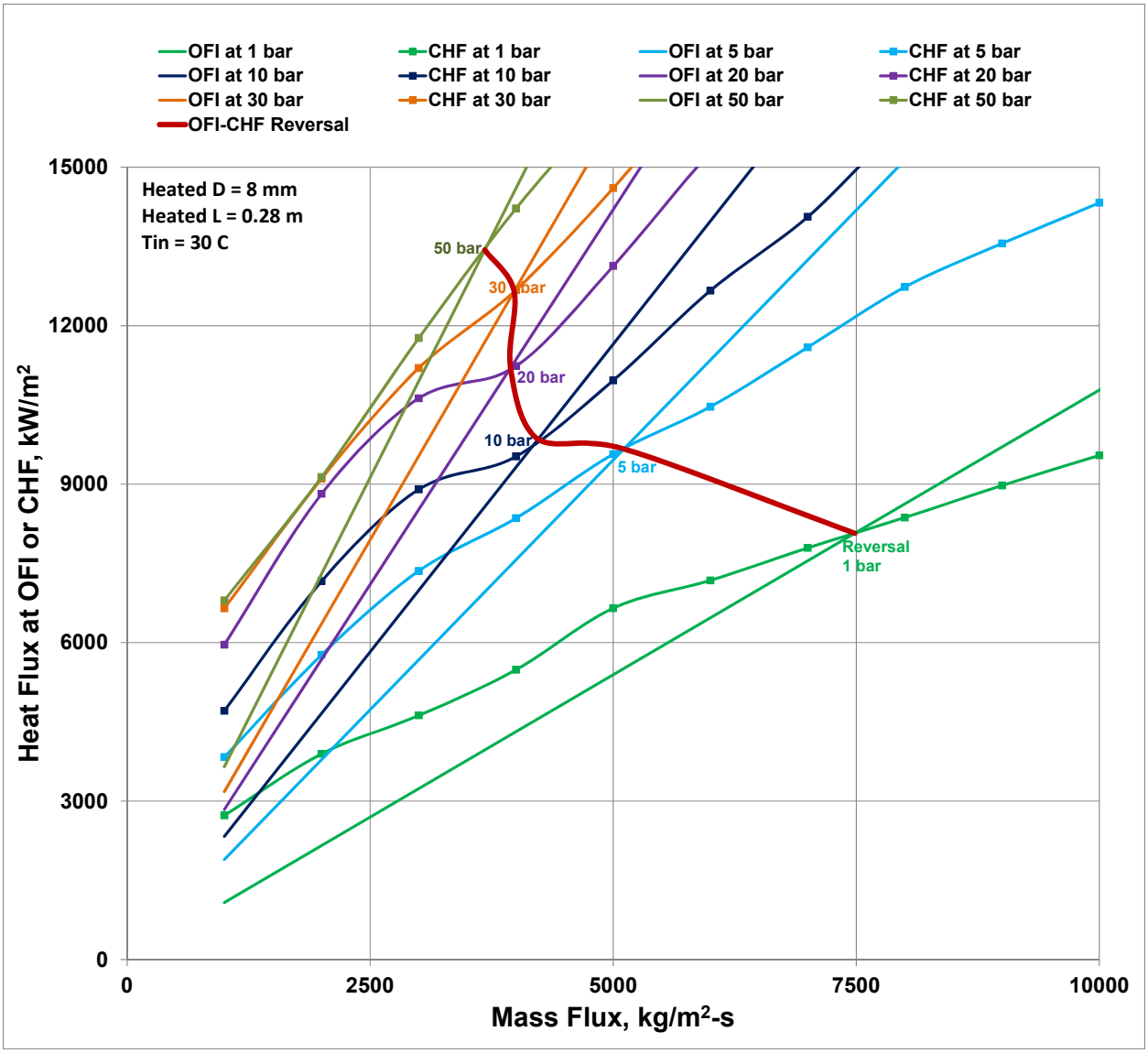

Fig. 5. Continued (Part 2 of 6): Intersection of OFI Heat Flux and CHF at Exit Pressures of 1 to 50 bar

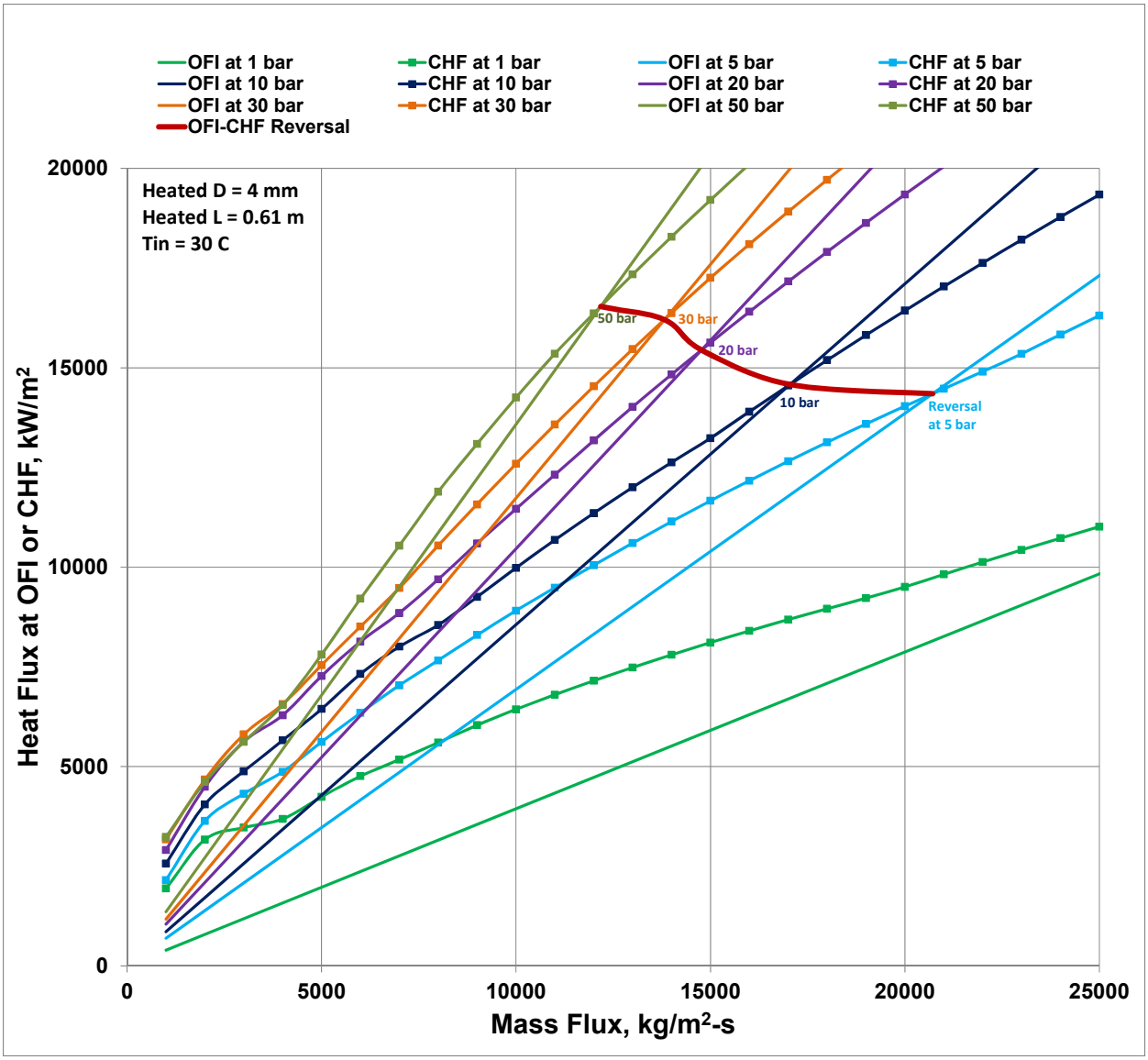

Fig. 5. Continued (Part 3 of 6): Intersection of OFI Heat Flux and CHF at Exit Pressures of 1 to 50 bar

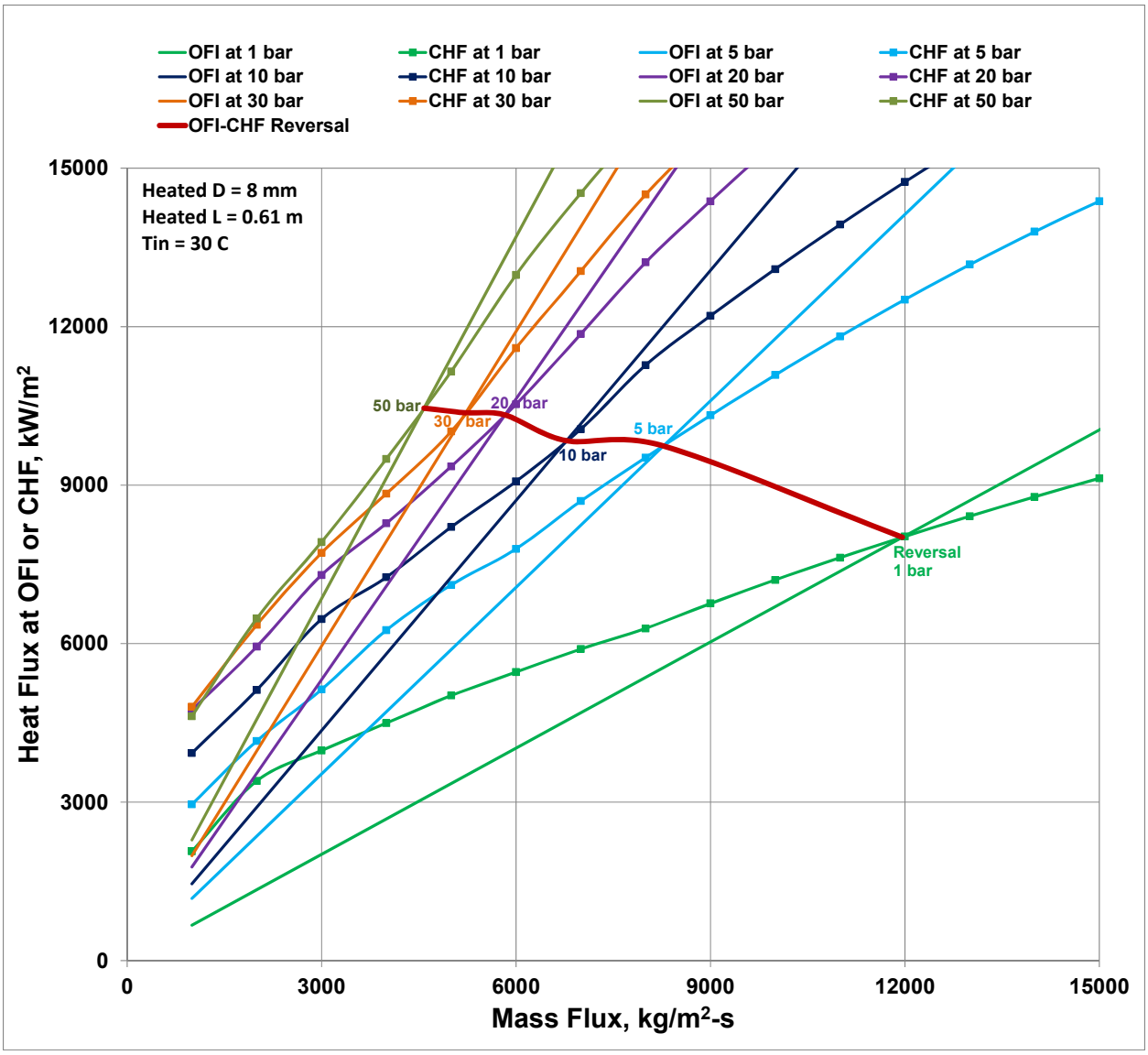

Fig. 5. Continued (Part 4 of 6): Intersection of OFI Heat Flux and CHF at Exit Pressures of 1 to 50 bar

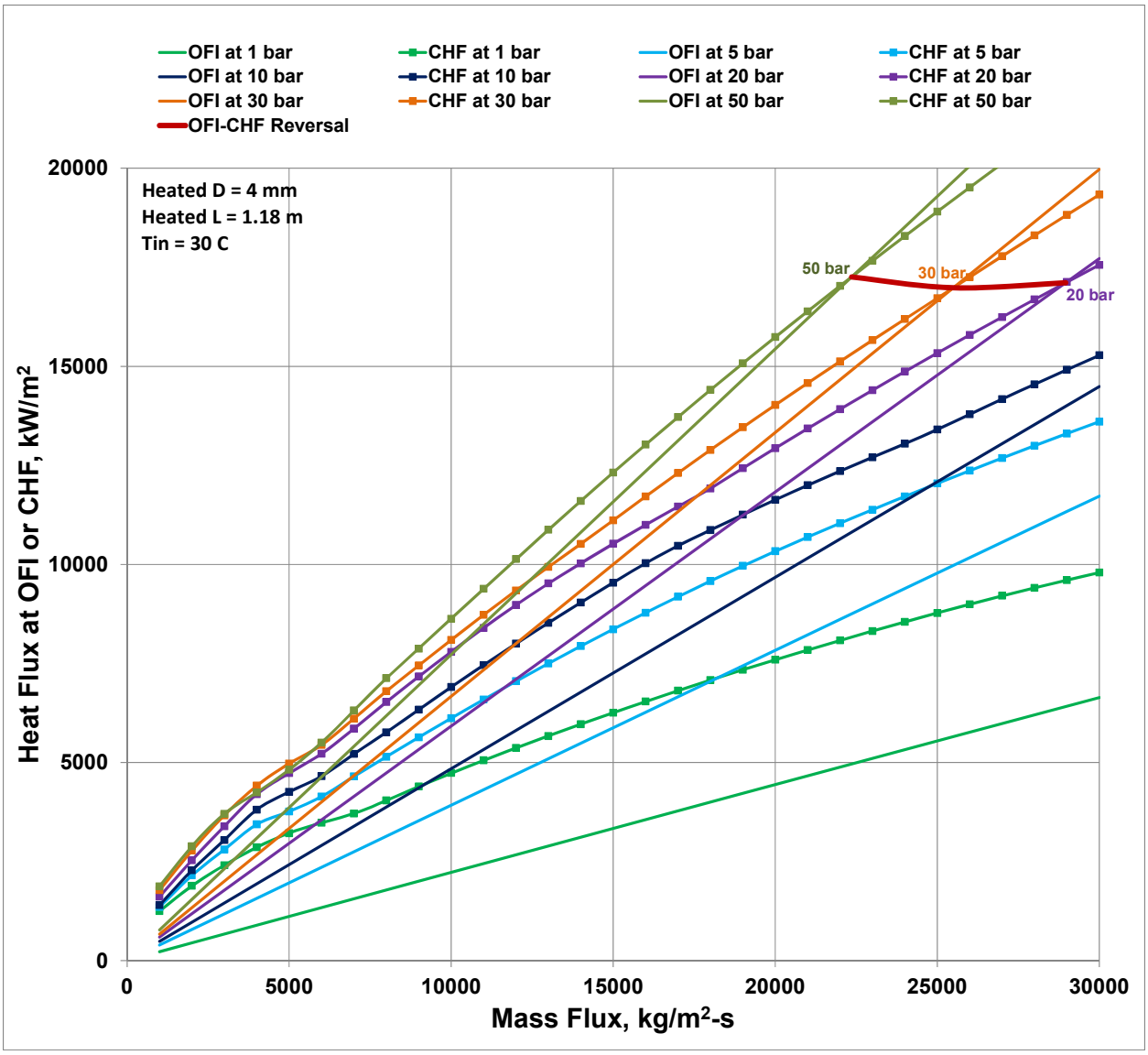

Fig. 5. Continued (Part 5 of 6): Intersection of OFI Heat Flux and CHF at Exit Pressures of 1 to 50 bar

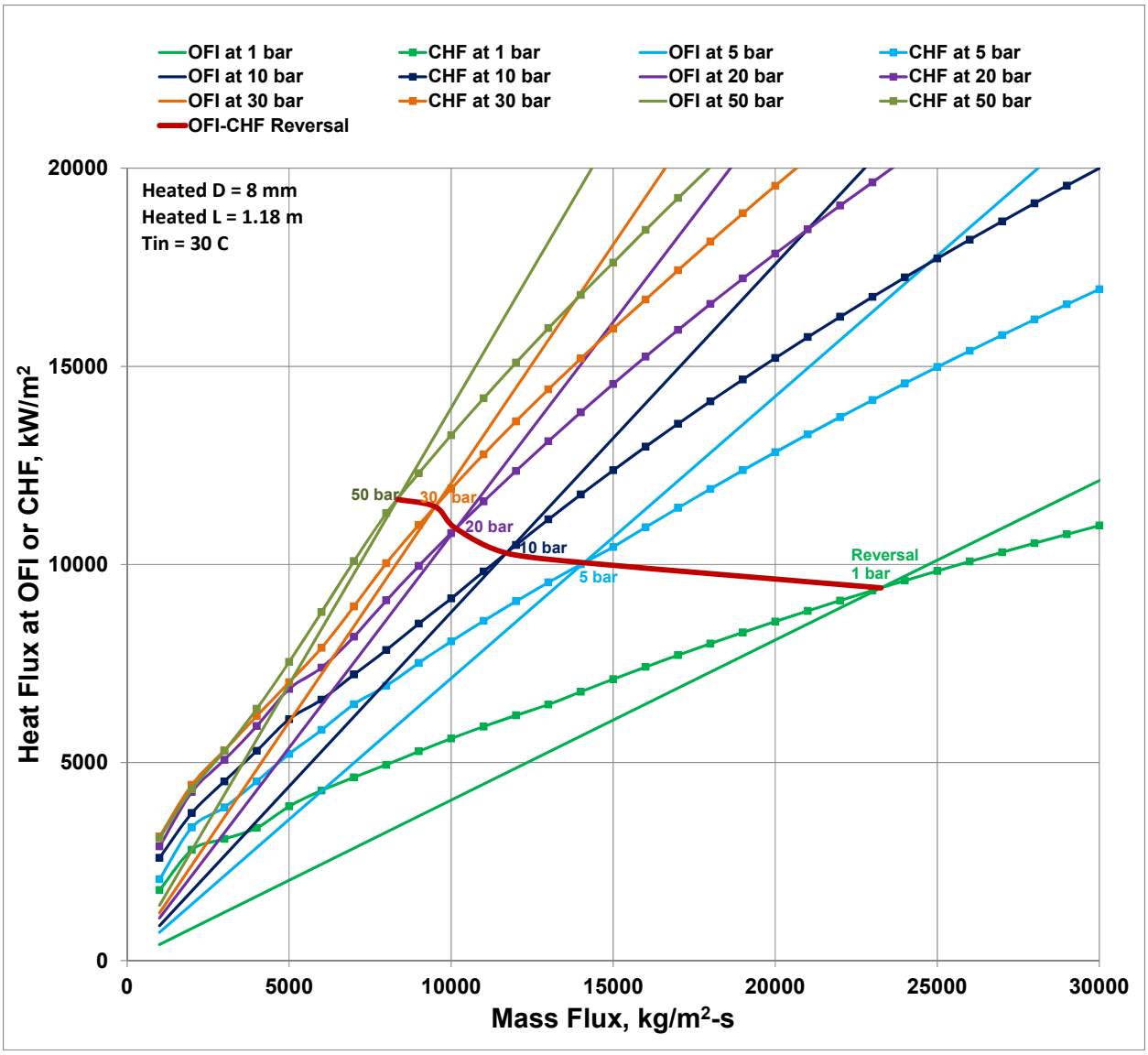

Fig. 5. Continued (Part 6 of 6): Intersection of OFI Heat Flux and CHF at Exit Pressures of 1 to 50 bar

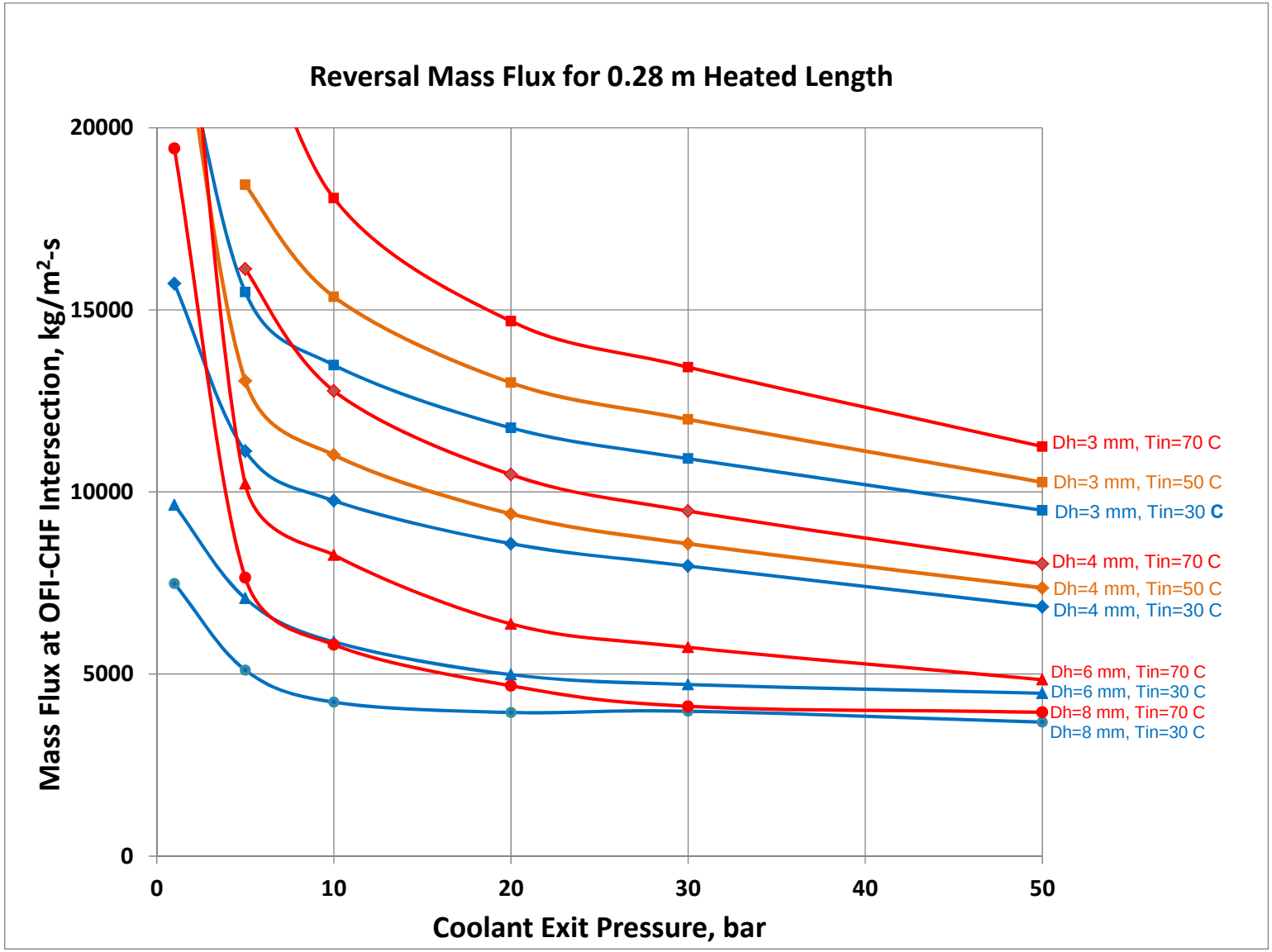

Fig. 6. (Part 1 of 6): Mass Flux at OFI-CHF Intersection (OFI-CHF Reversal Diagram)

The heated diameter and inlet temperature of each reactor, that determine the reversal line applicable to the reactor, are shown in parentheses. If the point representing a reactor lies below the applicable reversal line, the reactor is OFI-limited. It lies above, the reactor is CHF-limited.

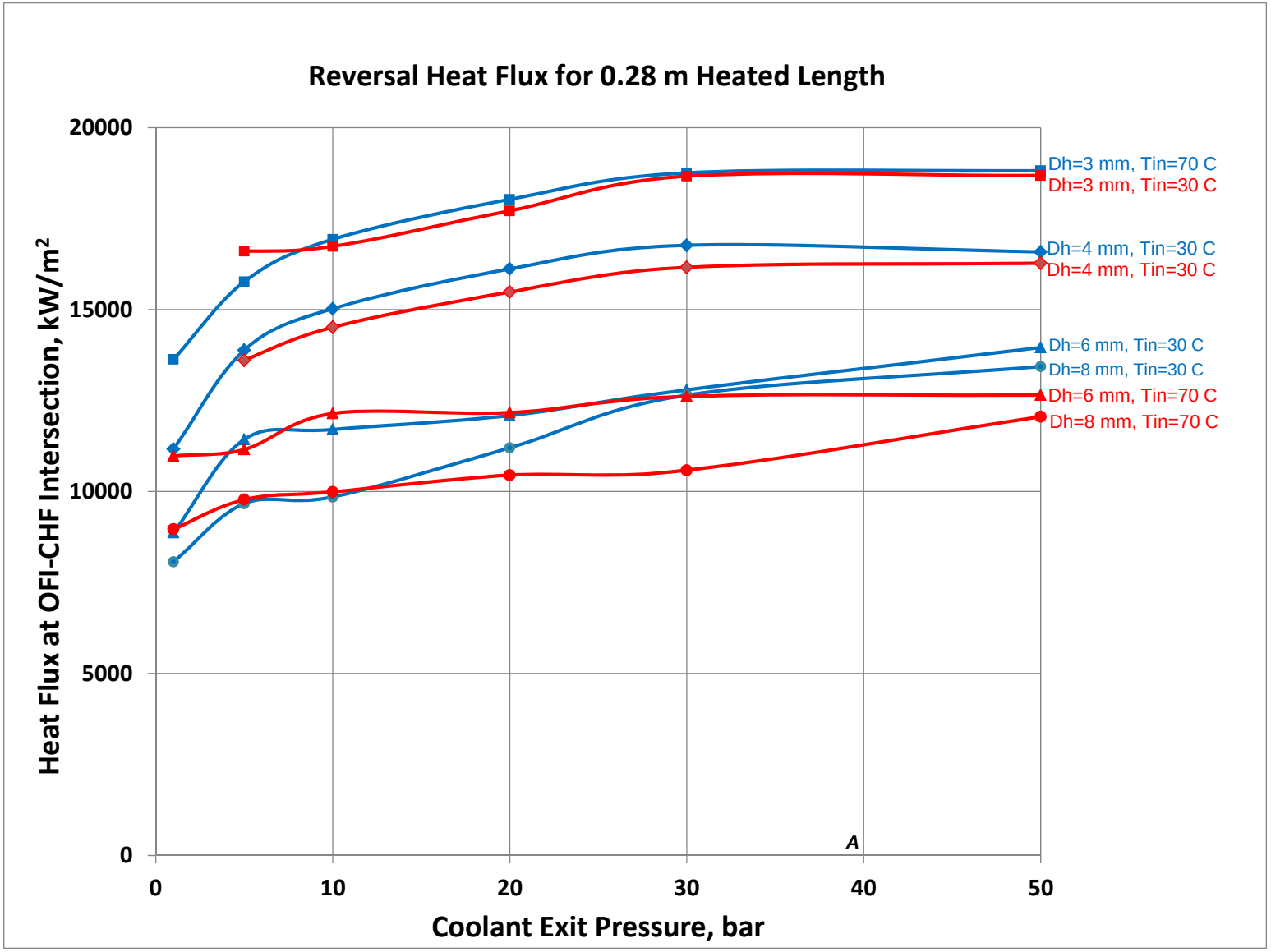

Fig. 6. Continued (Part 2 of 6): Heat Flux at OFI-CHF Intersection (OFI-CHF Reversal Diagram)

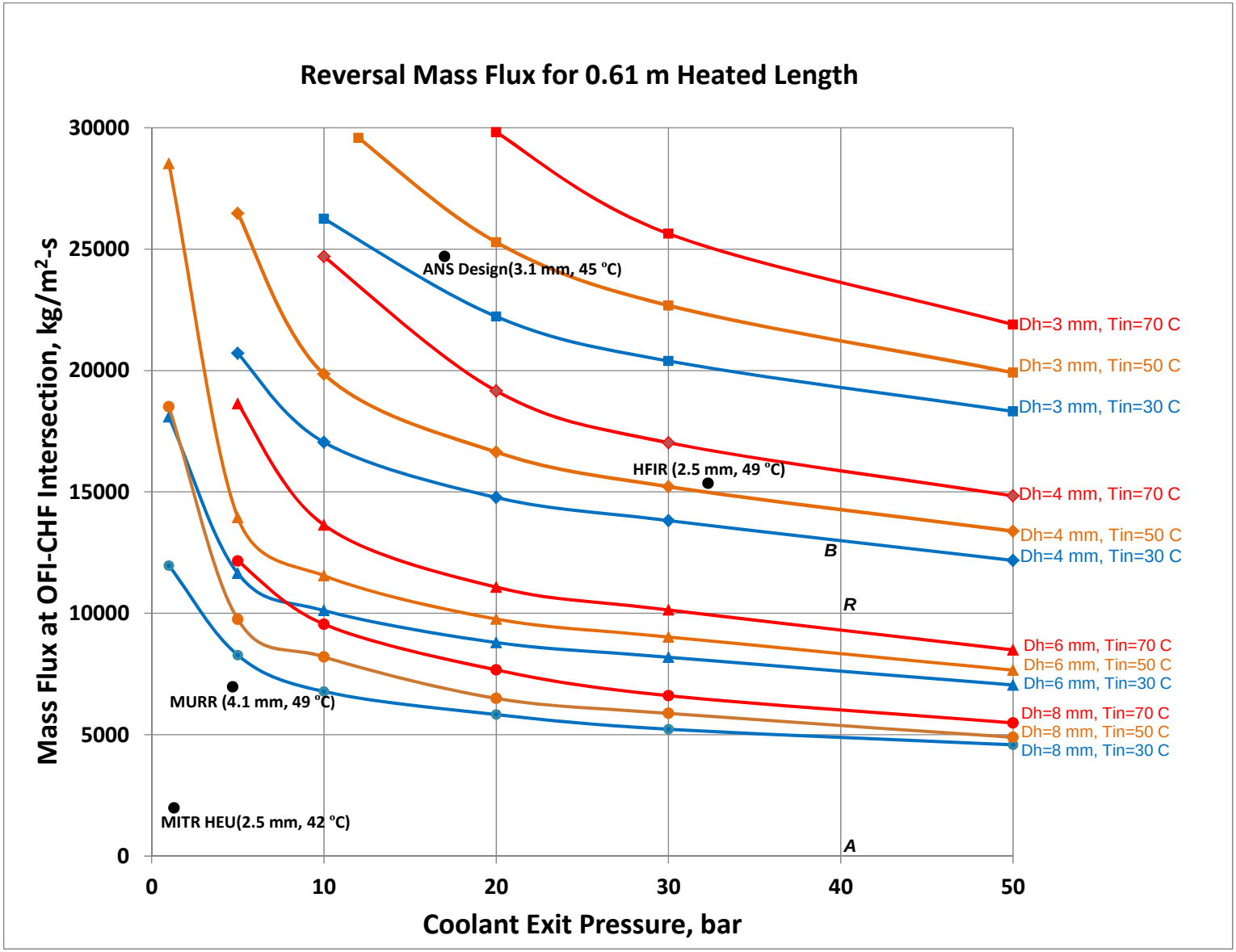

Fig. 6. Continued (Part 3 of 6): Mass Flux at OFI-CHF Intersection (OFI-CHF Reversal Diagram)

The heated diameter and inlet temperature of each reactor, that determine the reversal line applicable to the reactor, are shown in parentheses. If the point representing a reactor lies below the applicable reversal line, the reactor is OFI-limited. It lies above, the reactor is CHF-limited.

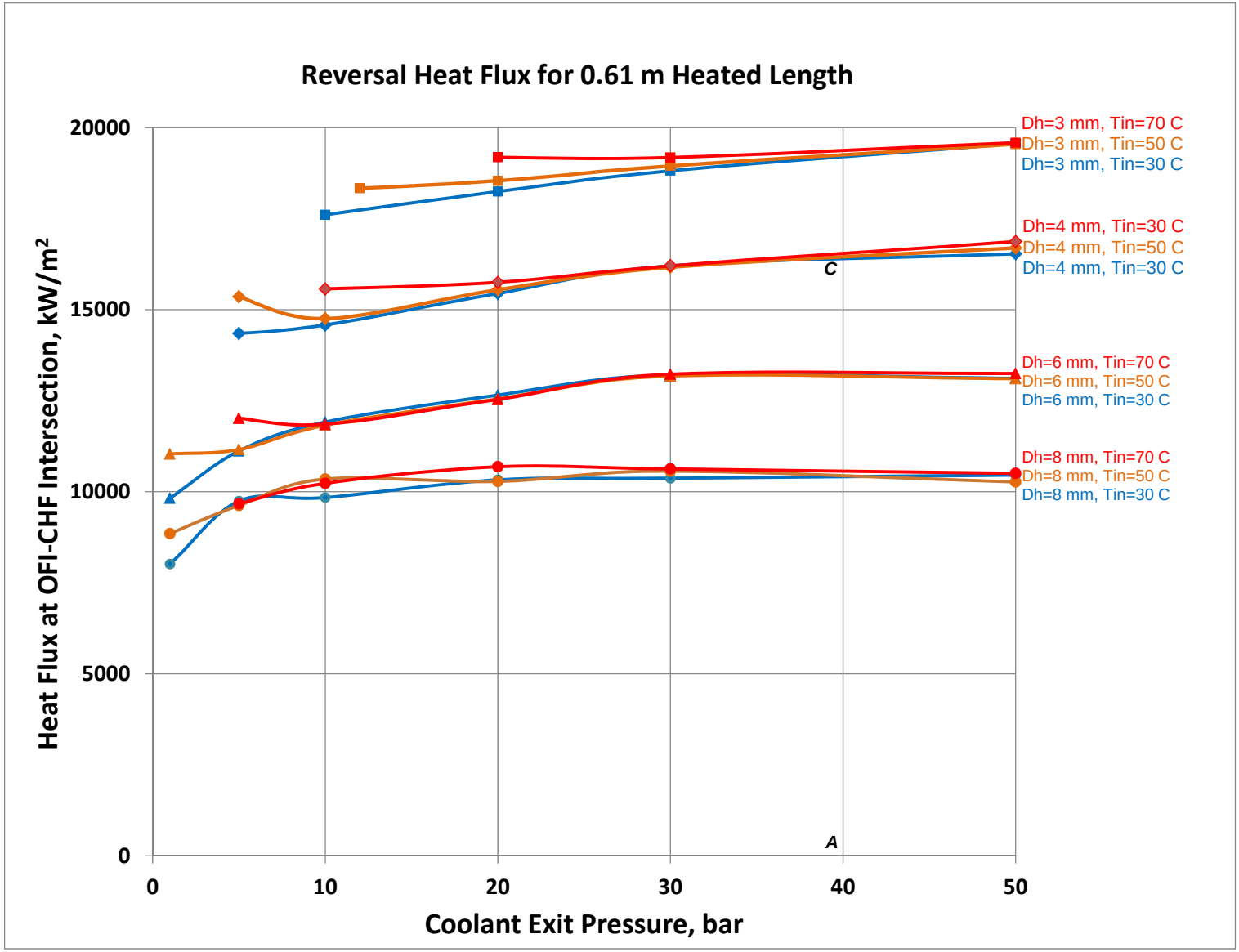

Fig. 6. Continued (Part 4 of 6): Heat Flux at OFI-CHF Intersection (OFI-CHF Reversal Diagram)

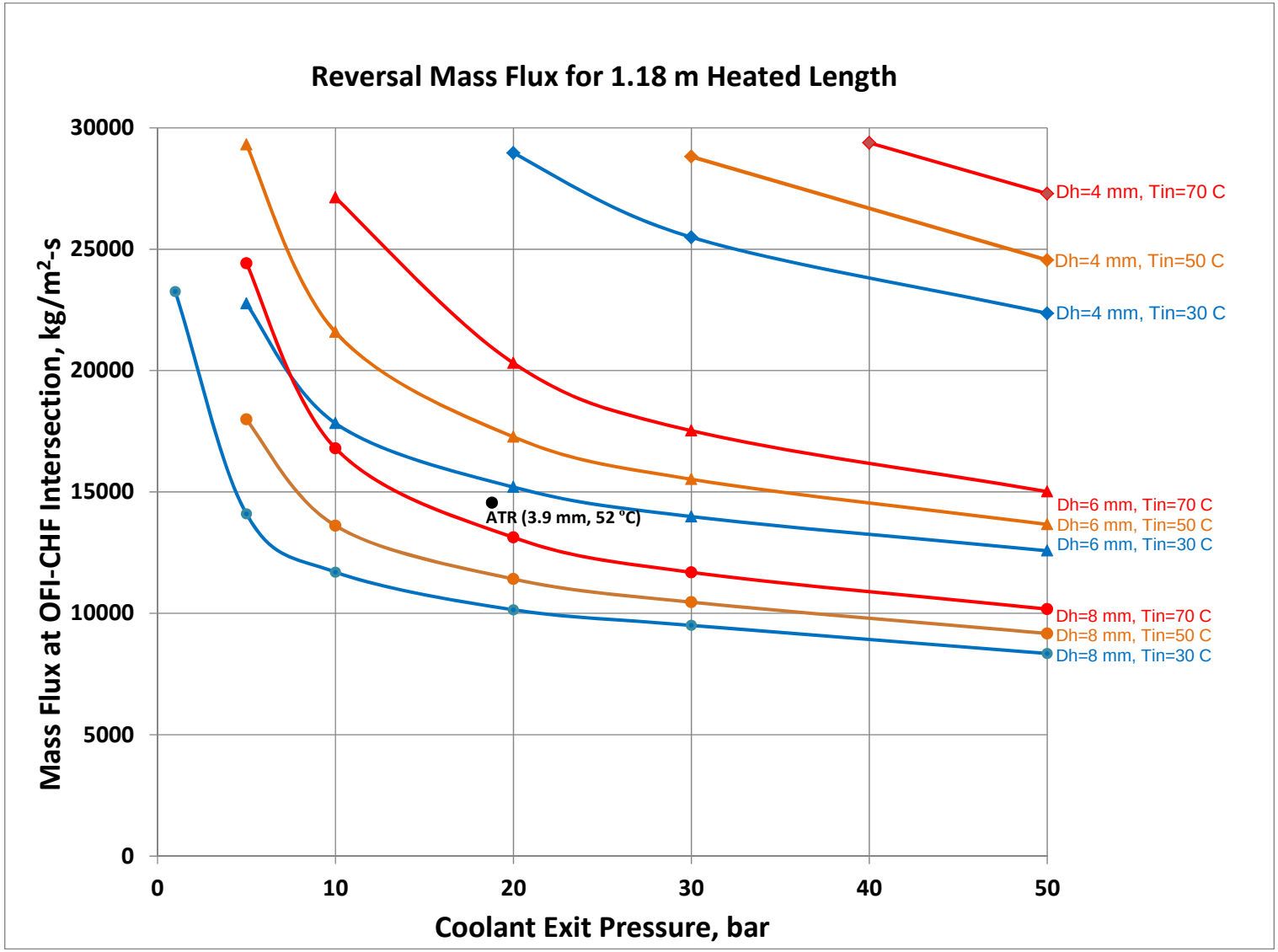

Fig. 6. Continued (Part 5 of 6): Mass Flux at OFI-CHF Intersection (OFI-CHF Reversal Diagram)

The heated diameter and inlet temperature of each reactor, that determine the reversal line applicable to the reactor, are shown in parentheses. If the point representing a reactor lies below the applicable reversal line, the reactor is OFI-limited. It lies above, the reactor is CHF-limited.

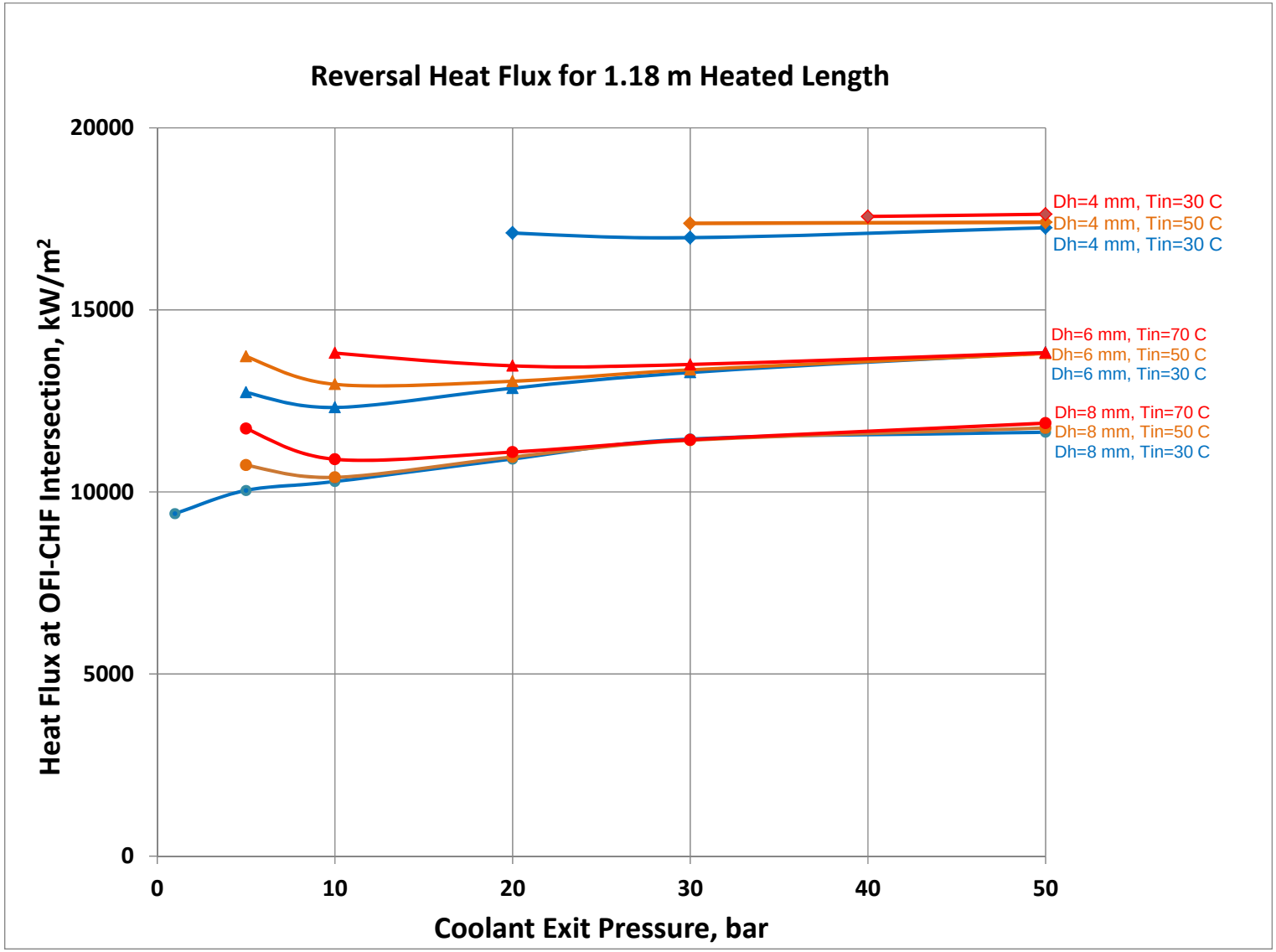

Fig. 6. Continued (Part 6 of 6): Heat Flux at OFI-CHF Intersection (OFI-CHF Reversal Diagram)

Table 1. CHF Mechanisms from Highly Subcooled to High Quality Conditions

Subcooling and Flow Pattern	CHF Model	Speed of Photography	CHF Mechanism
(1) High subcooling; Single-phase liquid flowing in the mainstream of coolant channel	Surface overheating due to poor heat transfer capability of the subcooled liquid core. Bankoff (1961)[14], Tong (1975)[15], Tong and Tang [Section 5.3.1.3 of Ref. 9]	20000 frames/s; ΔT_{sub}=33 to 111ºC; P = 1 to 11 bar; T_c = 4 to 88 ºC; V=0.76 to12.2 m/s; Heat flux = 2.45 to 10.63 MW/m^2; Rectangular duct 6.35×4.76 mm (1/4 × 3/16 inch)**.** CHF =1.7 to 35.6 MW/m^2. Gunther[11,12]	The CHF mechanism in *highly* subcooled nucleate boiling is the first of 5 CHF mechanisms described by Tong and Tang [Fig. 5.12 of Ref. 9]. It is based on Gunther's cinematographic study[11,12] of the mechanism of subcooled nucleate boiling of water and approach to CHF. Gunther conducted tests on subcooled flow boiling of water in two transparent channels (with axially uniform heat flux), and made high-speed (20000 frames/s), high resolution movie of bubbles, roughly hemispherical in shape, growing and collapsing while remaining attached to the heated surface. The cinematographic results showed that the coolant velocity did not detach the bubbles from the heated surface. The attached bubbles slid downstream during growth and collapse, producing turbulence in the *two-phase wall layer* (on-the-wall coolant layer of thickness equal to the maximum bubble radius) by their translational motion in addition to the turbulence caused by their growing and collapsing action. The sliding velocity was approximately 0.8 of the coolant velocity, increasing slightly with bubble size. The effect of an increase in coolant velocity or subcooling was to reduce bubble size and lifetime. An increase of heat flux caused bubble population to increase up to a point when bubbles coalesced to form vapor clumps. Gunther photographed the bubble coalescence to vapor clumps in a test at ΔT_{sub} = 105.6 ºC and V = 7.6 m/s when the heat flux was increased to 21.3 MW/m^2, i.e., within 10 % of CHF. This photograph indicates that bubble coalescence signifies *incipient* film boiling that results in CHF.
		50 frames/s; P = 5 to 30 bar; V = 3 to 7.5 m/s; T_i = 20 ºC; $\Delta T_{sub,in}$ = 132 to 214 ºC; Square duct 7.2×7.2 mm; Heater rod of diameter 2 mm. Celata et al.[13]	A recent, more detailed, photographic study (as the heat flux is increased in small steps) of the phenomena in *highly subcooled* flow boiling from ONB to CHF and from CHF to heater melting is provided by Celata et al.[13]. The inlet subcooling in these experiments was 132 to 214 ºC (T_i = 20 ºC, P = 5 to 30 bar, V = 3 to 7.5 m/s). He also observed that CHF occurred before bubble detachment in highly subcooled flow boiling.
			Bankoff[14] formulated a refined mechanistic method of calculating subcooled nucleate boiling heat transfer, analyzed Gunther's experiments[11], and found that the CHF occurs due to a relative inability of the turbulent core liquid to remove heat as fast as it is transmitted through the *two-phase wall layer*. Tong (1975)[15] has also done a CHF analysis in which the subcooled liquid core is the limiting cause.
			This mechanism leads to CHF before bubble detachment from the heated surface, i.e., before OFI.
(2) Medium or low subcooling; Single-phase liquid flowing in the mainstream of coolant	Formation of a dry patch on the heated wall under a nucleate bubble. (Kirby, et al., 1967)[31]	9000 frames/s; ΔT_{sub} = 5 to 46 ºC; Pressure is 1.7 bar (25 psia); Mass flux from 275 to 2700 kg/m^2-s [31]	The experimental work of earlier researchers has confirmed that under a nucleate bubble there is a very thin evaporating *liquid film* on the heated wall. The CHF in subcooled flow is caused by the formation of a stable dry patch on the heated wall under a nucleate. The high-speed motion pictures by Kirby of the bubble over a CHF site show that the heated wall is insulated (from the mainstream subcooled liquid flow in the channel) by a steam bubble (varying in thickness from 4 to 20 mils). The bubble is flattened in shape and does not resemble a nucleate bubble which is spherical. Kirby

channel			however argues that the dry patch which eventually causes burnout is formed under a nucleate bubble. This argument is based not on direct observation, but on physical reasoning and analysis of heat transfer of the site and the associated bubble. A stable dry patch on the heated wall under the nucleate bubble is formed if the thin liquid film evaporates completely due to the (high) heat flux from the heated wall and the wall temperature exceeds the Leidenfrost temperature in a few milliseconds of time that a rewetting takes. It was found that the flow pattern at the CHF site depended on subcooling; at high subcooling only nucleate bubbles were present, whereas at low subcooling the channel was full of large vapor bubbles. Clear photographs of the flow pattern at the CHF site could be taken only at high subcooling but these pictures did not clarify the early stages in the formation of the flattened bubble attached to the heated wall at the CHF site because an *intermittent* passage of larger bubbles obscured the view. This mechanism will lead to CHF after OSV and OFI because the larger bubbles which obscured the view of the CHF site during Kirby's experiments were obviously detached from the wall.
(3) Low quality; Bubbly flow, slug flow, or froth flow in the mainstream of coolant channel	Dryout under a vapor bubble. (Fiori and Bergles, 1968)[32]	Colored movie at 1200 frames/s; ΔT_{sub} =28 to 61 ºC; P < 6.9 bar; CHF from 3.15 to15.77 kW/m^2 [32]	The high-speed motion pictures by Fiori and Bergles show that the flow pattern at CHF for high heat flux (3.15 to15.77 kW/m^2), subcooling (28 to 61 ºC), at low pressures (less than 6.9 bar) is slug flow or froth flow, depending on the coolant mass velocity. The pin-holes observed in the burned-out test sections suggested that the CHF condition is extremely local. Bubble nucleation was seen to exist in the superheated liquid film on the wall near the CHF condition. As a large vapor bubble passes over the wall, these nucleating bubbles break the film and cause a stable dry spot which results in an increased local wall temperature. After the vapor bubble passes by and the liquid slug arrives at the site, the dry spot is quenched by the liquid slug, and the wall temperature drops. At CHF, the heat flux, the slug arriving frequency, and the void fraction are such that the wall temperature rise due to the passage of vapor bubble over the dry spot is greater than the temperature drop during quenching. This results in an unstable situation. The wall temperature at the dry spot continues to rise and reaches the Leidenfrost temperature, at which point quenching is prevented and destruction is inevitable.
	Crowding of bubbles near the wall reduces the ingress of the mainstream cold liquid into the near-wall bubbly boundary layer. (Weisman and Pei, 1983)[33]	Visual observations and measurements in various basic tests recorded by Tong and Tang [see Section 5.2.1 in Ref. 9]	Tong et al. (1966)[9] originated the idea that, in subcooled and low quality flow boiling, a *near-wall bubbly boundary layer* (2 to 4 bubble diameters thick) forms on the heated wall. Building on the presence of the near-wall bubbly boundary layer, Weisman and Pei (1983)[33] later postulated (in accord with the understanding of several other investigators) that the turbulent mass exchange (i.e., radially outward flow of vapor and inward flow of liquid) between the bubbly boundary layer and the mainstream of liquid in the channel is *the limiting mechanism* leading to CHF. As the heat flux increases to CHF, the bubbly layer thickness increases to a maximum; bubble crowding in the bubbly layer increases; and the volume fraction of vapor in the bubbly layer increases to a maximum critical void fraction. This critical void fraction (0.82) was obtained when the bubbly layer becomes crowded and packed with oblong bubbles (ratio of long-to-short axes = 3:1) touching each other. The bubbly layer void fraction was calculated based on the above-mentioned *limiting mechanism*, i.e., by a balance between the radially outward flow of vapor and inward flow of liquid at the bubbly layer-mainstream liquid interface. When the calculated void fraction in the bubbly layer just exceeds 0.82,

			effectively preventing the mainstream liquid from reaching the wall, the CHF occurs by vapor blanketing and forming a dry patch on the heated wall. Weisman predicted more than 1500 CHF data points (subcooled or at low quality at CHF location, void fraction ≤ 0.6, pressure 20 to 205 bar) within ± 20%. Weisman and others[34] have made further improvements to this model. In the low quality and bubbly flow regime, the sublayer dryout under a vapor blanket model developed by Lee and Mudawar (1988) and Celata (1994) is receiving significant attention. As one increases the heat flux and approaches CHF, the heated wall surface temperature exceeds the coolant saturation temperature; the liquid adjacent to the wall gets heated to above-saturation temperatures and a superheated liquid layer is formed on the heated wall, while the mainstream liquid (bulk liquid core) remains subcooled. A flattened vapor bubble elongated (and moving) in the flow direction forms in the superheated liquid layer due to the coalescence of smaller bubbles, with a very thin liquid sublayer in-between the flattened bubble and the wall surface. The CHF occurs when the thermal-hydraulic condition are such that the liquid sublayer evaporates during the passage time of the flattened bubble, thus insulating the heating surface from the bulk liquid core. The CHF is given by $q_c = \delta \rho_L h_{fg} U_B / L_B$ where δ is the initial thickness of liquid sublayer, ρ_L is the liquid sublayer density, h_{fg} is latent heat of vaporization, and U_B and L_B are the flattened bubble's velocity and length in the flow direction, respectively. Celata et al.[36] improved the model by removing most of the empirical constants in it. Celata et al. predicted 1888 subcooled CHF data ($25 \le \Delta T_{sub,in} \le 255$ ºC, pressure 1 to 84 bar, mass flux 1 to 90000 kg/m^2-s) with an RMS error of 17.2%, and 91% of CHF data predicted within ±30%. These mechanisms will lead to CHF obviously after OSV and OFI.
	Liquid sublayer dryout under a vapor blanket. (Lee and Mudawar, 1988)[35], (Celata et al., 1994)[36]	2000 frames/s; FC-72 coolant; ΔT_{sub} =10 to 40 ºC; $1.38 \le P \le 1.52$ bar; $0.5 \le V \le 1.2$ m/s; 5.0 × 2.5 mm rectangular channel by Zhang et al.[37]	
(4) Medium to High quality; Annular flow in channel	Liquid film dryout. Hewitt and Hall Taylor (1970)[38] , (Whalley et al., 1976)[39]	Measurements of liquid film flow rate by Hewitt (1970)[40]	In the annular flow regime, the CHF condition is reached as a result of drying out of the *liquid film* usually flowing on the heated channel wall (with vapor flowing in the center). The film dries out due to evaporation and entrainment of droplets from the film surface, despite the counteracting effect of the re-deposition of droplets on the film. Extensive experimental studies relating to this mechanism are given by Hewitt and Hall Taylor[38], and Whalley et al.[39]. Hewitt[43] conducted experiments in a vertical heated tube in which the liquid film flow rate was measured at the top of the heated length. This measurement was made by sucking the film off through a porous section of the tube wall. The liquid film flow rate decreased as the power to the heated length was increased. The CHF, identified by a dramatic drop in the heat transfer coefficient, occurred at the power which gave zero film flow rate at the tube outlet. This mechanism will lead to CHF obviously after OSV and OFI.

Table 2. Gunther's Data[11] for Approach to CHF in Highly Subcooled Nucleate Flow Boiling
(Pressure = 1.7 bar, T_{sat} = 115 ºC, Subcooling = 86.1 ºC, Velocity = 3.05 m/s)

Heat Flux	Maximum Bubble Radius	Bubble Formation Rate	Fraction of Wall Surface Covered by Bubbles	Bubble Lifetime	Wall Temp.	Temp. at Edge of Two-phase Wall Layer	Mean Bulk Temp.
MW/m^2	micron	Million bubbles/cm^2-s		micro-s	ºC	ºC	ºC
2.453	292.1		0.010	250	139.4	55.8	28.9
4.088	279.4	0.0620	0.020	250	141.1	65.3	28.9
5.723	266.7	0.1256	0.030	245	142.8	73.1	28.9
7.358	241.3	0.2170	0.045	220	144.2	81.4	28.9
8.993	203.2	0.5735	0.080	185	145.0	90.8	28.9
10.628	165.1	2.4878	0.160	150	146.1	101.9	28.9
12.263	127.0	8.4010	0.350	115	146.7	114.4	28.9

Table 3. Gunther's 35 CHF Test Data[12] for Subcooled Nucleate Flow Boiling

Test No.	Velocity	Outlet	T_{sat}	Outlet	ΔT_{sub}	Measured CHF	
	ft/s	psia	ºF	ºF	ºF	Btu/sq. in-s	kW/m^2
1	5.0	14.1	209.8	172	38	1.45	1880
4	12.3	15.6	215.1	162	53	2.55	5477
5	12.3	14.4	210.9	140	71	3.85	5575
6	12.3	14.6	211.6	140	72	3.55	7178
7	12.3	14.7	212.0	119	93	5.05	7178
8	12.3	14.6	211.6	101	111	5.50	8551
9	12.3	14.6	211.6	77	135	7.35	10415
10	12.3	29.4	249.1	80	170	9.30	13162
11	12.3	60.0	292.6	82	210	10.70	16187
12	12.3	60.0	292.6	83	210	10.70	16187
13	12.3	114.0	337.4	84	254	12.00	19620
14	12.3	113.0	336.7	86	251	12.00	19457
15	40.0	114.0	337.4	82	255	20.00	35480
16	40.0	30.9	252.0	187	65	5.30	9058
17	40.0	28.6	247.6	162	86	6.70	11903
18	40.0	28.1	246.6	135	112	9.50	15696
19	40.0	28.2	246.7	111	136	11.70	18966
20	40.0	28.4	247.2	96	152	13.70	21092
21	40.0	39.0	265.7	79	187	17.80	25997
22	40.0	81.0	312.9	81	232	20.40	32373
23	40.0	114.0	337.4	81	256	22.00	35643
24	12.3	114.0	337.4	86	251	11.20	19293
25	12.3	114.0	337.4	87	250	10.40	19457
26	12.3	113.0	336.7	94	242	11.20	18639
27	12.3	114.0	337.4	92	245	10.10	18966
28	12.3	29.0	248.4	85	164	8.90	12639
29	5.0	14.6	211.6	89	122	4.87	5902
30	5.0	114.0	337.4	99	238	7.10	12001
31	5.0	56.0	288.2	92	197	5.95	9532
32	4.8	28.2	246.7	92	155	5.60	7488
33	5.0	15.1	213.4	115	98	3.85	4742
34	5.0	14.5	211.3	138	73	2.60	3532
36	12.3	14.5	211.3	190	22	0.81	1700
37	12.3	14.6	211.6	173	39	2.00	3025
38	12.3	164.0	365.5	84	282	11.10	21746

Table 4. Mass Flux and Heat Flux at the Intersection of OFI and CHF for L_h = 0.28, 0.61, and 1.18 m

Case	Exit Pres.	Heated Dia.	Inlet Temp.	L_h = 0.28 m		L_h = 0.61 m		L_h = 1.18 m	
				Reversal Mass Flux	Reversal Heat Flux	Reversal Mass Flux	Reversal Heat Flux	Reversal Mass Flux	Reversal Heat Flux
	bar	mm	°C	kg/m^2-s	kW/m^2	kg/m^2-s	kW/m^2	kg/m^2-s	kW/m^2
1	1	3	30	23569	13630				
2	5	3	30	15490	15766				
3	10	3	30	13485	16931	26250	17610		
4	20	3	30	11759	18029	22222	18246		
5	30	3	30	10917	18758	20391	18817		
6	50	3	30	9496	18818	18313	19567		
7	1	4	30	15719	11169				
8	5	4	30	11118	13883	20712	14349		
9	10	4	30	9760	15026	17045	14580		
10	20	4	30	8579	16118	14770	15446	28961	17110
11	30	4	30	7968	16767	13818	16207	25493	16982
12	50	4	30	6846	16585	12177	16536	22357	17255
13	1	6	30	9643	8870	18090	9821		
14	5	6	30	7079	11431	11645	11121	22760	12731
15	10	6	30	5882	11704	10114	11915	17828	12320
16	20	6	30	4982	12087	8795	12655	15199	12848
17	30	6	30	4712	12796	8192	13212	13984	13282
18	50	6	30	4471	13958	7046	13116	12577	13828
19	1	8	30	7484	8071	11961	8014	23260	9406
20	5	8	30	5110	9668	8275	9743	14096	10042
21	10	8	30	4227	9850	6778	9841	11697	10286
22	20	8	30	3944	11201	5829	10329	10146	10906
23	30	8	30	3981	12649	5225	10371	9506	11456
24	50	8	30	3680	13435	4580	10458	8344	11641
25	1	3	50						
26	5	3	50	18438	15726				
27	10	3	50	15362	16764	29582[a]	18336[a]		
28	20	3	50	13002	17811	25284	18540		
29	30	3	50	11992	18655	22675	18951		
30	50	3	50	10266	18704	19913	19550		
31	1	4	50	24232	12287				
32	5	4	50	13048	13657	26473	15359		
33	10	4	50	11017	14744	19851	14755		
34	20	4	50	9396	15772	16641	15547		
35	30	4	50	8578	16344	15215	16169	28815	17376
36	50	4	50	7363	16373	13381	16699	24552	17408
37	1	6	50	14142	9293	28523	11041		
38	5	6	50	8445	11431	13943	11160	29303	13720
39	10	6	50	6700	11590	11552	11829	21578	12954

Case	Exit Pres.	Heated Dia.	Inlet Temp.	L_h = 0.28 m		L_h = 0.61 m		L_h = 1.18 m	
				Reversal Mass Flux	Reversal Heat Flux	Reversal Mass Flux	Reversal Heat Flux	Reversal Mass Flux	Reversal Heat Flux
	bar	mm	°C	kg/m^2-s	kW/m^2	kg/m^2-s	kW/m^2	kg/m^2-s	kW/m^2
40	20	6	50	5659	12268	9763	12551	17269	13040
41	30	6	50	5021	12342	9026	13180	15522	13353
42	50	6	50	4630	13276	7659	13106	13662	13803
43	1	8	50	10054	7748	18508	8854		
44	5	8	50	6066	9622	9753	9625	17988	10737
45	10	8	50	4918	9965	8203	10351	13609	10400
46	20	8	50	4191	10634	6496	10284	11414	10960
47	30	8	50	3993	11486	5881	10568	10458	11419
48	50	8	50	3803	12750	4890	10270	9170	11758
49	1	3	70						
50	5	3	70	24162	16604				
51	10	3	70	18066	16735				
52	20	3	70	14690	17714	29816	19189		
53	30	3	70	13426	18667	25634	19182		
54	50	3	70	11246	18684	21892	19588		
55	1	4	70						
56	5	4	70	16125	13605				
57	10	4	70	12776	14517	24692	15572		
58	20	4	70	10477	15483	19158	15753		
59	30	4	70	9476	16161	17026	16208	29385[b]	17564[b]
60	50	4	70	8022	16275	14834	16875	27286	17628
61	1	6	70	27961	10977				
62	5	6	70	10219	11154	18636	12020		
63	10	6	70	8269	12146	13636	11853	27124	13812
64	20	6	70	6376	12168	11078	12537	20309	13462
65	30	6	70	5733	12616	10137	13229	17524	13501
66	50	6	70	4843	12649	8491	13250	15013	13825
67	1	8	70	19435	8962				
68	5	8	70	7645	9779	12157	9672	24420	11740
69	10	8	70	5806	9990	9551	10233	16799	10896
70	20	8	70	4677	10448	7669	10689	13127	11096
71	30	8	70	4111	10584	6607	10628	11688	11433
72	50	8	70	3948	12056	5485	10507	10171	11889

a. This value (for Case 27 of heated length 0.61 m) corresponds to an exit pressure of 12 bar.
b. This value (for Case 59 of heated length 1.18 m) corresponds to an exit pressure of 40 bar.

Table 5. Error in ONB, OFI, and CHF due to Ignoring Frictional Pressure Drop (Using the Calculated Inlet Pressure vs. Assuming it Equal to the Exit Pressure)

B-R = Bergles and Rohsenow, W-F = Whittle-Forgan
S-Z = Saha-Zuber, Gro = Extended Groeneveld 2006 Table
H-M = Hall-Mudawar Inlet Conditions Correlation

	% Error				
	B-R ONB	W-F OFI	S-Z OFI	Gro CHF	H-M CHF
	For 0.28 m Heated Length				
Number of Data Points	2160	2160	2160	2160	1881
Mean Error %	0.02	0.05	0.03	0.02	0.03
Max. Absolute Error %	1.43 [b]	0.59	0.42	0.11	0.29
Case / Mass Flux [a]	53/7000	49/30000	49/30000	25/30000	55/30000
RMS Error %	0.23	0.08	0.05	0.03	0.04
	For 0.61 m Heated Length				
Number of Data Points	2160	2160	2160	2160	1448
Mean Error %	0.05	0.08	0.06	0.03	0.05
Max. Absolute Error %	0.86	1.11	0.95	0.16	0.33
Case / Mass Flux [a]	22/8000	49/30000	49/30000	7 /30000	7 /30000
RMS Error %	0.11	0.14	0.11	0.04	0.07
	For 1.18 m Heated Length				
Number of Data Points	2160	2160	2160	2160	845
Mean Error %	0.11	0.14	0.12	0.05	0.08
Max. Absolute Error %	1.33	2.02	1.91	0.26	0.39
Case / Mass Flux [a]	49/30000	49/30000	49/30000	1/30000	13/30000
RMS Error %	0.18	0.24	0.22	0.07	0.10

a. Case number (given in Table 4) and mass flux of the data point having the Maximum Absolute Error (MAE)
b. The MAE of 1.43 % was actually calculated for a heated length of 0.285 m (not for 0.28 m). This replacement was done to the following reason. The MAE was calculated for several heated lengths close to 0.28 m, which are tabulated below. The table below shows that the MAE has a discontinuous behavior near the heated length of 0.28 m. The discontinuity might be caused by a discontinuity in one of the coolant property subroutines, and it needs to be investigated further. However, the high value of MAE (8.13 %) for the 0.28 m heated length is not due to the reduced heated length. Otherwise the MAE for the heated length of 0.27 m would not be 1.23 %. An look at the variation of MAE for heated lengths from 0.27 to 1.18 m indicates that the actual MAE should be nearly 1% (not 8%).

L_h m	Mean Error %	Max Abs Error %	Case / Mass Flux	RMS Error %
0.27	0.024	1.23	48/27000	0.123
0.275	0.018	4.25	48/16000	0.156
0.28	0.018	8.13	53/17000	0.233
0.285	0.021	1.43	72/16000	0.14
0.29	0.018	10.0	60/4000	0.249
0.295	0.021	1.53	72/17000	0.136

Table 6. Difference between CHFs Calculated by the Extended Groeneveld Table and the Hall_Mudawar ICC, and Difference between OFIs Calculated by the Whittle-Forgan and the Saha-Zuber Correlations

Gro = Extended Groeneveld 2006 Table, H-M = Hall-Mudawar Inlet Conditions Correlation
W-F = Whittle-Forgan, S-Z = Saha-Zuber

	% Difference	
	Gro CHF vs. H-M CHF	W-F OFI vs. S-Z OFI [a]
	For 0.28 m Heated Length	
Number of Data Points	1881	2088
Mean Difference %	-2.84	-4.67
Max Absolute Diff. %	40.6	11.1
Case / Mass Flux [b]	67/6000	2/2000
RMS Difference %	8.50	5.19
	For 0.61 m Heated Length	
Number of Data Points	1448	2088
Mean Difference %	-5.75	-2.68
Max Absolute Diff. %	38.7	5.66
Case / Mass Flux [a]	67/18000	2/2000
RMS Difference %	8.56	3.03
	For 1.18 m Heated Length	
Number of Data Points	845	2088
Mean Difference %	-7.40	-1.54
Max Absolute Diff. %	28.0	3.16
Case / Mass Flux [a]	43/23000	67/5000
RMS Difference %	8.81	1.77

a. For G > 1000 kg/m^2-s
b. Case number (see Table 4) and mass flux of the data point that has the maximum absolute difference

Table 7. Heat Fluxes at ONB, OFI, and CHF for Coolant Channels of D_h = 8 mm, L_h = 0.28 m, and T_{in} = 30 °C

	Channel Exit Pressure																	
	1 bar						5 bar						10 bar					
Mass Flux	**ONB**	**OFI-WF**	**OFI-SZ**	**CHF-Gr**	**Quality Gr**	**CHF-HM**	**ONB**	**OFI-WF**	**OFI-SZ**	**CHF-Gr**	**Quality Gr**	**CHF-HM**	**ONB**	**OFI-WF**	**OFI-SZ**	**CHF-Gr**	**Quality Gr**	**CHF-HM**
kg/m^2-s	kW/m^2	kW/m^2	kW/m^2	kW/m^2		kW/m^2	kW/m^2	kW/m^2	kW/m^2	kW/m^2		kW/m^2	kW/m^2	kW/m^2	kW/m^2	kW/m^2		kW/m^2
1000	462	1079	1176	2727	0.0397		819	1892	2067	3832	0.0102		1030	2331	2525	4709	0.0114	
2000	873	2157	1989	3893	-0.0087	3017	1490	3784	3505	5768	-0.0528	5102	1868	4661	4333	7163	-0.0683	6169
3000	1278	3236	2983	4620	-0.034	4160	2128	5676	5257	7357	-0.0816	6953	2643	6992	6500	8901	-0.1118	8352
4000	1676	4314	3978	5486	-0.0445	5179	2746	7568	7010	8356	-0.1058	8580	3402	9322	8666	9524	-0.1533	10257
5000	2074	5393	4972	6652	-0.0471	6105	3355	9460	8762	9569	-0.1174	10045	4140	11653	10832	10965	-0.1665	11962
6000	2477	6471	5966	7179	-0.0554	6959	3956	11352	10514	10467	-0.1287	11385	4862	13983	12999	12666	-0.1723	13516
7000	2884	7549	6961	7792	-0.0605	7754	4544	13244	12267	11591	-0.1346	12625	5571	16313	15165	14060	-0.1796	14948
8000	3286	8627	7955	8369	-0.0647	8500	5127	15136	14019	12733	-0.1389	13781	6276	18644	17332	15831	-0.1817	16280
9000	3696	9705	8949	8975	-0.0677	9203	5704	17028	15771	13558	-0.1445	14868	6977	20974	19498	17018	-0.1879	17530
10000	4110	10784	9943	9545	-0.0704	9871	6284	18919	17523	14329	-0.1494	15895	7658	23304	21665	18136	-0.1934	18707
11000	4523	11861	10938	10083	-0.0728	10507	6853	20810	19275	15148	-0.1531	16869	8339	25634	23831	19195	-0.1982	19824
12000	4943	12939	11932	10594	-0.0749	11114	7426	22702	21027	15940	-0.1564	17798	9024	27964	25997	20213	-0.2025	20886
13000	5362	14017	12926	11081	-0.0767	11697	7990	24593	22780	16695	-0.1593	18686	9735	30294	28163	21192	-0.2063	21900
14000	5786	15094	13920	11546	-0.0785	12256	8562	26485	24531	17418	-0.162	19537	10356	32623	30329	22130	-0.2098	22871
15000	6208	16172	14914	11992	-0.08	12796	9135	28376	26283	18112	-0.1644	20356	11039	34953	32495	23030	-0.213	23804
16000	6638	17249	15907	12420	-0.0815	13316	9691	30266	28035	18779	-0.1666	21144	11702	37283	34661	23897	-0.216	24702
17000	7072	18327	16902	12833	-0.0828	13820	10257	32157	29787	19422	-0.1687	21906	12365	39611	36827	24733	-0.2187	25569
18000	7522	19403	17895	13231	-0.084	14307	10814	34048	31538	20043	-0.1706	22642	13015	41941	38993	25541	-0.2213	26406
19000	7944	20480	18888	13616	-0.0852	14780	11391	35939	33291	20644	-0.1724	23355	13681	44270	41158	26323	-0.2236	27216
20000	8389	21557	19882	13989	-0.0862	15240	11950	37828	35042	21226	-0.1741	24047	14326	46599	43325	27081	-0.2258	28001
21000	8833	22634	20876	14350	-0.0872	15686	12511	39718	36793	21791	-0.1757	24719	14982	48928	45490	27817	-0.2279	28764
22000	9284	23710	21869	14702	-0.0882	16121	13068	41609	38545	22340	-0.1772	25373	15629	51255	47655	28533	-0.2299	29506
23000	9727	24786	22863	15043	-0.089	16545	13630	43498	40296	22874	-0.1785	26009	16281	53584	49821	29229	-0.2317	30227
24000	10181	25862	23856	15376	-0.0899	16959	14182	45388	42047	23394	-0.1798	26629	16935	55913	51986	29908	-0.2335	30930
25000	10643	26938	24849	15700	-0.0906	17363	14742	47278	43799	23902	-0.1811	27235	17579	58240	54151	30569	-0.2351	31616
26000	11101	28014	25841	16016	-0.0914	17758	15302	49166	45550	24396	-0.1823	27826	18235	60568	56317	31215	-0.2367	32285
27000	11568	29089	26835	16324	-0.0921	18143	15859	51054	47300	24880	-0.1834	28403	18878	62896	58482	31846	-0.2382	32939
28000	12031	30163	27828	16626	-0.0928	18521	16413	52944	49051	25352	-0.1844	28968	19515	65223	60647	32462	-0.2396	33578
29000	12504	31238	28820	16921	-0.0934	18891	16973	54832	50801	25814	-0.1855	29521	20162	67549	62811	33066	-0.2409	34204
30000	12963	32314	29813	17209	-0.094	19254	17541	56721	52552	26266	-0.1864	30062	20934	69876	64976	33656	-0.2422	34816

Table 7. Continued

	Channel Exit Pressure																	
	20 bar						30 bar						50 bar					
Mass Flux	**ONB**	**OFI-WF**	**OFI-SZ**	**CHF-Gr**	**Quality Gr**	**CHF-HM**	**ONB**	**OFI-WF**	**OFI-SZ**	**CHF-Gr**	**Quality Gr**	**CHF-HM**	**ONB**	**OFI-WF**	**OFI-SZ**	**CHF-Gr**	**Quality Gr**	**CHF-HM**
kg/m^2-s	kW/m^2	kW/m^2	kW/m^2	kW/m^2		kW/m^2	kW/m^2	kW/m^2	kW/m^2	kW/m^2		kW/m^2	kW/m^2	kW/m^2	kW/m^2	kW/m^2		kW/m^2
1000	1288	2840	2993	5960	0.0278		1463	3178	3302	6649	0.0278		1719	3651	3621	6799	-0.0434	5378
2000	2317	5680	5324	8817	-0.0878	7362	2636	6355	5996	9106	-0.1356	8097	3106	7302	6968	9134	-0.2323	9002
3000	3288	8520	7986	10627	-0.1524	9888	3736	9533	8995	11198	-0.1996	10813	4380	10953	10452	11766	-0.2868	11911
4000	4214	11361	10648	11235	-0.2071	12074	4780	12710	11993	12677	-0.2435	13149	5599	14604	13936	14221	-0.3179	14389
5000	5127	14200	13309	13129	-0.2207	14019	5784	15888	14991	14606	-0.2628	15218	6787	18254	17420	16325	-0.3424	16571
6000	5995	17040	15971	15282	-0.2266	15782	6793	19065	17989	16734	-0.2731	17088	7934	21905	20903	18408	-0.3591	18533
7000	6855	19880	18633	17048	-0.2349	17402	7751	22243	20987	18608	-0.2833	18801	9061	25556	24387	20193	-0.3746	20324
8000	7756	22720	21295	18924	-0.2401	18905	8726	25420	23985	20312	-0.2926	20388	10178	29207	27871	21857	-0.3875	21977
9000	8559	25560	23956	20307	-0.2483	20310	9667	28597	26983	21772	-0.302	21869	11270	32857	31355	23386	-0.3988	23517
10000	9380	28400	26618	21607	-0.2554	21632	10565	31774	29981	23182	-0.3098	23261	12340	36508	34839	24838	-0.4085	24962
11000	10201	31239	29280	22836	-0.2617	22883	11491	34951	32979	24514	-0.3168	24576	13419	40158	38322	26209	-0.4171	26324
12000	11066	34079	31941	24002	-0.2674	24071	12423	38129	35977	25780	-0.3231	25824	14444	43808	41806	27509	-0.4247	27615
13000	11834	36918	34603	25114	-0.2724	25204	13304	41306	38974	26987	-0.3287	27013	15500	47459	45290	28747	-0.4315	28843
14000	12672	39757	37264	26176	-0.2771	26288	14194	44482	41972	28141	-0.3338	28150	16512	51109	48773	29930	-0.4378	30016
15000	13425	42597	39926	27195	-0.2813	27328	15109	47659	44970	29248	-0.3385	29239	17569	54759	52257	31063	-0.4434	31140
16000	14209	45436	42587	28175	-0.2852	28328	15993	50835	47968	30313	-0.3428	30287	18576	58409	55740	32151	-0.4486	32219
17000	15018	48275	45249	29119	-0.2888	29292	16849	54012	50966	31338	-0.3468	31295	19604	62058	59224	33198	-0.4534	33258
18000	15801	51113	47910	30029	-0.2921	30223	17743	57188	53963	32329	-0.3505	32269	20591	65708	62706	34209	-0.4578	34259
19000	16579	53952	50570	30910	-0.2952	31123	18600	60364	56961	33287	-0.3539	33211	21608	69358	66190	35186	-0.4619	35228
20000	17503	56790	53232	31764	-0.298	31996	19478	63540	59958	34215	-0.3571	34123	22632	73007	69673	36132	-0.4658	36165
21000	18117	59628	55893	32597	-0.3007	32842	20338	66715	62955	35116	-0.3601	35007	23568	76656	73157	37049	-0.4693	37073
22000	18911	62466	58554	33423	-0.3032	33665	21205	69891	65953	35990	-0.363	35866	24573	80304	76639	37940	-0.4727	37955
23000	19661	65304	61215	34227	-0.3055	34465	22060	73066	68949	36841	-0.3656	36702	25542	83953	80122	38805	-0.4758	38813
24000	20442	68142	63875	35010	-0.3077	35244	22915	76241	71946	37670	-0.3681	37515	26576	87602	83605	39648	-0.4788	39647
25000	21195	70980	66537	35773	-0.3097	36003	23729	79416	74944	38478	-0.3705	38308	27499	91250	87087	40469	-0.4816	40460
26000	21955	73816	69197	36518	-0.3117	36744	24597	82592	77940	39266	-0.3727	39081	28467	94899	90570	41270	-0.4843	41253
27000	22715	76654	71857	37245	-0.3136	37468	25430	85766	80937	40035	-0.3749	39836	29474	98546	94052	42052	-0.4868	42027
28000	23489	79490	74517	37956	-0.3153	38176	26290	88941	83933	40787	-0.3769	40574	30410	102194	97535	42815	-0.4892	42783
29000	24233	82328	77178	38652	-0.317	38867	27123	92114	86930	41523	-0.3788	41296	31346	105841	101017	43563	-0.4915	43523
30000	25001	85164	79838	39333	-0.3186	39545	27925	95289	89926	42243	-0.3807	42002	32308	109490	104500	44293	-0.4936	44246

Table 8. Heat Fluxes at ONB, OFI, and CHF for Coolant Channels of D_h = 4 mm, L_h = 0.28 m, and T_{in} = 30 °C

	Channel Exit Pressure																	
	1 bar						5 bar						10 bar					
Mass Flux	**ONB**	**OFI-WF**	**OFI-SZ**	**CHF-Gr**	**Quality Gr**	**CHF-HM**	**ONB**	**OFI-WF**	**OFI-SZ**	**CHF-Gr**	**Quality Gr**	**CHF-HM**	**ONB**	**OFI-WF**	**OFI-SZ**	**CHF-Gr**	**Quality Gr**	**CHF-HM**
kg/m^2-s	kW/m^2	kW/m^2	kW/m^2	kW/m^2		kW/m^2	kW/m^2	kW/m^2	kW/m^2	kW/m^2		kW/m^2	kW/m^2	kW/m^2	kW/m^2	kW/m^2		kW/m^2
1000	437	711	874	2513	0.1827		768	1249	1539	3468	0.2168		965	1540	1894	4661	0.3377	
2000	842	1422	1505	4083	0.1241		1433	2498	2647	4893	0.0809		1781	3080	3247	5910	0.0964	
3000	1238	2133	2021	4711	0.0655		2067	3747	3561	6068	0.0244		2566	4619	4402	7494	0.0317	
4000	1633	2844	2694	5393	0.0379		2686	4996	4747	7312	-0.0015	5881	3309	6159	5870	8610	-0.0172	7192
5000	2032	3555	3367	5983	0.019		3292	6244	5934	8418	-0.0207	7087	4055	7699	7337	9535	-0.0519	8640
6000	2433	4266	4041	6434	0.0036		3890	7493	7121	9120	-0.0425	8229	4778	9238	8804	10542	-0.0731	10007
7000	2836	4977	4714	6939	-0.0065	5480	4481	8742	8308	10110	-0.0525	9318	5490	10778	10271	11728	-0.0846	11304
8000	3237	5687	5388	7398	-0.0148	6115	5063	9990	9495	11037	-0.0611	10360	6192	12317	11738	13084	-0.0903	12542
9000	3646	6398	6061	7973	-0.0196	6727	5651	11239	10681	11997	-0.0673	11361	6885	13856	13206	14215	-0.0982	13728
10000	4064	7108	6734	8516	-0.0238	7319	6230	12487	11868	12910	-0.0729	12324	7577	15396	14673	15282	-0.1054	14867
11000	4477	7819	7407	9031	-0.0276	7893	6800	13736	13054	13784	-0.078	13255	8277	16935	16140	16298	-0.112	15965
12000	4900	8529	8080	9522	-0.0311	8450	7401	14984	14241	14622	-0.0826	14155	8943	18473	17606	17270	-0.118	17024
13000	5316	9239	8753	9990	-0.0342	8992	7951	16232	15427	15427	-0.0868	15027	9634	20013	19074	18205	-0.1235	18050
14000	5740	9949	9426	10439	-0.037	9520	8530	17480	16613	16204	-0.0907	15875	10306	21551	20540	19104	-0.1286	19044
15000	6171	10659	10098	10870	-0.0396	10035	9100	18728	17800	16953	-0.0943	16698	10981	23090	22007	19972	-0.1332	20009
16000	6606	11369	10771	11286	-0.042	10537	9673	19975	18985	17678	-0.0977	17500	11658	24628	23473	20811	-0.1376	20947
17000	7037	12078	11444	11687	-0.0442	11028	10237	21222	20171	18368	-0.1009	18282	12323	26167	24940	21623	-0.1417	21860
18000	7483	12788	12116	12074	-0.0463	11508	10813	22470	21357	19000	-0.1042	19044	12995	27705	26406	22410	-0.1454	22749
19000	7924	13497	12789	12449	-0.0482	11978	11382	23717	22543	19613	-0.1073	19789	13663	29243	27872	23175	-0.149	23617
20000	8370	14205	13461	12813	-0.05	12438	11952	24964	23728	20208	-0.1102	20517	14320	30781	29339	23969	-0.152	24465
21000	8822	14915	14133	13224	-0.0514	12889	12512	26211	24914	20786	-0.1129	21230	14974	32318	30805	24763	-0.1547	25293
22000	9266	15623	14805	13624	-0.0526	13331	13086	27457	26099	21349	-0.1155	21927	15648	33855	32270	25540	-0.1573	26103
23000	9728	16332	15477	14016	-0.0539	13765	13646	28704	27284	21897	-0.1179	22610	16298	35393	33736	26299	-0.1598	26896
24000	10180	17039	16149	14399	-0.055	14191	14215	29950	28470	22431	-0.1202	23280	16960	36930	35202	27042	-0.1621	27673
25000	10651	17747	16819	14773	-0.0561	14610	14778	31196	29655	22952	-0.1224	23937	17616	38467	36668	27771	-0.1644	28434
26000	11116	18455	17491	15140	-0.0572	15021	15347	32441	30840	23462	-0.1245	24582	18265	40003	38132	28485	-0.1665	29181
27000	11581	19163	18162	15499	-0.0582	15426	15918	33687	32025	23960	-0.1265	25215	18920	41539	39597	29184	-0.1686	29914
28000	12053	19869	18834	15851	-0.0592	15824	16483	34932	33208	24447	-0.1284	25838	19571	43076	41063	29871	-0.1706	30633
29000	12530	20576	19504	16197	-0.0601	16216	17053	36177	34393	24924	-0.1302	26449	20225	44611	42528	30545	-0.1725	31340
30000	12998	21283	20175	16536	-0.061	16602	17620	37422	35577	25391	-0.1319	27051	20878	46146	43992	31208	-0.1743	32035

Table 8. Continued

	Channel Exit Pressure																	
	20 bar						30 bar						50 bar					
Mass Flux	**ONB**	**OFI-WF**	**OFI-SZ**	**CHF-Gr**	**Quality Gr**	**CHF-HM**	**ONB**	**OFI-WF**	**OFI-SZ**	**CHF-Gr**	**Quality Gr**	**CHF-HM**	**ONB**	**OFI-WF**	**OFI-SZ**	**CHF-Gr**	**Quality Gr**	**CHF-HM**
kg/m^2-s	kW/m^2	kW/m^2	kW/m^2	kW/m^2		kW/m^2	kW/m^2	kW/m^2	kW/m^2	kW/m^2		kW/m^2	kW/m^2	kW/m^2	kW/m^2	kW/m^2		kW/m^2
1000	1202	1879	2296	5393	0.3876		1366	2104	2565	5619	0.3855		1588	2423	2914	5339	0.2848	
2000	2213	3758	3898	6840	0.0934		2508	4209	4331	7359	0.0831		2929	4845	4844	7403	0.0077	
3000	3161	5637	5409	8557	0.0088		3577	6313	6092	8980	-0.0239	7648	4172	7268	7079	9225	-0.0983	8694
4000	4078	7516	7212	9611	-0.0583	8700	4619	8418	8123	10226	-0.092	9666	5376	9691	9439	10953	-0.1553	10926
5000	4983	9394	9014	10909	-0.0912	10412	5624	10522	10153	11687	-0.1261	11536	6550	12113	11798	12905	-0.1819	12979
6000	5861	11273	10817	12201	-0.1133	12021	6612	12626	12184	13402	-0.1423	13286	7697	14536	14158	15010	-0.1953	14889
7000	6728	13152	12620	13748	-0.1237	13541	7578	14731	14214	15106	-0.1541	14935	8808	16958	16517	16872	-0.2108	16682
8000	7575	15030	14423	15358	-0.1302	14987	8531	16835	16245	16822	-0.1627	16500	9930	19381	18877	18555	-0.2262	18374
9000	8416	16909	16225	16671	-0.1403	16367	9476	18939	18275	18279	-0.1739	17990	11015	21803	21236	20122	-0.2403	19980
10000	9248	18787	18028	17919	-0.1493	17690	10401	21043	20306	19665	-0.1839	19414	12090	24225	23596	21610	-0.253	21510
11000	10077	20666	19830	19184	-0.1564	18960	11331	23147	22336	20991	-0.193	20781	13148	26647	25955	23029	-0.2644	22974
12000	10894	22544	21633	20408	-0.1629	20185	12238	25250	24366	22267	-0.2012	22095	14210	29069	28314	24387	-0.2747	24379
13000	11724	24422	23435	21588	-0.1688	21367	13154	27354	26396	23522	-0.2084	23362	15257	31491	30673	25690	-0.2842	25729
14000	12536	26300	25237	22729	-0.1744	22510	14062	29457	28426	24734	-0.215	24586	16295	33913	33033	26944	-0.2929	27032
15000	13328	28178	27039	23834	-0.1795	23618	14965	31561	30456	25906	-0.2212	25771	17330	36334	35391	28159	-0.3009	28290
16000	14146	30055	28841	24906	-0.1843	24694	15857	33664	32486	27041	-0.227	26919	18347	38756	37750	29369	-0.308	29507
17000	14917	31933	30644	25947	-0.1888	25739	16732	35767	34516	28142	-0.2324	28034	19519	41177	40109	30541	-0.3146	30687
18000	15720	33810	32446	26959	-0.1931	26756	17613	37870	36545	29212	-0.2374	29118	20393	43598	42468	31680	-0.3208	31833
19000	16524	35687	34247	27945	-0.1971	27747	18504	39973	38575	30252	-0.2422	30174	21417	46019	44826	32786	-0.3266	32947
20000	17299	37564	36049	28905	-0.2009	28714	19372	42076	40604	31265	-0.2467	31202	22401	48440	47185	33862	-0.332	34030
21000	18091	39441	37851	29839	-0.2045	29657	20236	44178	42634	32253	-0.251	32204	23396	50860	49543	34911	-0.3372	35086
22000	18872	41318	39652	30752	-0.208	30579	21108	46280	44663	33217	-0.255	33184	24406	53281	51901	35934	-0.3421	36115
23000	19636	43194	41453	31643	-0.2112	31480	22018	48382	46692	34158	-0.2589	34140	25394	55702	54259	36932	-0.3468	37120
24000	20424	45071	43255	32515	-0.2143	32363	22835	50484	48721	35078	-0.2625	35076	26381	58122	56617	37907	-0.3512	38102
25000	21197	46947	45056	33369	-0.2173	33226	23707	52585	50750	35978	-0.266	35992	27356	60541	58975	38861	-0.3555	39062
26000	21967	48822	46857	34205	-0.2202	34073	24556	54687	52778	36859	-0.2694	36889	28338	62961	61333	39794	-0.3595	40002
27000	22746	50698	48656	35025	-0.2229	34903	25415	56788	54807	37721	-0.2725	37767	29310	65380	63690	40708	-0.3633	40921
28000	23497	52573	50457	35829	-0.2255	35717	26266	58889	56836	38567	-0.2756	38629	30303	67799	66047	41603	-0.367	41823
29000	24274	54448	52258	36617	-0.228	36516	27110	60989	58864	39397	-0.2785	39475	31270	70219	68405	42480	-0.3706	42706
30000	25029	56323	54059	37392	-0.2304	37301	27950	63090	60891	40211	-0.2813	40305	32237	72637	70762	43341	-0.3739	43573

Table 9. Heat Fluxes at ONB, OFI, and CHF for Coolant Channels of D_h = 8 mm, L_h = 0.61 m, and T_{in} = 30 °C

	Channel Exit Pressure																	
	1 bar						5 bar						10 bar					
Mass Flux	ONB	OFI-WF	OFI-SZ	CHF-Gr	Quality Gr	CHF-HM	ONB	OFI-WF	OFI-SZ	CHF-Gr	Quality Gr	CHF-HM	ONB	OFI-WF	OFI-SZ	CHF-Gr	Quality Gr	CHF-HM
kg/m²-s	kW/m²	kW/m²	kW/m²	kW/m²		kW/m²	kW/m²	kW/m²	kW/m²	kW/m²		kW/m²	kW/m²	kW/m²	kW/m²	kW/m²		kW/m²
1000	388	670	707	2069	0.1505		683	1177	1243	2957	0.1839		858	1452	1526	3929	0.2838	
2000	745	1341	1274	3400	0.1005		1277	2355	2244	4157	0.0566		1589	2904	2775	5122	0.073	
3000	1097	2011	1910	3977	0.0498		1842	3532	3367	5131	0.0032		2283	4355	4162	6464	0.0104	
4000	1446	2681	2547	4494	0.0224		2394	4710	4489	6255	-0.0181	5217	2956	5807	5550	7257	-0.0421	6362
5000	1800	3351	3184	5018	0.0062		2933	5887	5611	7111	-0.0386	6264	3619	7259	6937	8207	-0.0687	7613
6000	2156	4021	3821	5460	-0.0065	4270	3470	7064	6733	7793	-0.0565	7250	4265	8711	8324	9071	-0.0887	8788
7000	2511	4691	4457	5899	-0.0156	4842	4000	8242	7855	8700	-0.0646	8187	4899	10162	9712	10060	-0.1002	9900
8000	2873	5361	5094	6287	-0.0233	5391	4523	9419	8977	9522	-0.0722	9080	5539	11614	11099	11273	-0.1045	10956
9000	3233	6031	5730	6761	-0.028	5918	5047	10596	10099	10325	-0.0784	9935	6164	13065	12486	12206	-0.1126	11964
10000	3599	6701	6367	7206	-0.0321	6427	5564	11773	11221	11087	-0.084	10756	6785	14517	13873	13091	-0.1199	12931
11000	3967	7370	7003	7628	-0.0358	6918	6083	12950	12343	11815	-0.089	11547	7403	15968	15260	13935	-0.1264	13859
12000	4336	8040	7640	8030	-0.0391	7395	6599	14127	13465	12511	-0.0936	12310	8017	17419	16647	14740	-0.1323	14753
13000	4709	8710	8276	8412	-0.0421	7857	7112	15303	14586	13178	-0.0978	13048	8628	18870	18034	15513	-0.1377	15617
14000	5089	9379	8913	8778	-0.0448	8307	7629	16480	15708	13801	-0.1018	13763	9236	20321	19421	16255	-0.1427	16452
15000	5468	10048	9549	9130	-0.0473	8744	8138	17656	16830	14375	-0.1058	14457	9840	21772	20808	16970	-0.1473	17261
16000	5856	10717	10184	9468	-0.0495	9170	8655	18833	17951	14927	-0.1095	15132	10478	23223	22194	17684	-0.1513	18047
17000	6235	11386	10820	9836	-0.0513	9586	9164	20009	19073	15461	-0.1129	15788	11054	24673	23581	18416	-0.1547	18810
18000	6623	12055	11457	10203	-0.0529	9991	9674	21185	20194	15976	-0.116	16427	11654	26124	24968	19128	-0.1578	19553
19000	7012	12723	12092	10560	-0.0544	10388	10190	22361	21315	16476	-0.119	17051	12250	27574	26354	19821	-0.1608	20276
20000	7408	13392	12728	10908	-0.0558	10776	10695	23537	22436	16960	-0.1217	17660	12846	29024	27740	20496	-0.1636	20982
21000	7806	14060	13363	11246	-0.0571	11156	11211	24712	23557	17430	-0.1243	18255	13448	30474	29126	21155	-0.1663	21671
22000	8198	14728	13999	11577	-0.0584	11528	11715	25887	24677	17888	-0.1268	18837	14036	31924	30512	21797	-0.1689	22344
23000	8605	15396	14634	11899	-0.0596	11892	12224	27062	25798	18333	-0.1291	19406	14625	33373	31898	22426	-0.1713	23002
24000	9005	16064	15269	12214	-0.0607	12250	12731	28237	26919	18767	-0.1313	19964	15223	34823	33284	23040	-0.1736	23646
25000	9411	16731	15903	12521	-0.0618	12601	13240	29412	28039	19190	-0.1333	20510	15817	36272	34669	23641	-0.1758	24277
26000	9822	17398	16538	12822	-0.0628	12946	13755	30587	29159	19603	-0.1353	21046	16403	37721	36055	24230	-0.1779	24895
27000	10236	18066	17173	13117	-0.0638	13284	14262	31762	30280	20007	-0.1372	21572	16998	39170	37441	24807	-0.1799	25500
28000	10654	18732	17808	13406	-0.0647	13617	14764	32935	31400	20402	-0.139	22088	17582	40619	38826	25372	-0.1818	26095
29000	11070	19399	18442	13689	-0.0656	13944	15276	34110	32520	20788	-0.1407	22595	18173	42067	40211	25927	-0.1837	26678
30000	11490	20065	19077	13967	-0.0665	14266	15786	35283	33640	21167	-0.1423	23093	18751	43515	41597	26472	-0.1855	27251

Table 9. Continued

	Channel Exit Pressure																	
	20 bar						30 bar						50 bar					
Mass Flux	ONB	OFI-WF	OFI-SZ	CHF-Gr	Quality Gr	CHF-HM	ONB	OFI-WF	OFI-SZ	CHF-Gr	Quality Gr	CHF-HM	ONB	OFI-WF	OFI-SZ	CHF-Gr	Quality Gr	CHF-HM
kg/m^2-s	kW/m^2	kW/m^2	kW/m^2	kW/m^2		kW/m^2	kW/m^2	kW/m^2	kW/m^2	kW/m^2		kW/m^2	kW/m^2	kW/m^2	kW/m^2	kW/m^2		kW/m^2
1000	1064	1772	1835	4744	0.354		1205	1985	2040	4806	0.3256		1408	2283	2287	4626	0.2339	
2000	1966	3544	3409	5943	0.0661		2230	3970	3840	6355	0.0491		2597	4567	4462	6475	-0.0219	5518
3000	2822	5316	5114	7299	-0.0214	6076	3191	5955	5760	7718	-0.0537	6757	3716	6850	6693	7921	-0.132	7650
4000	3645	7088	6819	8278	-0.0804	7668	4115	7940	7680	8839	-0.1153	8497	4791	9133	8924	9496	-0.1811	9563
5000	4447	8860	8523	9354	-0.1127	9141	5020	9925	9600	10016	-0.1503	10099	5847	11416	11155	11153	-0.2075	11312
6000	5233	10631	10228	10529	-0.1315	10517	5903	11910	11520	11594	-0.1624	11591	6869	13699	13386	12980	-0.2199	12930
7000	6013	12403	11932	11862	-0.1413	11812	6775	13894	13440	13052	-0.1739	12991	7880	15982	15618	14530	-0.2361	14441
8000	6772	14175	13637	13218	-0.1481	13039	7629	15879	15360	14504	-0.1826	14313	8879	18265	17848	15942	-0.2513	15863
9000	7533	15946	15341	14373	-0.1571	14207	8485	17864	17280	15722	-0.1939	15569	9854	20548	20079	17246	-0.2654	17209
10000	8292	17718	17046	15488	-0.1649	15323	9317	19848	19199	16891	-0.2037	16766	10826	22831	22310	18482	-0.278	18487
11000	9025	19489	18750	16555	-0.172	16392	10154	21833	21119	18026	-0.2122	17911	11788	25114	24541	19658	-0.2892	19707
12000	9771	21261	20454	17580	-0.1785	17419	10978	23817	23038	19113	-0.22	19010	12734	27397	26771	20781	-0.2994	20875
13000	10504	23032	22158	18567	-0.1845	18409	11800	25801	24958	20158	-0.2272	20068	13682	29679	29002	21893	-0.3082	21996
14000	11236	24803	23862	19519	-0.19	19365	12608	27785	26878	21165	-0.2338	21087	14625	31962	31233	22965	-0.3163	23075
15000	11960	26574	25567	20439	-0.1951	20290	13424	29769	28797	22137	-0.2399	22072	15545	34244	33463	23998	-0.3237	24115
16000	12681	28345	27270	21330	-0.1999	21186	14233	31753	30717	23076	-0.2455	23026	16472	36526	35694	24997	-0.3306	25121
17000	13402	30115	28974	22191	-0.2044	22056	15017	33737	32636	23987	-0.2508	23950	17390	38808	37924	25964	-0.3371	26094
18000	14116	31886	30678	23028	-0.2086	22901	15831	35720	34554	24870	-0.2558	24848	18303	41090	40154	26902	-0.3431	27038
19000	14831	33657	32382	23841	-0.2126	23723	16611	37704	36473	25728	-0.2605	25720	19218	43372	42384	27812	-0.3488	27954
20000	15529	35427	34085	24633	-0.2164	24524	17396	39687	38392	26563	-0.2649	26570	20120	45654	44614	28696	-0.3541	28844
21000	16236	37197	35788	25404	-0.2199	25305	18186	41670	40312	27376	-0.269	27397	21025	47935	46844	29557	-0.3591	29711
22000	16948	38967	37492	26157	-0.2233	26067	18975	43653	42230	28168	-0.273	28204	21927	50216	49074	30396	-0.3639	30556
23000	17650	40737	39195	26892	-0.2265	26811	19752	45636	44149	28941	-0.2767	28992	22835	52498	51303	31214	-0.3684	31379
24000	18354	42506	40898	27610	-0.2295	27539	20522	47619	46067	29696	-0.2803	29762	23704	54778	53533	32012	-0.3726	32184
25000	19058	44275	42601	28312	-0.2324	28252	21316	49601	47986	30434	-0.2836	30514	24605	57059	55762	32792	-0.3767	32969
26000	19776	46045	44304	28999	-0.2352	28949	22075	51584	49904	31156	-0.2869	31251	25485	59340	57992	33555	-0.3806	33737
27000	20444	47814	46006	29673	-0.2378	29632	22848	53565	51822	31863	-0.2899	31972	26378	61620	60221	34302	-0.3843	34489
28000	21139	49583	47709	30332	-0.2404	30302	23626	55547	53740	32555	-0.2929	32679	27246	63901	62450	35032	-0.3878	35225
29000	21838	51351	49412	30979	-0.2428	30959	24390	57529	55658	33234	-0.2957	33372	28129	66180	64679	35749	-0.3912	35946
30000	22524	53119	51114	31614	-0.2451	31604	25148	59510	57575	33899	-0.2984	34052	28997	68460	66908	36451	-0.3945	36653

Table 10. Heat Fluxes at ONB, OFI, and CHF for Coolant Channels of D_h = 4 mm, L_h = 0.61 m, and T_{in} = 30 °C

	Channel Exit Pressure																	
	1 bar						5 bar						10 bar					
Mass Flux	ONB	OFI-WF	OFI-SZ	CHF-Gr	Quality Gr	CHF-HM	ONB	OFI-WF	OFI-SZ	CHF-Gr	Quality Gr	CHF-HM	ONB	OFI-WF	OFI-SZ	CHF-Gr	Quality Gr	CHF-HM
kg/m^2-s	kW/m^2	kW/m^2	kW/m^2	kW/m^2		kW/m^2	kW/m^2	kW/m^2	kW/m^2	kW/m^2		kW/m^2	kW/m^2	kW/m^2	kW/m^2	kW/m^2		kW/m^2
1000	308	394	440	1941	0.3959		532	694	775	2153	0.3794		660	856	956	2567	0.4694	
2000	603	789	813	3168	0.2992		1019	1387	1432	3635	0.2822		1261	1712	1763	4050	0.3025	
3000	896	1183	1148	3468	0.1833		1489	2081	2022	4317	0.1725		1838	2568	2500	4880	0.1797	
4000	1191	1577	1530	3684	0.1197		1952	2774	2696	4867	0.1081		2400	3424	3334	5657	0.1143	
5000	1493	1971	1913	4238	0.0998		2414	3468	3370	5616	0.081		2958	4280	4167	6443	0.0755	
6000	1790	2366	2295	4758	0.085		2867	4161	4044	6345	0.0619		3507	5135	5000	7322	0.0545	
7000	2097	2760	2677	5173	0.0705		3319	4854	4718	7037	0.0468		4063	5991	5833	8006	0.0309	
8000	2401	3154	3059	5599	0.0598		3772	5547	5392	7660	0.0329		4593	6847	6667	8549	0.0077	
9000	2710	3547	3441	6038	0.052		4216	6240	6066	8300	0.0227		5132	7702	7500	9253	-0.0047	7942
10000	3024	3941	3824	6434	0.0446		4662	6934	6739	8907	0.0136		5666	8558	8333	9982	-0.0139	8693
11000	3338	4335	4206	6802	0.0378		5111	7626	7413	9485	0.0053		6195	9413	9166	10682	-0.0223	9428
12000	3652	4728	4587	7151	0.0317		5554	8319	8087	10047	-0.0019	8281	6723	10268	9998	11354	-0.03	10147
13000	3975	5122	4969	7484	0.0263		6000	9012	8760	10605	-0.0081	8865	7253	11123	10831	12002	-0.037	10851
14000	4297	5515	5351	7802	0.0213		6452	9704	9433	11144	-0.0139	9438	7777	11978	11663	12627	-0.0436	11542
15000	4618	5908	5733	8108	0.0168		6893	10397	10106	11664	-0.0192	10001	8303	12833	12497	13233	-0.0496	12219
16000	4949	6301	6114	8401	0.0126		7330	11089	10779	12167	-0.0241	10555	8830	13688	13329	13897	-0.0538	12885
17000	5277	6694	6496	8684	0.0088		7777	11781	11452	12655	-0.0288	11100	9350	14542	14161	14552	-0.0577	13539
18000	5608	7087	6876	8957	0.0052		8219	12473	12125	13129	-0.0331	11636	9872	15396	14993	15192	-0.0614	14182
19000	5944	7479	7257	9221	0.0019		8662	13165	12798	13590	-0.0372	12164	10387	16251	15826	15819	-0.0648	14814
20000	6283	7872	7638	9504	-0.0008	7417	9106	13857	13471	14038	-0.041	12684	10911	17105	16657	16434	-0.0682	15436
21000	6630	8264	8019	9819	-0.0029	7726	9546	14548	14143	14475	-0.0447	13197	11427	17958	17489	17037	-0.0714	16049
22000	6966	8656	8400	10128	-0.0048	8031	9994	15239	14815	14900	-0.0481	13703	11945	18812	18320	17629	-0.0744	16653
23000	7309	9047	8780	10430	-0.0067	8332	10436	15930	15487	15350	-0.051	14202	12463	19666	19152	18210	-0.0774	17248
24000	7655	9439	9161	10725	-0.0084	8630	10879	16621	16159	15833	-0.0532	14694	12984	20519	19983	18781	-0.0802	17835
25000	8006	9830	9540	11014	-0.0101	8924	11325	17311	16830	16308	-0.0553	15180	13495	21372	20814	19342	-0.0829	18414
26000	8357	10221	9920	11298	-0.0117	9215	11764	18002	17502	16775	-0.0574	15660	14009	22225	21645	19893	-0.0855	18985
27000	8713	10612	10300	11576	-0.0133	9503	12211	18692	18174	17235	-0.0593	16134	14525	23077	22476	20436	-0.088	19548
28000	9065	11002	10680	11848	-0.0148	9788	12653	19382	18845	17687	-0.0612	16602	15038	23930	23307	20970	-0.0904	20104
29000	9426	11393	11059	12116	-0.0162	10069	13096	20072	19515	18133	-0.0631	17065	15554	24782	24137	21496	-0.0928	20654
30000	9785	11783	11437	12379	-0.0176	10348	13548	20761	20187	18572	-0.0648	17522	16073	25633	24967	22015	-0.095	21196

Table 10. Continued

	Channel Exit Pressure																	
	20 bar						30 bar						50 bar					
Mass Flux	ONB	OFI-WF	OFI-SZ	CHF-Gr	Quality Gr	CHF-HM	ONB	OFI-WF	OFI-SZ	CHF-Gr	Quality Gr	CHF-HM	ONB	OFI-WF	OFI-SZ	CHF-Gr	Quality Gr	CHF-HM
kg/m^2-s	kW/m^2	kW/m^2	kW/m^2	kW/m^2		kW/m^2	kW/m^2	kW/m^2	kW/m^2	kW/m^2		kW/m^2	kW/m^2	kW/m^2	kW/m^2	kW/m^2		kW/m^2
1000	816	1046	1166	2906	0.5275		918	1173	1308	3173	0.5872		1064	1358	2200	3235	0.5739	
2000	1547	2092	2139	4491	0.3129		1744	2347	2391	4672	0.3028		2020	2716	2720	4612	0.2315	
3000	2254	3139	3072	5624	0.1924		2531	3520	3460	5806	0.1668		2933	4075	4021	5616	0.0714	
4000	2942	4185	4096	6286	0.0939		3304	4693	4613	6562	0.0666		3824	5433	5361	6539	-0.016	6185
5000	3616	5231	5120	7270	0.0558		4060	5866	5767	7541	0.0217		4694	6791	6701	7805	-0.0432	7510
6000	4279	6277	6144	8131	0.0237		4801	7039	6920	8512	-0.0087	7646	5556	8149	8041	9209	-0.0528	8778
7000	4941	7323	7167	8849	-0.0059	7798	5542	8212	8073	9474	-0.0308	8731	6399	9507	9381	10537	-0.0637	9997
8000	5587	8369	8191	9692	-0.0229	8748	6269	9385	9226	10544	-0.0429	9780	7235	10865	10721	11890	-0.0707	11173
9000	6236	9415	9215	10595	-0.0341	9671	6994	10558	10379	11573	-0.0537	10799	8070	12223	12061	13090	-0.0824	12311
10000	6878	10460	10238	11461	-0.0442	10570	7704	11731	11532	12591	-0.0628	11789	8894	13580	13401	14252	-0.0932	13414
11000	7519	11506	11262	12316	-0.0528	11447	8423	12903	12685	13577	-0.0712	12754	9710	14938	14740	15352	-0.1041	14485
12000	8154	12551	12285	13179	-0.0597	12304	9124	14076	13838	14535	-0.0791	13694	10519	16295	16080	16363	-0.1159	15526
13000	8789	13597	13308	14018	-0.0662	13141	9835	15248	14990	15466	-0.0864	14613	11332	17653	17420	17340	-0.1268	16541
14000	9419	14642	14332	14834	-0.0722	13961	10531	16421	16143	16372	-0.0932	15510	12129	19010	18759	18287	-0.137	17531
15000	10045	15687	15355	15630	-0.0779	14764	11230	17593	17295	17256	-0.0997	16389	12930	20367	20098	19206	-0.1465	18498
16000	10665	16732	16378	16406	-0.0833	15551	11924	18765	18448	18097	-0.1062	17249	13727	21724	21438	20109	-0.1552	19442
17000	11285	17777	17401	17164	-0.0884	16324	12608	19937	19601	18915	-0.1125	18092	14518	23081	22777	20995	-0.1632	20367
18000	11907	18821	18424	17905	-0.0932	17082	13304	21109	20753	19714	-0.1184	18918	15304	24438	24116	21858	-0.1708	21272
19000	12523	19866	19447	18630	-0.0978	17828	13988	22280	21905	20495	-0.124	19730	16091	25794	25455	22701	-0.178	22159
20000	13143	20910	20468	19343	-0.1021	18560	14674	23451	23056	21259	-0.1293	20527	16871	27151	26793	23525	-0.1848	23028
21000	13758	21954	21491	20045	-0.1062	19281	15351	24623	24208	22007	-0.1344	21310	17660	28507	28132	24330	-0.1913	23882
22000	14373	22998	22513	20734	-0.1101	19990	16028	25794	25359	22739	-0.1392	22080	18437	29863	29471	25118	-0.1975	24719
23000	14983	24042	23535	21410	-0.1138	20687	16718	26964	26511	23457	-0.1438	22837	19206	31219	30809	25911	-0.203	25543
24000	15596	25086	24558	22074	-0.1174	21375	17387	28135	27662	24161	-0.1483	23583	19977	32574	32148	26706	-0.2081	26352
25000	16204	26129	25578	22726	-0.1209	22052	18063	29306	28813	24871	-0.1523	24316	20756	33930	33485	27486	-0.213	27147
26000	16812	27172	26600	23368	-0.1242	22720	18739	30476	29964	25582	-0.156	25039	21515	35285	34823	28253	-0.2177	27930
27000	17421	28215	27621	23998	-0.1274	23378	19411	31646	31114	26281	-0.1595	25751	22281	36640	36160	29006	-0.2222	28700
28000	18021	29258	28643	24619	-0.1305	24027	20077	32815	32266	26969	-0.163	26453	23047	37994	37498	29748	-0.2265	29458
29000	18633	30300	29663	25230	-0.1334	24668	20746	33985	33415	27647	-0.1663	27145	23811	39349	38835	30477	-0.2307	30206
30000	19236	31342	30685	25831	-0.1363	25300	21416	35154	34566	28314	-0.1695	27828	24569	40703	40172	31195	-0.2348	30942

Table 11. Heat Fluxes at ONB, OFI, and CHF for Coolant Channels of D_h = 8 mm, L_h = 1.18 m, and T_{in} = 30 °C

	Channel Exit Pressure																	
	1 bar						5 bar						10 bar					
Mass Flux	ONB	OFI-WF	OFI-SZ	CHF-Gr	Quality Gr	CHF-HM	ONB	OFI-WF	OFI-SZ	CHF-Gr	Quality Gr	CHF-HM	ONB	OFI-WF	OFI-SZ	CHF-Gr	Quality Gr	CHF-HM
kg/m^2-s	kW/m^2	kW/m^2	kW/m^2	kW/m^2		kW/m^2	kW/m^2	kW/m^2	kW/m^2	kW/m^2		kW/m^2	kW/m^2	kW/m^2	kW/m^2	kW/m^2		kW/m^2
1000	294	405	418	1777	0.3357		510	713	737	2052	0.3307		635	880	907	2592	0.451	
2000	573	811	786	2794	0.2362		973	1425	1384	3361	0.2265		1204	1759	1712	3725	0.2337	
3000	850	1216	1178	3068	0.1381		1420	2138	2077	3867	0.1167		1755	2639	2567	4523	0.1278	
4000	1130	1621	1571	3349	0.0896		1860	2851	2769	4523	0.0723		2290	3518	3423	5294	0.0729	
5000	1411	2026	1964	3892	0.0742		2297	3564	3461	5216	0.0478		2817	4398	4279	6091	0.0415	
6000	1696	2431	2356	4293	0.0577		2727	4276	4153	5821	0.0274		3342	5277	5135	6585	0.0055	
7000	1982	2836	2749	4626	0.0434		3154	4989	4845	6470	0.0145		3858	6157	5990	7219	-0.0142	6252
8000	2268	3241	3142	4941	0.0321		3583	5701	5537	6938	-0.0015	5713	4370	7036	6846	7839	-0.0295	7001
9000	2559	3646	3534	5283	0.0241		4007	6413	6229	7511	-0.0107	6315	4881	7915	7701	8505	-0.0399	7727
10000	2853	4051	3927	5603	0.0171		4431	7126	6921	8056	-0.0188	6901	5386	8794	8557	9138	-0.0492	8432
11000	3148	4456	4319	5905	0.0109		4852	7838	7613	8574	-0.0261	7473	5891	9673	9412	9821	-0.0555	9119
12000	3446	4860	4711	6190	0.0055		5271	8550	8304	9069	-0.0327	8031	6393	10552	10267	10488	-0.061	9788
13000	3746	5265	5103	6462	0.0006		5693	9262	8996	9544	-0.0388	8577	6894	11431	11123	11135	-0.0662	10441
14000	4049	5669	5495	6784	-0.0027	5335	6130	9974	9688	10000	-0.0444	9111	7393	12310	11978	11764	-0.0711	11079
15000	4354	6073	5888	7102	-0.0056	5651	6534	10686	10379	10439	-0.0495	9634	7891	13189	12833	12375	-0.0756	11703
16000	4661	6477	6280	7411	-0.0083	5962	6953	11397	11070	10935	-0.053	10146	8386	14067	13688	12970	-0.0799	12314
17000	4969	6881	6671	7710	-0.0108	6267	7374	12109	11762	11426	-0.0561	10649	8880	14945	14543	13550	-0.0839	12912
18000	5281	7285	7063	8000	-0.0132	6567	7793	12820	12453	11905	-0.0591	11143	9372	15823	15397	14115	-0.0877	13499
19000	5596	7689	7454	8283	-0.0154	6862	8208	13531	13144	12374	-0.062	11628	9866	16702	16253	14668	-0.0914	14075
20000	5910	8092	7846	8558	-0.0175	7153	8630	14242	13834	12831	-0.0647	12104	10357	17580	17107	15208	-0.0948	14640
21000	6228	8496	8237	8825	-0.0195	7440	9049	14953	14525	13280	-0.0672	12573	10845	18457	17961	15737	-0.0981	15195
22000	6549	8899	8628	9087	-0.0213	7723	9467	15664	15216	13718	-0.0697	13034	11339	19335	18815	16252	-0.1012	15741
23000	6874	9302	9019	9342	-0.0231	8001	9889	16374	15906	14148	-0.072	13488	11831	20212	19669	16752	-0.1043	16278
24000	7197	9704	9410	9591	-0.0248	8276	10306	17085	16597	14570	-0.0743	13935	12319	21089	20523	17243	-0.1072	16806
25000	7523	10107	9801	9834	-0.0264	8546	10724	17795	17286	14983	-0.0764	14375	12803	21966	21377	17724	-0.11	17325
26000	7852	10509	10190	10073	-0.028	8814	11144	18505	17977	15389	-0.0785	14809	13293	22843	22231	18196	-0.1127	17837
27000	8184	10911	10581	10306	-0.0294	9078	11562	19214	18667	15788	-0.0805	15236	13783	23720	23084	18659	-0.1153	18341
28000	8519	11313	10972	10535	-0.0309	9338	11982	19924	19357	16180	-0.0824	15658	14267	24596	23937	19114	-0.1178	18838
29000	8852	11715	11361	10759	-0.0322	9596	12400	20633	20045	16565	-0.0842	16074	14757	25472	24791	19562	-0.1202	19327
30000	9190	12116	11751	10979	-0.0335	9850	12821	21342	20735	16944	-0.086	16485	15241	26348	25643	20001	-0.1225	19810

Table 11. Continued

	Channel Exit Pressure																	
	20 bar						30 bar						50 bar					
Mass Flux	ONB	OFI-WF	OFI-SZ	CHF-Gr	Quality Gr	CHF-HM	ONB	OFI-WF	OFI-SZ	CHF-Gr	Quality Gr	CHF-HM	ONB	OFI-WF	OFI-SZ	CHF-Gr	Quality Gr	CHF-HM
kg/m^2-s	kW/m^2	kW/m^2	kW/m^2	kW/m^2		kW/m^2	kW/m^2	kW/m^2	kW/m^2	kW/m^2		kW/m^2	kW/m^2	kW/m^2	kW/m^2	kW/m^2		kW/m^2
1000	784	1075	1100	2880	0.4884		883	1205	1229	3131	0.5382		1025	1395	1397	3086	0.4817	
2000	1484	2150	2103	4259	0.2526		1669	2411	2369	4436	0.2381		1936	2791	2753	4323	0.152	
3000	2154	3225	3155	5065	0.114		2423	3616	3553	5303	0.0901		2809	4186	4129	5288	0.0098	
4000	2809	4300	4206	5918	0.0483		3160	4821	4737	6173	0.0164		3659	5581	5505	6355	-0.0522	6055
5000	3448	5375	5257	6855	0.0142		3880	6026	5922	7022	-0.0291	6388	4490	6977	6881	7539	-0.081	7306
6000	4086	6450	6309	7394	-0.0293	6672	4586	7231	7106	7894	-0.0583	7451	5304	8372	8257	8794	-0.096	8494
7000	4708	7525	7360	8175	-0.0496	7597	5288	8436	8290	8940	-0.071	8469	6116	9767	9633	10082	-0.1051	9628
8000	5329	8600	8411	9096	-0.0593	8490	5980	9641	9474	10031	-0.0786	9450	6909	11162	11009	11296	-0.1152	10715
9000	5943	9674	9463	9959	-0.0688	9353	6663	10846	10658	10989	-0.0894	10395	7701	12557	12385	12301	-0.1313	11760
10000	6554	10749	10514	10789	-0.0775	10189	7347	12051	11842	11911	-0.0992	11310	8484	13952	13761	13260	-0.1458	12767
11000	7158	11823	11565	11589	-0.0854	11001	8023	13256	13026	12778	-0.1089	12197	9267	15347	15137	14192	-0.1586	13741
12000	7762	12898	12616	12361	-0.0928	11791	8694	14460	14210	13611	-0.1178	13058	10033	16741	16513	15093	-0.1701	14684
13000	8363	13972	13667	13109	-0.0996	12560	9364	15665	15394	14417	-0.1261	13896	10799	18136	17889	15962	-0.1808	15599
14000	8959	15046	14718	13841	-0.1058	13310	10030	16869	16578	15196	-0.1339	14711	11565	19530	19264	16802	-0.1906	16488
15000	9551	16120	15768	14552	-0.1116	14042	10687	18074	17761	15952	-0.1411	15506	12320	20925	20640	17615	-0.1998	17353
16000	10147	17194	16819	15244	-0.117	14758	11348	19278	18945	16686	-0.1478	16282	13083	22319	22015	18442	-0.2076	18195
17000	10737	18268	17870	15918	-0.1222	15458	12005	20482	20128	17422	-0.1537	17041	13836	23713	23390	19248	-0.2148	19017
18000	11322	19342	18920	16575	-0.127	16143	12659	21686	21312	18150	-0.1591	17782	14580	25107	24765	20033	-0.2217	19819
19000	11911	20416	19970	17217	-0.1316	16815	13313	22889	22495	18862	-0.1642	18508	15327	26501	26140	20799	-0.2281	20604
20000	12493	21489	21021	17844	-0.136	17473	13963	24093	23678	19557	-0.1691	19219	16070	27895	27515	21548	-0.2343	21371
21000	13083	22562	22071	18457	-0.1402	18119	14606	25297	24861	20238	-0.1737	19916	16808	29288	28890	22279	-0.2402	22121
22000	13660	23635	23121	19057	-0.1441	18753	15250	26500	26043	20904	-0.1782	20600	17592	30682	30265	22995	-0.2457	22857
23000	14238	24708	24171	19644	-0.1479	19376	15897	27703	27226	21557	-0.1824	21271	18282	32075	31640	23695	-0.251	23577
24000	14823	25781	25220	20236	-0.1513	19988	16537	28906	28409	22197	-0.1864	21930	19022	33468	33014	24381	-0.2561	24284
25000	15400	26853	26269	20839	-0.1543	20591	17181	30109	29590	22825	-0.1903	22577	19760	34861	34389	25054	-0.261	24978
26000	15970	27925	27319	21431	-0.1572	21182	17815	31311	30773	23441	-0.194	23214	20478	36253	35763	25714	-0.2657	25659
27000	16548	28998	28368	22013	-0.16	21765	18451	32513	31955	24047	-0.1976	23840	21211	37646	37136	26361	-0.2702	26329
28000	17122	30070	29417	22587	-0.1627	22339	19087	33716	33137	24647	-0.201	24456	21937	39038	38510	26997	-0.2745	26986
29000	17701	31141	30465	23151	-0.1653	22904	19724	34917	34318	25248	-0.2041	25062	22670	40430	39884	27622	-0.2786	27633
30000	18266	32212	31515	23707	-0.1678	23461	20357	36119	35500	25839	-0.2072	25658	23380	41822	41257	28236	-0.2826	28270

Table 12. Heat Fluxes at ONB, OFI, and CHF for Coolant Channels of D_h = 4 mm, L_h = 1.18 m, and T_{in} = 30 °C

	Channel Exit Pressure																	
	1 bar						5 bar						10 bar					
Mass Flux	ONB	OFI-WF	OFI-SZ	CHF-Gr	Quality Gr	CHF-HM	ONB	OFI-WF	OFI-SZ	CHF-Gr	Quality Gr	CHF-HM	ONB	OFI-WF	OFI-SZ	CHF-Gr	Quality Gr	CHF-HM
kg/m^2-s	kW/m^2	kW/m^2	kW/m^2	kW/m^2		kW/m^2	kW/m^2	kW/m^2	kW/m^2	kW/m^2		kW/m^2	kW/m^2	kW/m^2	kW/m^2	kW/m^2		kW/m^2
1000	198	223	237	1248	0.5241		340	392	417	1353	0.514		421	485	515	1399	0.5128	
2000	393	446	453	1888	0.3648		663	785	799	2149	0.3581		815	969	985	2278	0.3573	
3000	590	669	657	2404	0.2901		980	1177	1158	2803	0.2794		1204	1453	1432	3043	0.2832	
4000	789	891	876	2861	0.245		1295	1569	1544	3437	0.2372		1586	1938	1909	3809	0.2462	
5000	988	1114	1095	3215	0.2072		1609	1961	1930	3764	0.1776		1966	2422	2386	4258	0.1861	
6000	1192	1337	1314	3481	0.1743		1921	2353	2316	4140	0.1423		2342	2907	2863	4652	0.1407	
7000	1395	1559	1533	3709	0.1479		2232	2745	2702	4648	0.1278		2719	3391	3340	5214	0.1225	
8000	1602	1782	1751	4041	0.135		2541	3137	3087	5140	0.1157		3091	3875	3817	5762	0.1079	
9000	1812	2004	1970	4395	0.1262		2850	3529	3473	5635	0.1065		3464	4359	4294	6333	0.098	
10000	2022	2227	2189	4733	0.1183		3160	3921	3858	6115	0.0983		3834	4843	4771	6904	0.0901	
11000	2234	2449	2407	5055	0.1112		3471	4313	4244	6590	0.0914		4203	5327	5248	7459	0.0827	
12000	2448	2671	2625	5365	0.1046		3778	4704	4629	7052	0.085		4573	5811	5724	7998	0.0759	
13000	2664	2893	2844	5666	0.0988		4089	5096	5015	7501	0.079		4940	6294	6200	8524	0.0695	
14000	2880	3115	3062	5966	0.0937		4398	5487	5400	7937	0.0734		5307	6778	6677	9037	0.0634	
15000	3099	3336	3280	6257	0.089		4708	5878	5785	8362	0.0682		5675	7261	7153	9539	0.0577	
16000	3320	3558	3498	6539	0.0846		5017	6269	6170	8777	0.0632		6041	7744	7629	10029	0.0523	
17000	3545	3779	3715	6814	0.0805		5326	6660	6555	9183	0.0585		6407	8228	8105	10470	0.0458	
18000	3766	4001	3933	7080	0.0767		5636	7051	6939	9579	0.054		6774	8710	8581	10867	0.0386	
19000	3991	4222	4150	7340	0.073		5947	7441	7323	9965	0.0498		7138	9193	9057	11254	0.0319	
20000	4218	4443	4367	7593	0.0695		6255	7832	7708	10331	0.0454		7504	9676	9533	11630	0.0255	
21000	4447	4663	4585	7840	0.0663		6565	8222	8092	10688	0.0411		7868	10158	10008	11997	0.0194	
22000	4675	4884	4801	8081	0.0632		6875	8612	8476	11037	0.0371		8232	10640	10483	12355	0.0137	
23000	4908	5104	5018	8316	0.0602		7187	9002	8860	11380	0.0333		8596	11122	10959	12704	0.0082	
24000	5139	5324	5234	8547	0.0574		7495	9391	9243	11715	0.0296		8962	11604	11433	13046	0.003	
25000	5373	5544	5451	8772	0.0547		7805	9780	9627	12045	0.0261		9326	12086	11908	13403	-0.0014	11440
26000	5608	5763	5667	8993	0.0521		8118	10170	10010	12368	0.0227		9688	12567	12382	13790	-0.0048	11833
27000	5844	5982	5883	9208	0.0496		8429	10559	10392	12685	0.0194		10053	13048	12856	14170	-0.008	12222
28000	6083	6202	6099	9407	0.047		8737	10947	10776	12996	0.0163		10414	13529	13331	14545	-0.0112	12607
29000	6320	6421	6315	9603	0.0445		9049	11336	11158	13302	0.0133		10779	14010	13804	14913	-0.0142	12989
30000	6561	6639	6530	9794	0.0421		9363	11724	11540	13603	0.0104		11141	14490	14278	15277	-0.0172	13369

Table 12. Continued

	Channel Exit Pressure																	
	20 bar						30 bar						50 bar					
Mass Flux	ONB	OFI-WF	OFI-SZ	CHF-Gr	Quality Gr	CHF-HM	ONB	OFI-WF	OFI-SZ	CHF-Gr	Quality Gr	CHF-HM	ONB	OFI-WF	OFI-SZ	CHF-Gr	Quality Gr	CHF-HM
kg/m^2-s	kW/m^2	kW/m^2	kW/m^2	kW/m^2		kW/m^2	kW/m^2	kW/m^2	kW/m^2	kW/m^2		kW/m^2	kW/m^2	kW/m^2	kW/m^2	kW/m^2		kW/m^2
1000	514	592	630	1613	0.5974		578	667	708	1777	0.6773		671	773	818	1874	0.7175	
2000	999	1184	1202	2533	0.3795		1120	1334	1348	2776	0.4215		1299	1545	1548	2885	0.4101	
3000	1470	1776	1759	3390	0.2935		1647	2002	1981	3663	0.3117		1912	2318	2302	3703	0.2615	
4000	1933	2369	2345	4198	0.2429		2168	2669	2642	4414	0.2346		2514	3090	3070	4244	0.138	
5000	2392	2961	2932	4730	0.1779		2680	3336	3302	4973	0.163		3107	3863	3837	4816	0.0682	
6000	2847	3553	3518	5220	0.1301		3189	4003	3962	5441	0.1053		3696	4635	4605	5501	0.0351	
7000	3300	4144	4104	5855	0.1091		3695	4670	4623	6110	0.083		4283	5408	5372	6314	0.0247	
8000	3751	4736	4690	6525	0.096		4193	5337	5283	6799	0.0679		4862	6180	6139	7128	0.0168	
9000	4198	5328	5276	7169	0.0841		4692	6004	5943	7448	0.0533		5439	6952	6906	7874	0.0053	
10000	4643	5920	5862	7791	0.0732		5188	6670	6603	8094	0.0414		6012	7724	7673	8625	-0.0035	8128
11000	5087	6511	6448	8393	0.0631		5684	7337	7263	8726	0.0308		6583	8496	8440	9387	-0.01	8841
12000	5529	7103	7034	8977	0.0537		6176	8003	7923	9340	0.021		7155	9268	9207	10136	-0.0161	9541
13000	5968	7694	7620	9519	0.0438		6665	8670	8583	9936	0.0119		7722	10040	9974	10874	-0.022	10230
14000	6406	8285	8205	10027	0.0338		7154	9336	9242	10517	0.0033		8284	10812	10740	11600	-0.0275	10908
15000	6846	8876	8790	10520	0.0244		7643	10002	9902	11112	-0.0035	10060	8847	11583	11507	12316	-0.0329	11575
16000	7303	9467	9376	10997	0.0157		8128	10668	10561	11715	-0.0092	10642	9410	12355	12273	13022	-0.0379	12233
17000	7721	10058	9961	11462	0.0075		8614	11334	11220	12307	-0.0146	11217	9971	13126	13040	13719	-0.0428	12881
18000	8154	10649	10546	11916	-0.0002	10513	9097	12000	11879	12889	-0.0197	11784	10530	13897	13806	14406	-0.0475	13520
19000	8591	11239	11130	12429	-0.0051	11019	9577	12665	12538	13461	-0.0246	12345	11094	14668	14572	15079	-0.0523	14151
20000	9024	11829	11715	12934	-0.0097	11519	10059	13331	13197	14024	-0.0294	12899	11550	15439	15338	15738	-0.057	14774
21000	9457	12419	12300	13430	-0.0142	12014	10541	13996	13856	14578	-0.0339	13447	12093	16209	16103	16387	-0.0617	15389
22000	9887	13009	12885	13917	-0.0185	12504	11020	14661	14514	15124	-0.0383	13989	12644	16980	16869	17029	-0.0661	15996
23000	10321	13599	13468	14397	-0.0226	12989	11497	15326	15173	15662	-0.0425	14524	13192	17750	17635	17662	-0.0704	16596
24000	10751	14189	14053	14869	-0.0266	13468	11975	15990	15831	16192	-0.0466	15055	13734	18520	18399	18288	-0.0746	17189
25000	11182	14778	14636	15334	-0.0304	13944	12455	16655	16489	16718	-0.0505	15579	14279	19290	19165	18906	-0.0787	17775
26000	11613	15367	15220	15792	-0.0341	14414	12927	17319	17147	17253	-0.0538	16098	14820	20060	19929	19517	-0.0826	18354
27000	12044	15956	15803	16243	-0.0377	14880	13401	17983	17804	17782	-0.057	16612	15361	20829	20694	20121	-0.0864	18927
28000	12470	16545	16386	16688	-0.0412	15342	13875	18646	18461	18306	-0.0602	17121	15902	21598	21458	20719	-0.0901	19494
29000	12898	17133	16970	17127	-0.0445	15800	14349	19310	19119	18822	-0.0632	17625	16446	22367	22222	21310	-0.0937	20055
30000	13331	17721	17552	17560	-0.0478	16253	14824	19973	19775	19334	-0.0662	18124	16986	23136	22987	21894	-0.0972	20611

Table 13. Key Parameters of Some Experimental Reactors Plotted on the OFI-CHF Reversal Diagram of Fig. 6

D_h = Heated diameter, D_e = Hydraulic diameter
C = Under construction, D = Design, O = Operational, S = Shutdown

No.	Reactor	Status	Power	Exit Pres.	Coolant Vel.	Mass Flux	D_e	D_h	Heated Length	Inlet Temp.
			MW_{th}	bar	m/s	kg/m^2-s	mm	mm	m	°C
1	ANS Design, Oak Ridge, USA[26]	D	350	17	25.0	24700	2.54	3.05[a]	0.474	45
2	HFIR, USA[28]	O	85	32.30	15.4	15355		2.54	0.508	49
3	MITR, HEU Core, USA[30]	O	6	1.30	2.0	1980	2.19	2.48	0.568	42
4	MURR, USA[29]	O	10	4.70	7.00	6969		4.06	0.610	49
5	ATR, USA[27]	O	250	18.8	14.60	14552		3.94	1.181	51.7

a. The heated diameter was estimated as 1.2 times the hydraulic diameter.

Table 14. Scoping Results Whether the Reactors Listed in Table 13 Are OFI-limited or CHF-limited

No.	Reactor	Comments	Results
		Reactors with L_h = ~0.61 m Plotted on Fig. 6 Part 3	
1	ANS Design, Oak Ridge, USA	The point representing the ANS Design (3.1 mm, 45 ºC) is below the orange reversal line (3 mm, 50 ºC). It is also below the interpolated reversal line (3.1 mm, 45 ºC) applicable to the reactor.	OFI-limited
2	HFIR, USA	The reversal line applicable to this reactor (2.5 mm, 49 ºC) lies above the line (3 mm, 49 ºC) which is not drawn, and the latter lies above the blue line (3.0 mm, 30 ºC). The point representing the HFIR (2.5 mm, 49 ºC) is below the blue line (3 mm, 30 ºC). So, the HFIR is far *below* the applicable reversal line (2.5 mm, 49 ºC).	OFI-limited
3	MITR, HEU Core, USA	The point representing the MITR (2.5 mm, 42 ºC) is below the lowest reversal line (8 mm, 30 ºC), and therefore farther *below* the applicable reversal line (2.5 mm, 42 ºC).	OFI-limited
4	MURR, USA	The point representing the MURR (4.1 mm, 49 ºC) is below the lowest reversal line (8 mm, 30 ºC), and therefore farther *below* the applicable reversal line (4.1 mm, 49 ºC).	OFI-limited
		Reactors with L_h = ~1.18 m Plotted on Fig. 6 Part 5	
5	ATR, USA	The point representing the ATR (3.9 mm, 52 ºC) is far below the orange reversal line (4 mm, 50 ºC). Therefore, the ATR is farther *below* the reversal line (3.9 mm, 52 ºC). This is because a decrease in heated diameter raises the reversal line; and also an increase in inlet temperature raises the reversal line.	OFI-limited

APPENDIX A. METHODS USED IN THE COMPUTER PROGRAM FOR CALCULATING ONB, OFI, AND CHF

Throughout this work, the heat flux to the coolant channel was assumed to be uniform over the heated length and the heated perimeter. Then the ONB, OFI, and CHF all occur at the channel exit. The ONB heat flux, OFI heat flux, and CHF were calculated iteratively, using the heat balance method (HBM) as agreed upon in 1996 by a panel of experts (Celata, Groeneveld, Hejzlar and Todreas, and Inasaka and Nariai)[41,42], for given values of five independent parameters: exit pressure, heated length, heated diameter, inlet temperature, mass flux. The methods used in the FORTRAN program developed for this purpose (listed in Appendix F) are outlined below.

A.1. ONB Heat Flux by the Bergles-Rohsenow Correlation

The ONB heat flux was calculated based on the Bergles-Rohsenow correlation[16] using the following iterative steps. As mentioned above, the values of the following five independent parameters are given: exit pressure P, heated length L_h , heated diameter D_h , coolant inlet temperature T_i , mass flux G.

Step 1: At the given exit pressure P, find the saturation temperature T_{sat} , saturated liquid enthalpy h_{fo} , saturated vapor enthalpy h_{go} , and the heat of vaporization Δh_{fgo} .

Step 2: Guess a value for the coolant exit temperature T_o at ONB. The first guess used in the program is $T_o = T_i+1$. Find the exit enthalpy $h_o = h(P, T_o)$.

Step 3: To iteratively calculate the inlet pressure P_i , guess $P_i = P$.

Step 4: At the average pressure $0.5(P_i + P)$ and average temperature $0.5(T_i + T_o)$, find the coolant density ρ_{ave} , viscosity μ_{ave} , Reynolds number Re_{ave} , friction factor f_{ave} , the frictional pressure drop $f_{ave} L_h/D_e$, and the gravity head $\rho_{ave} g L_h$.

Step 5: Calculate a new estimate of the inlet pressure.

$$P_{i,new} = P + f_{ave} L_h/D_e + \rho_{ave} g L_h \quad \text{(in upflow)}$$
$$P_{i,new} = P + f_{ave} L_h/D_e - \rho_{ave} g L_h \quad \text{(in downflow)}$$

Iterate over Steps 4 to 5 until $P_{i,new}$ converges to P_i . Three iterations were found to be sufficient for convergence.

Step 6: Find the inlet enthalpy h_i at the inlet temperature T_i and the converged inlet pressure P_i . Find the heat flux based on heat balance. This is a guessed value for the ONB heat flux corresponding to the guessed value of the exit temperature T_o.

$$q_{ONB,guess} = \frac{D_h G (h_o - h_i)}{4 L_h}$$

Step 7: Calculate coolant properties at the channel exit (temperature T_o and pressure P). Calculate the heat transfer coefficient H_o at the exit, using the Petukhov-Popov correlation Nu for single-phase forced convection. At the channel exit, calculate the temperature drop from the heated wall to bulk coolant ΔT_h , the wall temperature T_w , the wall superheat ΔT_{sat} , and the ONB heat flux using the Bergles-Rohsenow correlation, as follows.

$$\Delta T_h = \frac{q_{ONB,guess}}{H_o}$$

$$T_w = T_o + \Delta T_h$$

$$\Delta T_{sat} = T_w - T_{sat}$$

$$x = 2.16/P^{0.0234}$$

$$q_{ONB}\ (kW/m^2) = 1082.9 \times 10^{-3}\ P^{1.156}\ (1.8\ \Delta T_{sat})^x$$

Iterate over Steps 2 to 7 until q_{ONB} calculated in Step 7 converges to $q_{ONB,guess}$ found by heat balance in Step 6. The converged value is the desired ONB heat flux.

A.2. OFI Heat Flux by the Whittle-Forgan Correlation

The OFI heat flux based on the Whittle-Forgan correlation[4,21] ($\eta = 32.5$) was calculated using the following iterative steps, starting from the given values of the following five independent parameters: exit pressure P, heated length L_h , heated diameter D_h , inlet temperature T_i , mass flux G. According to the Whittle-Forgan correlation, the flow instability occurs when the ratio of the bulk coolant temperature rise ($T_o - T_i$) to the difference (T_{sat} - T_i) between the inlet temperature and the saturation temperature at the exit, equals a value R determined purely the channel geometry.

$$\frac{T_o - T_i}{T_{sat} - T_i} = R = \frac{1}{1 + (\eta D_h / L_h)}$$

Step 1: At the given exit pressure P, find the saturation temperature T_{sat} , saturated liquid enthalpy h_{fo} , saturated vapor enthalpy h_{go} , and the heat of vaporization Δh_{fgo} .

Step 2: Calculate the ratio R using $\eta = 32.5$ on the right hand side of the Whittle-Forgan correlation. Calculate the exit temperature and exit enthalpy.

$$T_o = T_i + R(T_{sat} - T_i)$$

$$h_o = h(P, T_o)$$

Step 3: To iteratively calculate the inlet pressure P_i , guess $P_i = P$.

Step 4: At the average pressure $0.5(P_i + P)$ and average temperature $0.5(T_i + T_o)$, find the coolant density ρ_{ave} , viscosity μ_{ave} , Reynolds number Re_{ave} , friction factor f_{ave} , the frictional pressure drop $f_{ave}\ L_h/D_e$, and the gravity head $\rho_{ave} g\ L_h$.

Step 5: Calculate a new estimate of the inlet pressure.

$P_{i,new} = P + f_{ave}\, L_h/D_e + \rho_{ave} g\, L_h$ (in upflow)
$P_{i,new} = P + f_{ave}\, L_h/D_e - \rho_{ave} g\, L_h$ (in downflow)

Iterate over Steps 4 to 5 until $P_{i,new}$ converges to P_i . Three iterations were found to be sufficient for convergence.

Step 6: Find the inlet enthalpy h_i at the inlet temperature T_i and the converged inlet pressure P_i . Find the heat flux based on heat balance. This is the desired OFI heat flux.

$$q_{OFI-WF} = \frac{D_h\, G\,(h_o - h_i)}{4\, L_h}$$

A.3. OFI Heat Flux by the Saha-Zuber Correlation

The OFI heat flux is assumed to be equal to the heat flux at the onset of significant voids (OSV) given by the following Saha-Zuber correlation[5].

$$q_{OFI-SZ} = -G\, h_{fg,o}\, X_o\, \mathrm{Max}\left(\frac{455}{Pe}, 0.0065\right) \qquad \text{where} \quad Pe = \frac{G\, D_h\, C_{pf,o}}{K_{f,o}}$$

The OFI heat flux was calculated using the following iterative steps, starting from the given values of the following five independent parameters: the exit pressure P, the heated length L_h , the heated diameter D_h , the inlet temperature T_i , and the mass flux G.

Step 1: At the given exit pressure P, find the saturation temperature T_{sat} , saturated liquid enthalpy h_{fo} , saturated vapor enthalpy h_{go} , and the heat of vaporization Δh_{fgo} .

Step 2: Guess a value for the coolant exit temperature T_o at OFI. The first guess used in the program is $T_o = T_i+1$. Find the exit enthalpy $h_o = h(P, T_o)$.

Step 3: To iteratively calculate the inlet pressure P_i , guess $P_i = P$.

Step 4: At the average pressure $0.5(P_i + P)$ and average temperature $0.5(T_i + T_o)$, find the coolant density ρ_{ave} , viscosity μ_{ave} , Reynolds number Re_{ave} , friction factor f_{ave} , the frictional pressure drop $f_{ave}\, L_h/D_e$, and the gravity head $\rho_{ave} g\, L_h$.

Step 5: Calculate a new estimate of the inlet pressure.

$P_{i,new} = P + f_{ave}\, L_h/D_e + \rho_{ave} g\, L_h$ (in upflow)
$P_{i,new} = P + f_{ave}\, L_h/D_e - \rho_{ave} g\, L_h$ (in downflow)

Iterate over Steps 4 to 5 until $P_{i,new}$ converges to P_i . Three iterations were found to be sufficient for convergence.

Step 6: Find the inlet enthalpy h_i at the inlet temperature T_i and the converged inlet pressure P_i. Find the heat flux based on heat balance. This is a guessed value for the ONB heat flux corresponding to the guessed value of the exit temperature T_o.

$$q_{OFI,guess} = \frac{D_h\, G\,(h_o - h_i)}{4\, L_h}$$

Step 7: Calculate coolant properties at the channel exit (temperature T_o and pressure P). Using the coolant properties at the exit, calculate the Peclet number Pe at the exit, the quality X_o at the exit, and the OFI heat flux using the Saha-Zuber correlation, as follows.

$$Pe = \frac{G\, D_h\, C_{pf,o}}{K_{f,o}}$$

$$X_o = \frac{h_o - h_{f,o}}{h_{fg,o}}$$

$$q_{OFI-SZ} = -G\, h_{fg,o}\, X_o\, Max\left(\frac{455}{Pe}, 0.0065\right)$$

Iterate over Steps 2 to 7 until q_{OFI-SZ} calculated in Step 7 converges to $q_{OFI,guess}$ found by heat balance in Step 6. The converged value is the desired OFI heat flux.

A.4. CHF by the Extended Groeneveld 2006 Table

The critical heat flux (CHF) based on an extension[8] of the Groeneveld 2006 table[18] was calculated using the following iterative steps, starting from the values of the following five independent parameters: the exit pressure P, the heated length L_h, the heated diameter D_h, the inlet temperature T_i, and the mass flux G.

Step 1: At the given exit pressure P, find the saturation temperature T_{sat}, saturated liquid enthalpy h_{fo}, saturated vapor enthalpy h_{go}, and the heat of vaporization Δh_{fgo}.

Step 2: Guess a value for the CHF. The first guess used in the program is $q_{c\text{-}guess} = 500$ kW/m^2.

Step 3: To iteratively calculate the inlet pressure P_i, guess $P_i = P$.

Step 4: At the average pressure $0.5(P_i + P)$ and average temperature $0.5(T_i + T_o)$, find the coolant density ρ_{ave}, viscosity μ_{ave}, Reynolds number Re_{ave}, friction factor f_{ave}, the frictional pressure drop $f_{ave}\, L_h/D_e$, and the gravity head $\rho_{ave} g\, L_h$.

Step 5: Calculate a new estimate of the inlet pressure.

$P_{i,new} = P + f_{ave}\, L_h/D_e + \rho_{ave} g\, L_h$ (in upflow)
$P_{i,new} = P + f_{ave}\, L_h/D_e - \rho_{ave} g\, L_h$ (in downflow)

Iterate over Steps 4 to 5 until $P_{i,new}$ converges to P_i . Three iterations were found to be sufficient for convergence.

Step 6: Find the inlet enthalpy h_i at the inlet temperature T_i and the converged inlet pressure P_i . Using the inlet enthalpy and the guessed heat flux, calculate the exit enthalpy based on heat balance. Find the exit quality X_o. Interpolate the Groeneveld 2006 table and calculate the CHF using the equation given below.

$$h_o = h_i + \frac{4 L_h q_{c-guess}}{D_h G}$$

$$X_o = \frac{h_o - h_{fo}}{h_{fg,o}}$$

$$q_c(D_h, P, G, X_o) = \begin{cases} q_c(0.008, P, G, X_o)\left(\frac{0.008}{D_h}\right)^{0.312} & \text{if } G \le 8000 \\ q_c(0.008, P, 8000, X_o)\left(\frac{0.008}{D_h}\right)^{0.312}\left(\frac{G}{8000}\right)^{0.376} & \text{if } G > 8000 \end{cases}$$

Iterate over Steps 2 to 6 until q_c calculated in Step 6 converges to $q_{c,guess}$ assumed in Step 2. The converged value is the desired CHF.

A.5. CHF by the Hall-Mudawar Inlet Conditions Correlation

The critical heat flux (CHF) based on the Hall-Mudawar inlet conditions correlation[19] was calculated using the following iterative steps, starting from the values of the following five independent parameters: the exit pressure P, the heated length L_h , the heated diameter D_h , the inlet temperature T_i , and the mass flux G. There would have been no need to iterate if the inlet pressure were also known. Since the inlet pressure depends (although weakly) on the heat flux and the resulting coolant temperature distribution, the inlet pressure needs to be found iteratively.

Step 1: At the given exit pressure P, find the saturation temperature T_{sat} , saturated liquid enthalpy h_{fo} , saturated vapor enthalpy h_{go} , and the heat of vaporization Δh_{fgo} .

Step 2: Guess a value for the CHF. The first guess used in the program is $q_{c\text{-}guess} = 500$ kW/m^2.

Step 3: To iteratively calculate the inlet pressure P_i , guess $P_i = P$.

Step 4: At the average pressure $0.5(P_i + P)$ and average temperature $0.5(T_i + T_o)$, find the coolant density ρ_{ave} , viscosity μ_{ave} , Reynolds number Re_{ave} , friction factor f_{ave} , the frictional pressure drop $f_{ave} L_h/D_e$, and the gravity head $\rho_{ave} g L_h$.

Step 5: Calculate a new estimate of the inlet pressure.

$P_{i,new} = P + f_{ave} L_h/D_e + \rho_{ave} g L_h$ (in upflow)

$P_{i,new} = P + f_{ave}\, L_h/D_e - \rho_{ave} g\, L_h$ (in downflow)

Iterate over Steps 4 to 5 until $P_{i,new}$ converges to P_i . Three iterations were found to be sufficient for convergence.

Step 6: Find the inlet enthalpy h_i at the inlet temperature T_i and the converged inlet pressure P_i . Using the saturated liquid and vapor properties at the channel exit pressure P, find the pseudo-inlet quality X_i^*, and then calculate the CHF using the equation given below.

$$X_i^* = \frac{h_i - h_{fo}}{h_{fg,o}}$$

$$\frac{q_c}{G\, h_{fg,o}} = \frac{C_1 \left(\frac{G^2 D}{\rho_f \sigma} \right)^{C_2} (\rho_f/\rho_g)^{C_3} \left[1 - C_4 (\rho_f/\rho_g)^{C_5} X_i^* \right]}{1 + 4 C_1 C_4 \left(\frac{G^2 D}{\rho_f \sigma} \right)^{C_2} (\rho_f/\rho_g)^{C_3 + C_5} (L_h/D_h)}$$

where $C_1 = 0.0722$, $C_2 = -0.312$, $C_3 = -0.644$, $C_4 = 0.900$, $C_5 = 0.724$

Iterate over Steps 2 to 6 until q_c calculated in Step 6 converges to $q_{c,guess}$ assumed in Step 2. The converged value is the desired CHF.

APPENDIX B. COMPARISON OF HEAT FLUXES AT ONB, OFI, AND CHF

The onset of nucleate boiling (ONB), onset of flow instability OFI), and CHF are the three limiting heat fluxes that are used to determine the maximum allowed operating power of a research reactor. The three limiting heat fluxes (calculated using the Bergles and Rohsenow ONB correlation, the Whittle-Forgan OFI correlation with $\eta = 32.5$, and the extended Groeneveld 2006 CHF table) are plotted and compared in Fig. 7 over the mass flux range of 1000 to 25000 kg/m^2-s. The calculations were done for 72 cases (6 exit pressures × 4 heated diameters × 3 inlet temperatures) for each of 3 heated lengths, altogether 216 cases. However, only 18 cases are shown in Fig. 7 (having 18 parts) for the following values of parameters. For brevity, only one of the 3 inlet temperatures (30, 50, 70 °C) and only one of the 4 heated diameters (3, 4, 6, 8 mm) are plotted in Fig. 7.

3 heated lengths L_h = 0.28, 0.61, 1.18 m, 6 exit pressures P = 1, 5, 10, 20, 30, 50 bar,
Heated diameter D_h = 4 mm, Inlet temperature T_{in} = 30 °C

The CHFs obtained by the extended Groeneveld 2006 table and the Hall-Mudawar inlet conditions correlation (ICC) were found to be in close agreement and the most reliable available at present[8]. However, the CHF obtained by the extended Groeneveld 2006 table, rather than the Hall-Mudawar ICC, was preferred for plotting in Fig. 7 because the former is applicable to both subcooled and saturated CHF (i.e., when the thermodynamic quality is negative or positive) whereas the latter is applicable to subcooled CHF only. In some of the 216 cases mentioned above, the Hall-Mudawar ICC is therefore found to be inapplicable, as shown by the extensive comparison of these two correlations in Fig. 8 (having 36 parts) in Appendix C.

The OFI heat flux obtained by the Whittle-Forgan correlation, rather than the Saha-Zuber correlation, was preferred for plotting in Fig. 7 because the former is a correlation for the onset of *flow instability* whereas the latter is actually a correlation for the onset of *significant void* (OSV) or bubble detachment from the heated wall[5]. Basically, the OSV occurs before flow instability and is therefore used as a slightly early indicator of flow instability as indicated by Whittle-Forgan[4] and others[3]. This is also found in the extensive comparison of these two correlations in Fig. 10 (having 36 parts) in Appendix D.

It is important to note in Fig. 7 that there is an intersection of the OFI heat flux and CHF at a certain mass flux and heat flux in 13 out of the 18 cases plotted. The point of intersection is referred to as the reversal point. The corresponding mass flux and heat flux are referred to as the reversal mass flux (G_{rev}) and reversal heat flux (q_{rev}).

It is noted in Fig. 7 Part 13 that the ONB and OFI heat fluxes are practically equal in this case, i.e., the case with P = 1 bar, D_h = 4 mm, L_h = 1.18 m, and T_{in} = 30 °C. This plot was found to be reliable by studying the difference between the OFI and ONB heat fluxes when the heated length is gradually increased from 0.28 to 1.18 m at fixed values of other parameters (P, D_h, T_{in} and mass flux G). With increasing heated length, the OFI and ONB heat fluxes both decrease. The OFI decreases faster than the ONB, making the difference between the two smaller and smaller. The difference becomes practically negligible at L_h = 1.18 m.

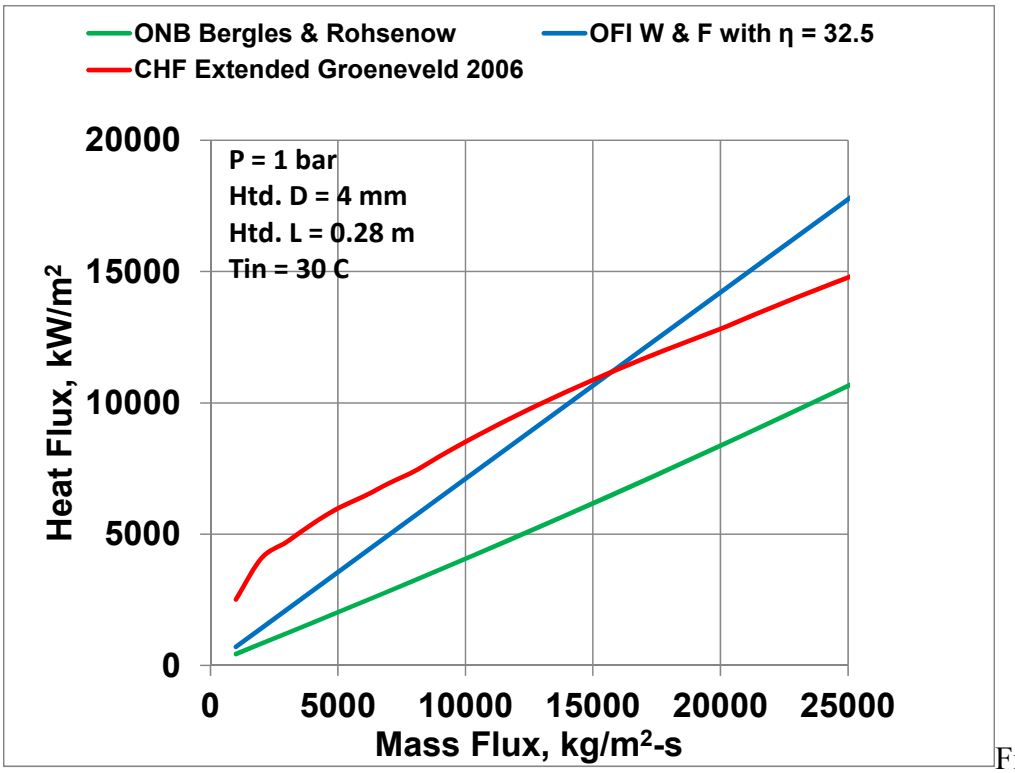

Fig. 7, Part 1 of 18

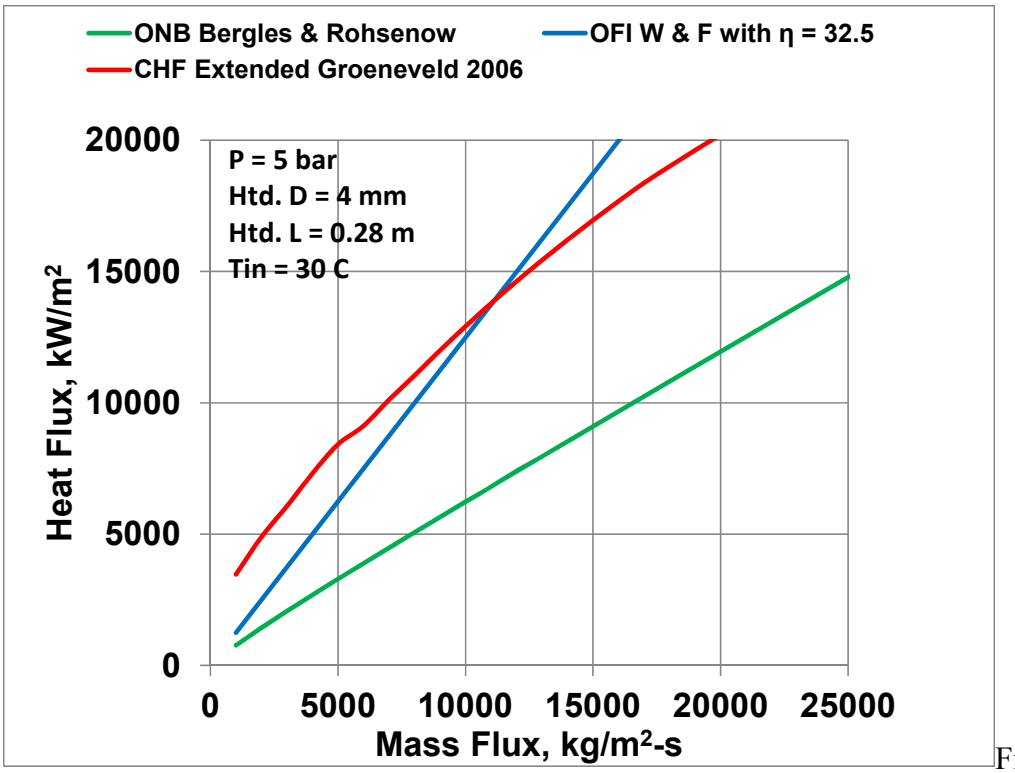

Fig. 7, Part 2 of 18

Fig. 7. Comparison of Heat Fluxes at CHF, OFI and ONB

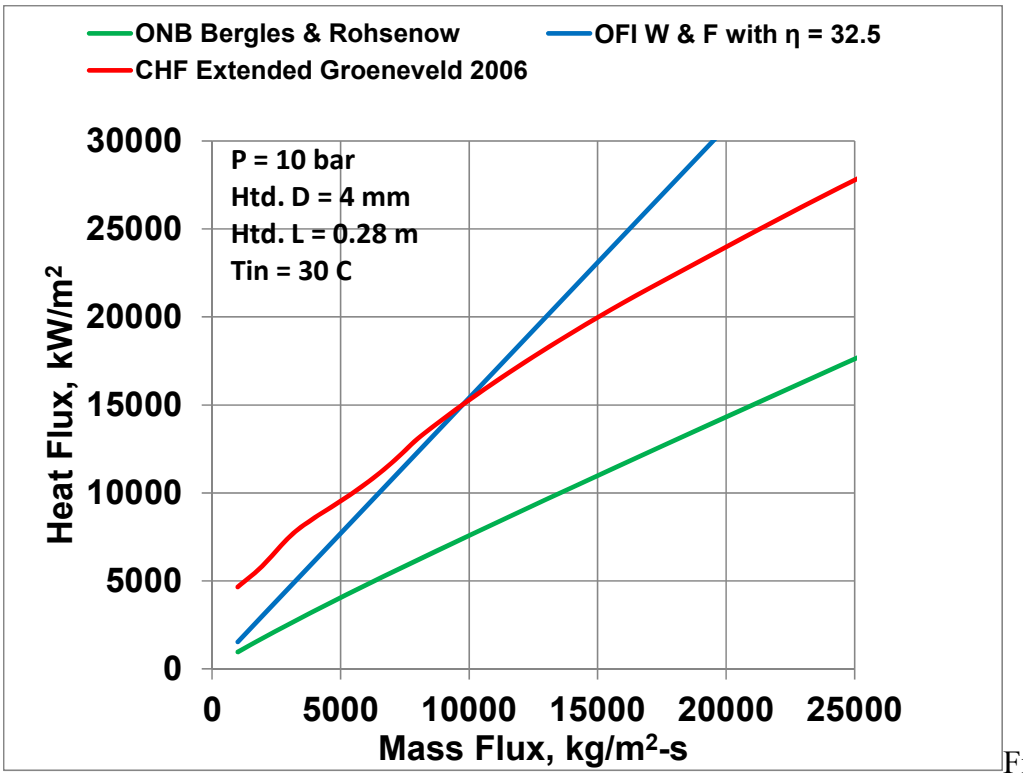

Fig. 7, Part 3 of 18

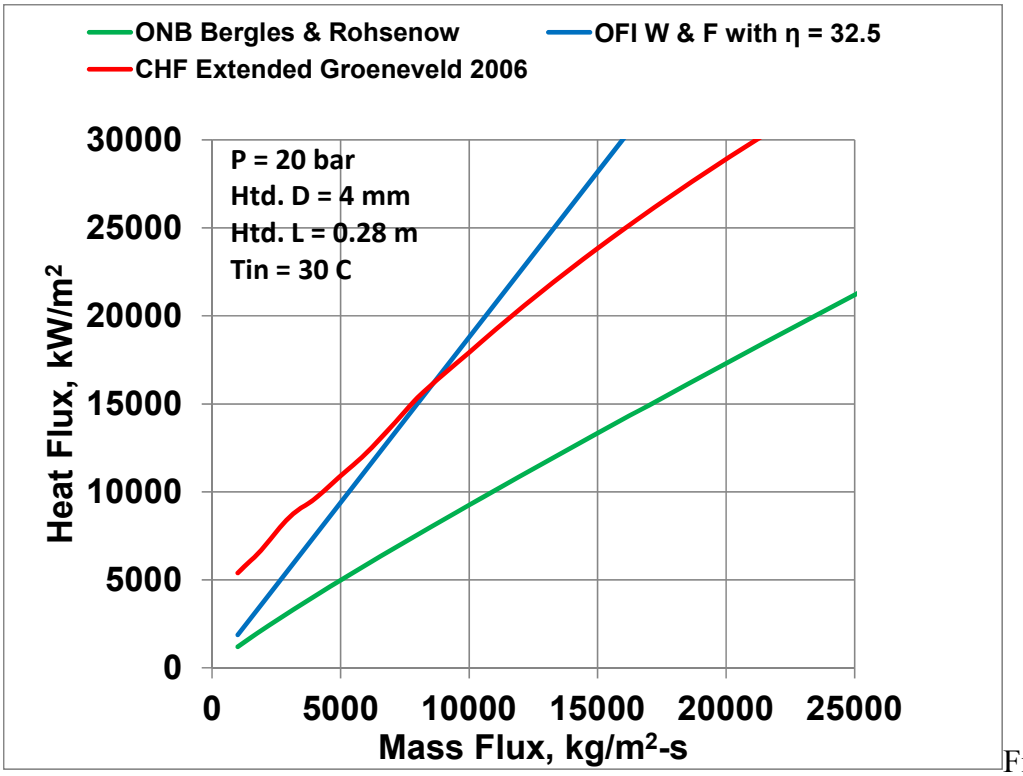

Fig. 7, Part 4 of 18

Fig. 7. Continued: Comparison of Heat Fluxes at CHF, OFI and ONB

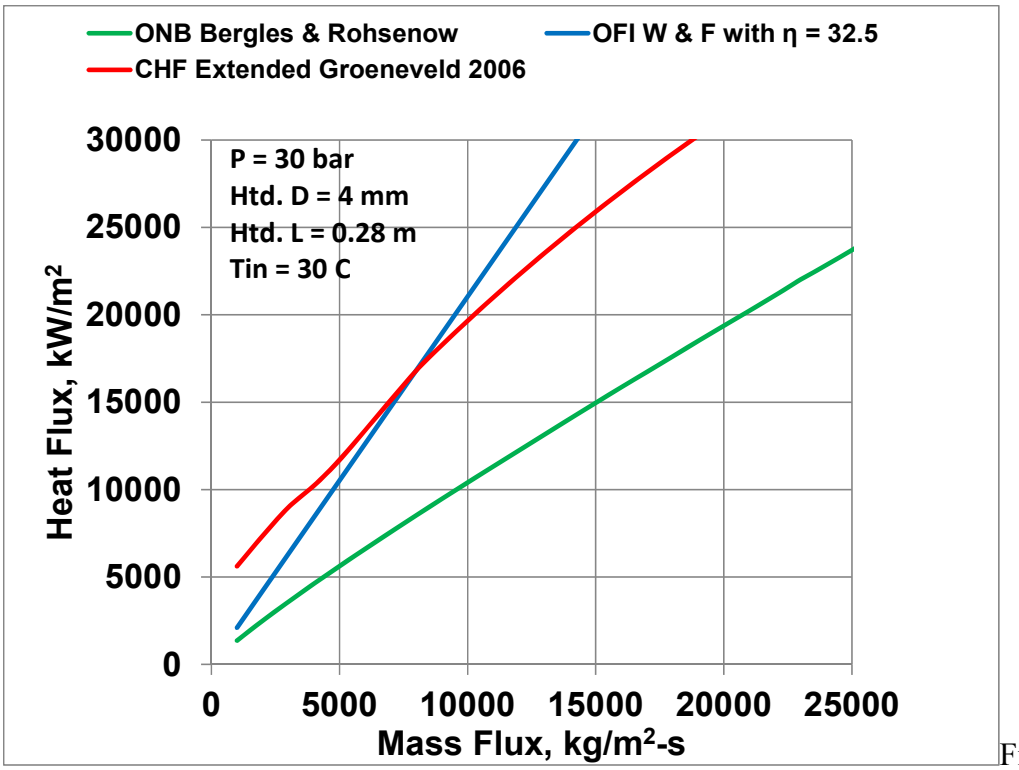

Fig. 7, Part 5 of 18

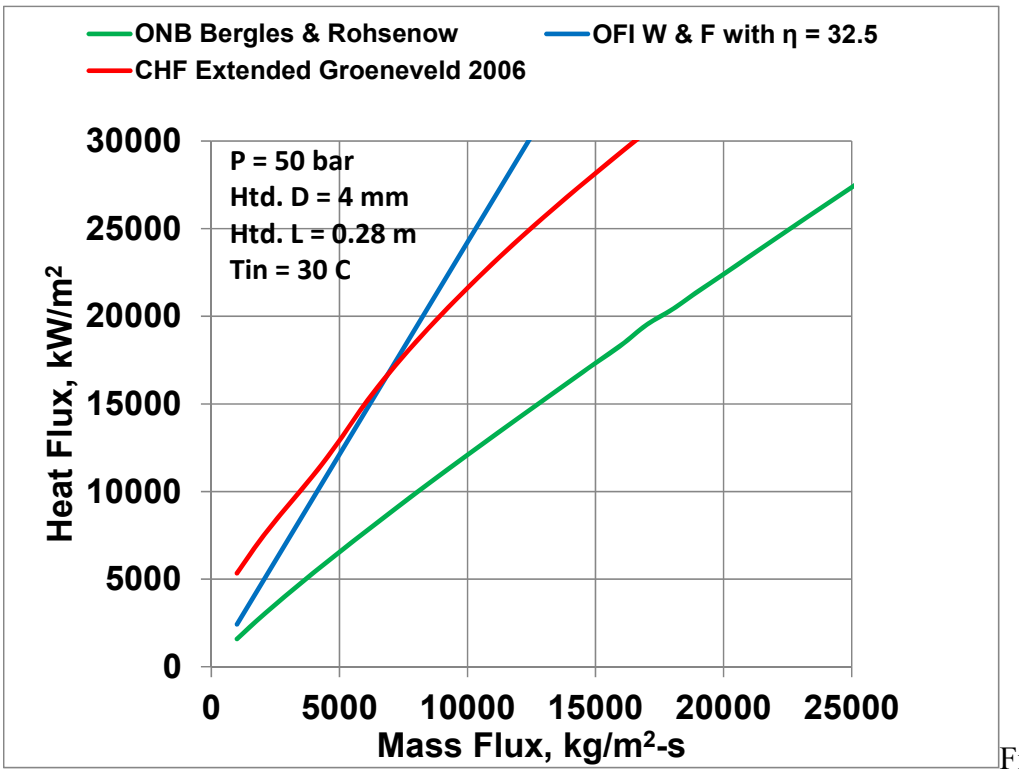

Fig. 7, Part 6 of 18

Fig. 7. Continued: Comparison of Heat Fluxes at CHF, OFI and ONB

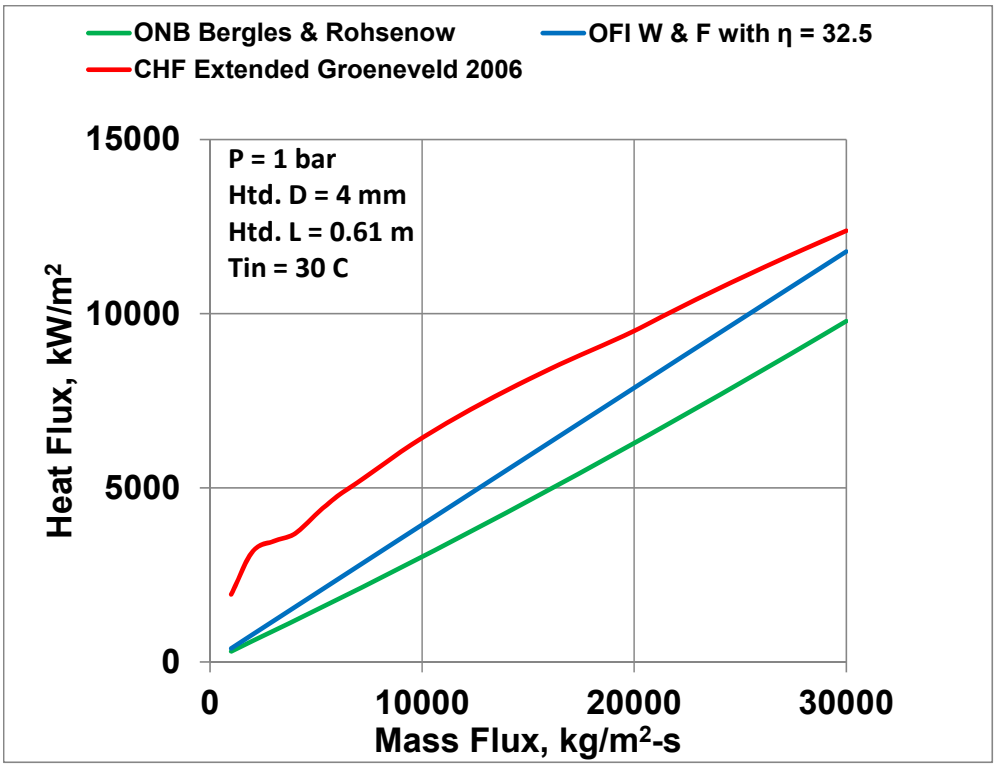

Fig. 7, Part 7 of 18

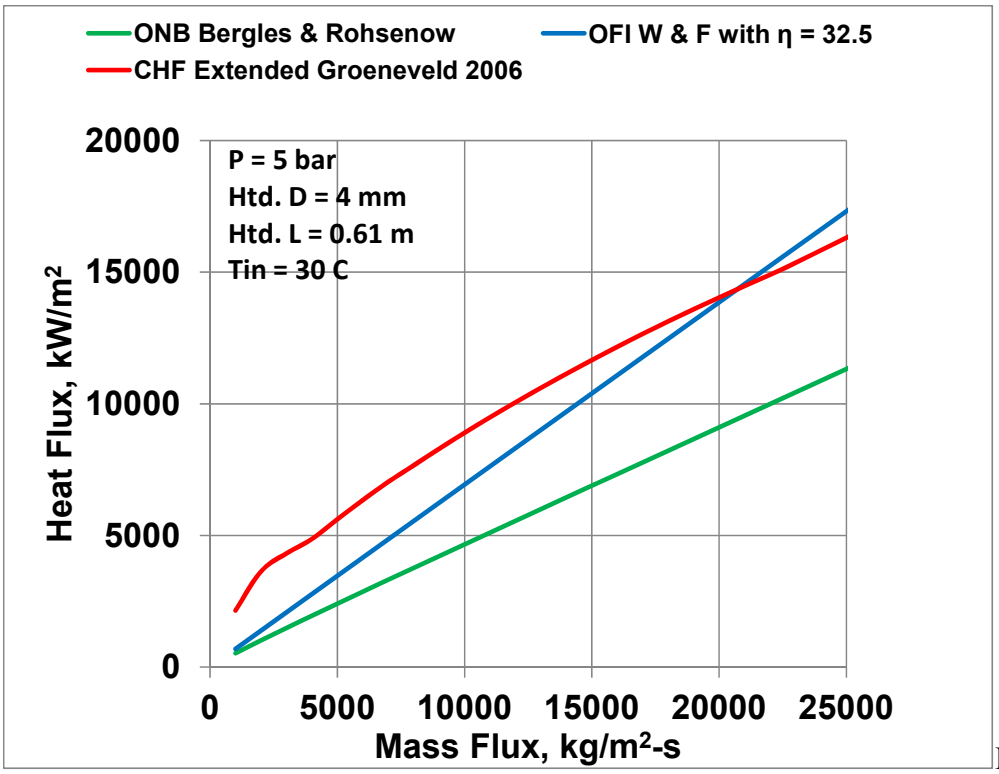

Fig. 7, Part 8 of 18

Fig. 7. Continued: Comparison of Heat Fluxes at CHF, OFI and ONB

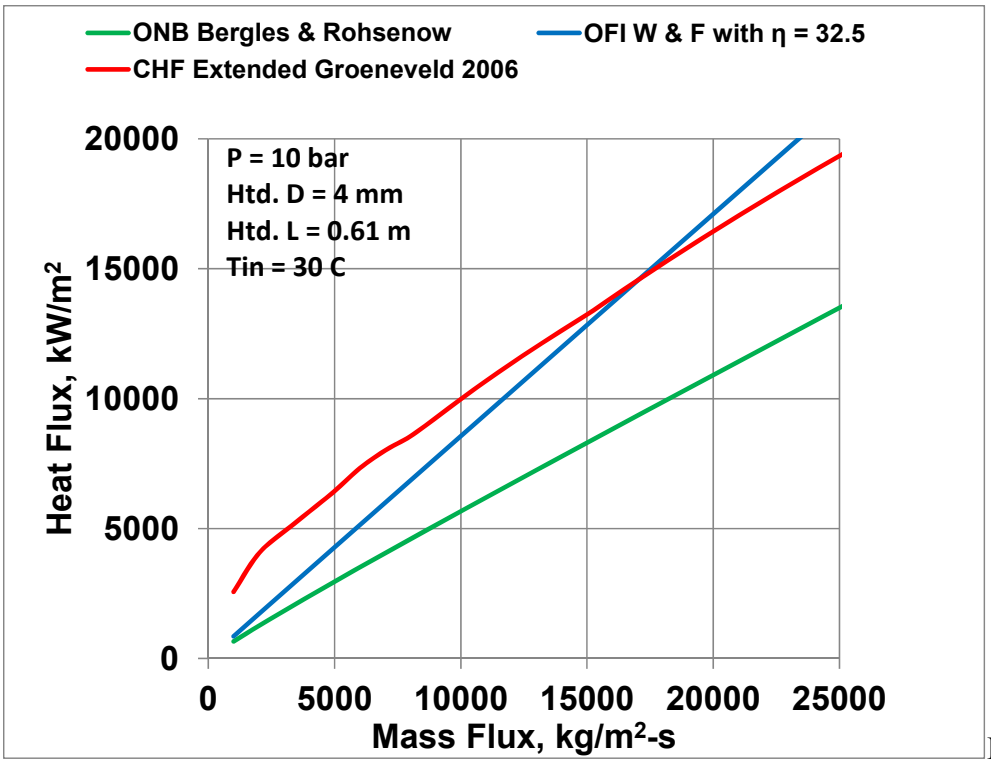

Fig. 7, Part 9 of 18

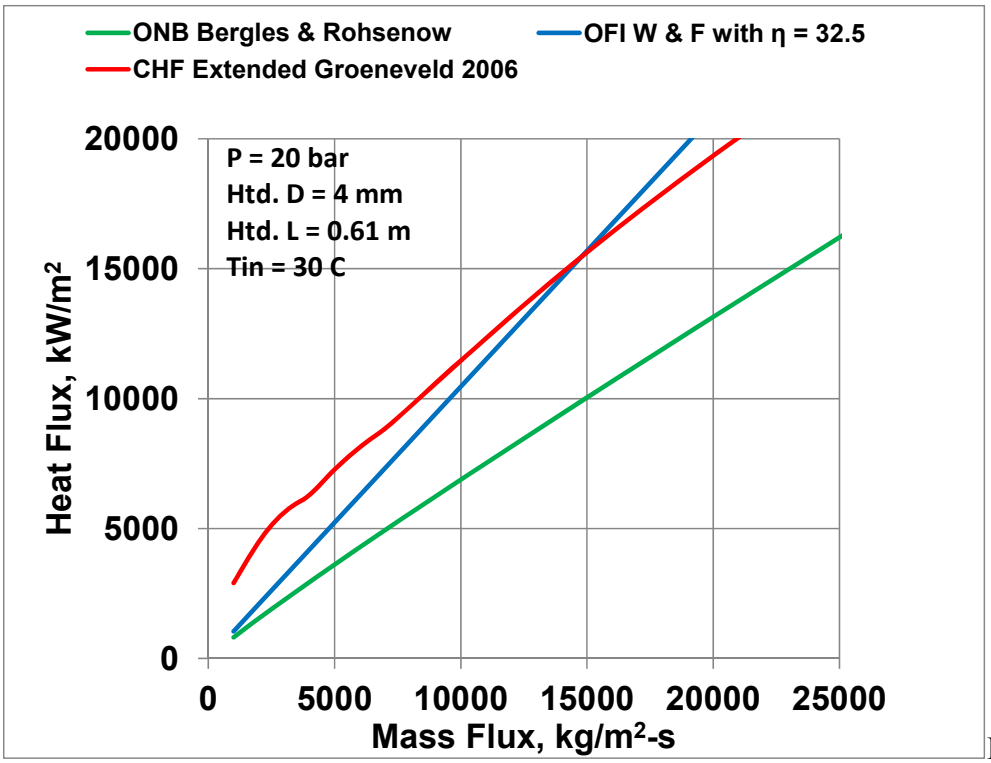

Fig. 7, Part 10 of 18

Fig. 7. Continued: Comparison of Heat Fluxes at CHF, OFI and ONB

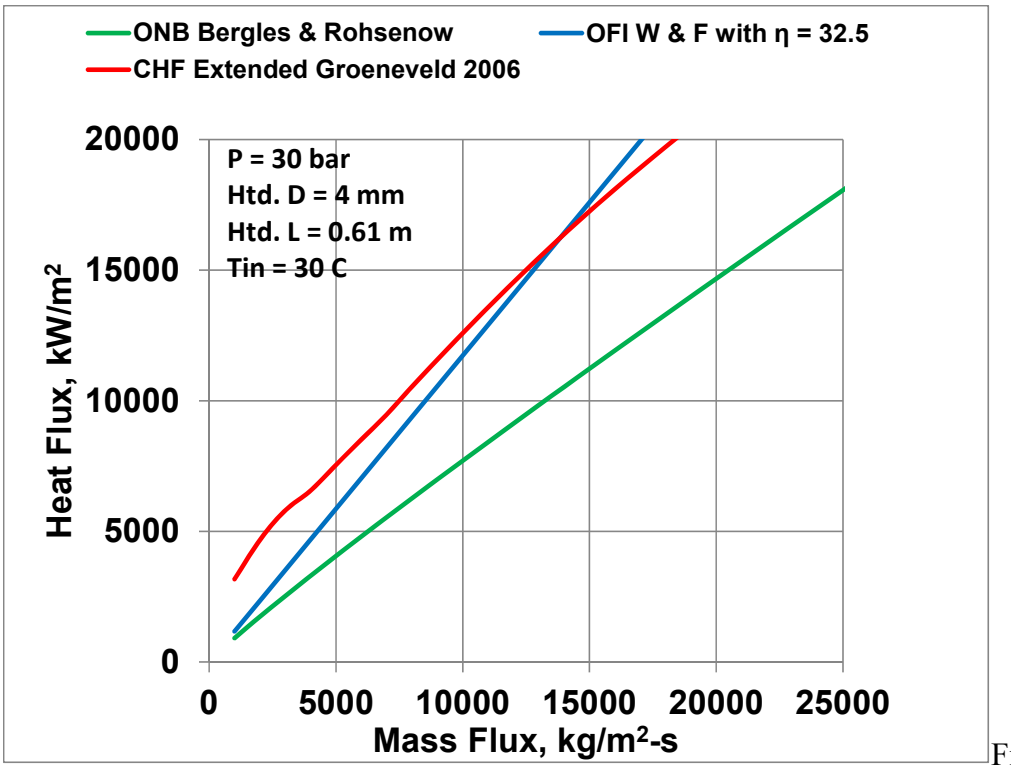

Fig. 7, Part 11 of 18

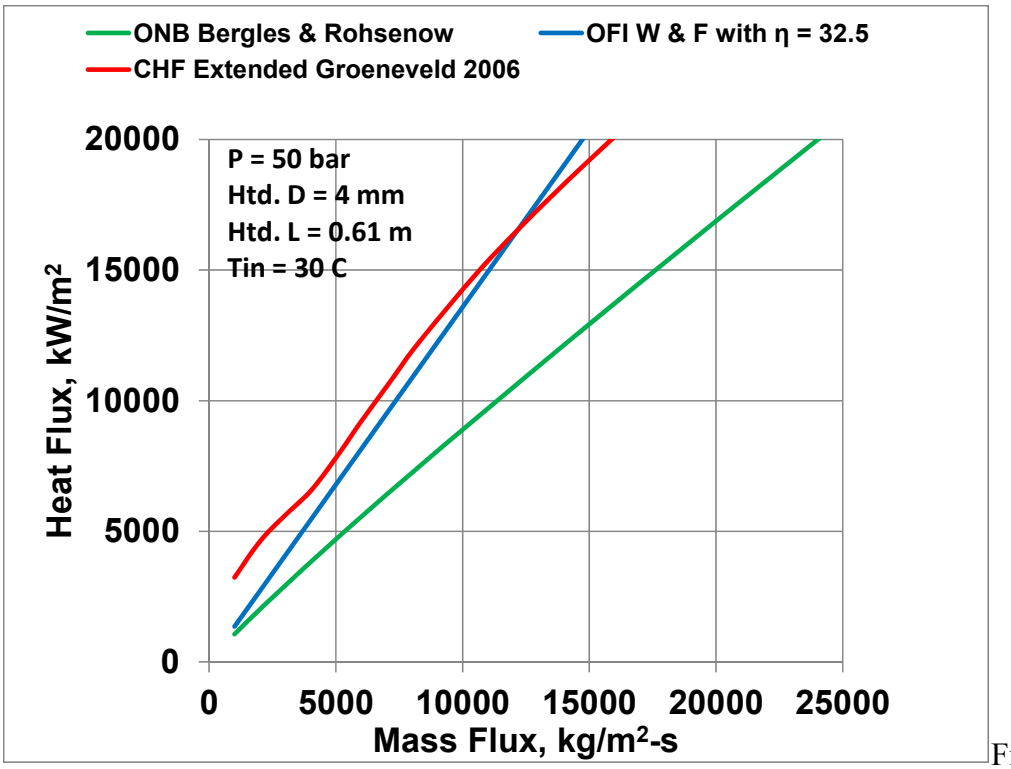

Fig. 7, Part 12 of 18

Fig. 7. Continued: Comparison of Heat Fluxes at CHF, OFI and ONB

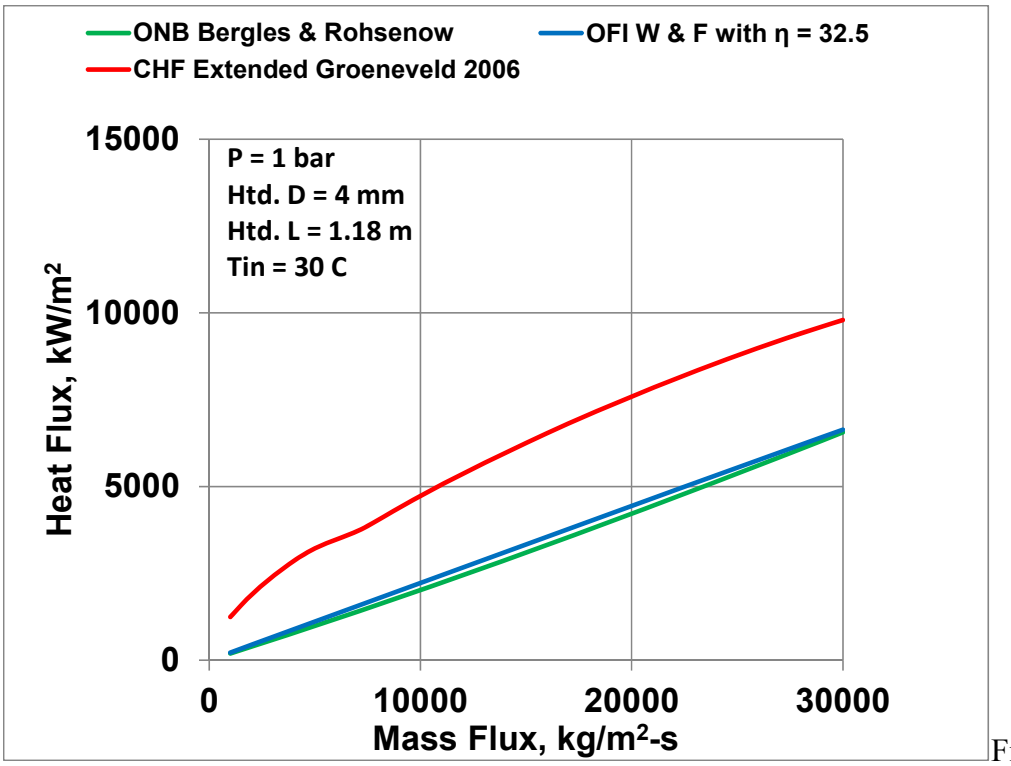

Fig. 7, Part 13 of 18

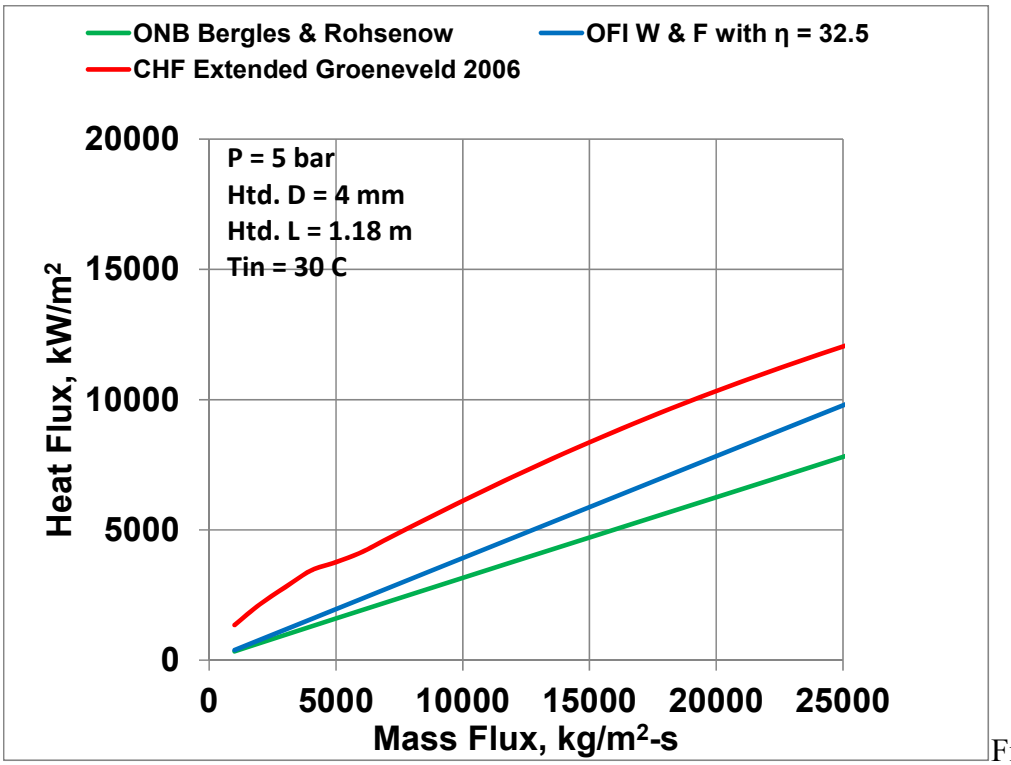

Fig. 7, Part 14 of 18

Fig. 7. Continued: Comparison of Heat Fluxes at CHF, OFI and ONB

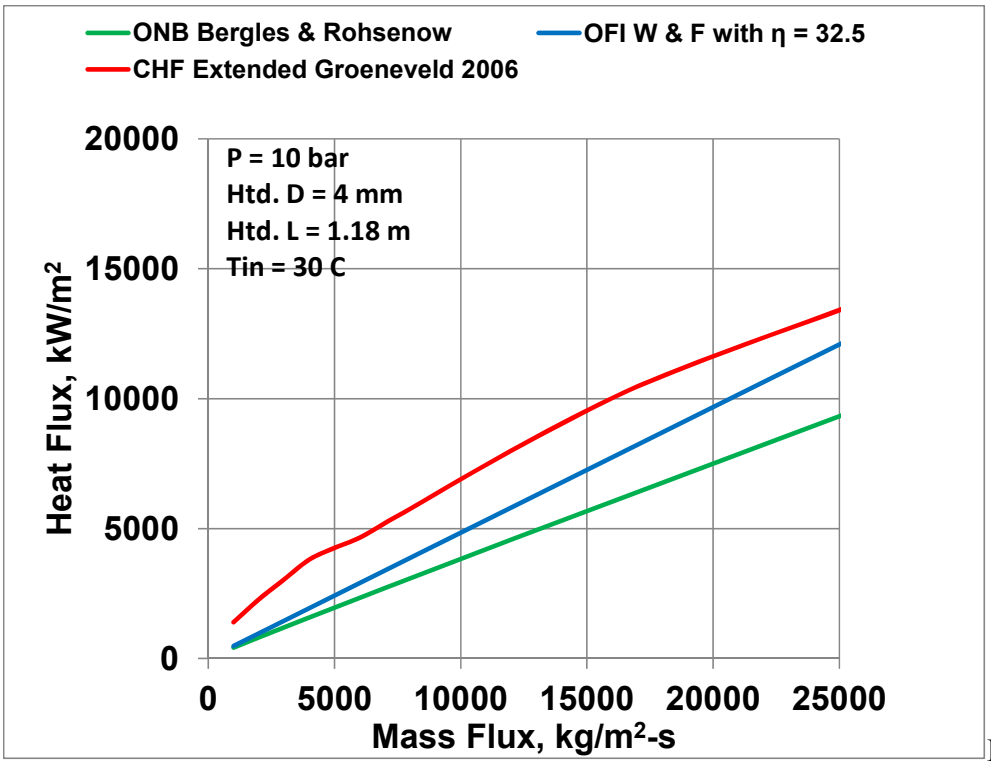

Fig. 7, Part 15 of 18

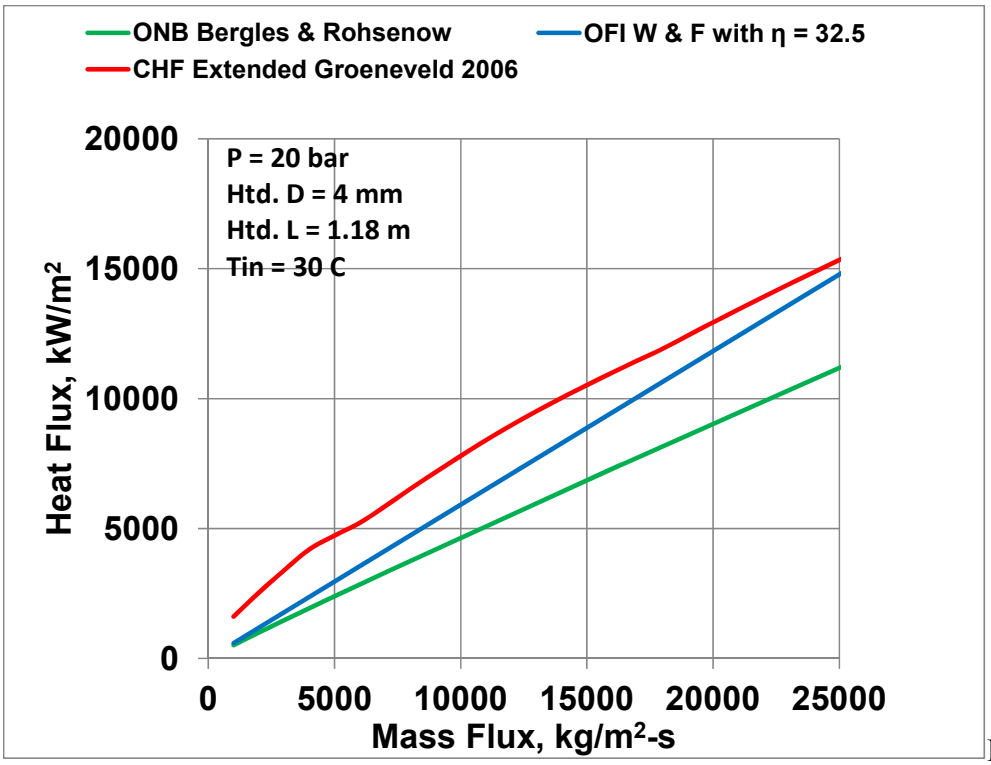

Fig. 7, Part 16 of 18

Fig. 7. Continued: Comparison of Heat Fluxes at CHF, OFI and ONB

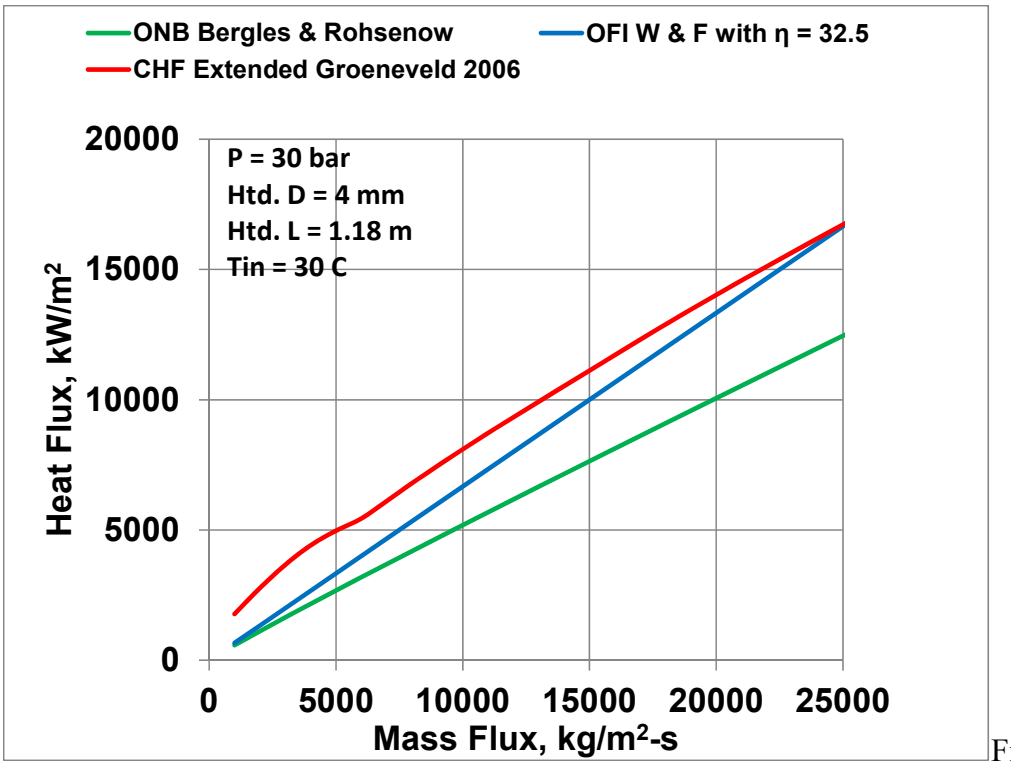

Fig. 7, Part 17 of 18

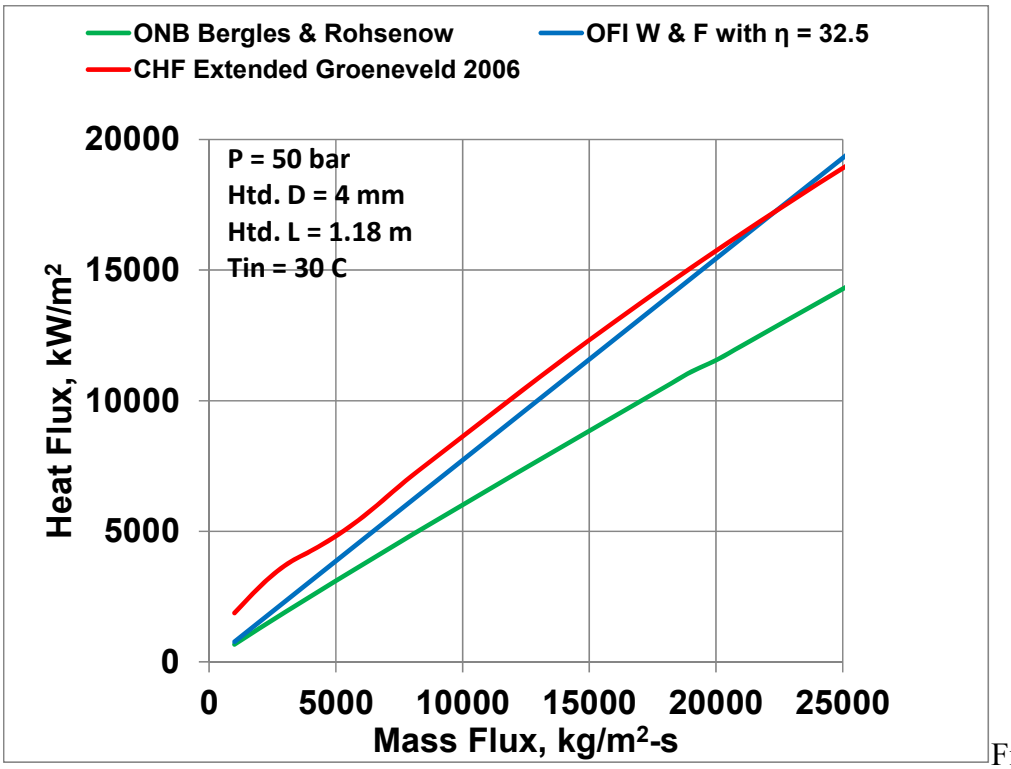

Fig. 7, Part 18 of 18

Fig. 7. Continued: Comparison of Heat Fluxes at CHF, OFI and ONB

APPENDIX C. COMPARISON OF CHFs BY THE EXTENDED GROENEVELD 2006 TABLE AND THE HALL-MUDAWAR INLET CONDITIONS CORRELATION

The critical heat flux (CHF) obtained by the extended Groeneveld 2006 table (calculated iteratively as described in Appendix A) was used in making the OFI-CHF reversal diagrams. Before plotting the reversal diagrams, the CHFs obtained by two world-class methods, the Groeneveld table and the Hall-Mudawar ICC were plotted and compared over the mass flux range of 1000 to 30000 kg/m^2-s for 72 cases (6 exit pressures × 4 heated diameters × 3 inlet temperatures) for each of 3 heated lengths, altogether 216 cases. The following are the values of the independent parameters:

3 heated lengths L_h = 0.28, 0.61, 1.18 m
6 exit pressures P = 1, 5, 10, 20, 30, 50 bar
4 heated diameters D_h = 3, 4, 6, 8 mm
3 inlet temperatures T_{in} = 30, 50, 70 º C

Figure 8 (having 36 parts) shows the comparison for all 216 cases. The blue curves are for the Groeneveld table and the red curves for the Hall-Mudawar inlet conditions correlation (ICC). Since the Hall-Mudawar ICC holds only for exit quality $X_o \leq 0$ (subcooled CHF), it is not plotted when the exit quality is positive. The exit quality relied upon here (for truncating the Hall-Mudawar curve) is that calculated using the value of CHF obtained by the Groeneveld table. Selected numerical results are also tabulated in Tables 4 to 9.

The difference between the two prediction methods over the 72 cases of each heated length is given in Table 3. There is a close agreement between the two prediction methods. The RMS difference is 8.50 %, 8.56 %, and 8.81 % for the heated lengths of 0.28, 0.61, and 1.18 m respectively. The comparison for all the data points in the 72 cases of heated length 0.28 m is shown in Fig. 2A. Figures 2B and 2C are similar plots for heated lengths of 0.61 m and 1.18 m. Comparing the scatter in these figures, it is obvious that the maximum absolute error for L_h=0.28 m is more than that for L_h=1.18 m. This observation is consistent with Table 3.

The CHF is a function of five independent parameters: P, L_h , D_h , G, and T_i . The effect of heated diameter D_h or inlet temperature T_i on the CHF obtained by the extended Groeneveld 2006 table is shown in Fig. 9 (having 18 parts). In these separate-effect plots, only one parameter is changed at a time, holding the other four parameters constant. The parts 1 to 6 of Fig. 9 are for L_h=0.28 m, the parts 7 to 12 for L_h=0.61 m, and the parts 13 to 18 for L_h=1.18 m. At each heated length, the CHF *increases* with increasing heated diameter at constant P, L_h , T_{in} , and G (see Fig. 9 parts 1 and 2) while the CHF *decreases* with increasing heated diameter at constant P, L_h , T_{in} , and X_o (see Fig. 9 parts 3 and 4). The CHF decreases with increasing inlet temperature at constant P, L_h , D_h , and G (see Fig. 9 parts 5 and 6).

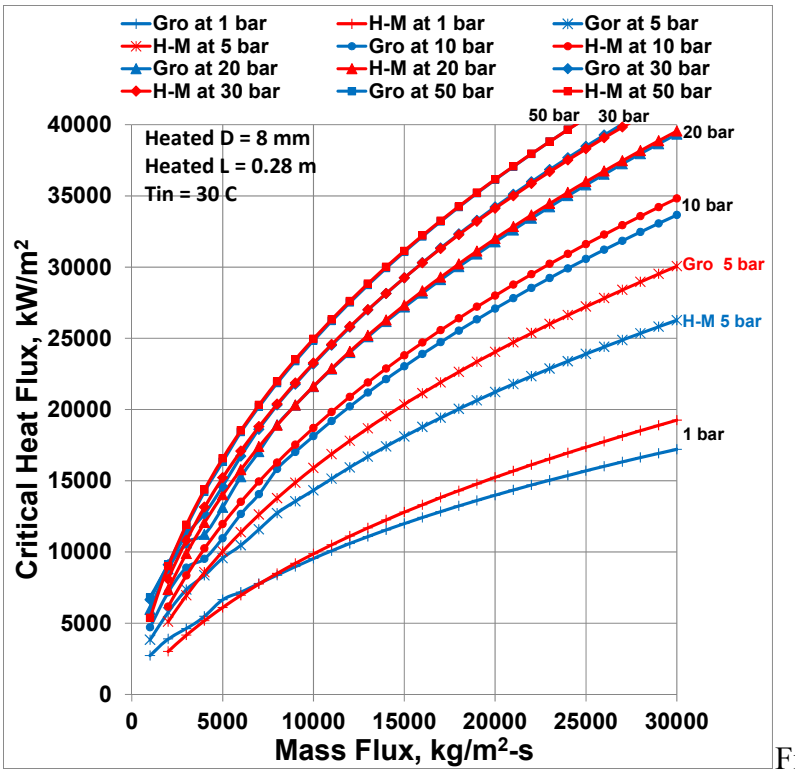

Fig. 8, Part 1 of 36

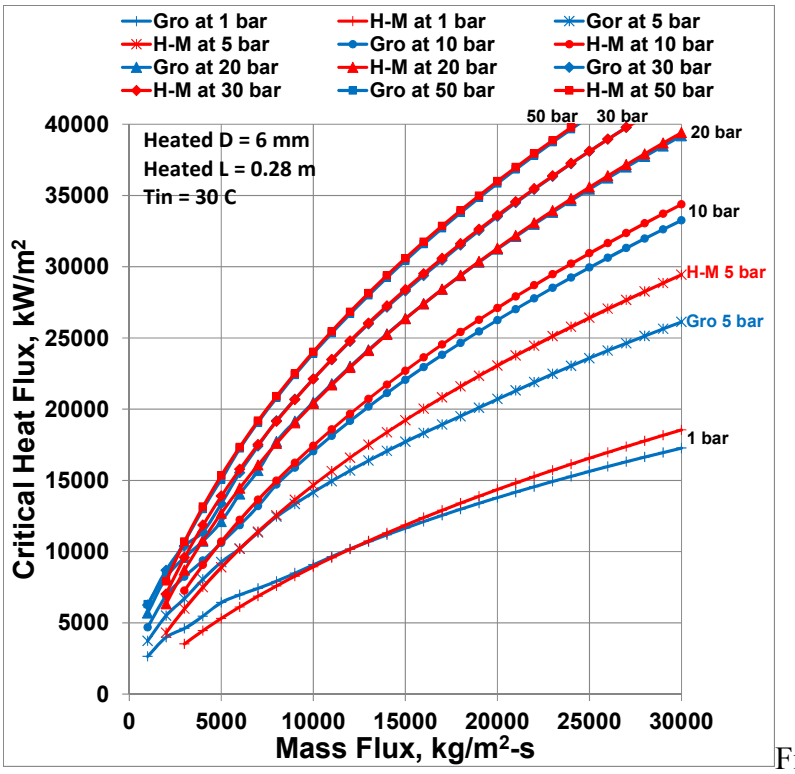

Fig. 8, Part 2 of 36

Fig. 8. Comparison of the Extended Groeneveld 2006 CHF Table and the Hall-Mudawar Inlet Conditions Correlation

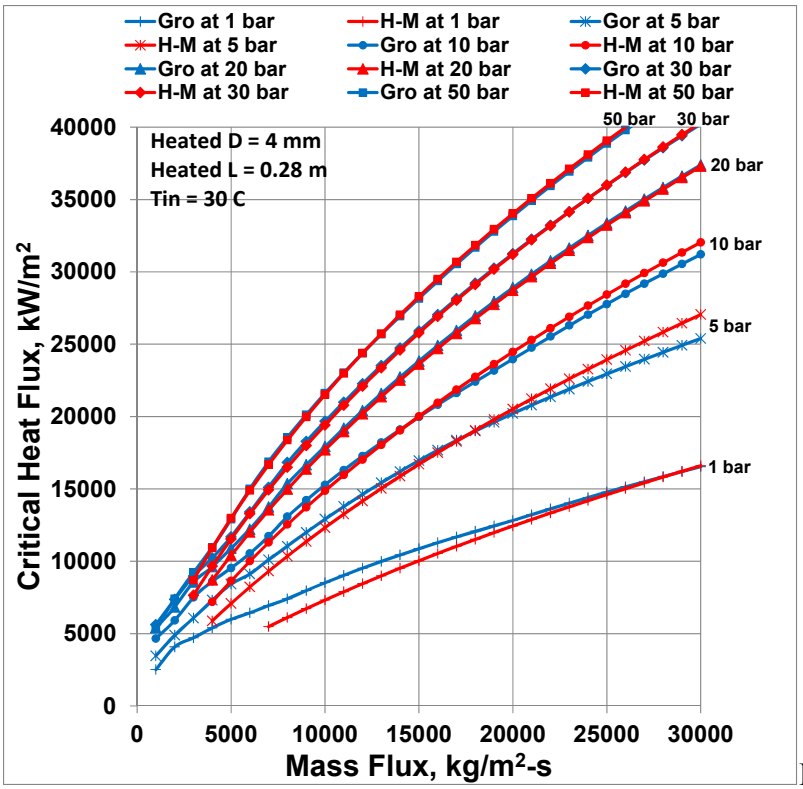

Fig. 8, Part 3 of 36

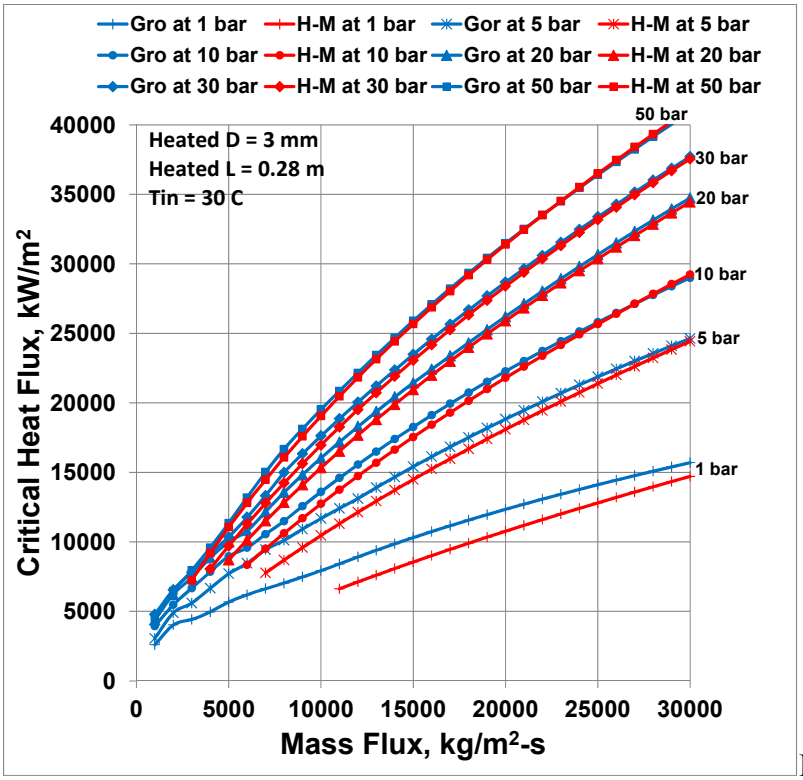

Fig. 8, Part 4 of 36

Fig. 8. Continued

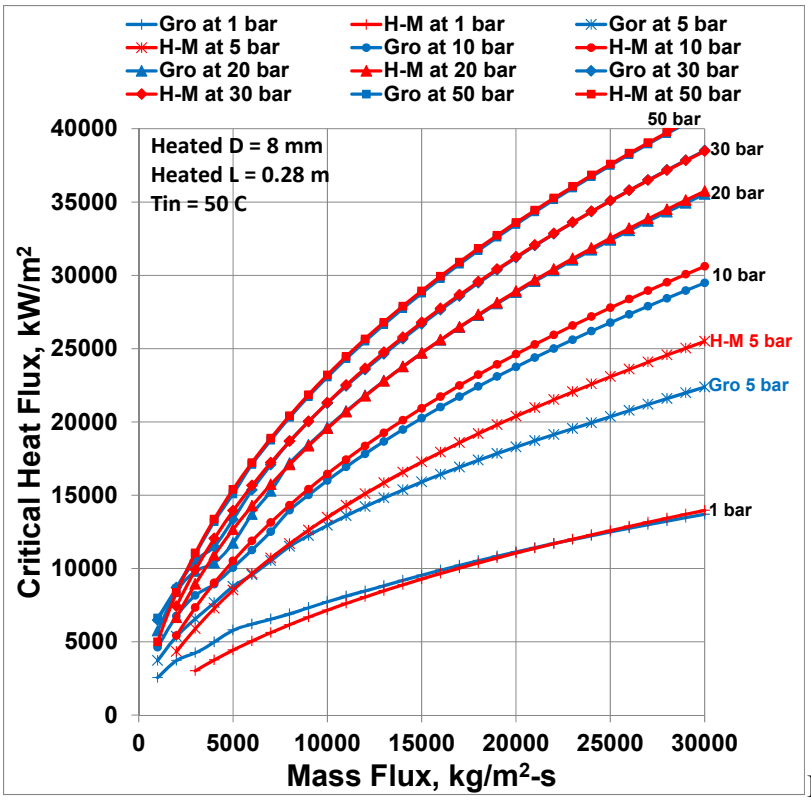

Fig. 8, Part 5 of 36

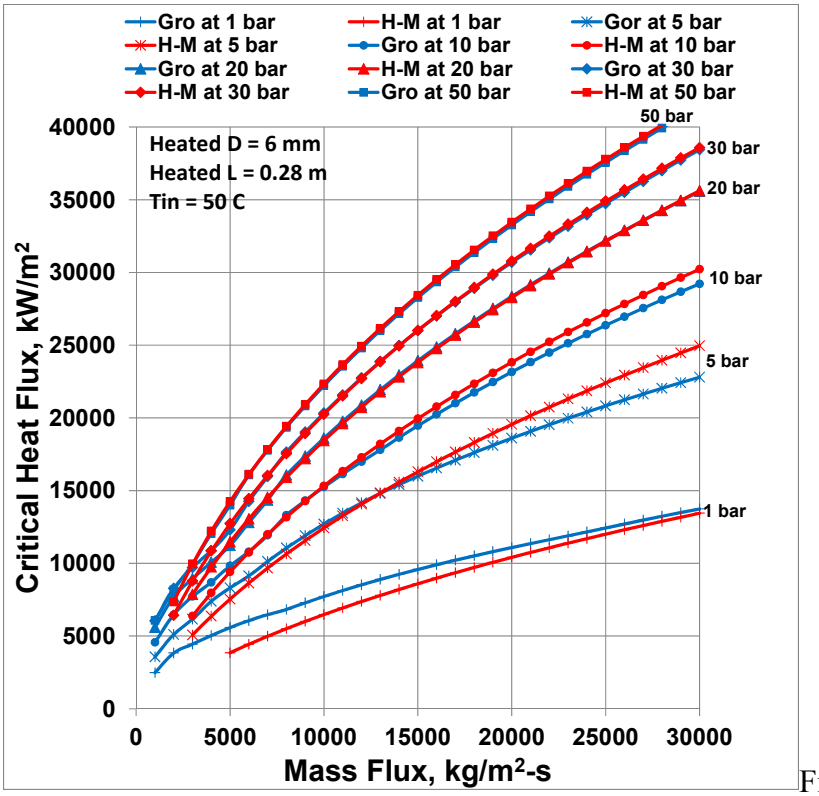

Fig. 8, Part 6 of 36

Fig. 8. Continued

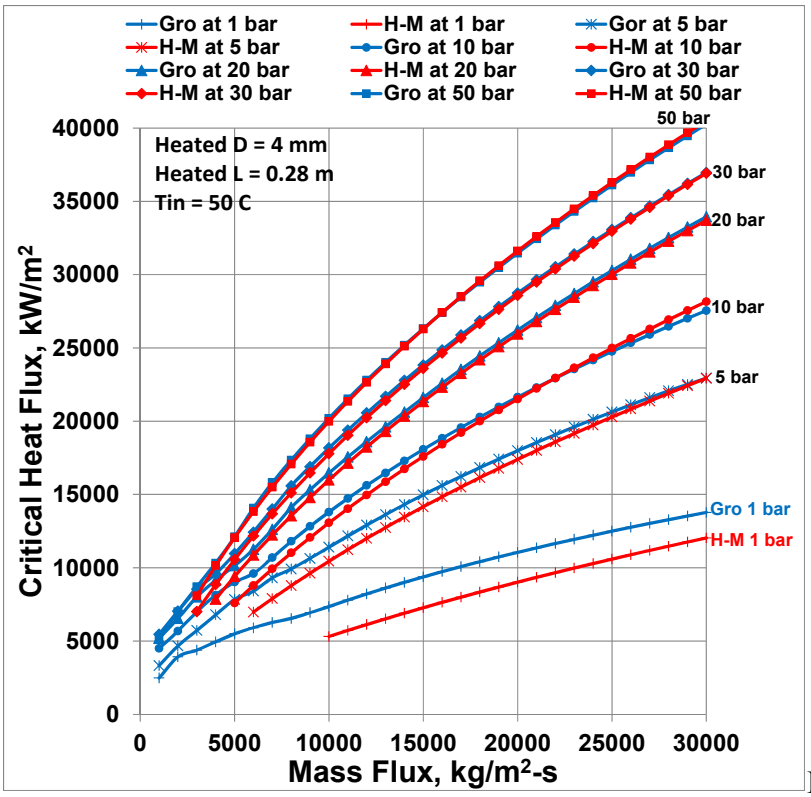

Fig. 8, Part 7 of 36

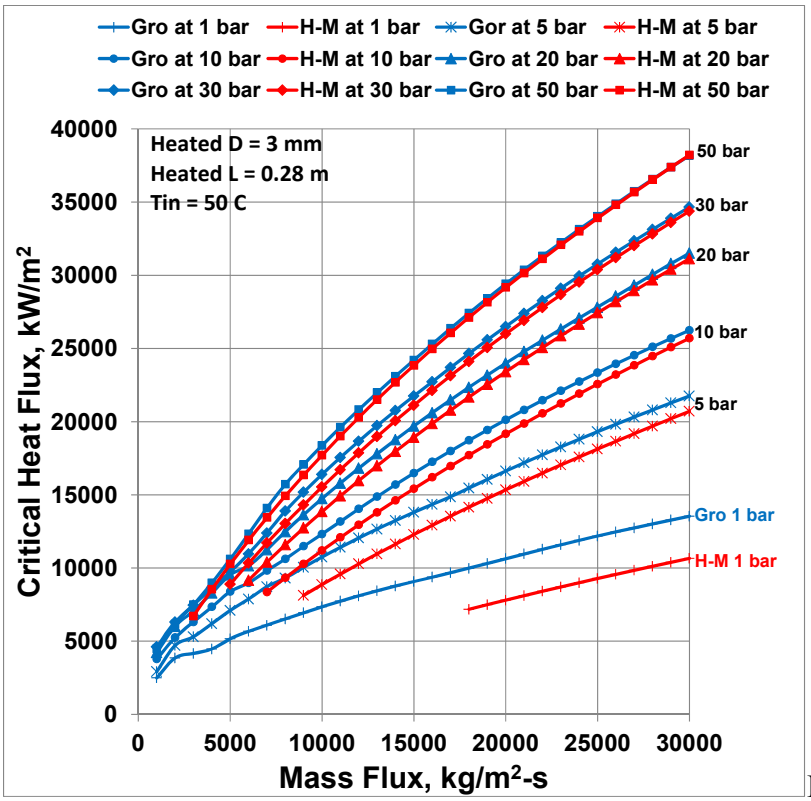

Fig. 8, Part 8 of 36

Fig. 8. Continued

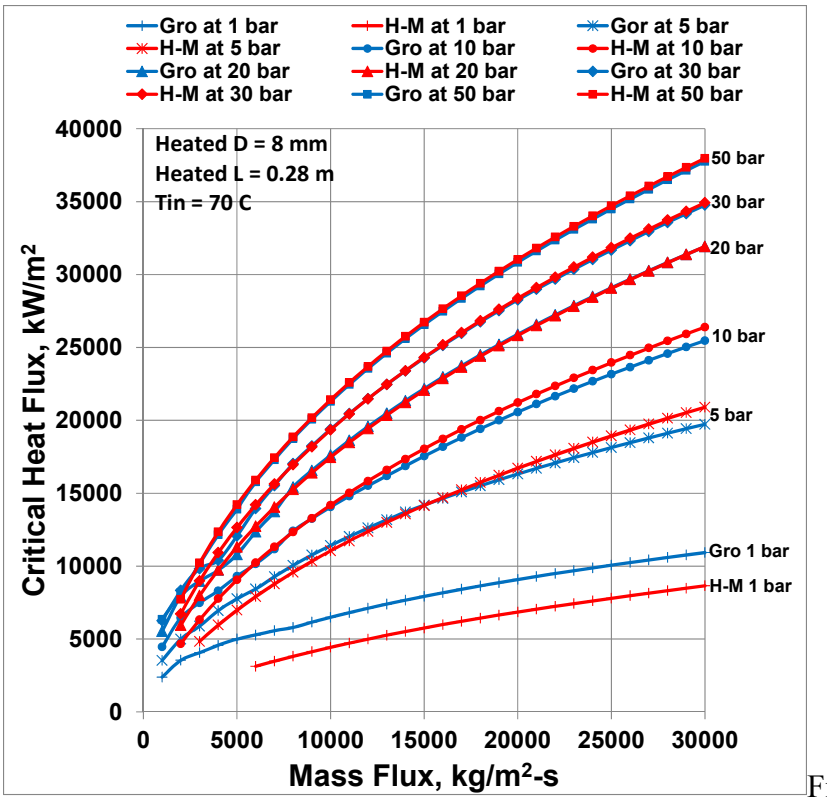

Fig. 8, Part 9 of 36

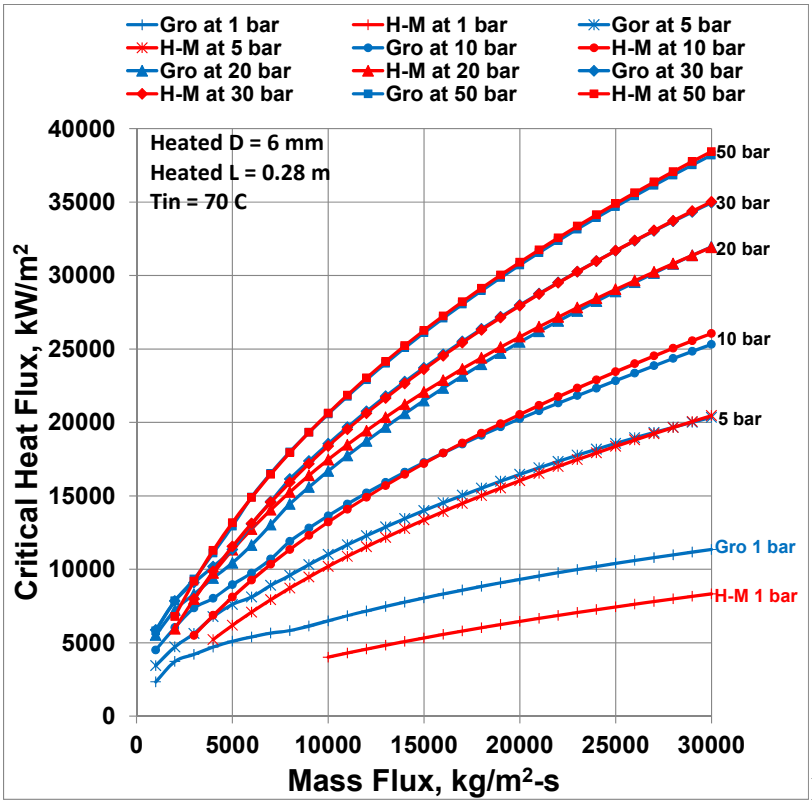

Fig. 8, Part 10 of 36

Fig. 8. Continued

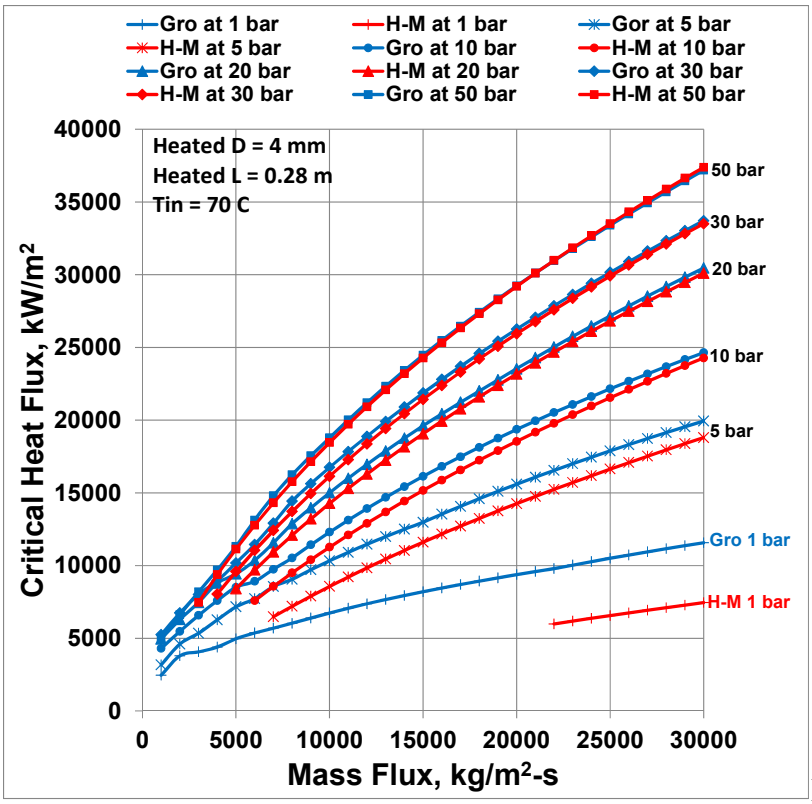

Fig. 8, Part 11 of 36

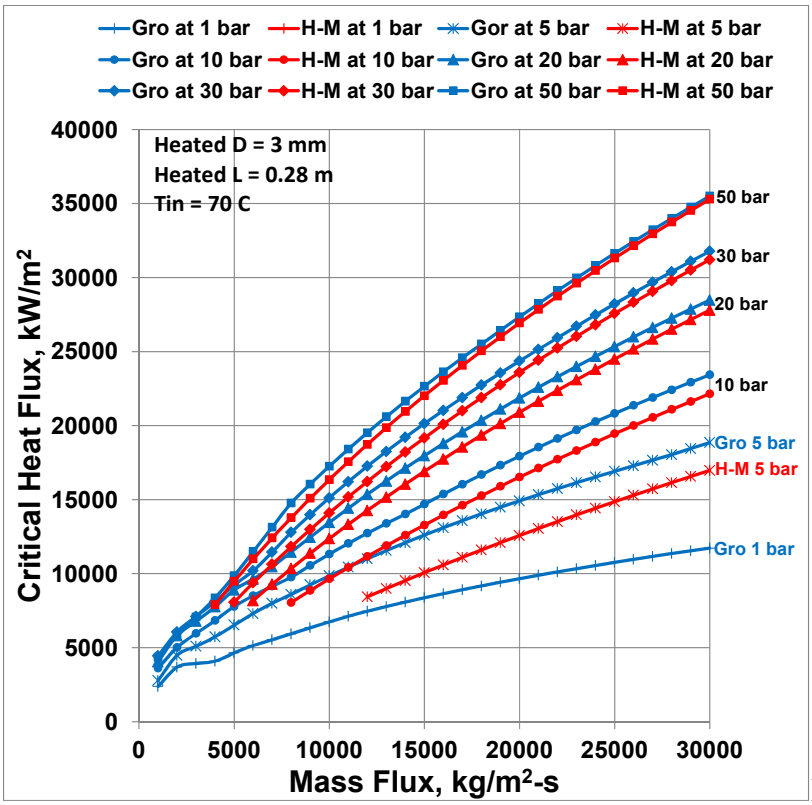

Fig. 8, Part 12 of 36

Fig. 8. Continued

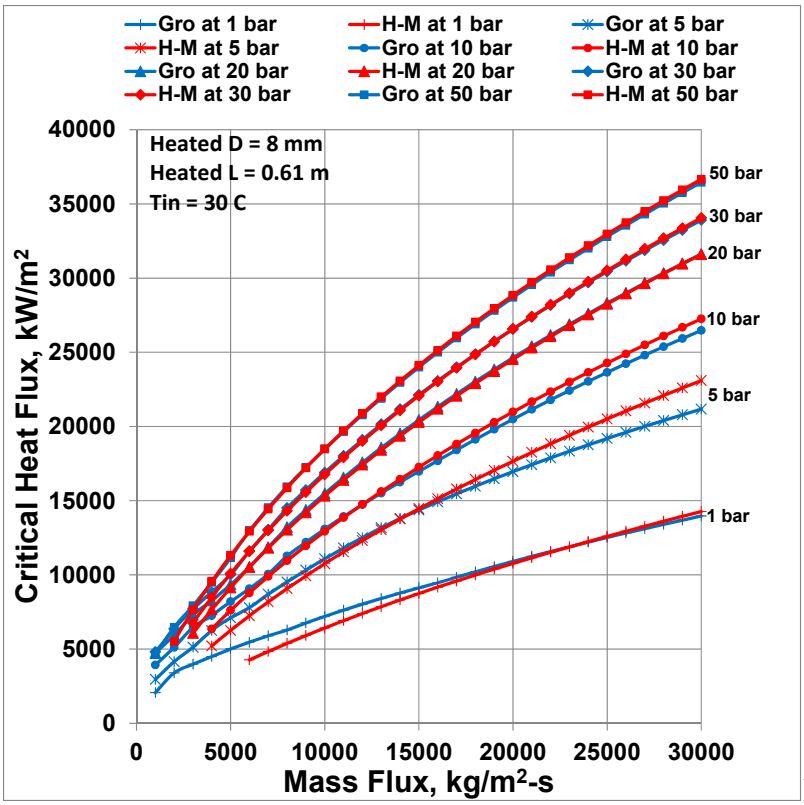

Fig. 8, Part 13 of 36

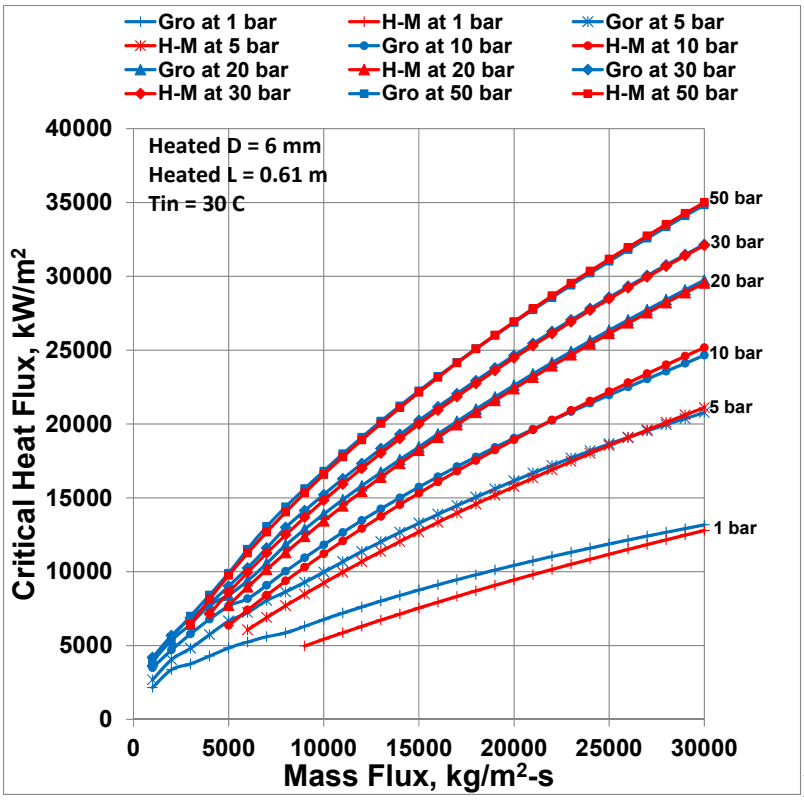

Fig. 8, Part 14 of 36

Fig. 8. Continued

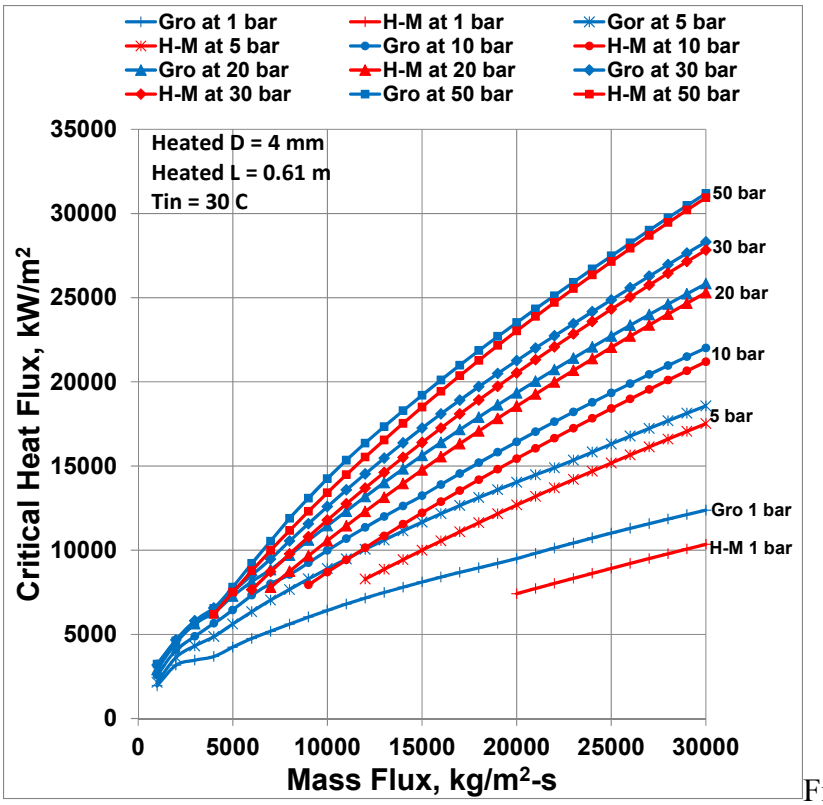

Fig. 8, Part 15 of 36

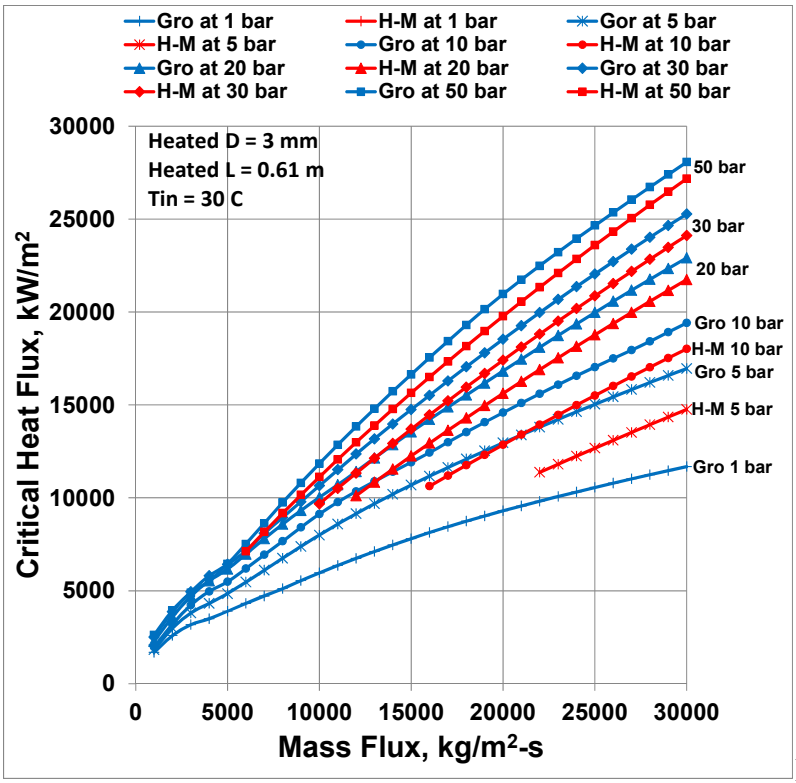

Fig. 8, Part 16 of 36

Fig. 8. Continued

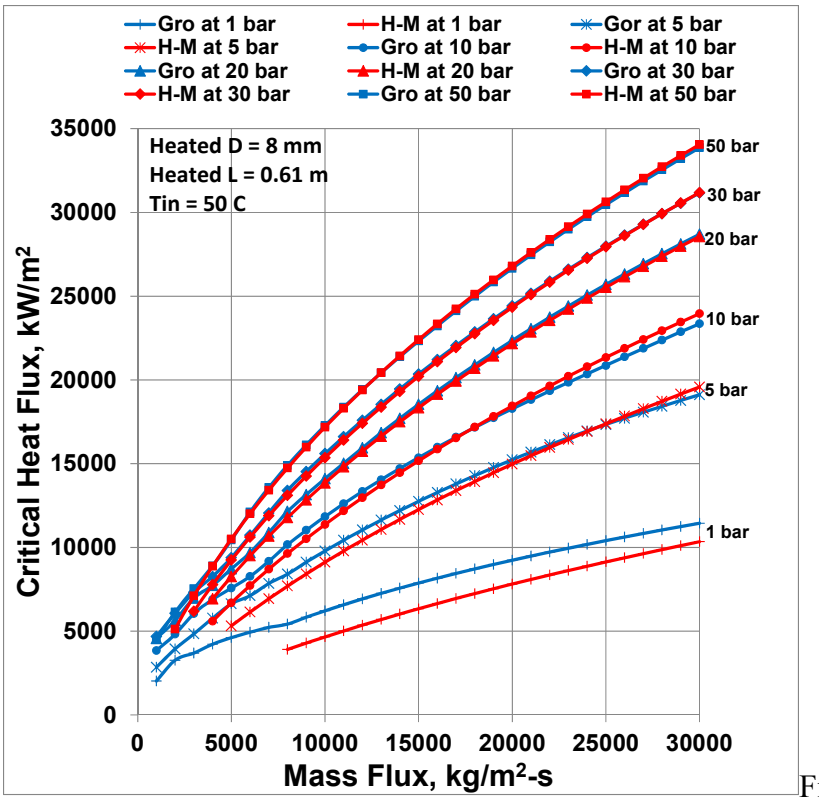

Fig. 8, Part 17 of 36

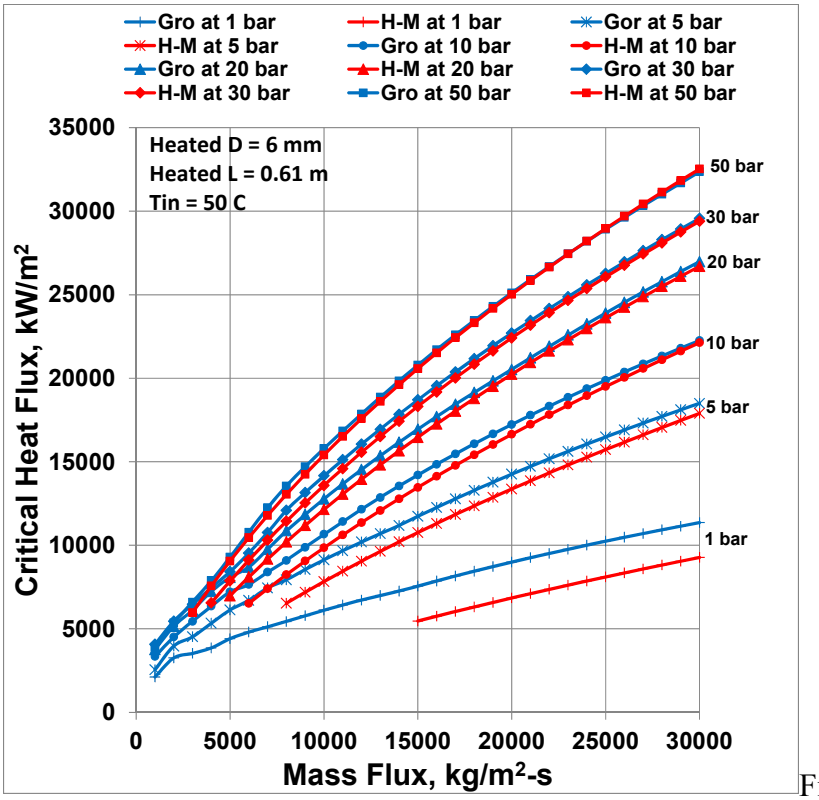

Fig. 8, Part 18 of 36

Fig. 8. Continued

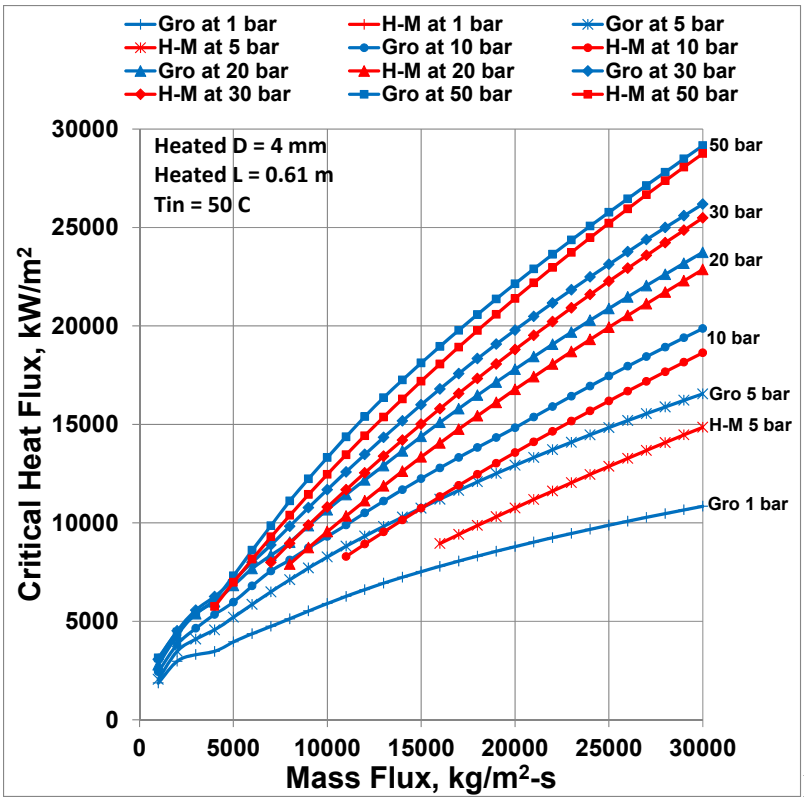

Fig. 8, Part 19 of 36

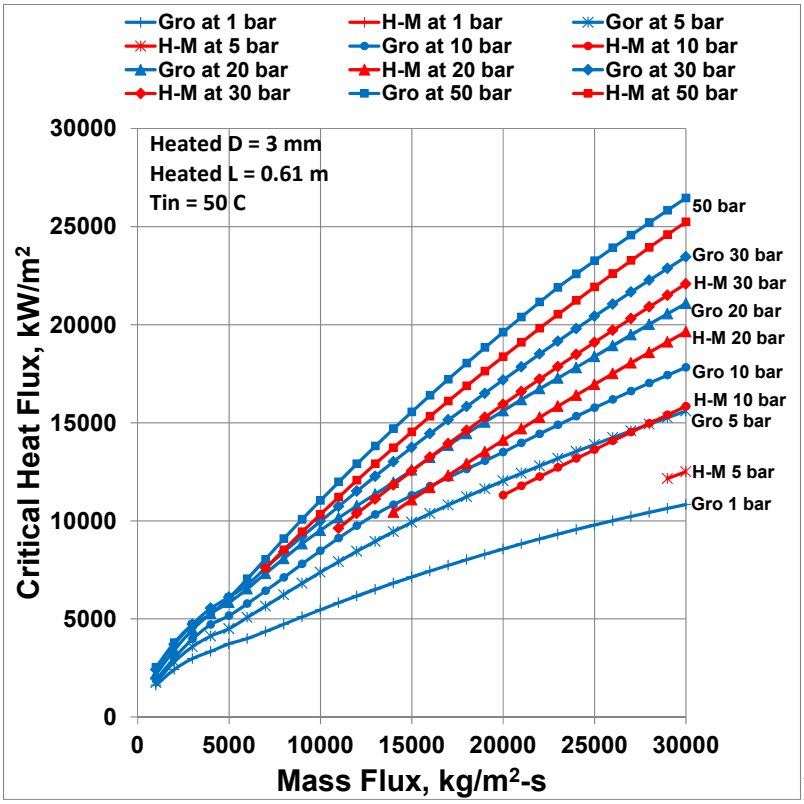

Fig. 8, Part 20 of 36

Fig. 8. Continued

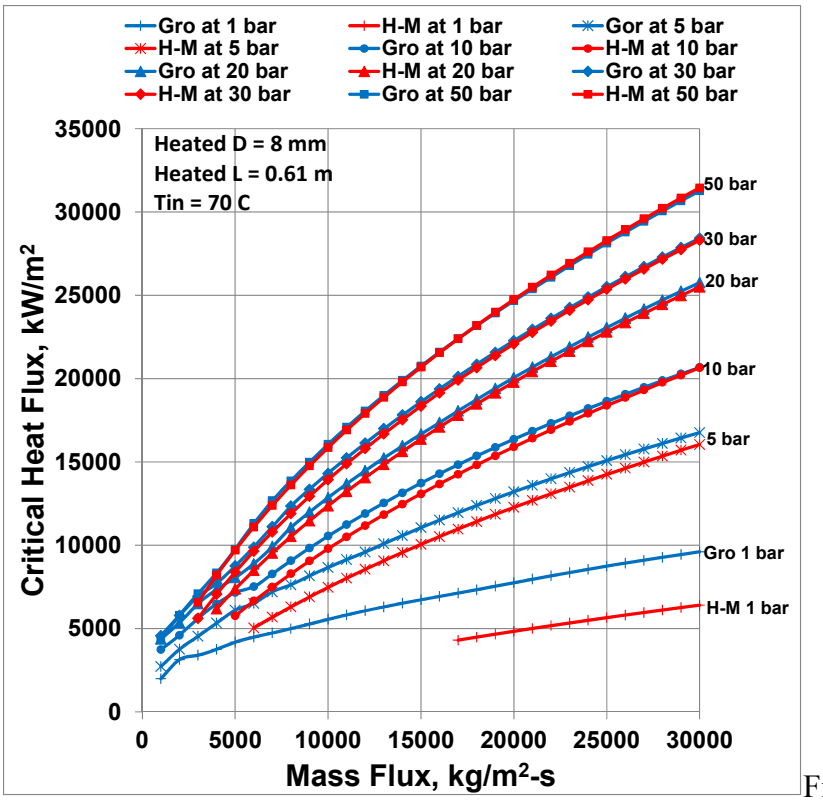

Fig. 8, Part 21 of 36

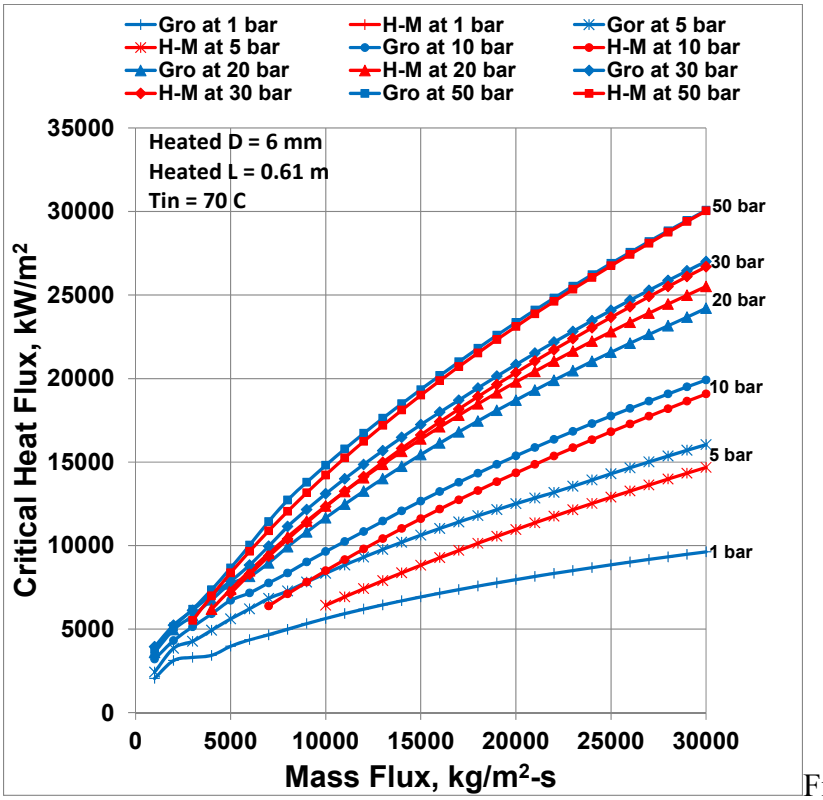

Fig. 8, Part 22 of 36

Fig. 8. Continued

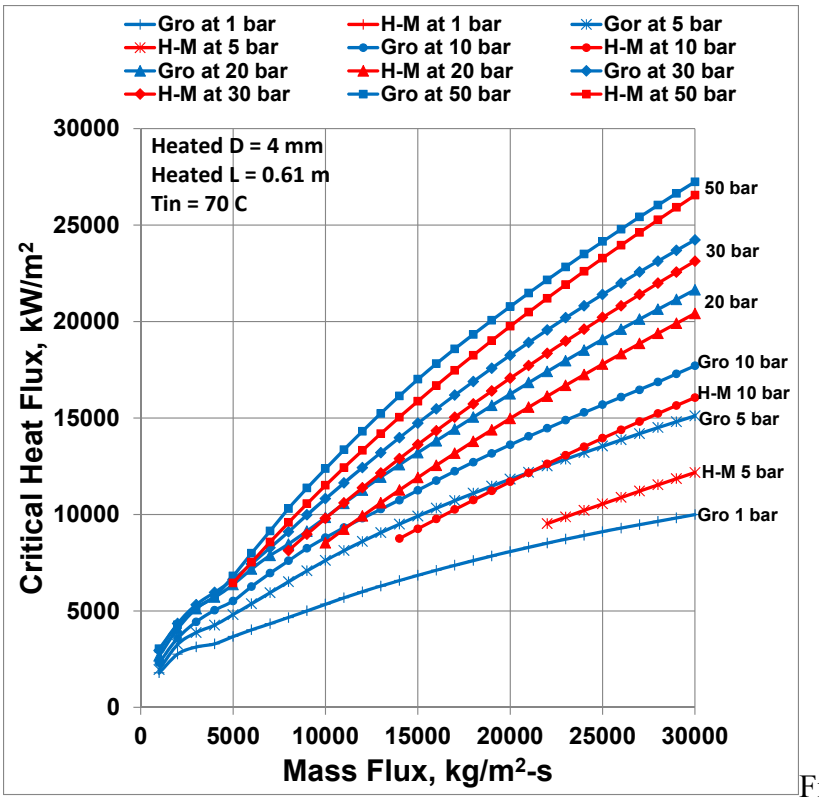

Fig. 8, Part 23 of 36

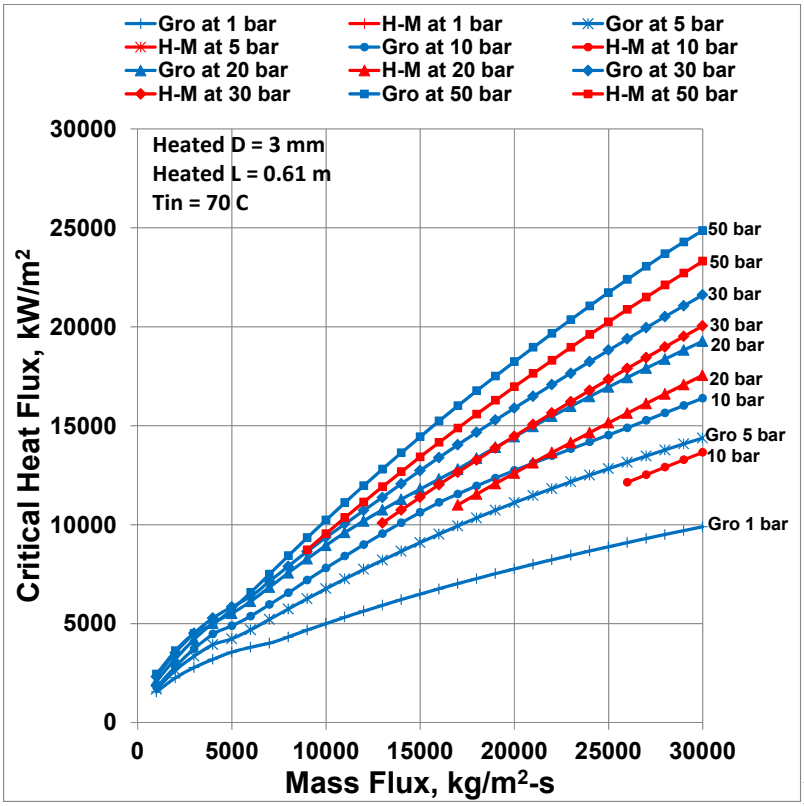

Fig. 8, Part 24 of 36

Fig. 8. Continued

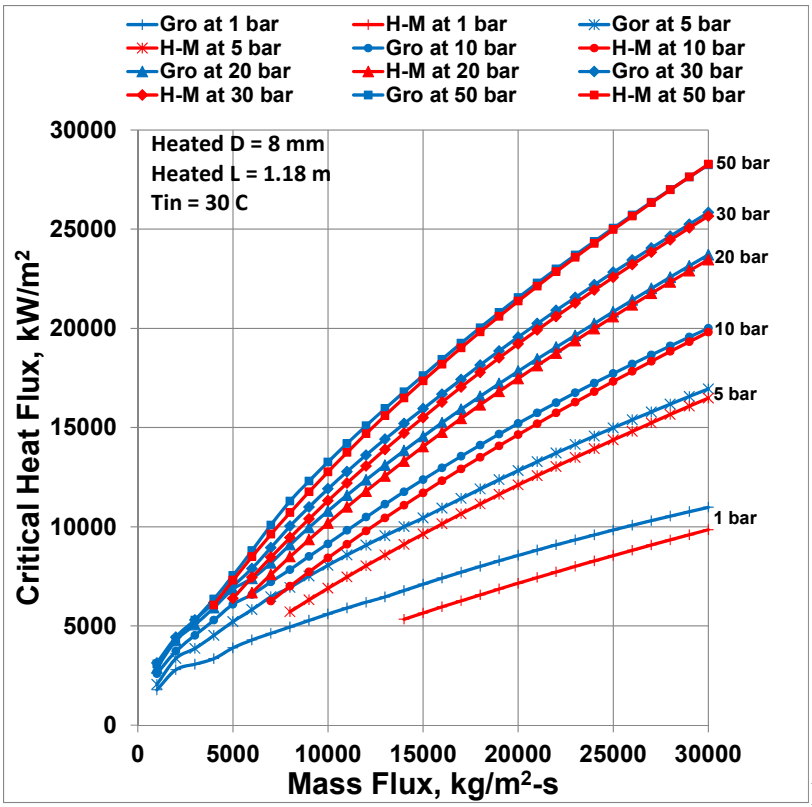

Fig. 8, Part 25 of 36

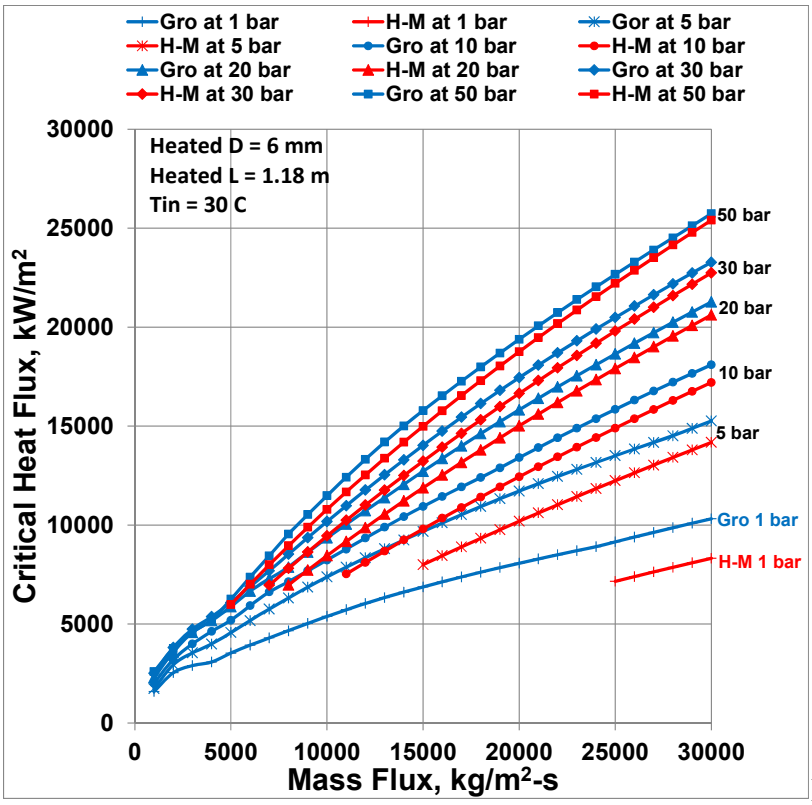

Fig. 8, Part 26 of 36

Fig. 8. Continued

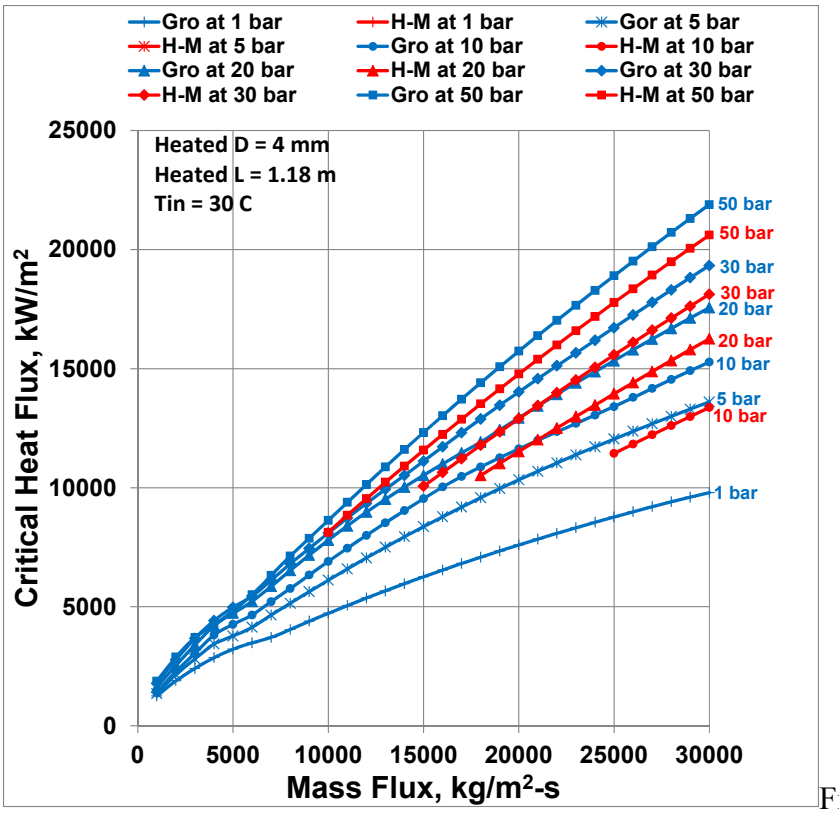

Fig. 8, Part 27 of 36

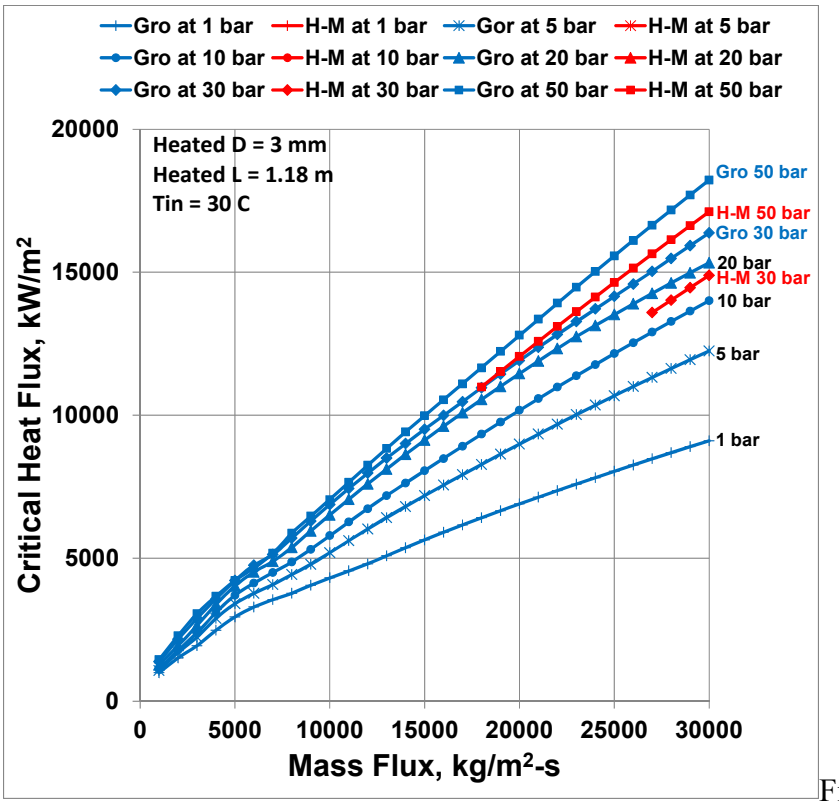

Fig. 8, Part 28 of 36

Fig. 8. Continued

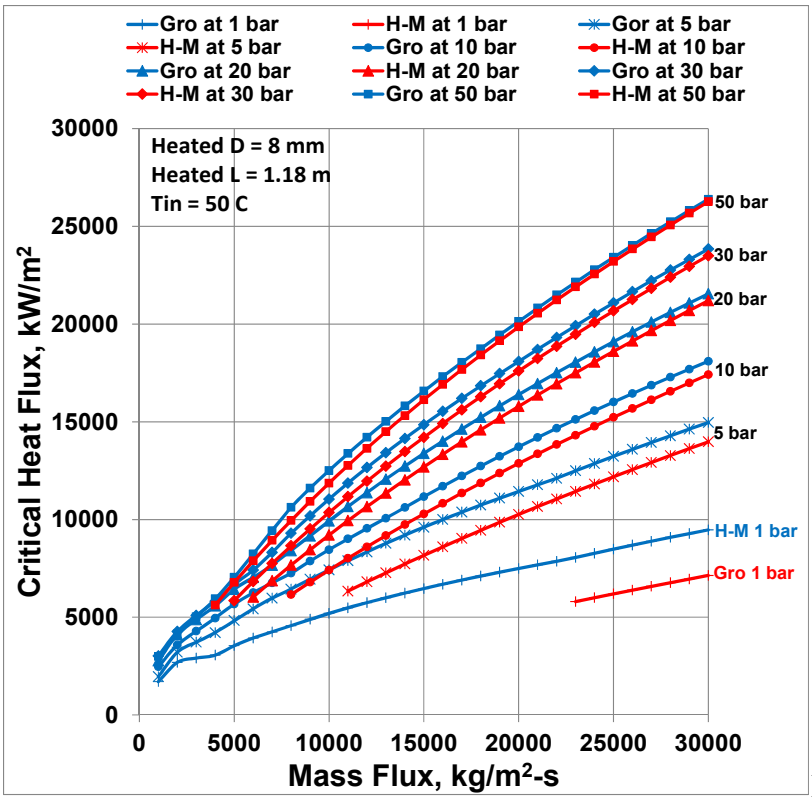

Fig. 8, Part 29 of 36

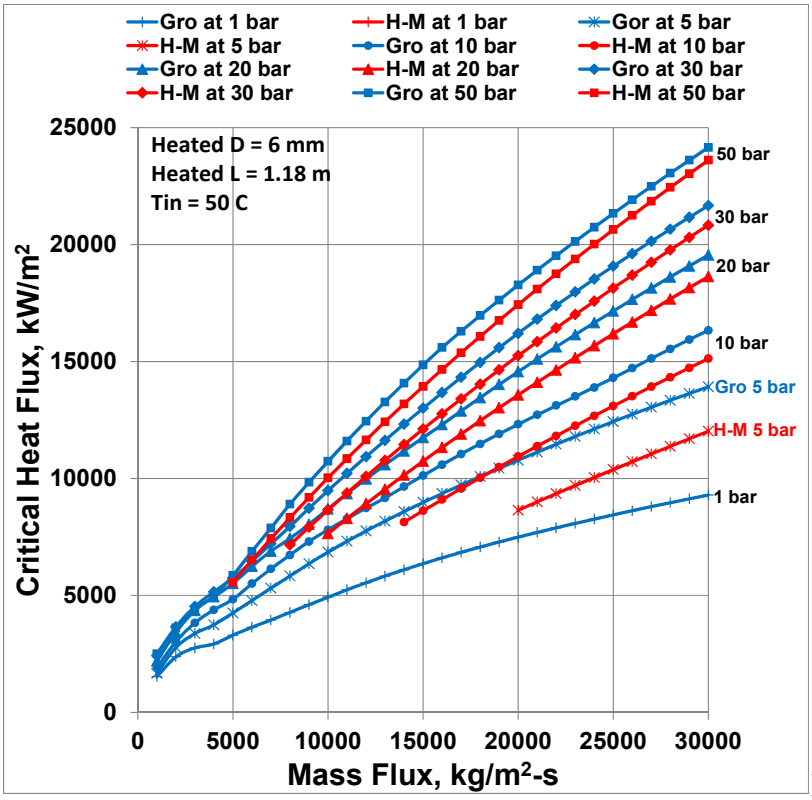

Fig. 8, Part 30 of 36

Fig. 8. Continued

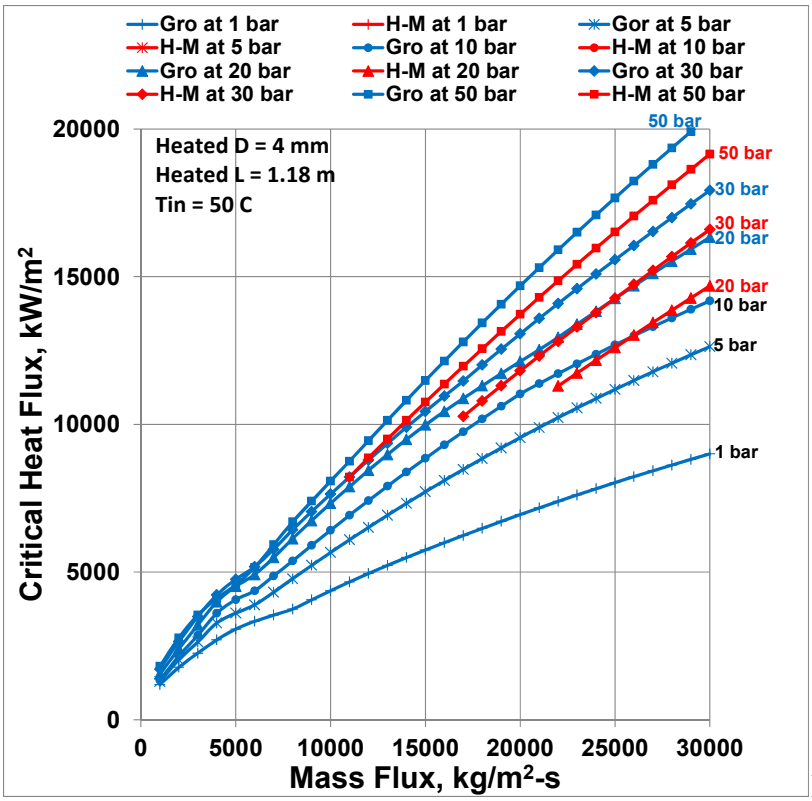

Fig. 8, Part 31 of 36

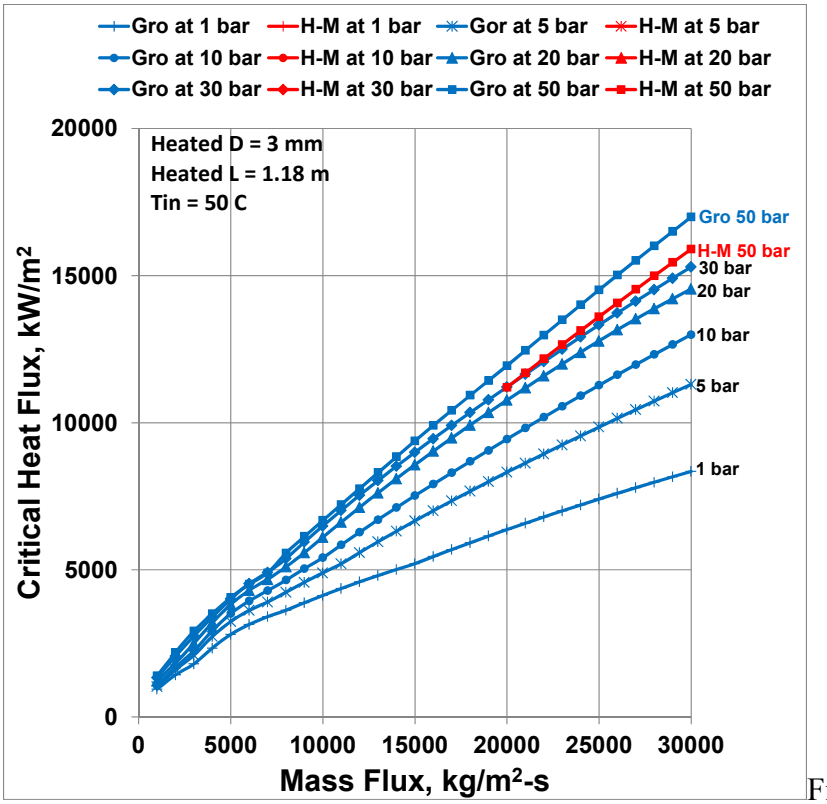

Fig. 8, Part 32 of 36

Fig. 8. Continued

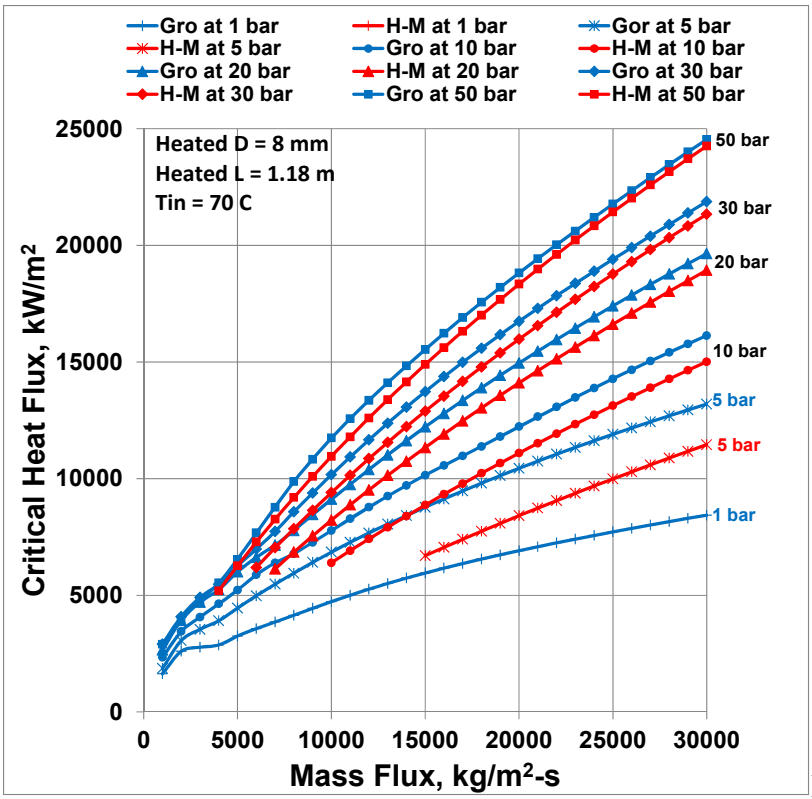

Fig. 8, Part 33 of 36

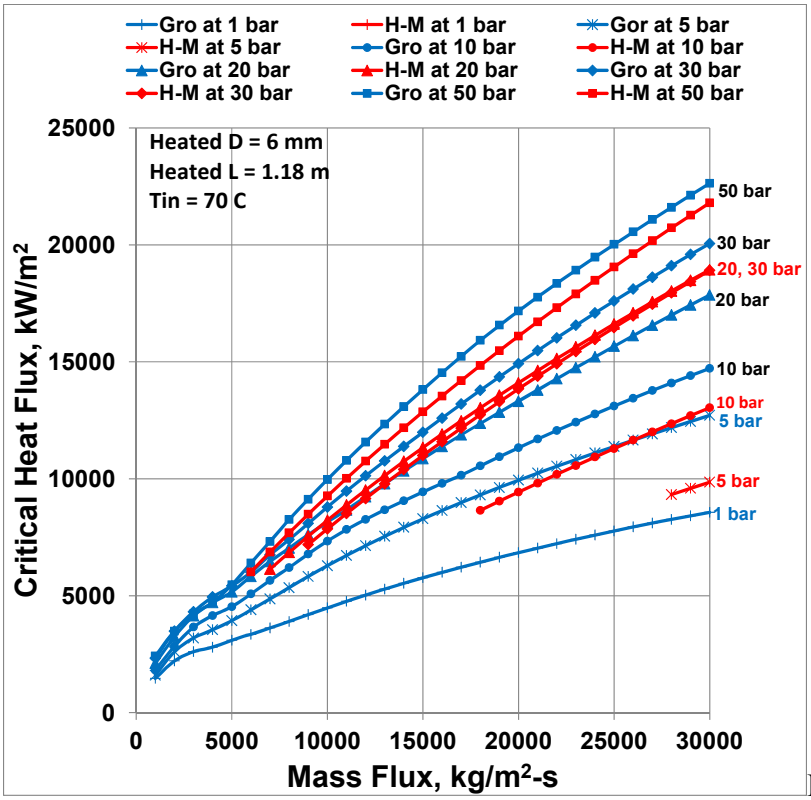

Fig. 8, Part 34 of 36

Fig. 8. Continued

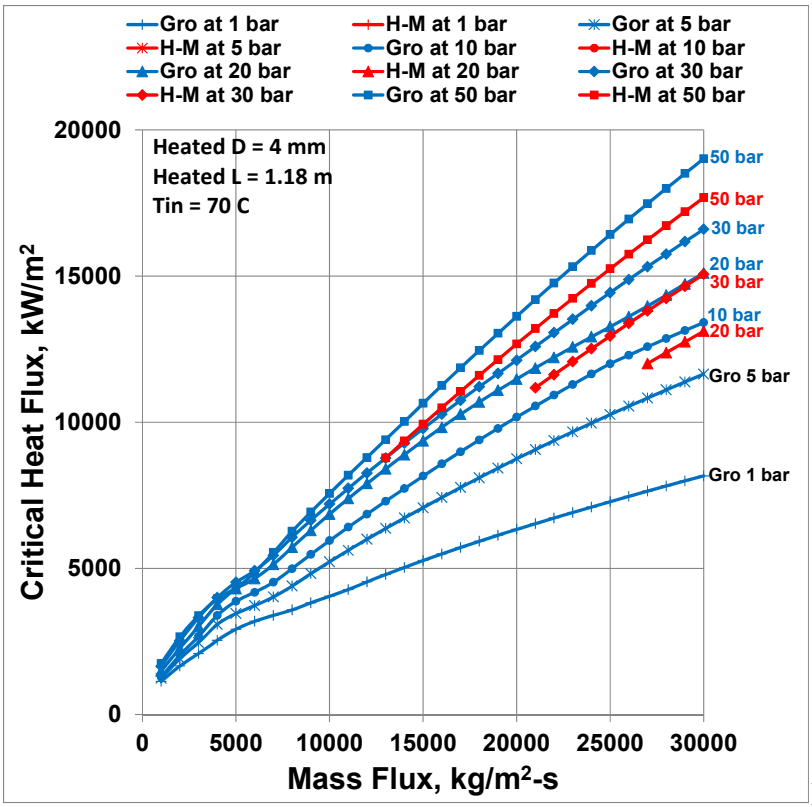

Fig. 8, Part 35 of 36

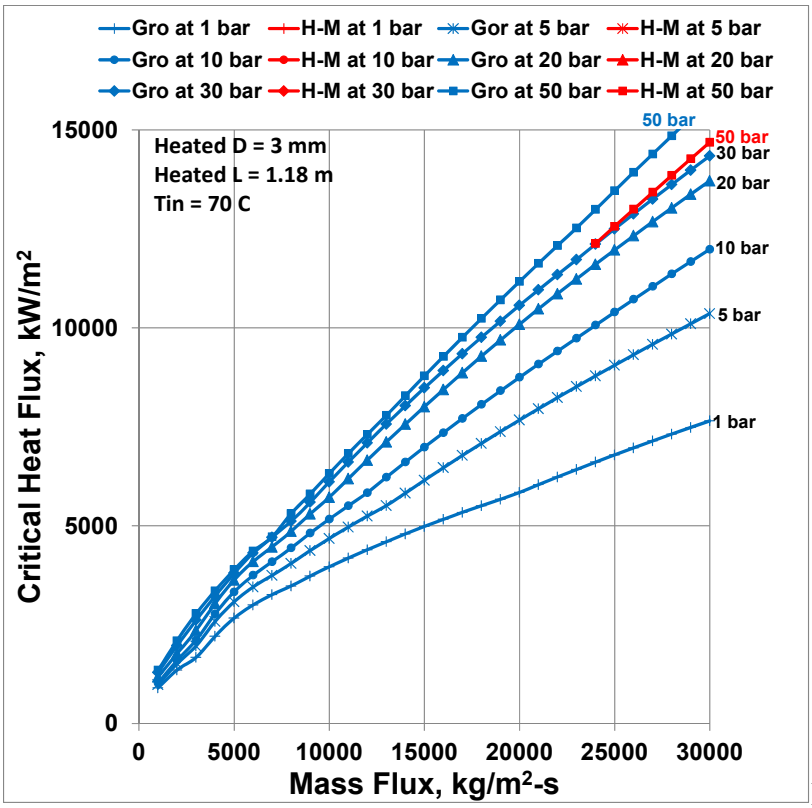

Fig. 8, Part 36 of 36

Fig. 8. Continued

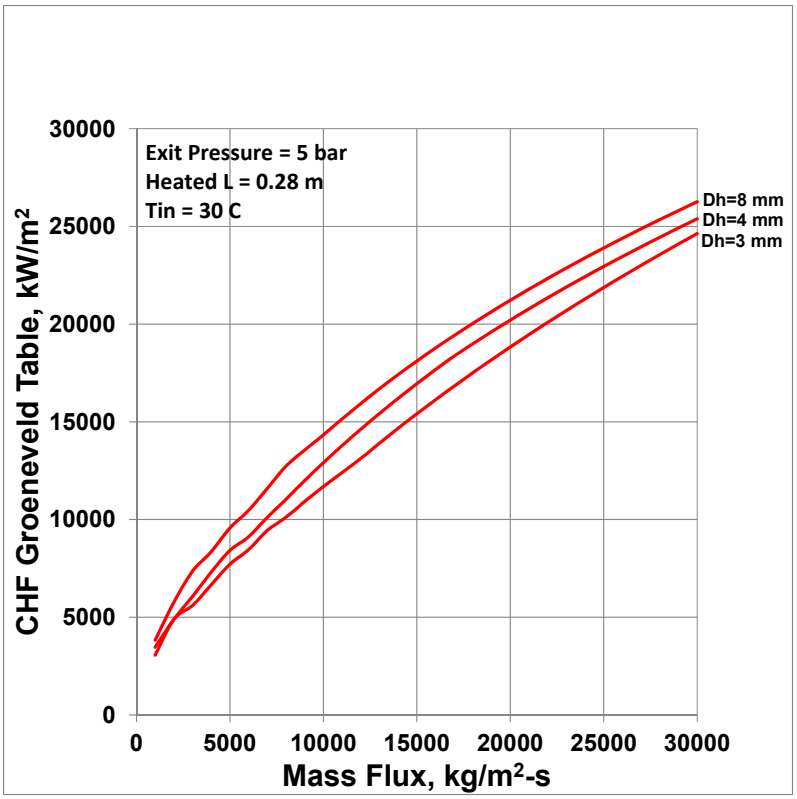

Fig. 9, Part 1 of 18

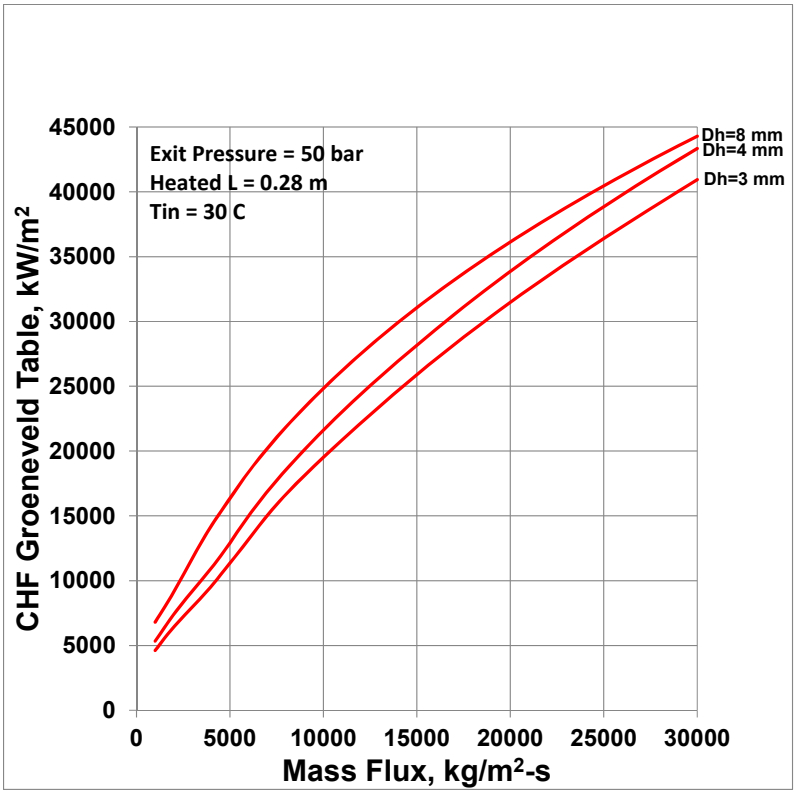

Fig. 9, Part 2 of 18

Fig. 9. Effect of Heated Diameter or Inlet Temperature on CHF

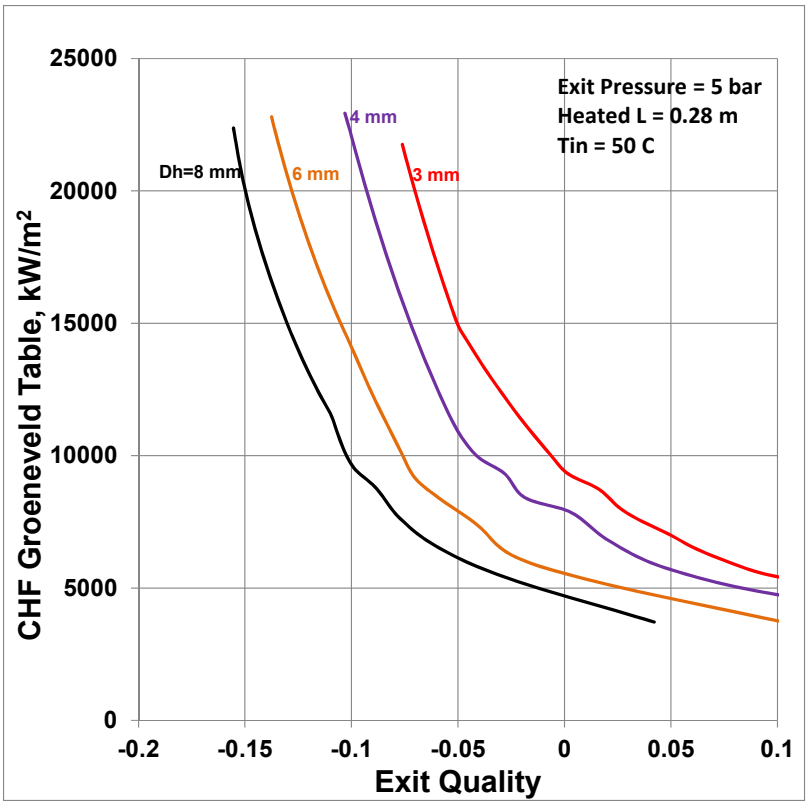

Fig. 9, Part 3 of 18

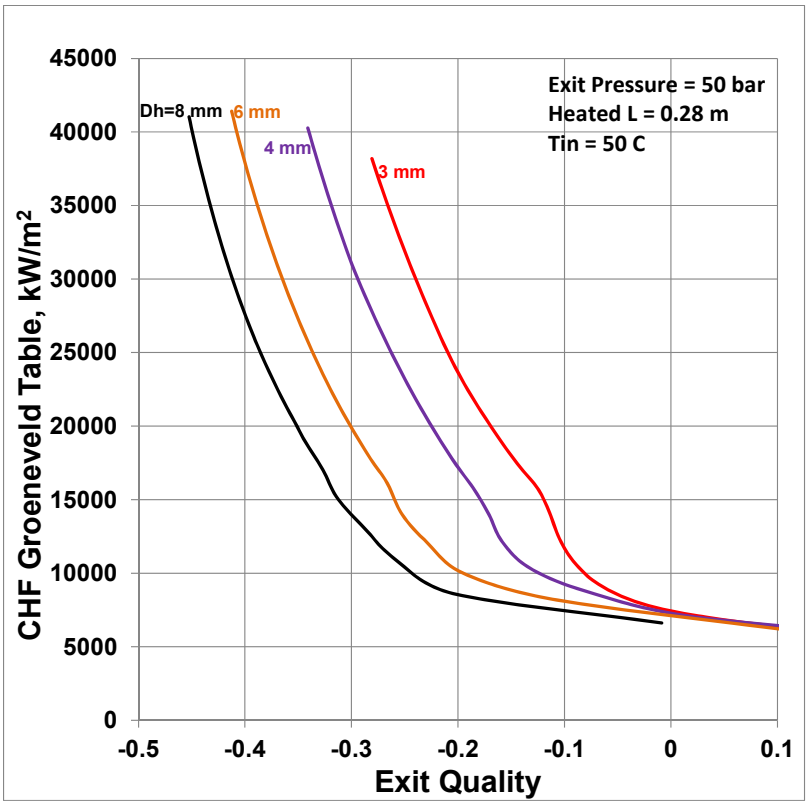

Fig. 9, Part 4 of 18

Fig. 9. Continued: Effect of Heated Diameter or Inlet Temperature on CHF

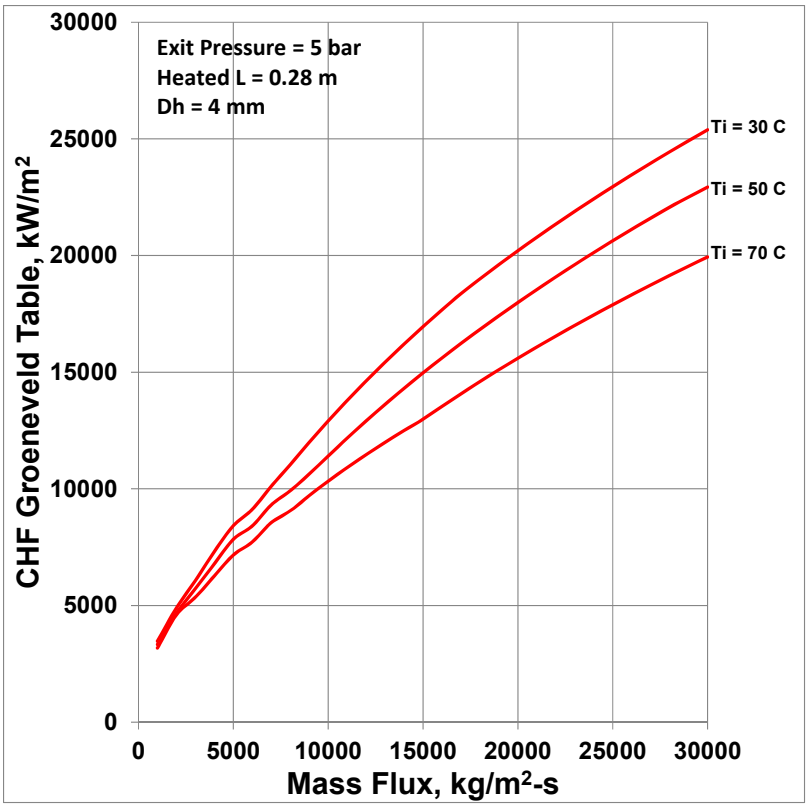

Fig. 9, Part 5 of 18

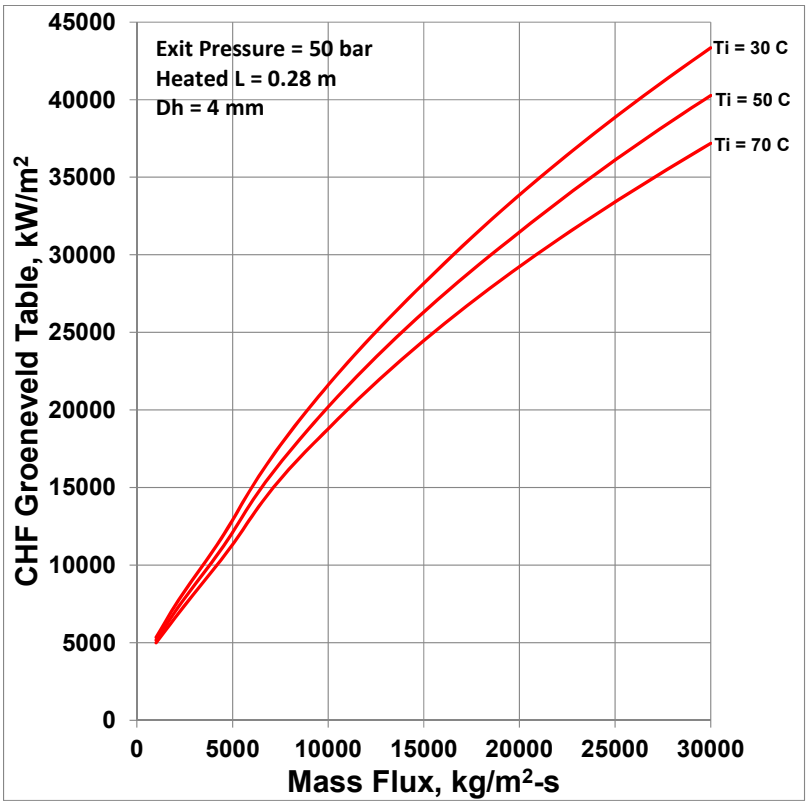

Fig. 9, Part 6 of 18

Fig. 9. Continued: Effect of Heated Diameter or Inlet Temperature on CHF

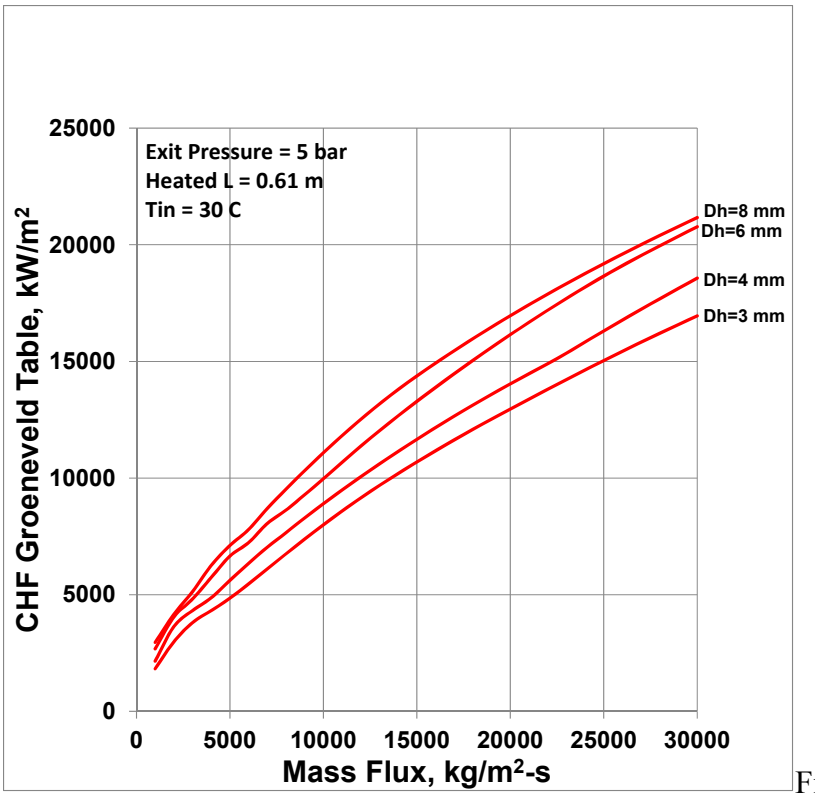

Fig. 9, Part 7 of 18

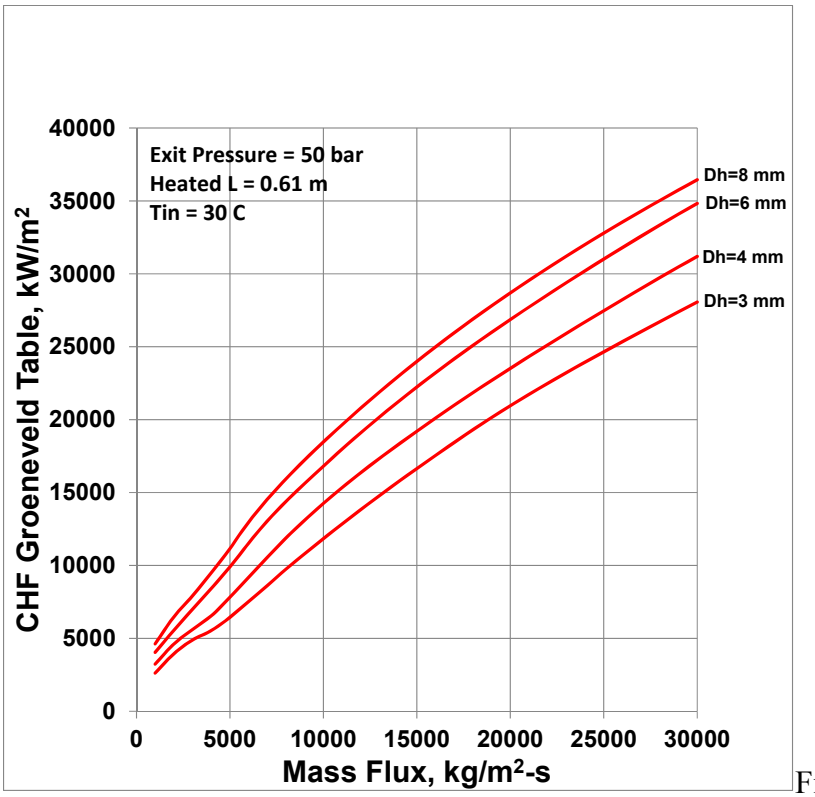

Fig. 9, Part 8 of 18

Fig. 9. Continued: Effect of Heated Diameter or Inlet Temperature on CHF

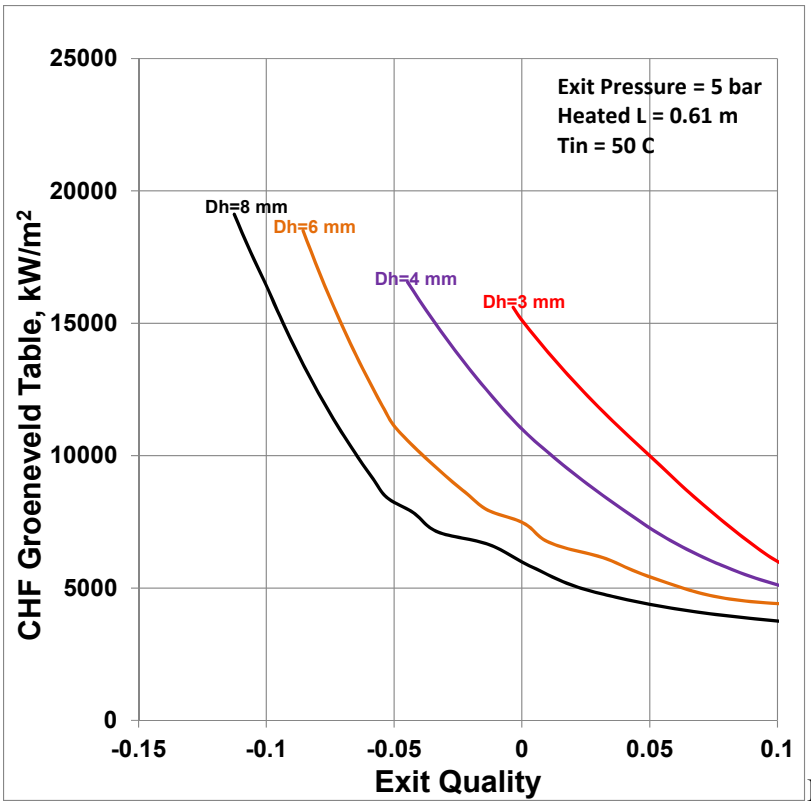

Fig. 9, Part 9 of 18

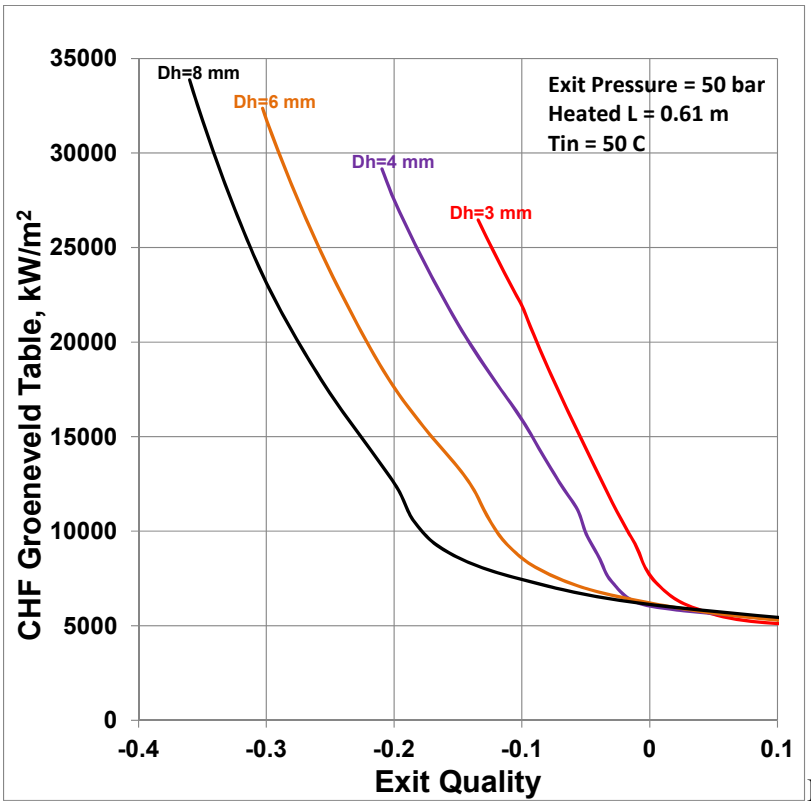

Fig. 9, Part 10 of 18

Fig. 9. Continued: Effect of Heated Diameter or Inlet Temperature on CHF

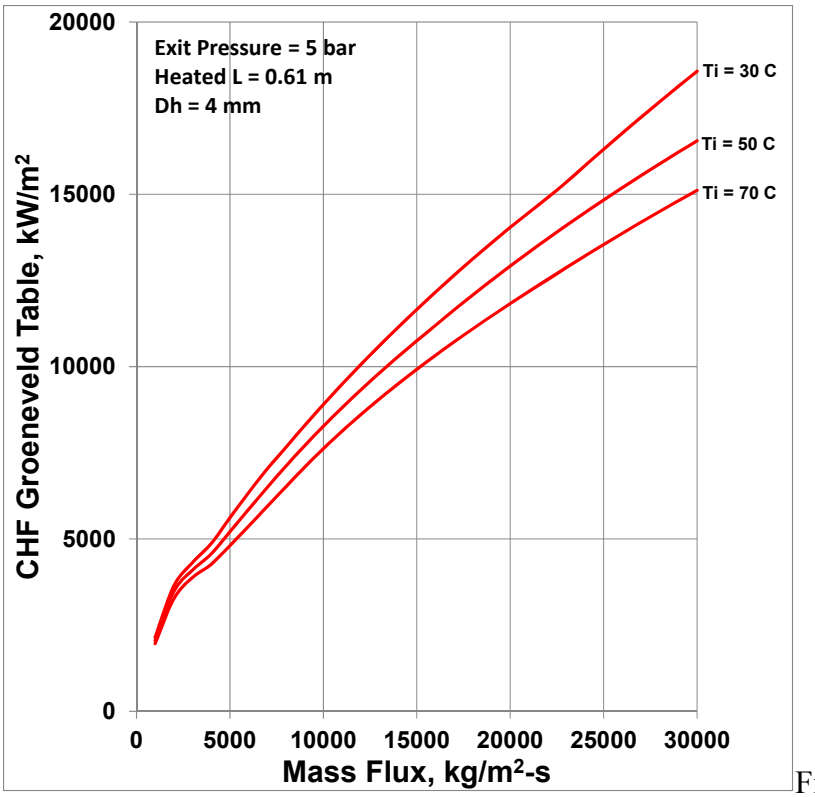

Fig. 9, Part 11 of 18

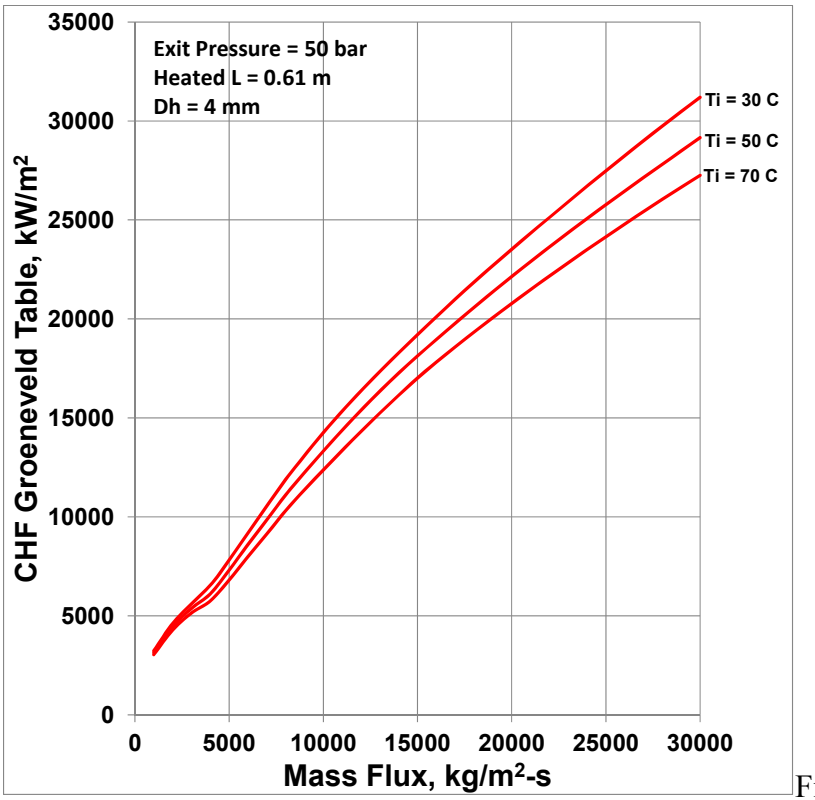

Fig. 9, Part 12 of 18

Fig. 9. Continued: Effect of Heated Diameter or Inlet Temperature on CHF

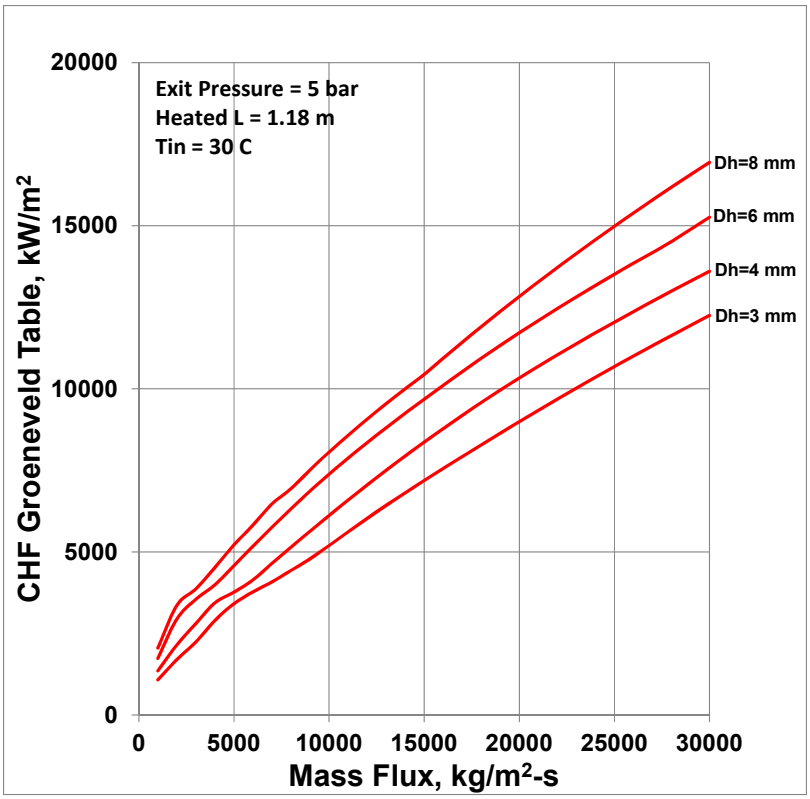

Fig. 9, Part 13 of 18

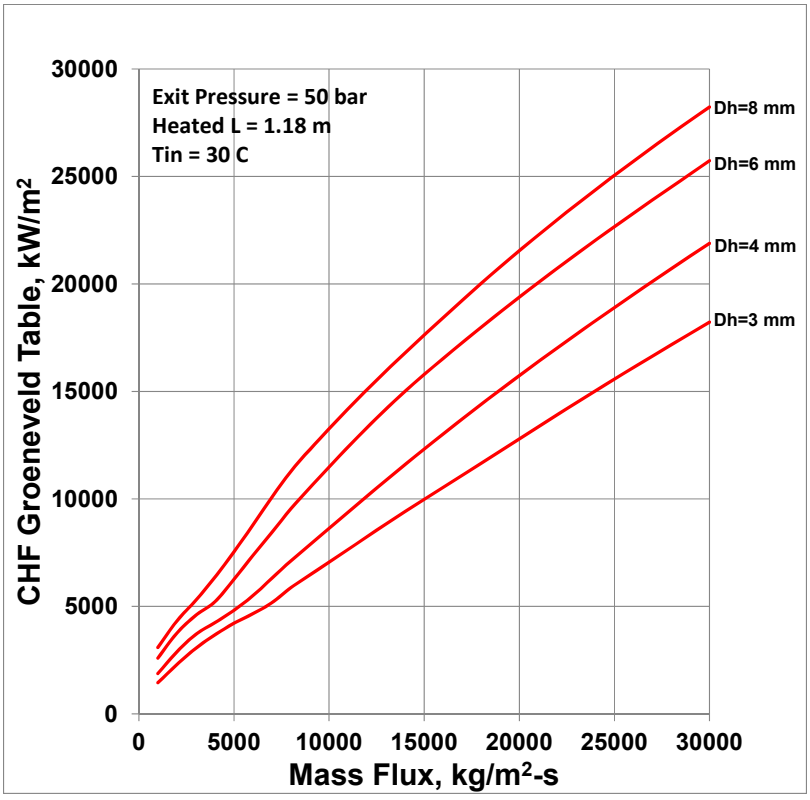

Fig. 9, Part 14 of 18

Fig. 9. Continued: Effect of Heated Diameter or Inlet Temperature on CHF

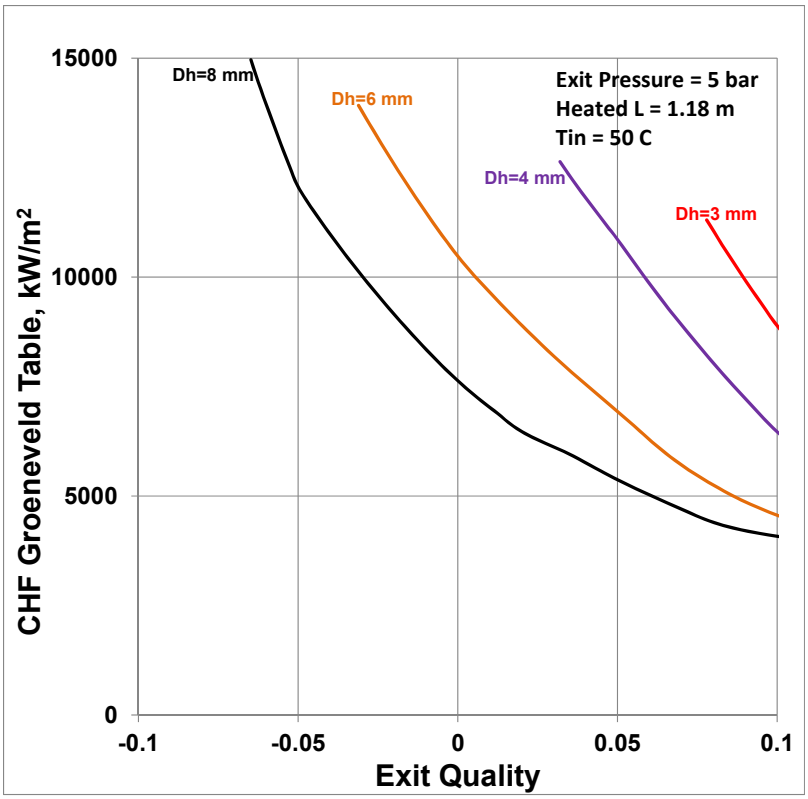

Fig. 9, Part 15 of 18

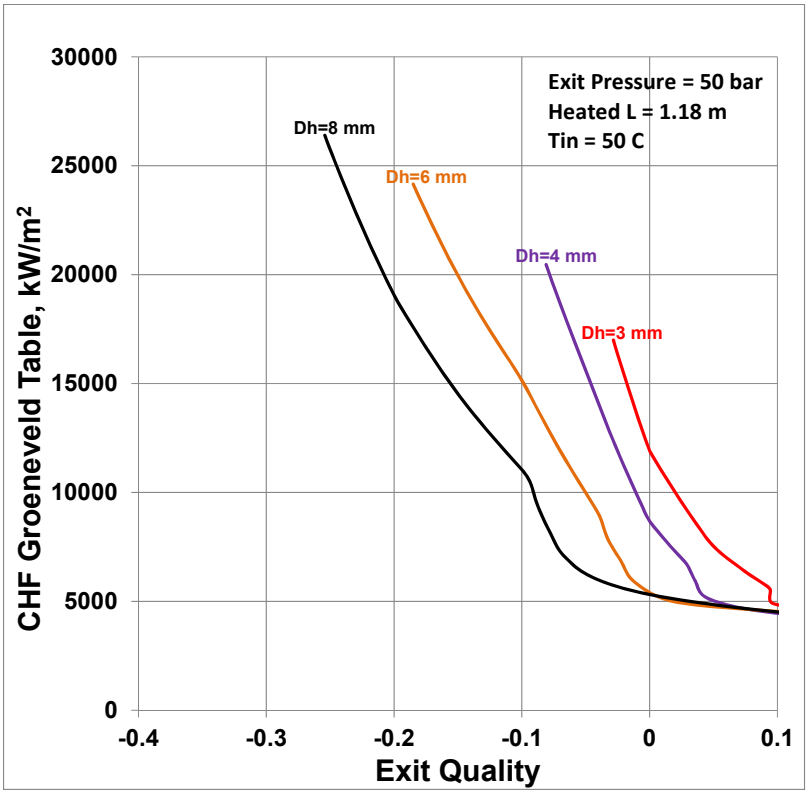

Fig. 9, Part 16 of 18

Fig. 9. Continued: Effect of Heated Diameter or Inlet Temperature on CHF

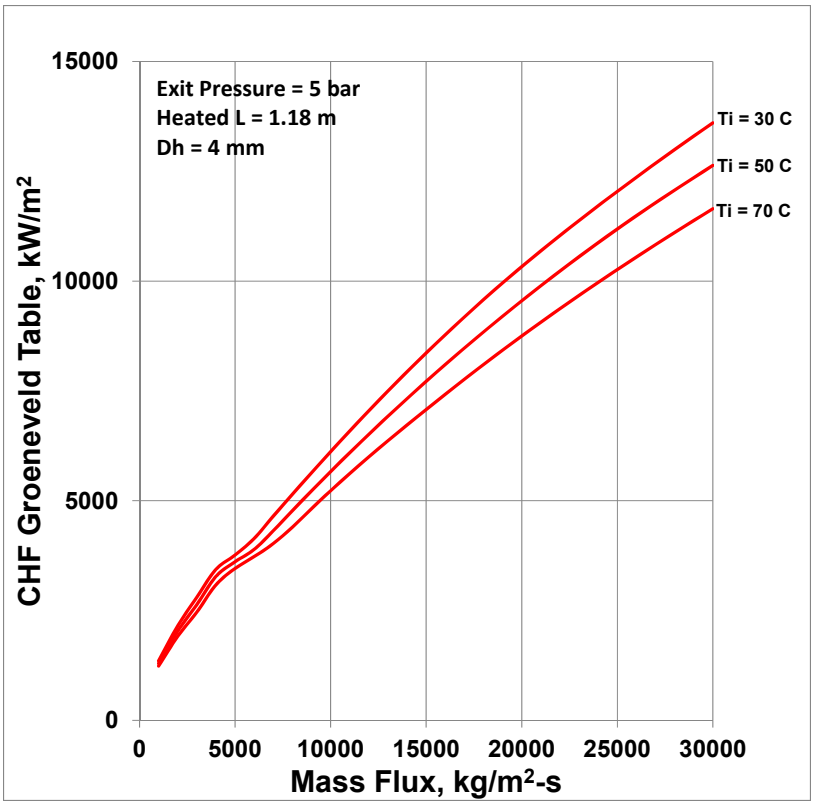

Fig. 9, Part 17 of 18

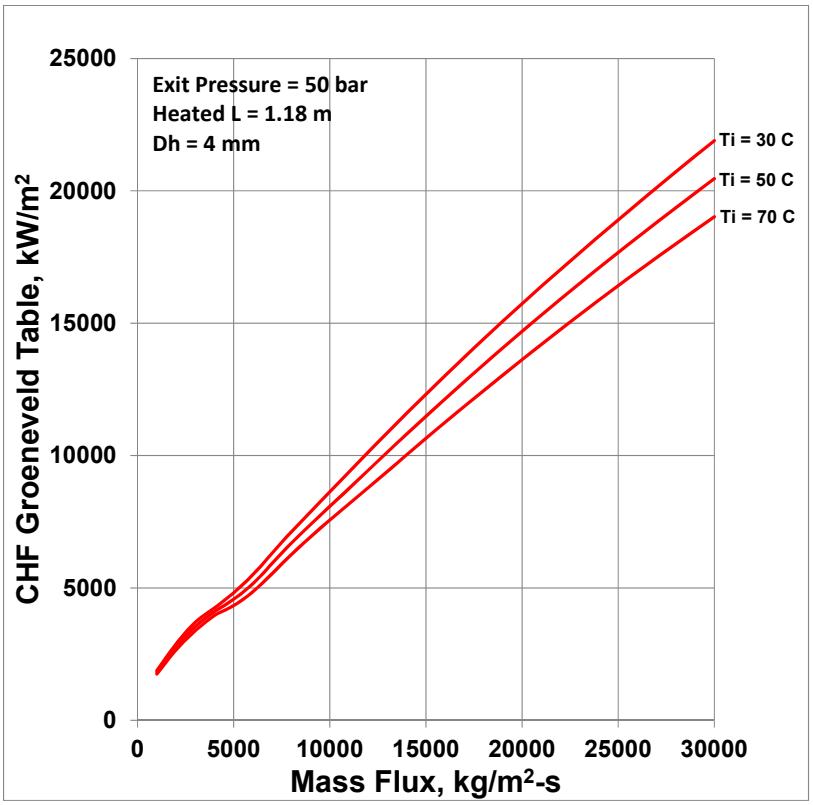

Fig. 9, Part 18 of 18

Fig. 9. Continued: Effect of Heated Diameter or Inlet Temperature on CHF

APPENDIX D. COMPARISON OF OFI HEAT FLUXES BY THE WHITTLE-FORGAN (η=32.5) AND THE SAHA-ZUBER CORRELATIONS

The heat flux at the onset of flow instability (OFI) obtained by the Whittle-Forgan correlation using η = 32.5 (calculated iteratively as described in Appendix A) was used in making the OFI-CHF reversal diagrams. Before plotting the reversal diagrams, the OFIs obtained by two widely used methods, the Whittle-Forgan and the Saha-Zuber were plotted and compared over the mass flux range of 1000 to 30000 kg/m^2-s for 72 cases (6 exit pressures × 4 heated diameters × 3 inlet temperatures) for each of 3 heated lengths, altogether 216 cases. The following are the values of the independent parameters:

3 heated lengths L_h = 0.28, 0.61, 1.18 m
6 exit pressures P = 1, 5, 10, 20, 30, 50 bar
4 heated diameters D_h = 3, 4, 6, 8 mm
3 inlet temperatures T_{in} = 30, 50, 70 º C

Figure 10 (having 36 parts) shows the comparison for all 216 cases. The blue curves are for the Whittle-Forgan correlation and the red curves for the Saha-Zuber. Selected numerical results are also tabulated in Tables 4 to 9. For uniform heat flux, the Saha-Zuber correlation consistently gives slightly lower OFI heat flux. It could be the other way around (Saha-Zuber correlation could give slightly higher OFI heat flux) for axially non-uniform heat flux having the axial peak near the mid-height and lower heat flux values near the channel exit (where the OSV occurs). This is because the Saha-Zuber correlation is based the local thermal-hydraulic conditions whereas the Whittle-Forgan correlation is based on the total rise of bulk coolant temperature.

The difference between the two prediction methods over the 72 cases for each heated length is given in Table 3. There is a close agreement between the two prediction methods. The RMS difference is 5.19 %, 3.03 %, and 1.77 % for the heated lengths of 0.28, 0.61, and 1.18 m respectively. The comparison for all the data points in the 72 cases of heated length 0.28 m is shown in Fig. 1A. Figures 1B and 1C are similar plots for heated lengths of 0.61 m and 1.18 m. Comparing the scatter in these figures, it is obvious that the maximum absolute error for L_h=0.28 m is more than that for L_h=1.18 m. This observation is consistent with Table 3.

The OFI heat flux is a function of five independent parameters: P, L_h , D_h , G, and T_i . The effect of exit pressure P, heated diameter D_h or inlet temperature T_i on the OFI obtained by the Whittle-Forgan (η = 32.5) is shown in Fig. 11 (having 15 parts). In these separate-effect plots, only one parameter is changed at a time, holding the other four parameters constant. The parts 1 to 5 of Fig. 11 are for L_h=0.28 m, the parts 6 to 10 for L_h=0.61 m, and the parts 11 to 15 for L_h=1.18 m. At each heated length, the OFI heat flux increases with increasing exit pressure at constant D_h , L_h , T_{in} , and G (see Fig. 11 part 1). The OFI increases with increasing heated diameter at constant P, L_h , T_{in} , and G (see Fig. 11 parts 2 and 3). The OFI decreases with increasing inlet temperature at constant P, L_h , D_h , and G (see Fig. 11 parts 4 and 5).

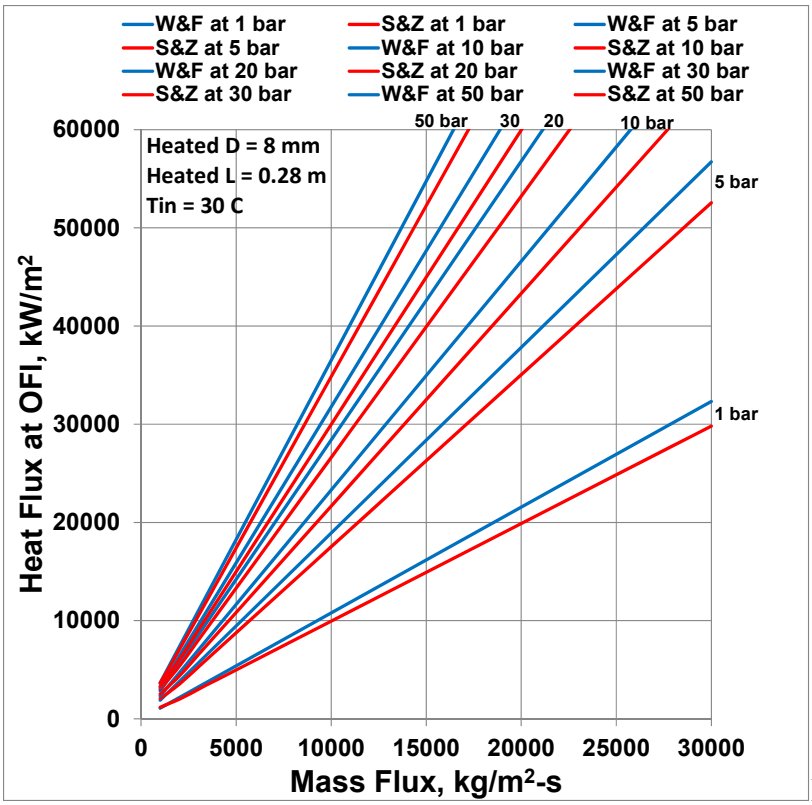

Fig. 9, Part 1 of 36

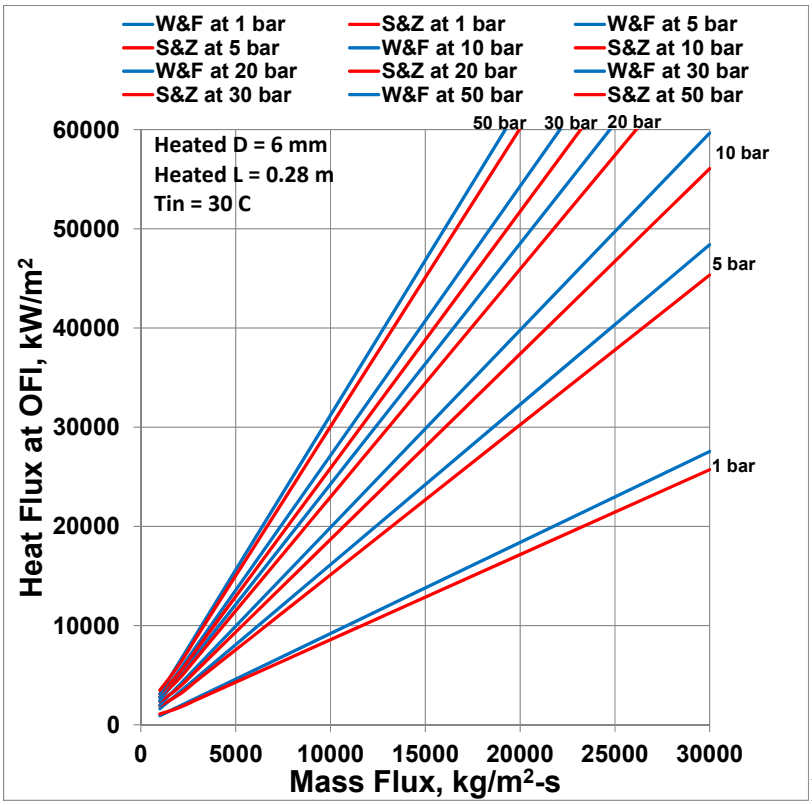

Fig. 10, Part 2 of 36

Fig. 10. Comparison of OFI Heat Fluxes by Whittle-Forgan (η=32.5) and Saha-Zuber Correlations

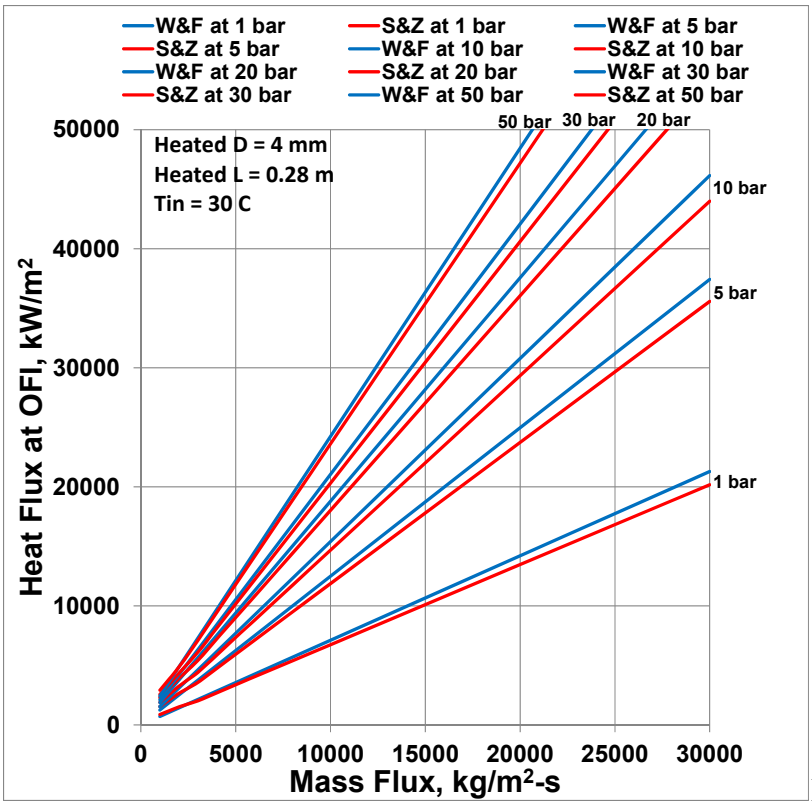

Fig. 10, Part 3 of 36

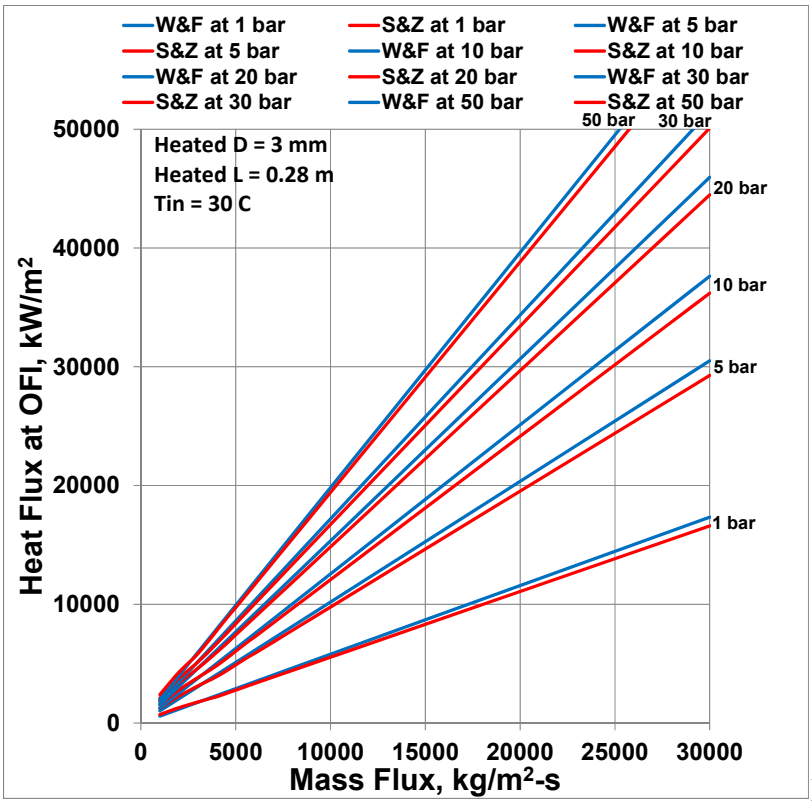

Fig. 10, Part 4 of 36

Fig. 10. Continued

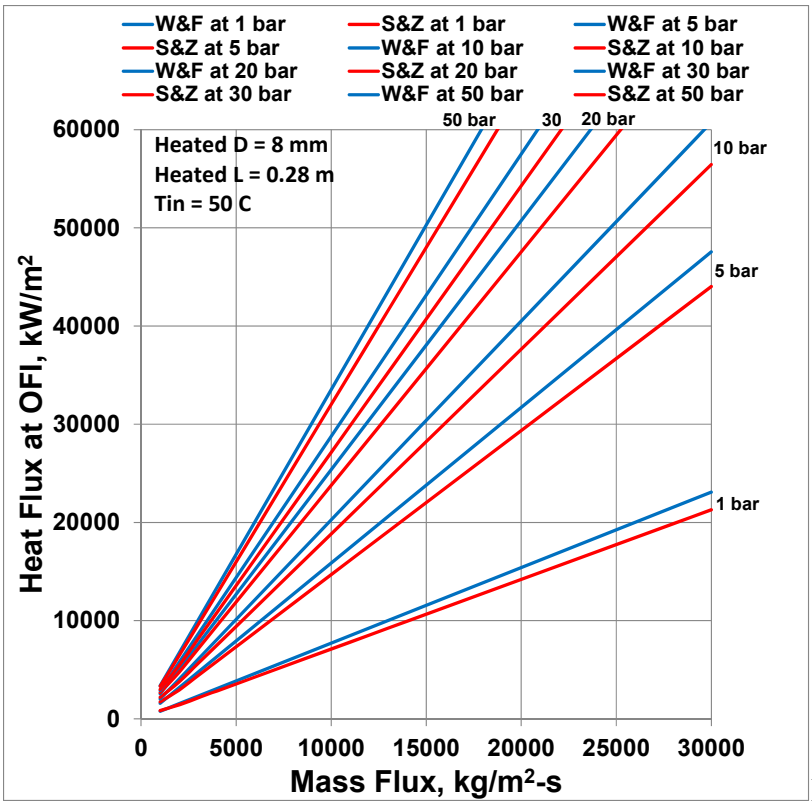

Fig. 10, Part 5 of 36

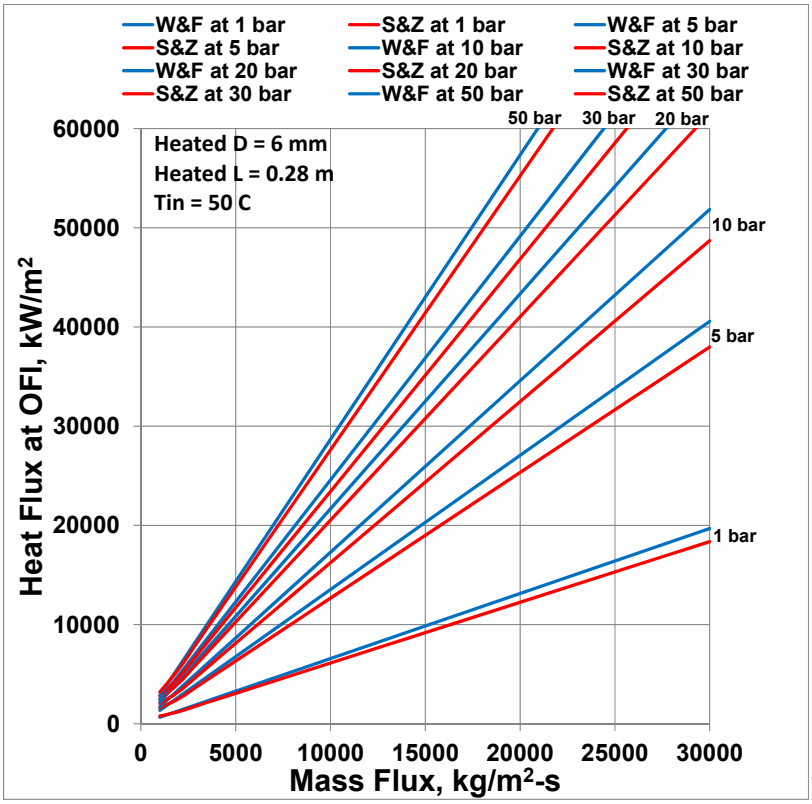

Fig. 10, Part 6 of 36

Fig. 10. Continued

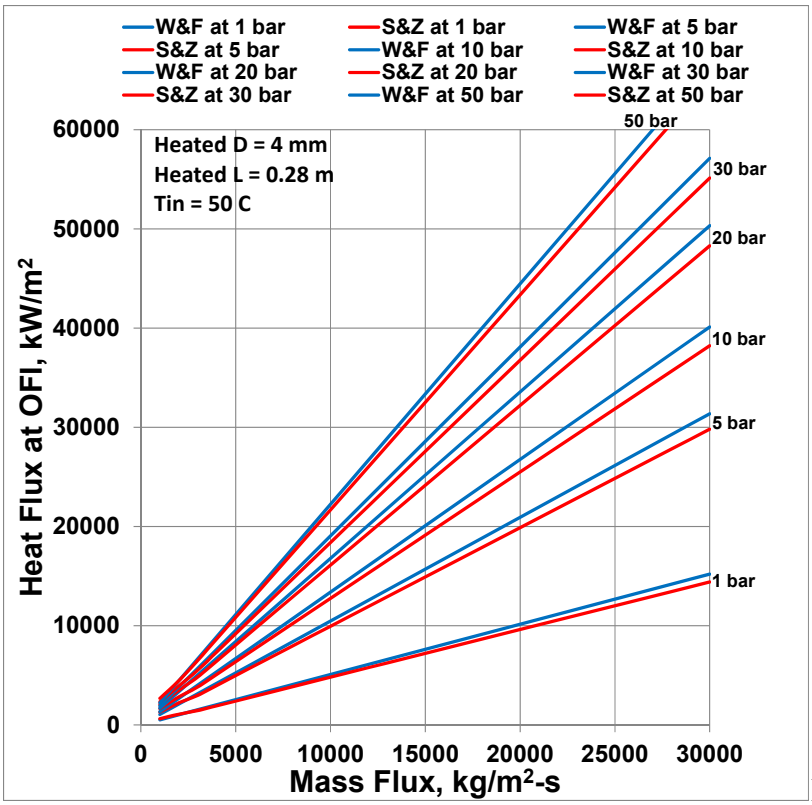

Fig. 10, Part 7 of 36

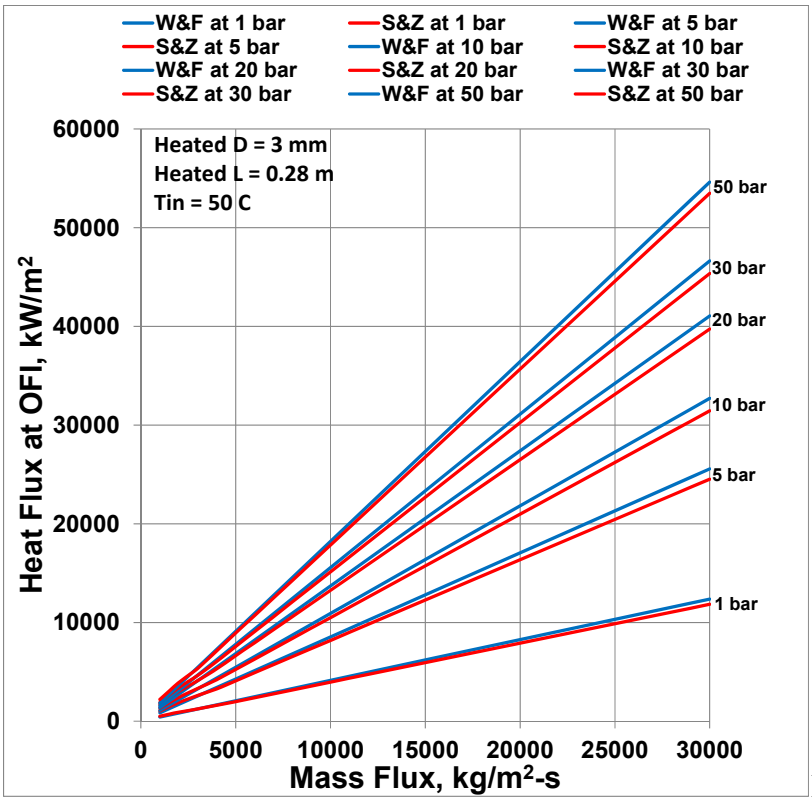

Fig. 10, Part 8 of 36

Fig. 10. Continued

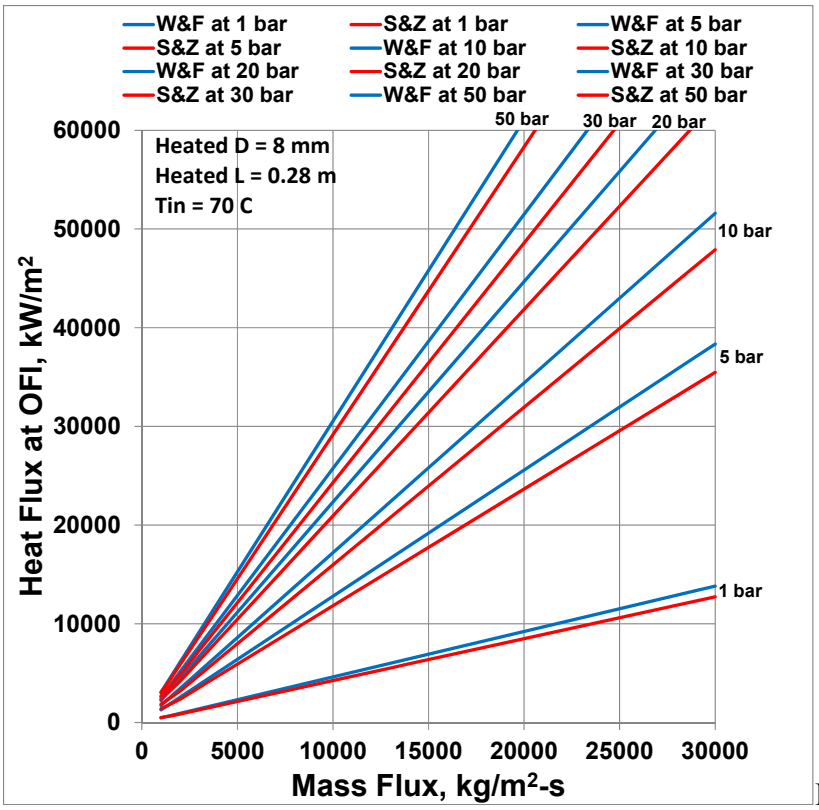

Fig. 10, Part 9 of 36

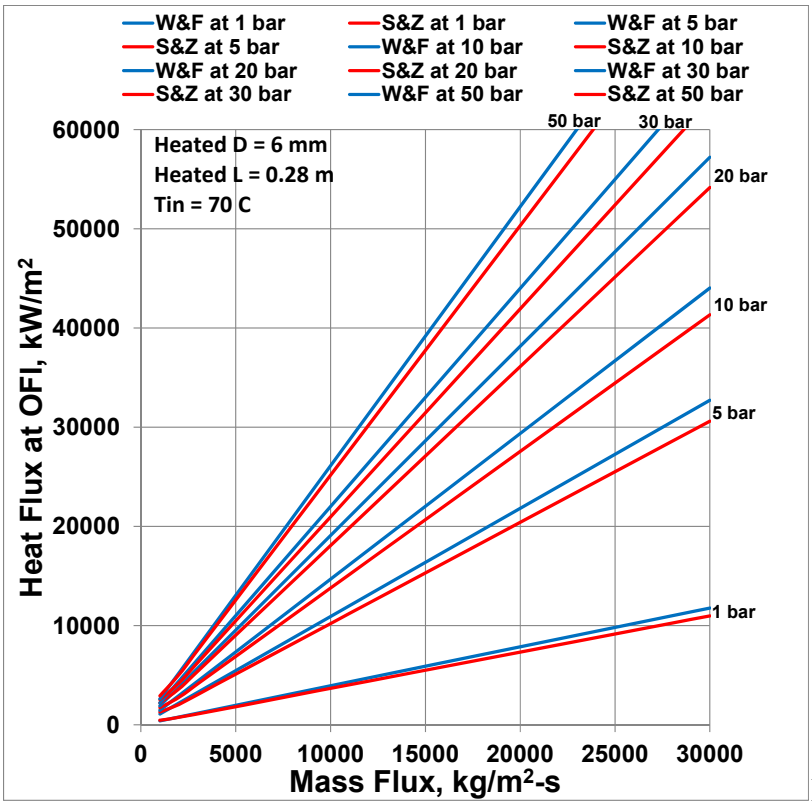

Fig. 10, Part 10 of 36

Fig. 10. Continued

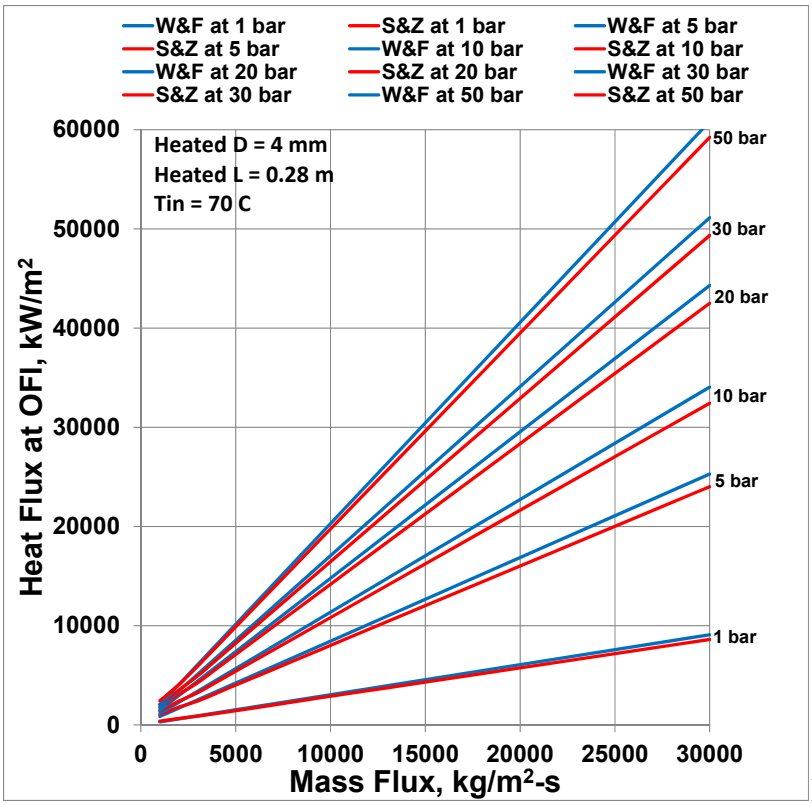

Fig. 10, Part 11 of 36

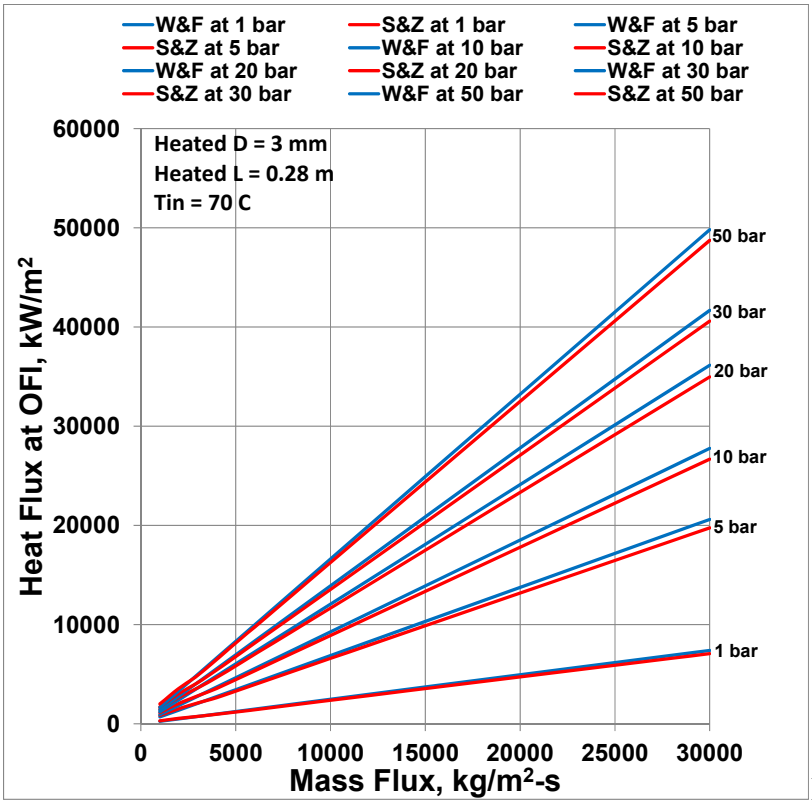

Fig. 10, Part 12 of 36

Fig. 10. Continued

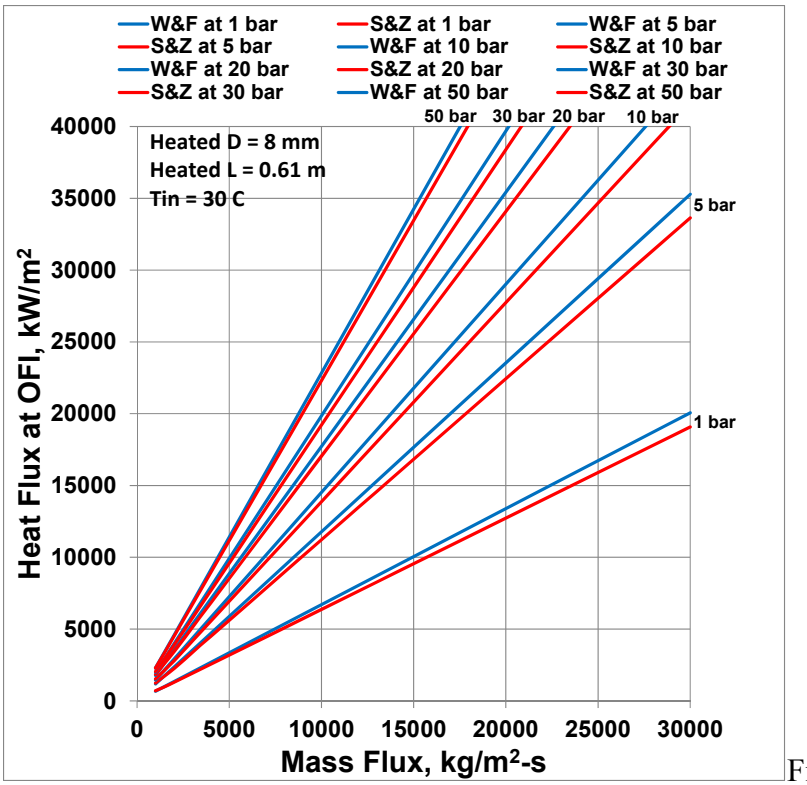

Fig. 10, Part 13 of 36

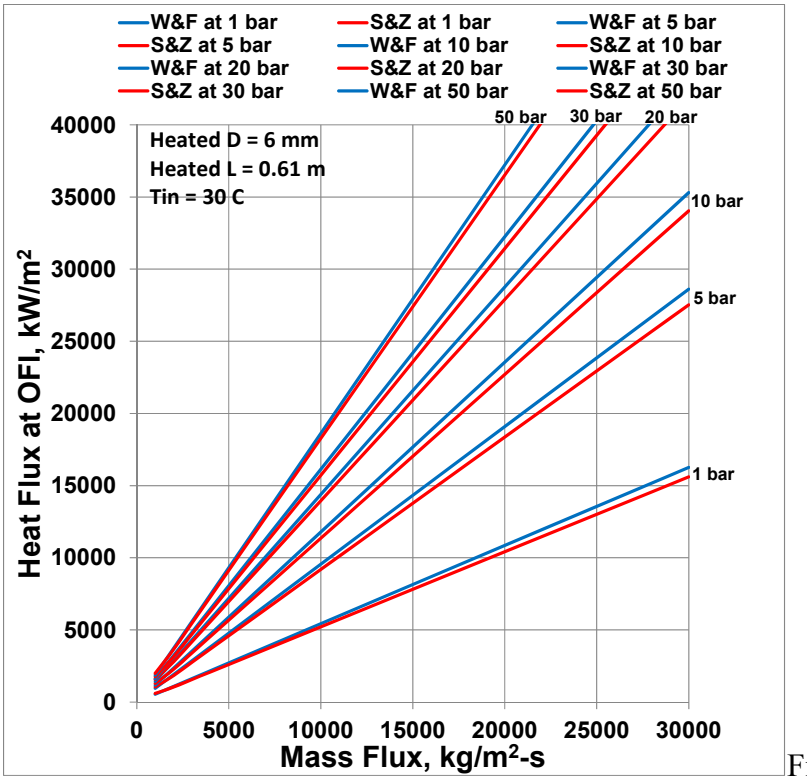

Fig. 10, Part 14 of 36

Fig. 10. Comparison of OFI Heat Fluxes by Whittle-Forgan (η=32.5) and Saha-Zuber Correlations

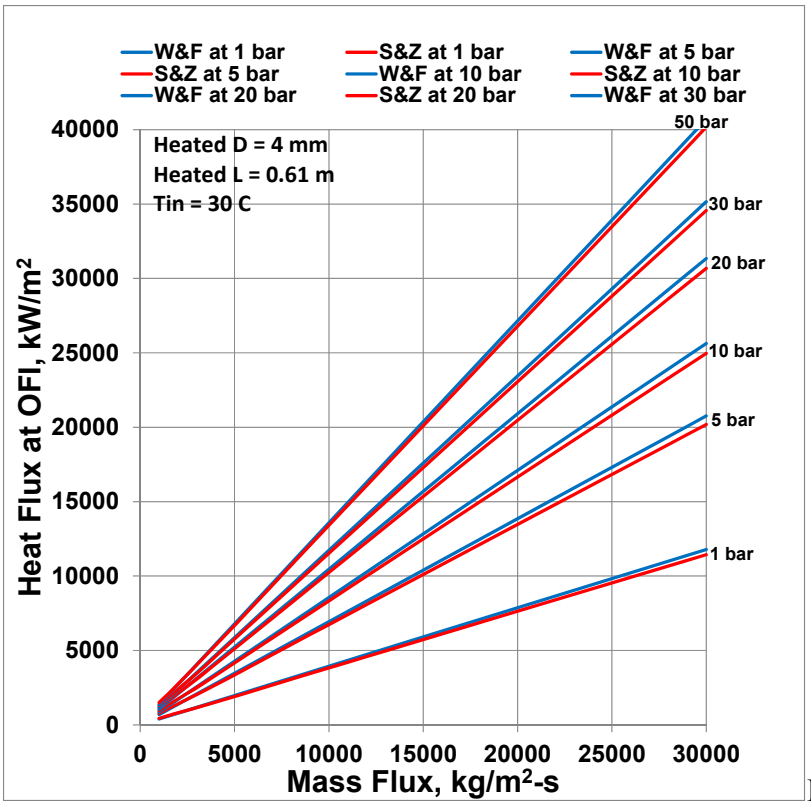

Fig. 10, Part 15 of 36

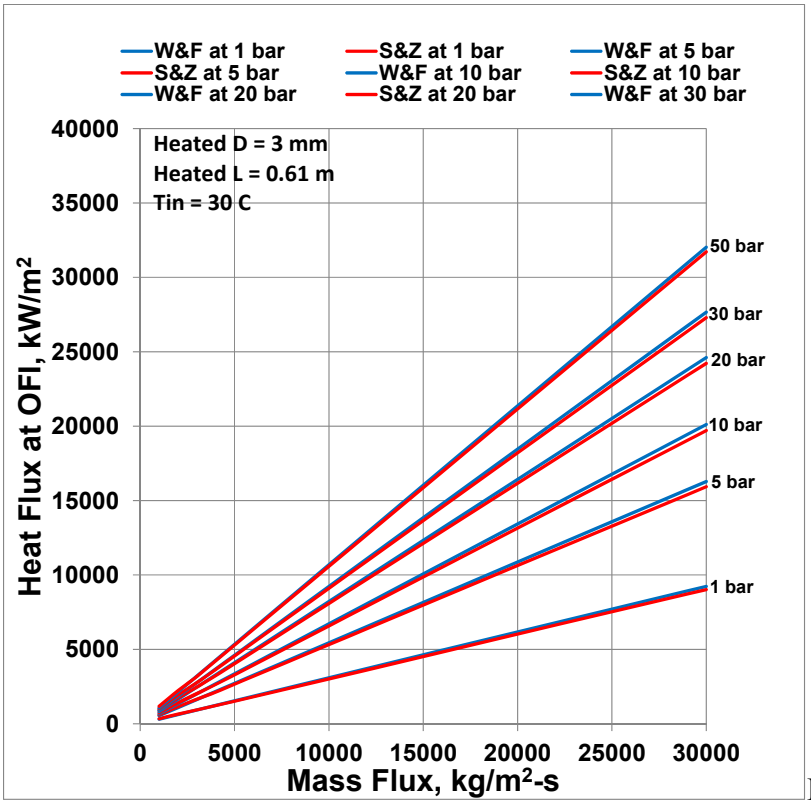

Fig. 10, Part 16 of 36

Fig. 10. Continued

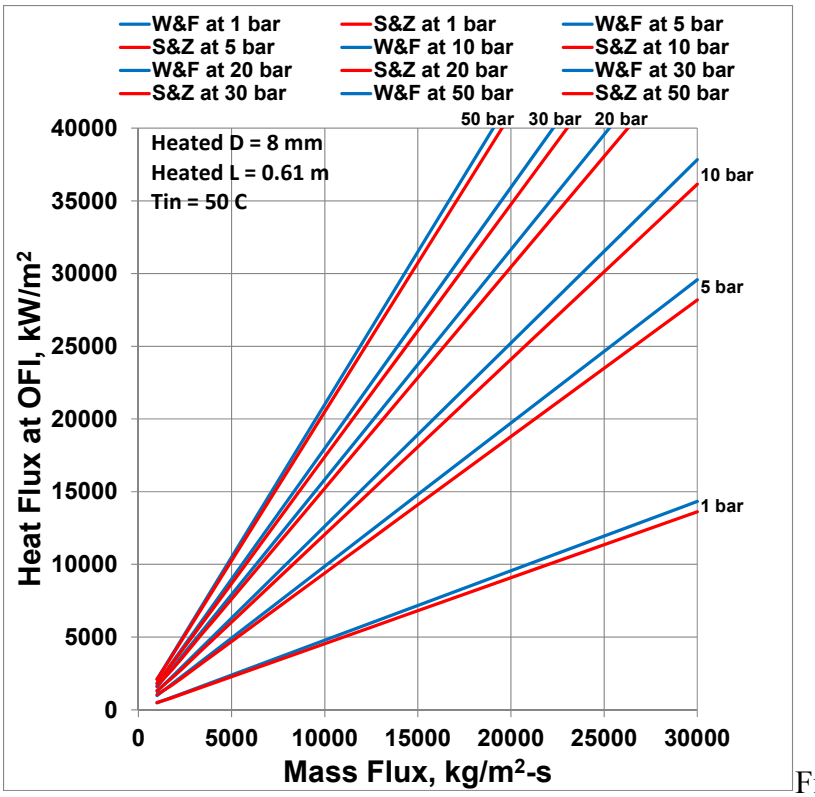

Fig. 10, Part 17 of 36

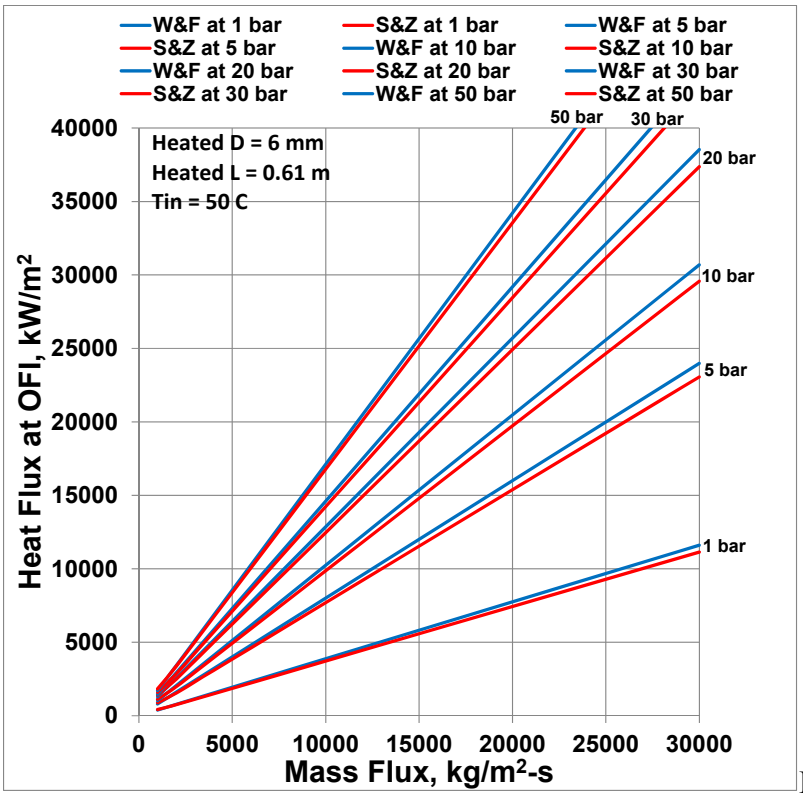

Fig. 10, Part 18 of 36

Fig. 10. Continued

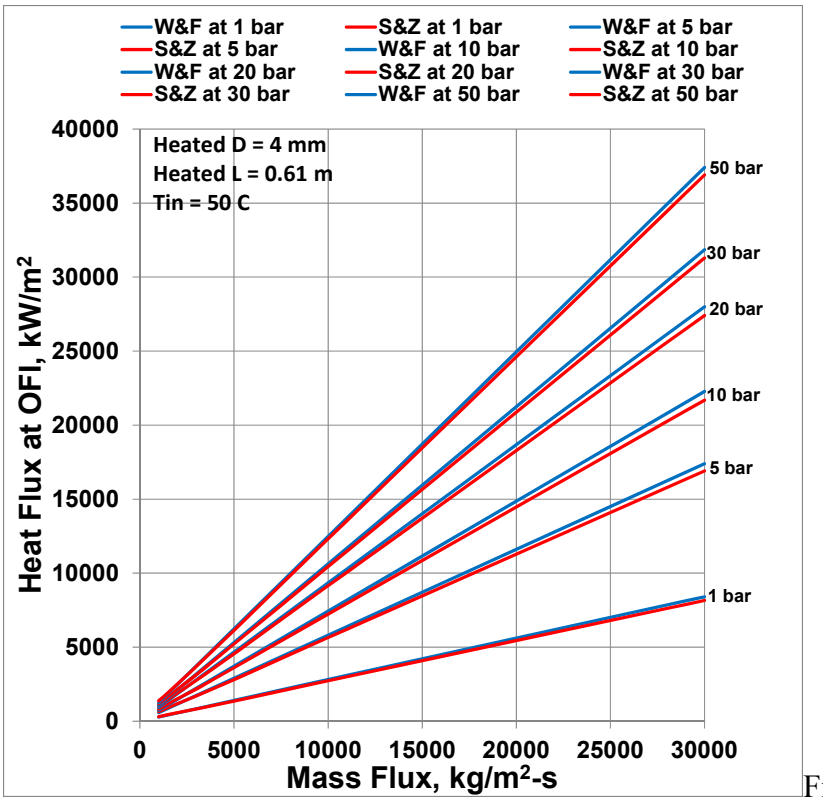

Fig. 10, Part 19 of 36

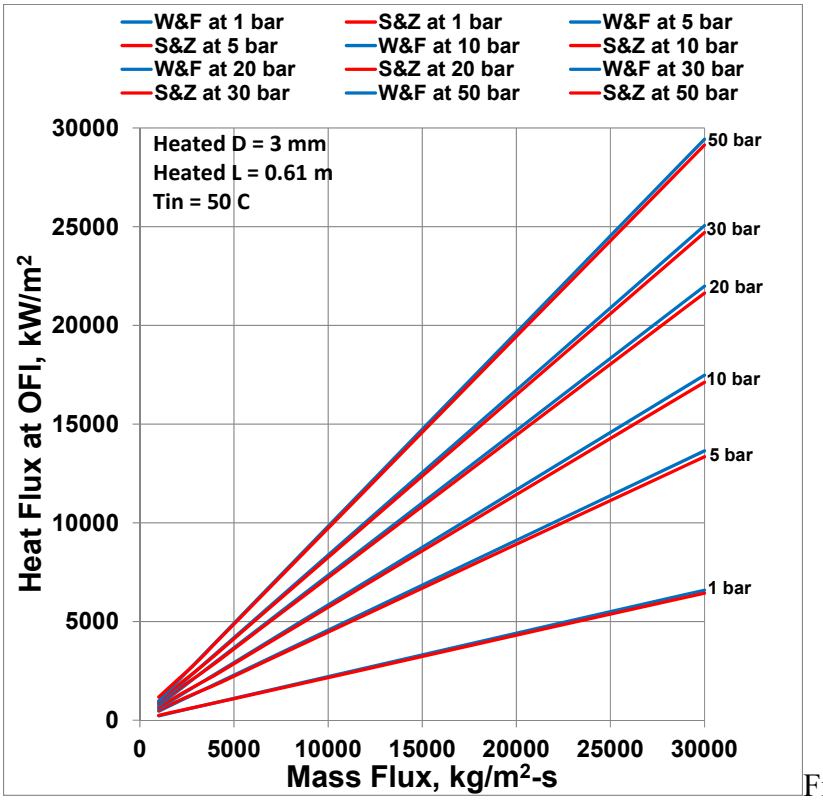

Fig. 10, Part 20 of 36

Fig. 10. Continued

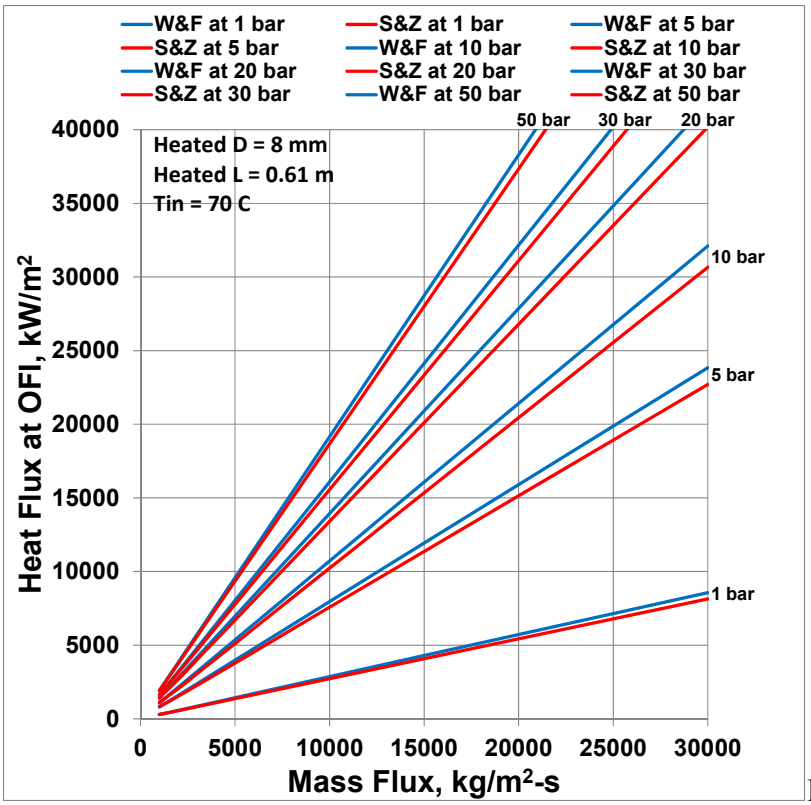

Fig. 10, Part 21 of 36

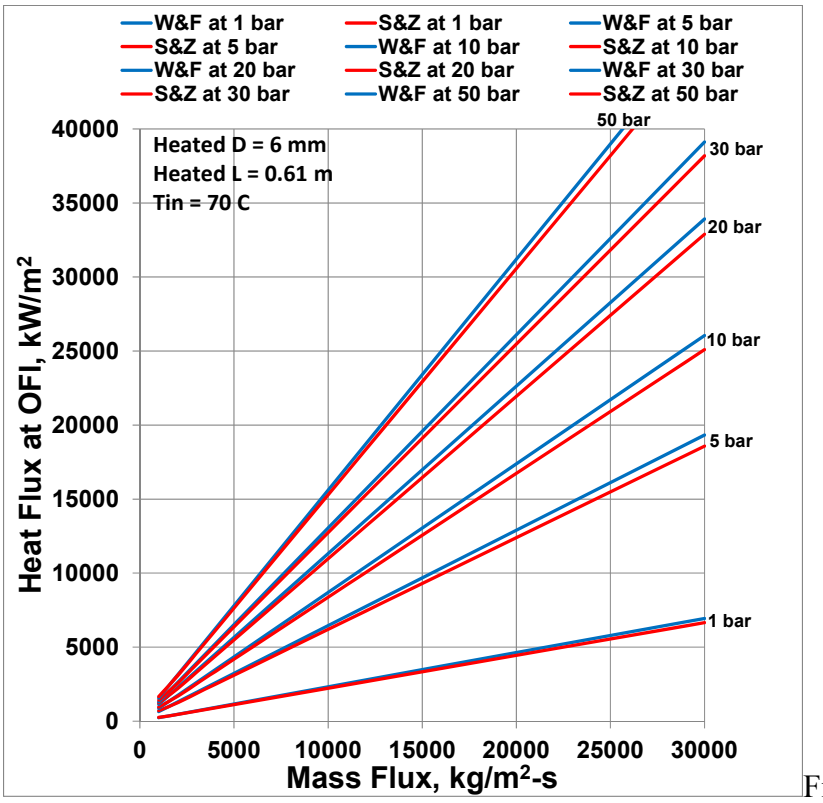

Fig. 10, Part 22 of 36

Fig. 10. Continued

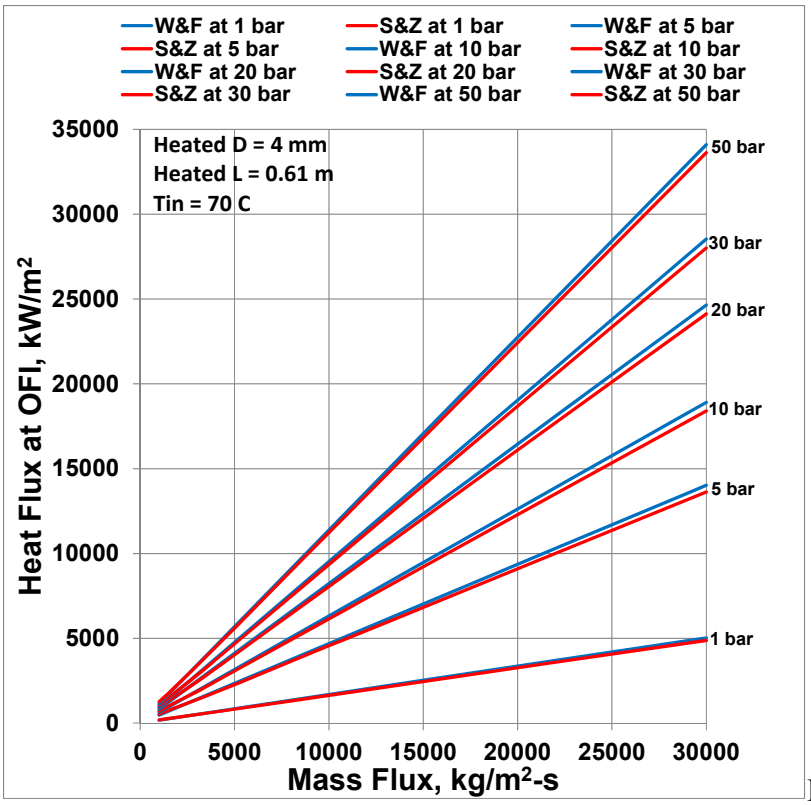

Fig. 10, Part 23 of 36

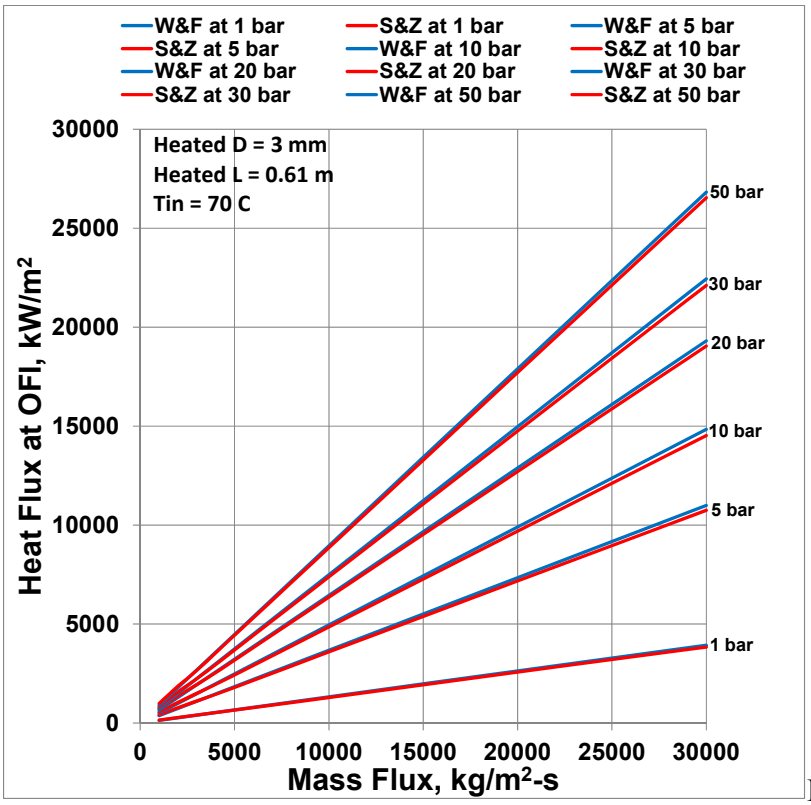

Fig. 10, Part 24 of 36

Fig. 10. Continued

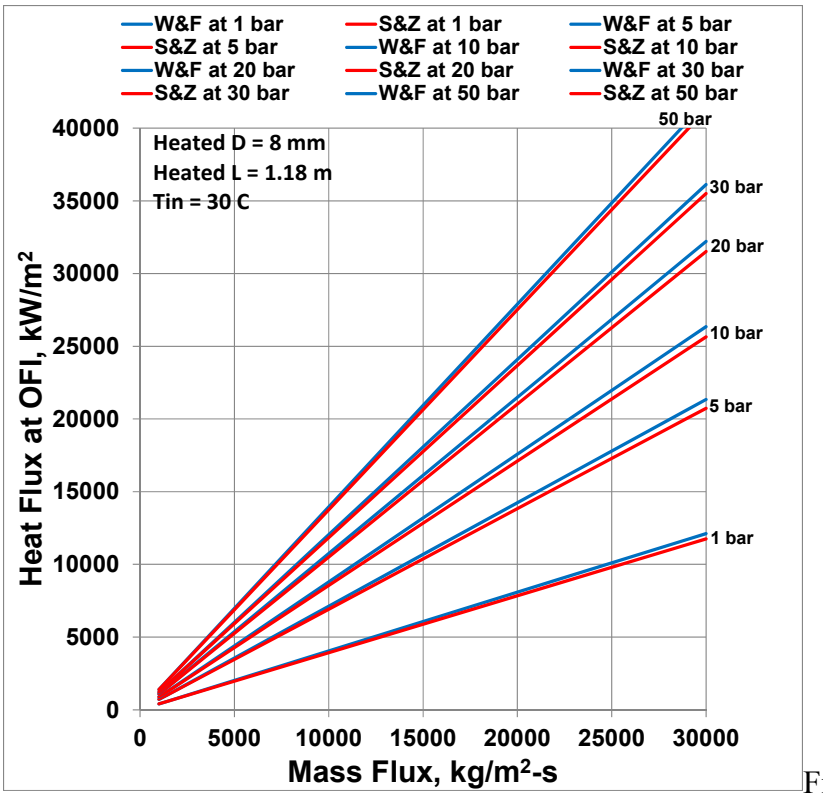

Fig. 10, Part 25 of 36

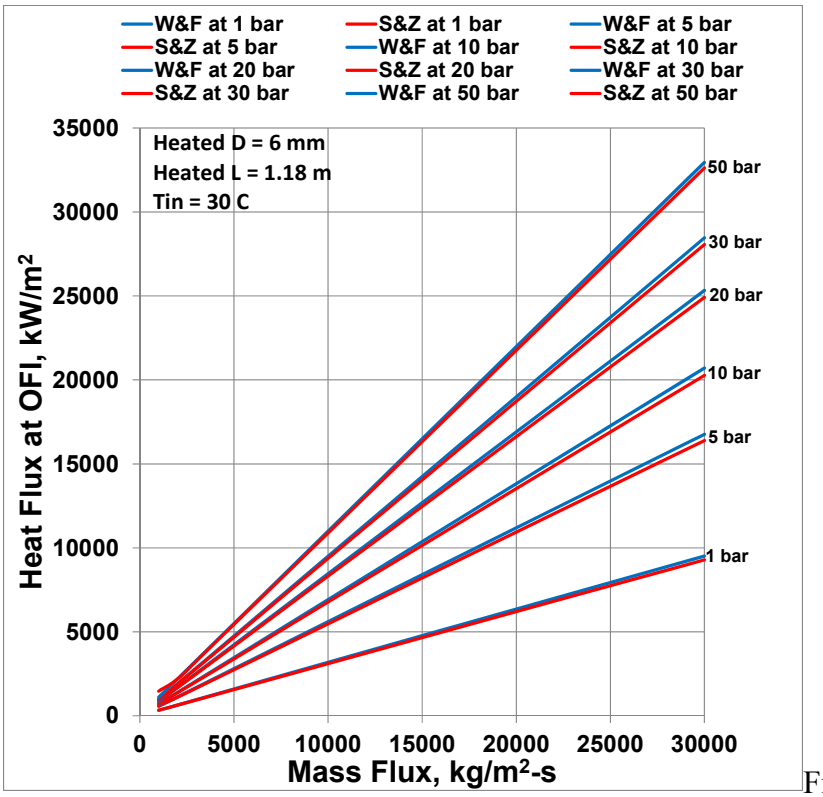

Fig. 10, Part 26 of 36

Fig. 10. Continued

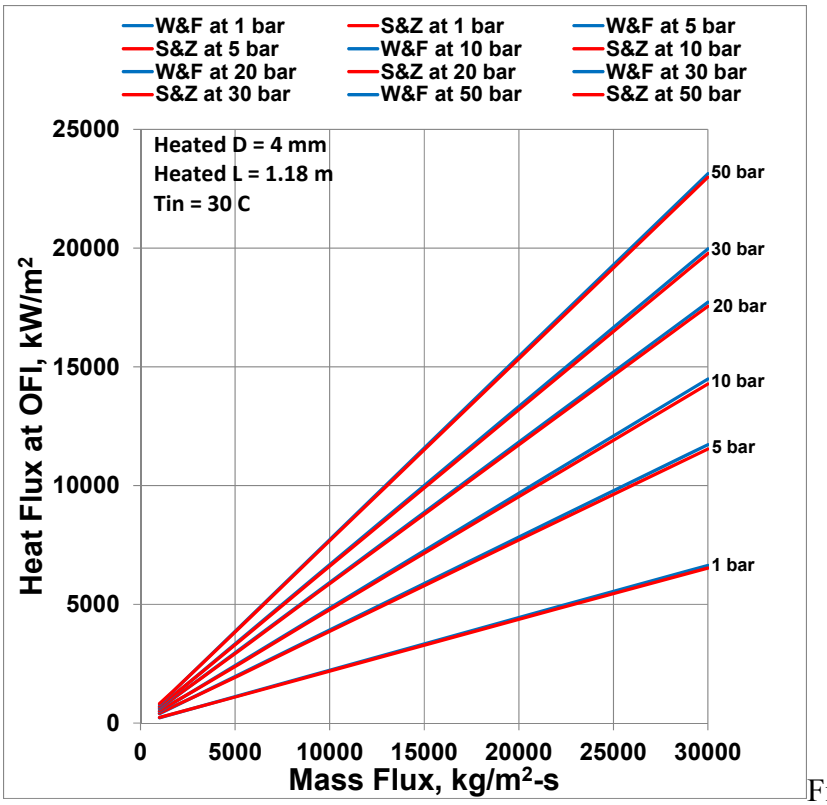

Fig. 10, Part 27 of 36

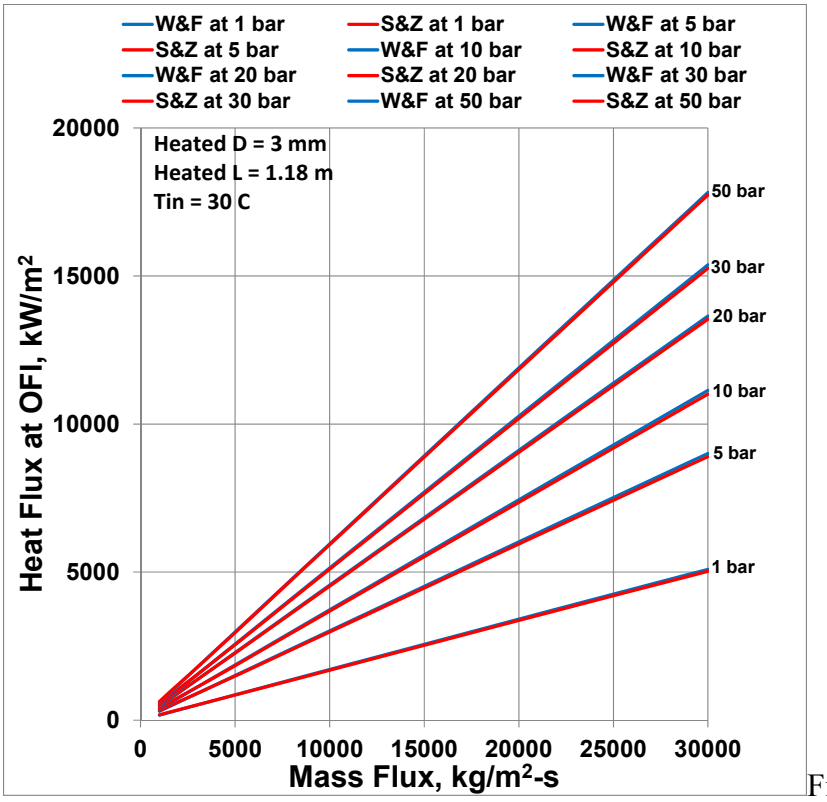

Fig. 10, Part 28 of 36

Fig. 10. Continued

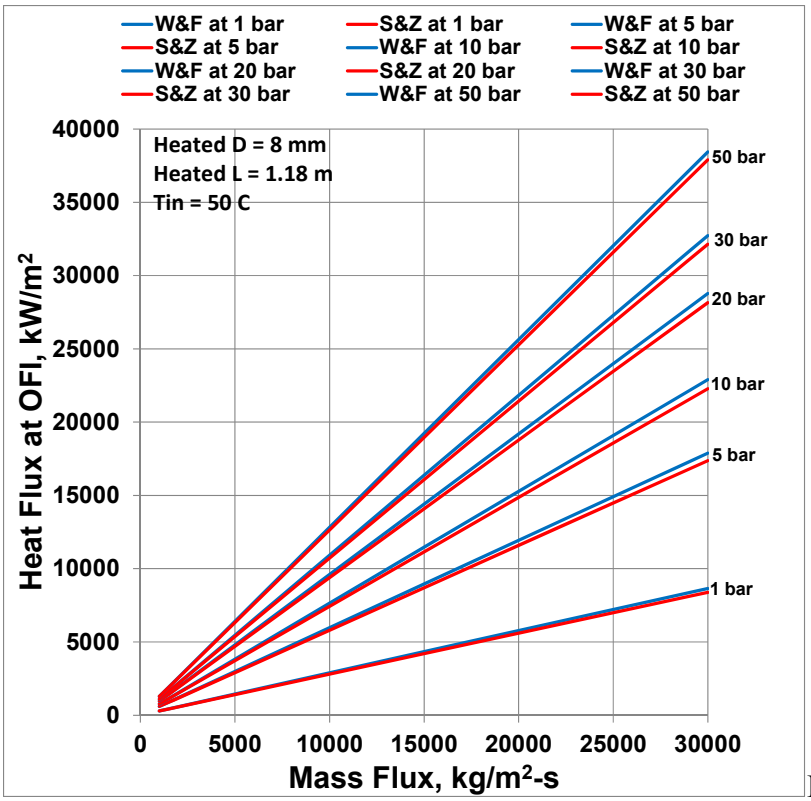

Fig. 10, Part 29 of 36

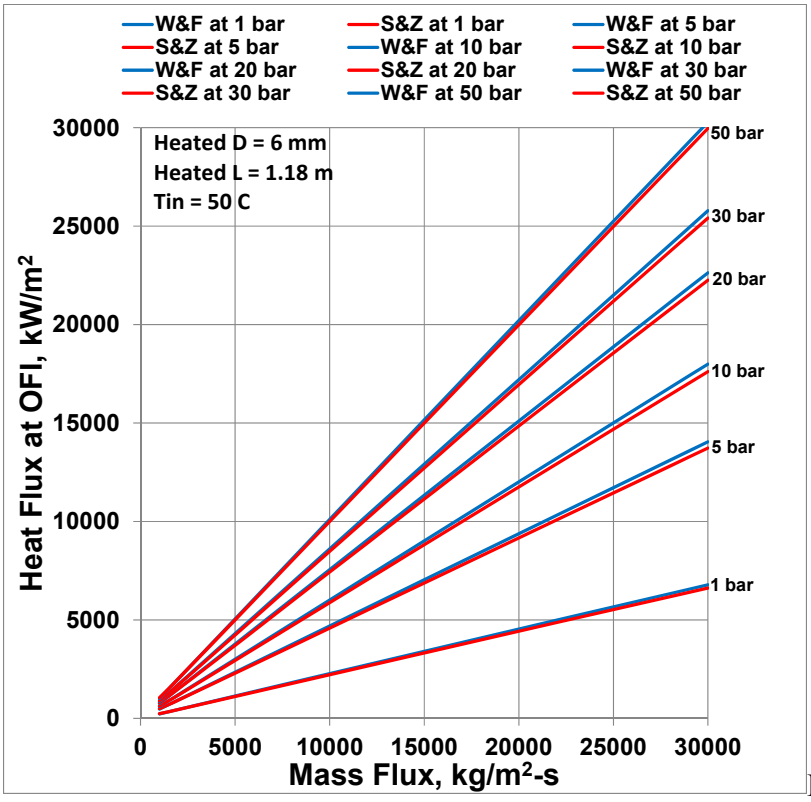

Fig. 10, Part 30 of 36

Fig. 10. Continued

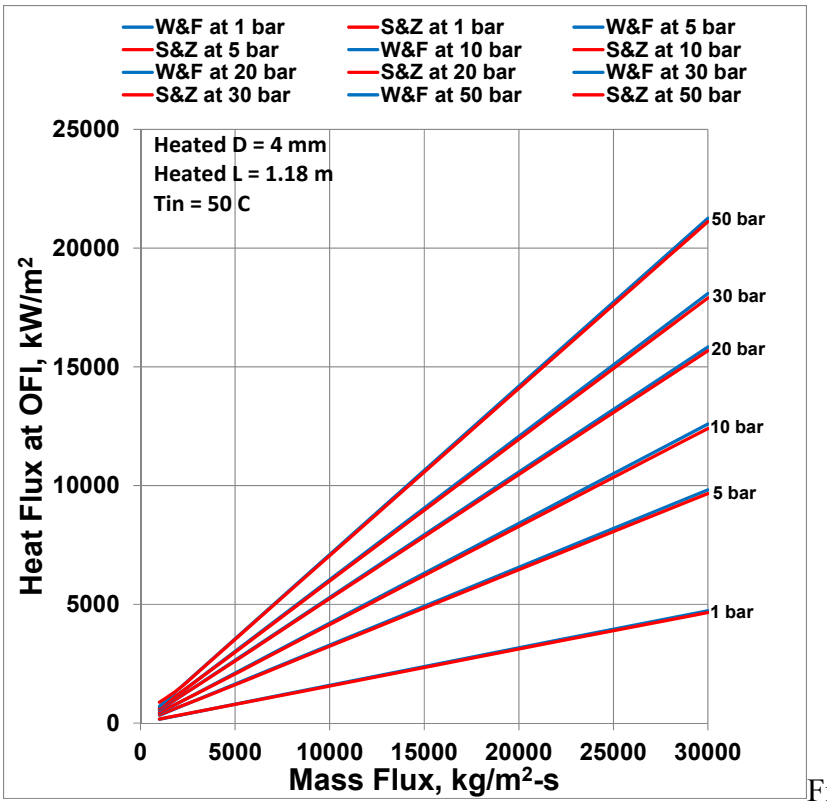

Fig. 10, Part 31 of 36

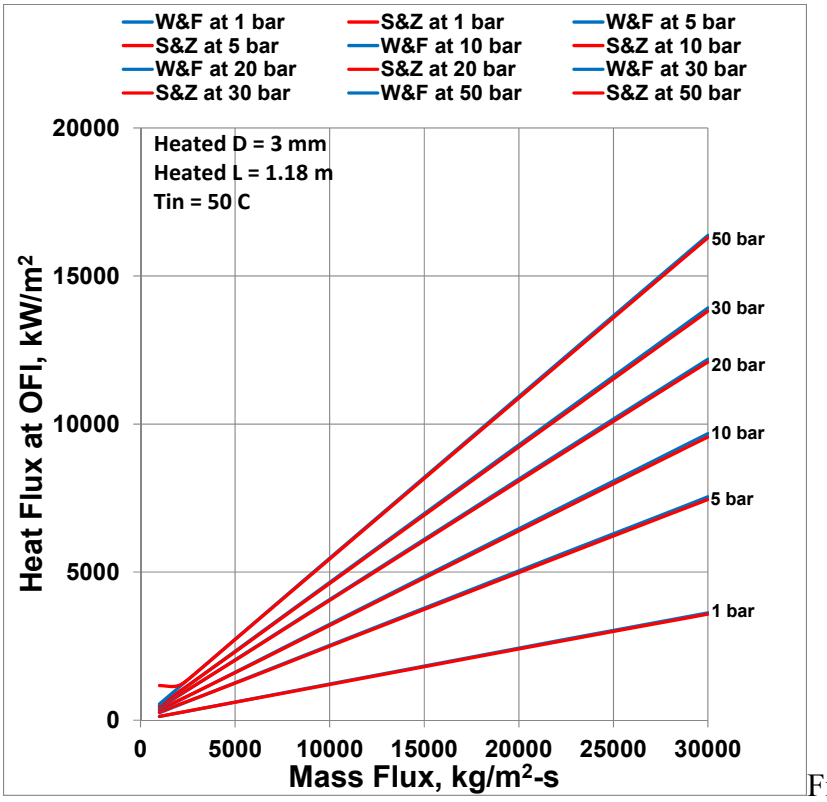

Fig. 10, Part 32 of 36

Fig. 10. Continued

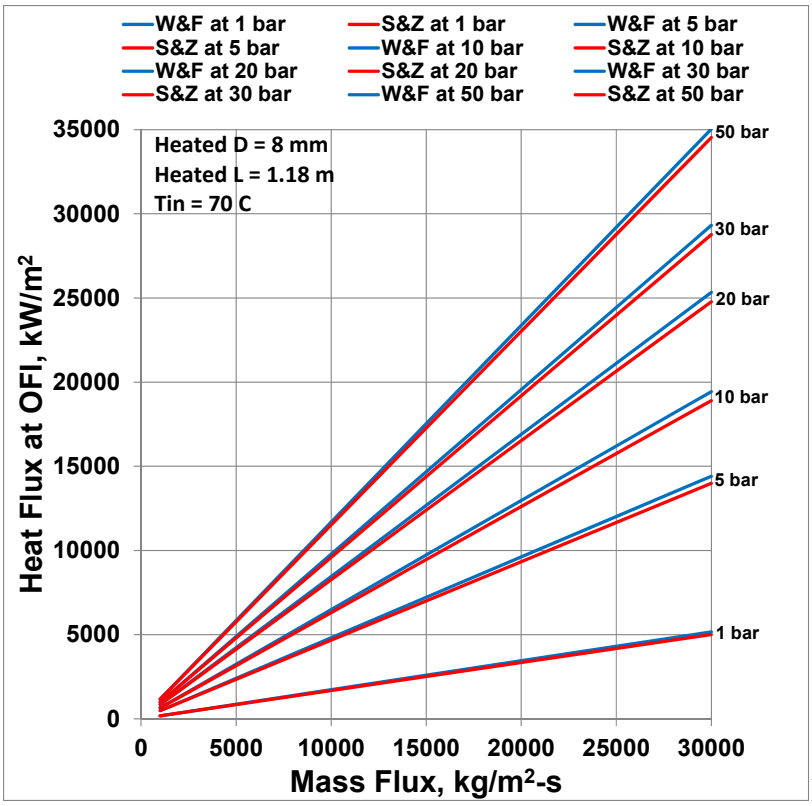

Fig. 10, Part 33 of 36

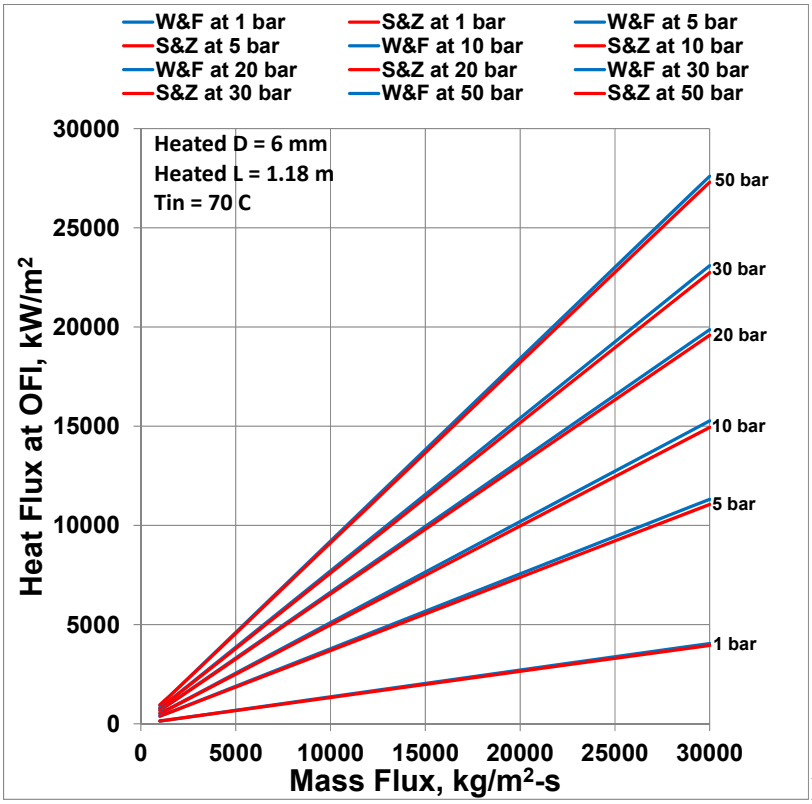

Fig. 10, Part 34 of 36

Fig. 10\9. Continued

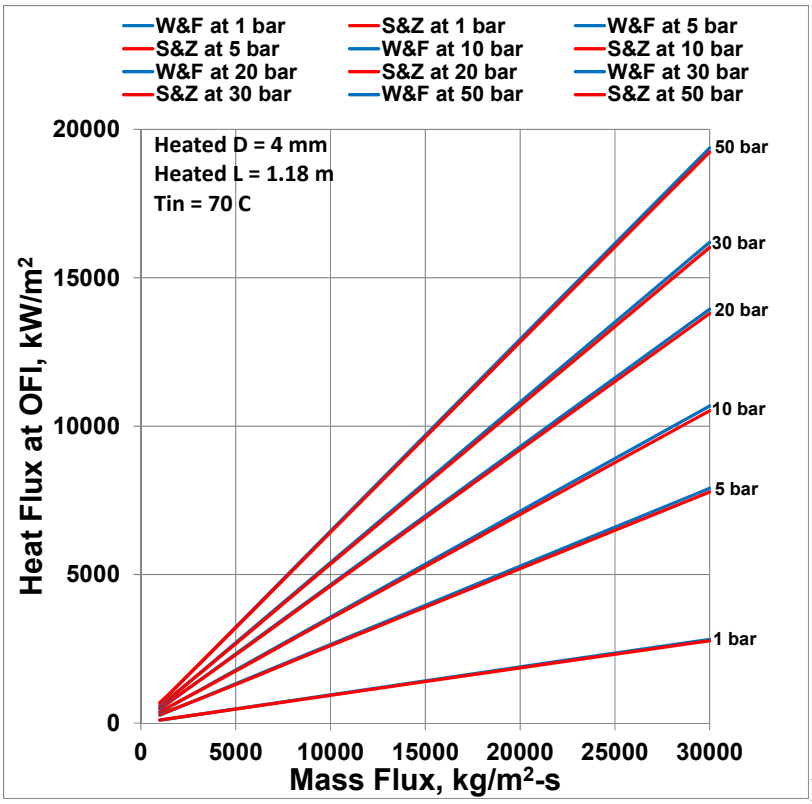

Fig. 10, Part 35 of 36

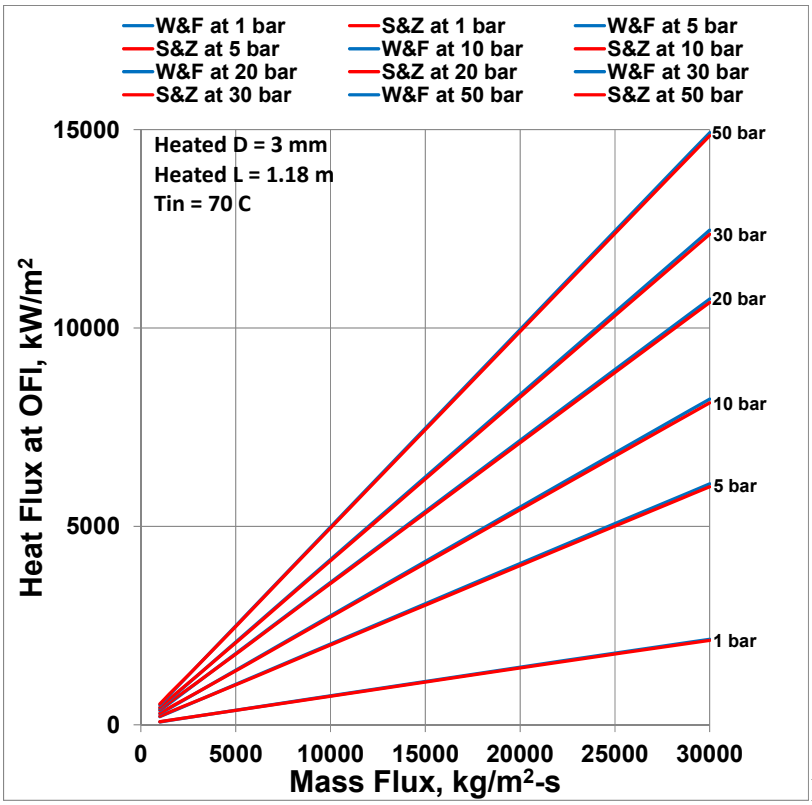

Fig. 10, Part 36 of 36

Fig. 10. Continued

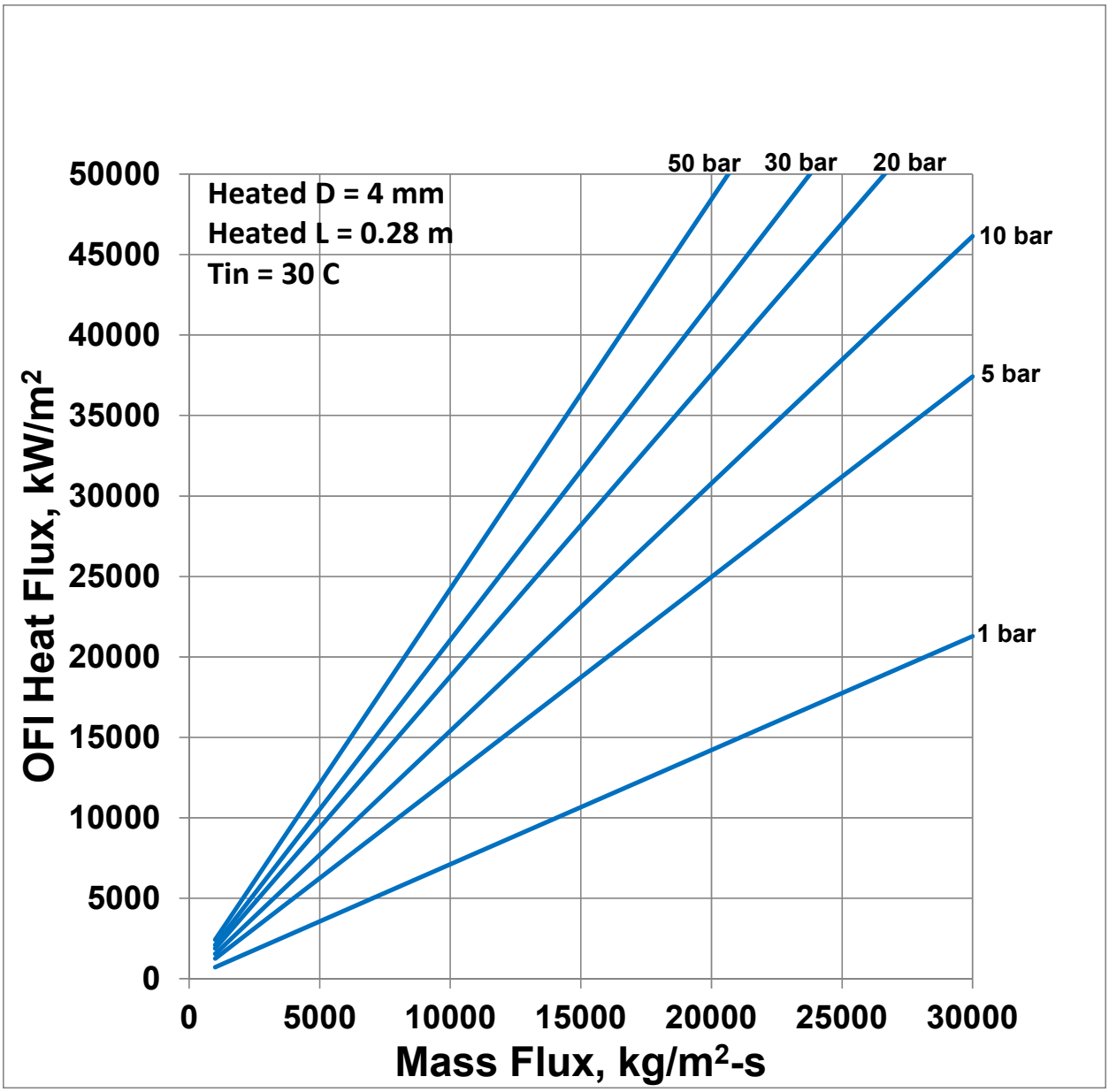

Fig. 11, Part 1 of 15

Fig. 11. Parametric Variation of OFI Heat Flux by Whittle-Forgan (η=32.5) Criterion

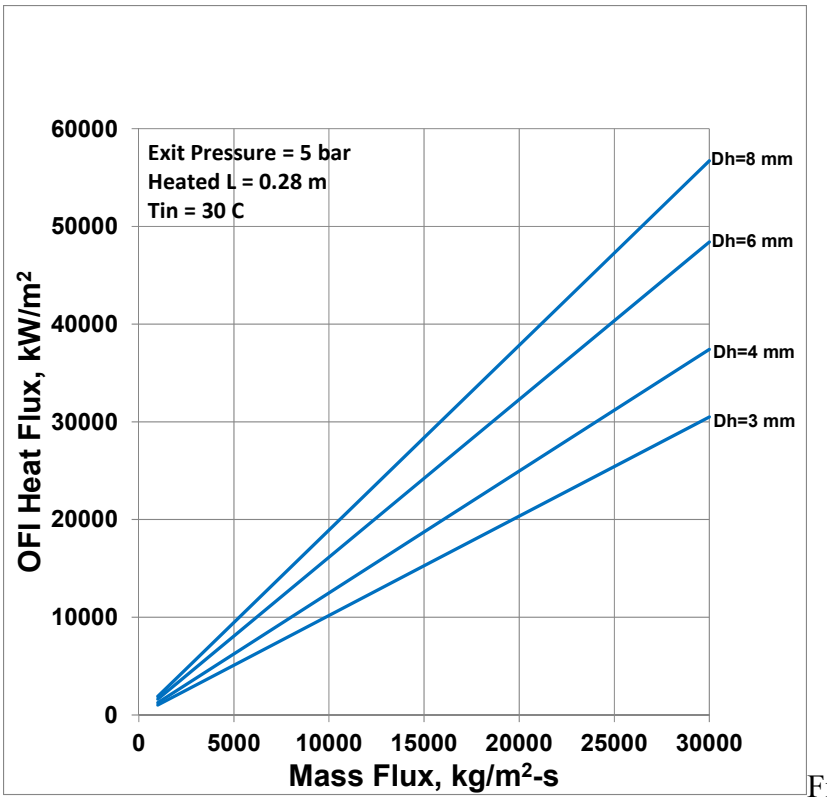

Fig. 11, Part 2 of 15

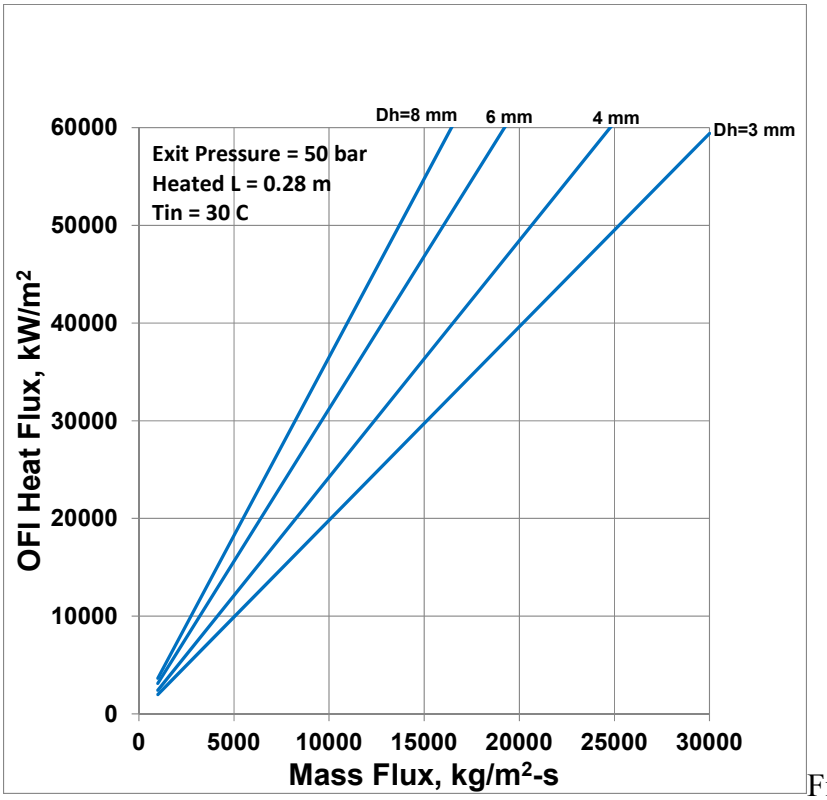

Fig. 11, Part 3 of 15

Fig. 11. Continued

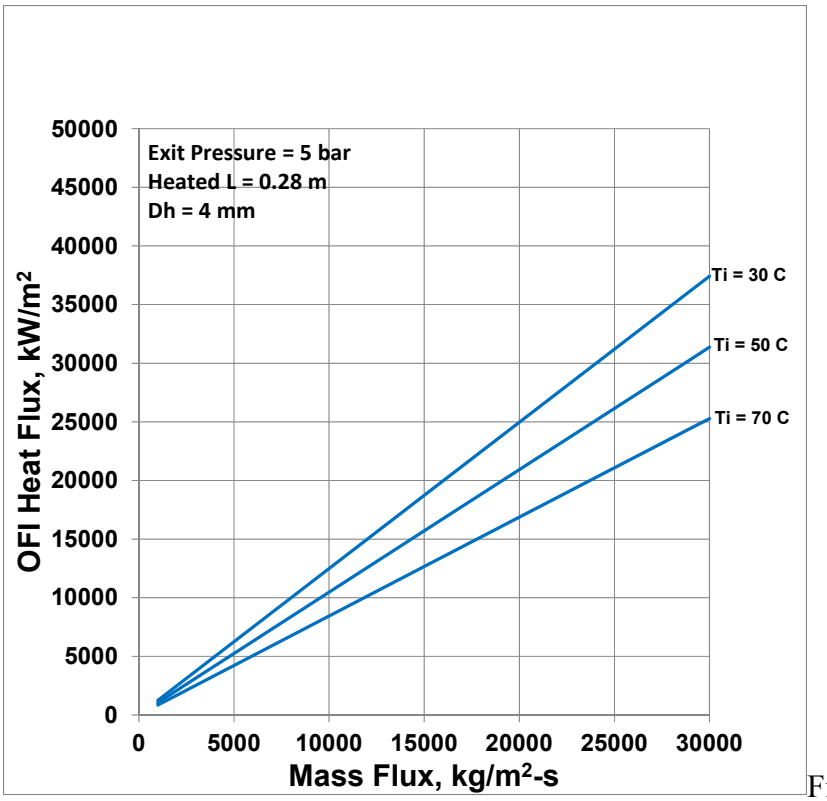

Fig. 11, Part 4 of 15

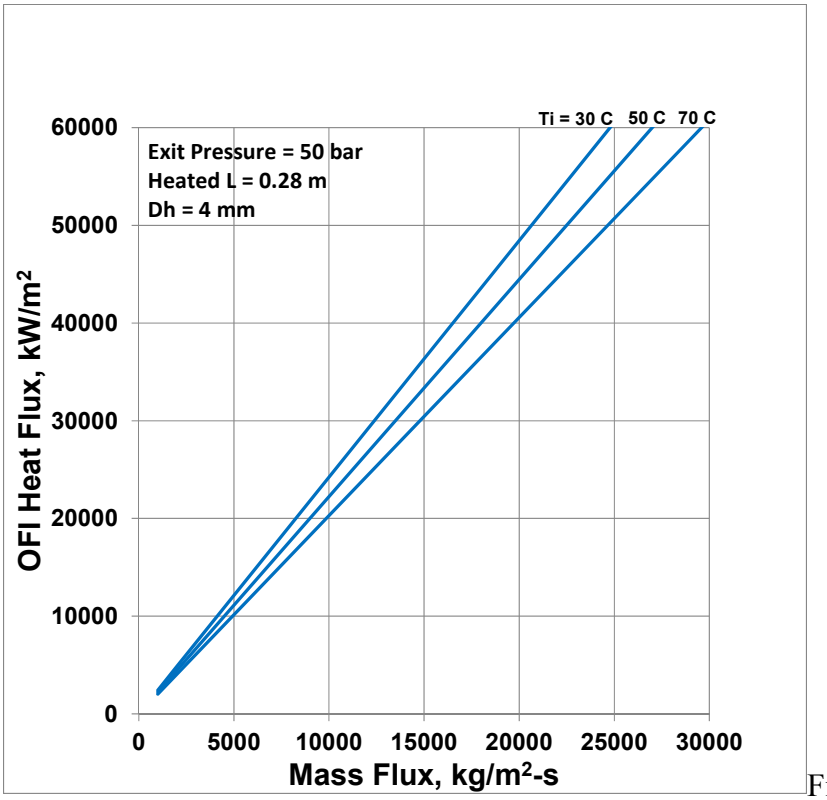

Fig. 11, Part 5 of 15

Fig. 11. Continued

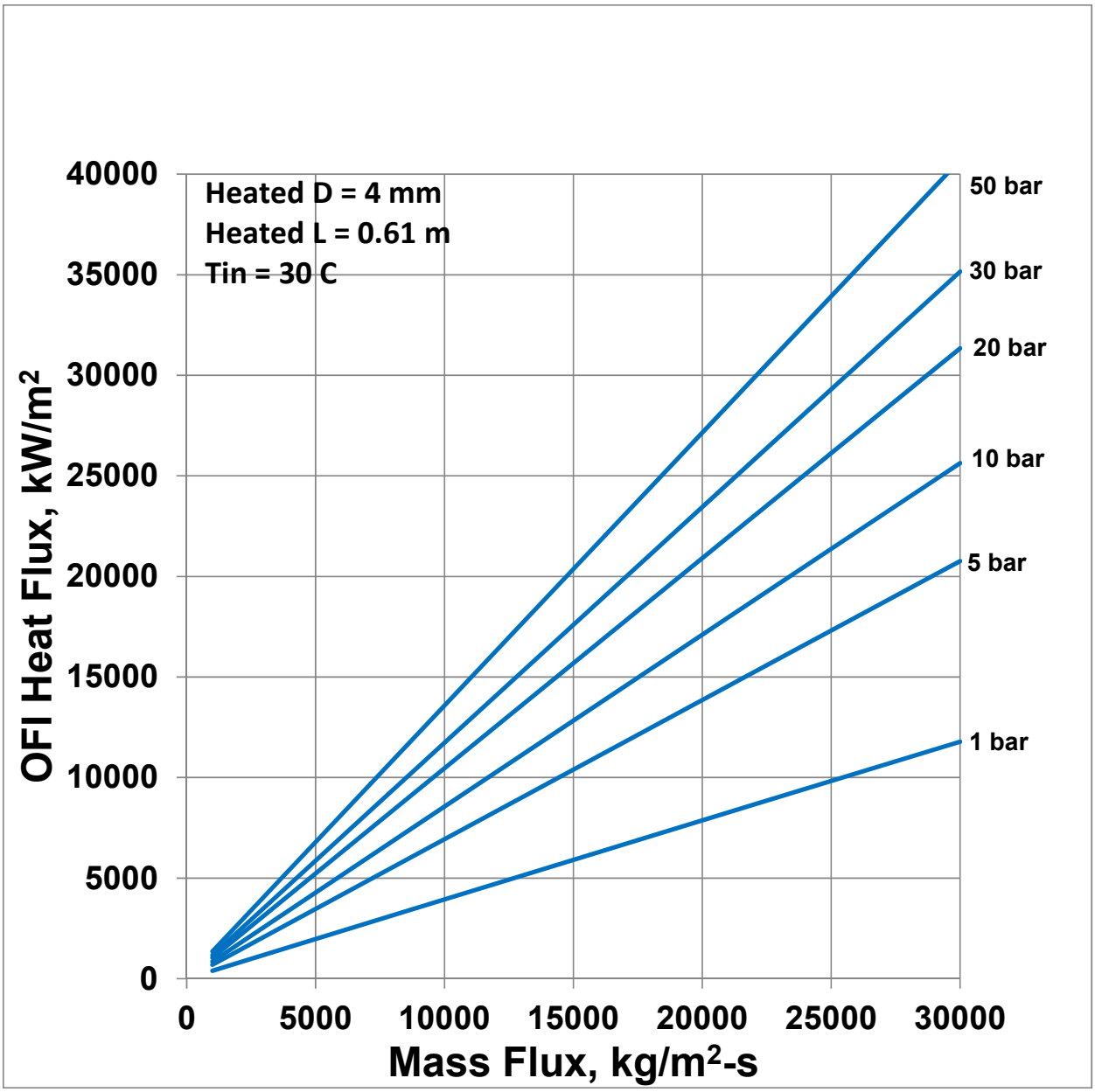

Fig. 11, Part 6 of 15

Fig. 11. Continued

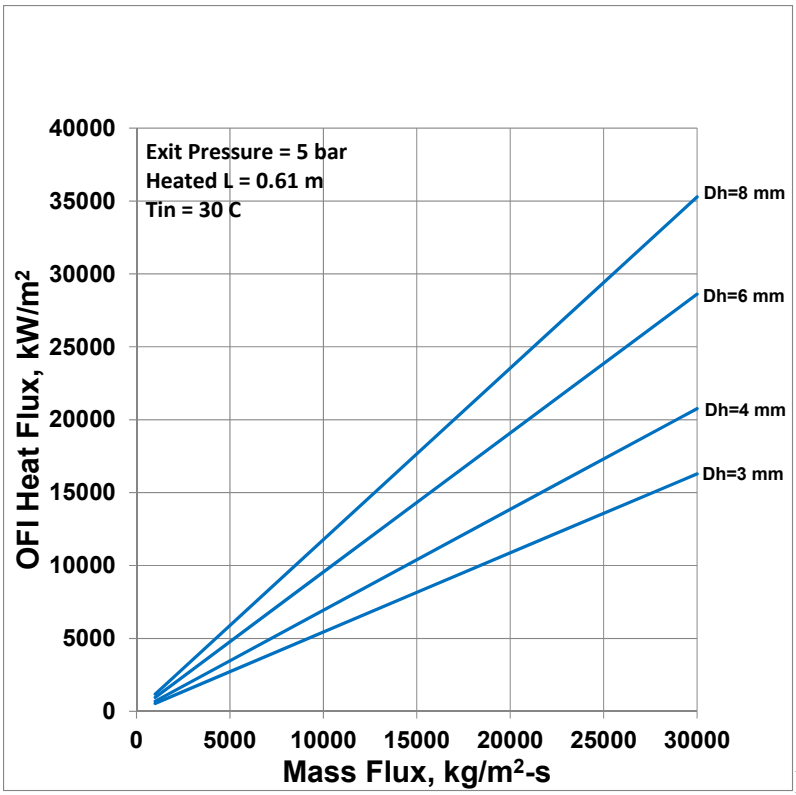

Fig. 11, Part 7 of 15

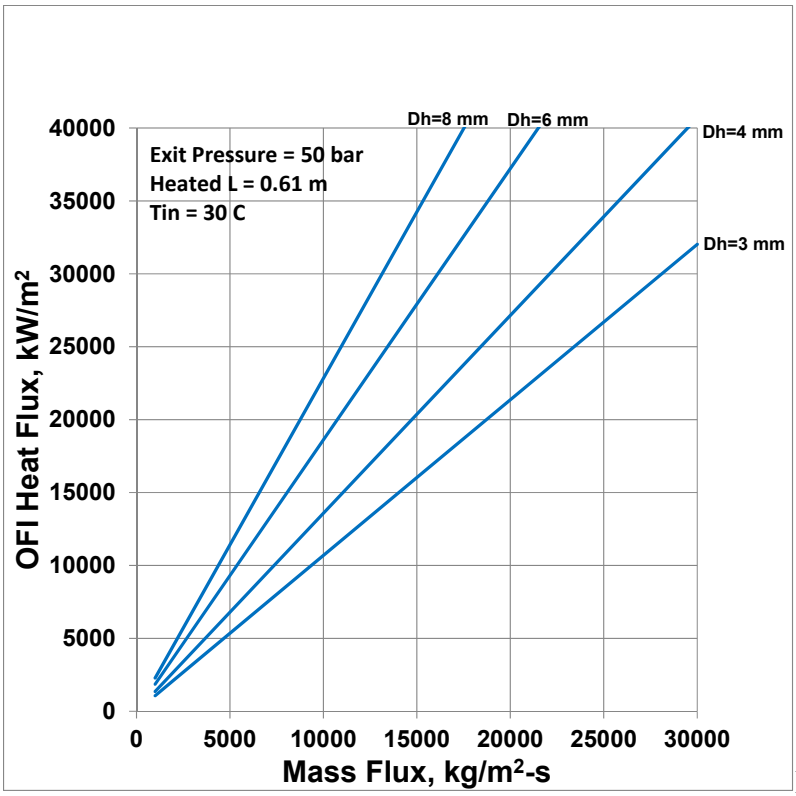

Fig. 11, Part 8 of 15

Fig. 11. Continued

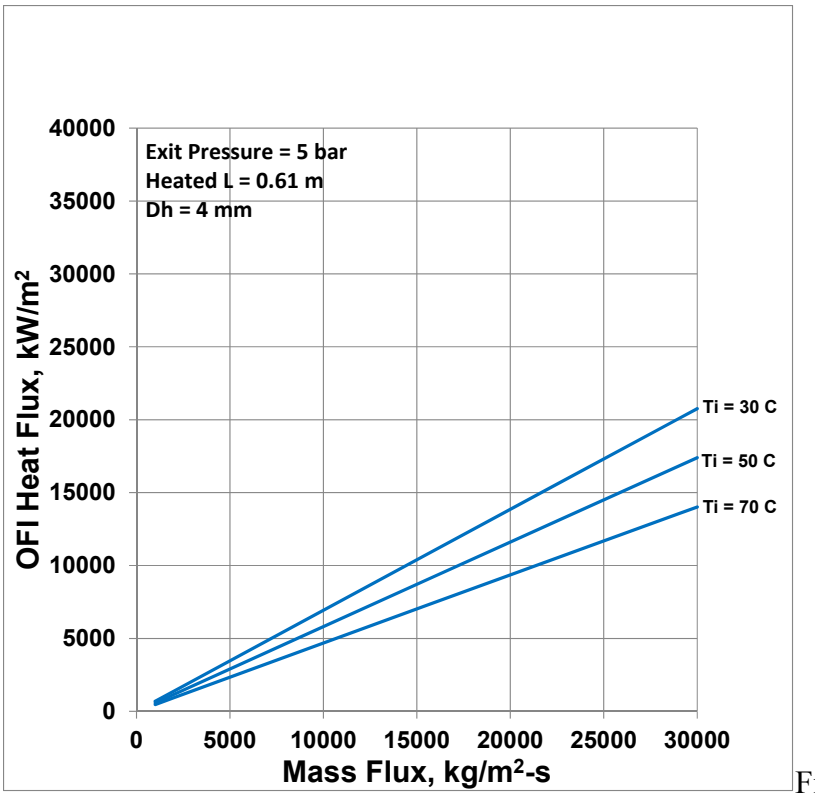

Fig. 11, Part 9 of 15

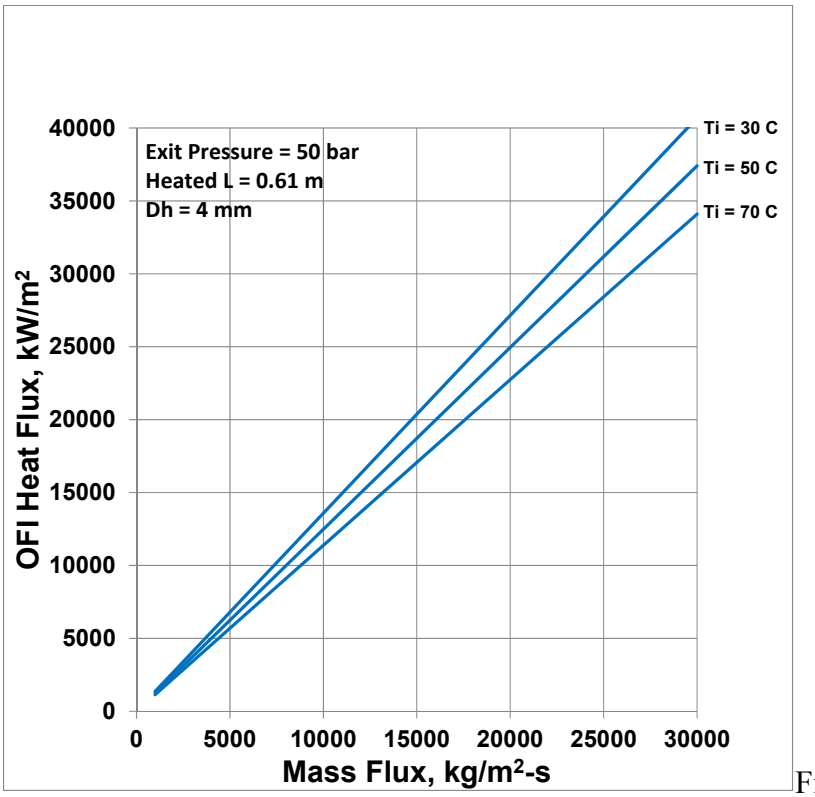

Fig. 11, Part 10 of 15

Fig. 11. Continued

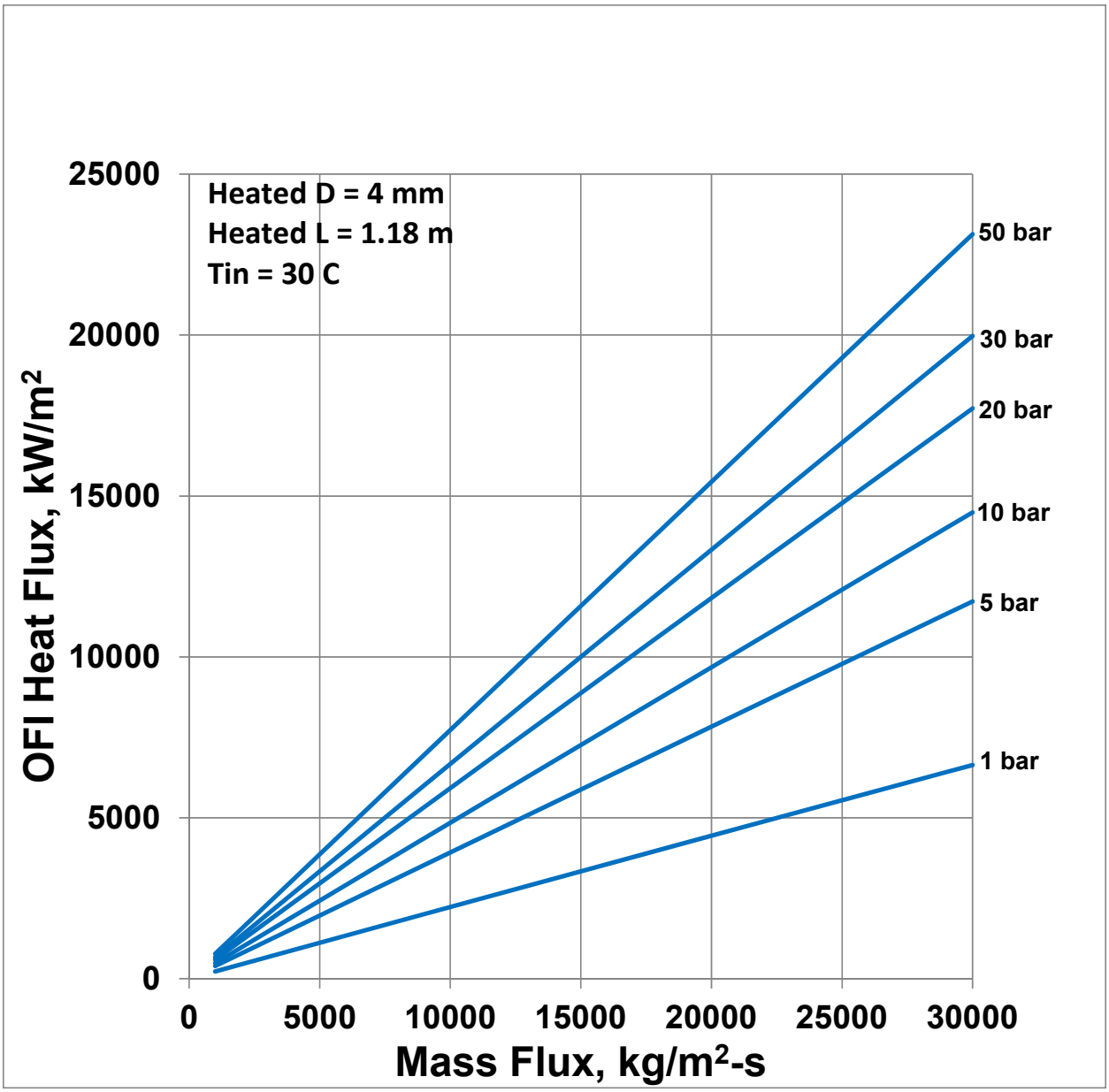

Fig. 11, Part 11 of 15

Fig. 11. Continued

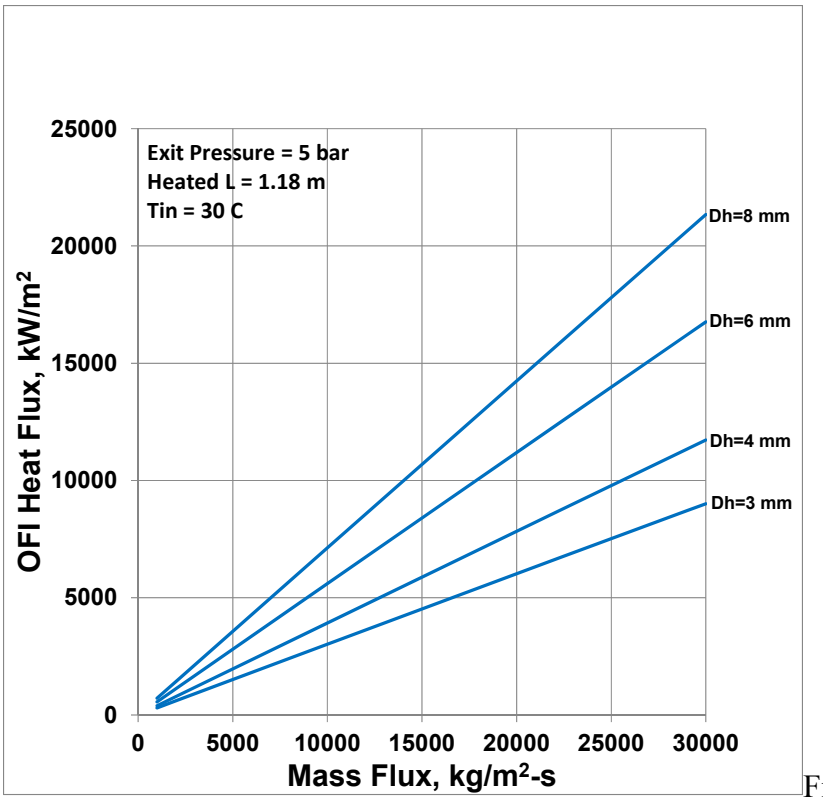

Fig. 11, Part 12 of 15

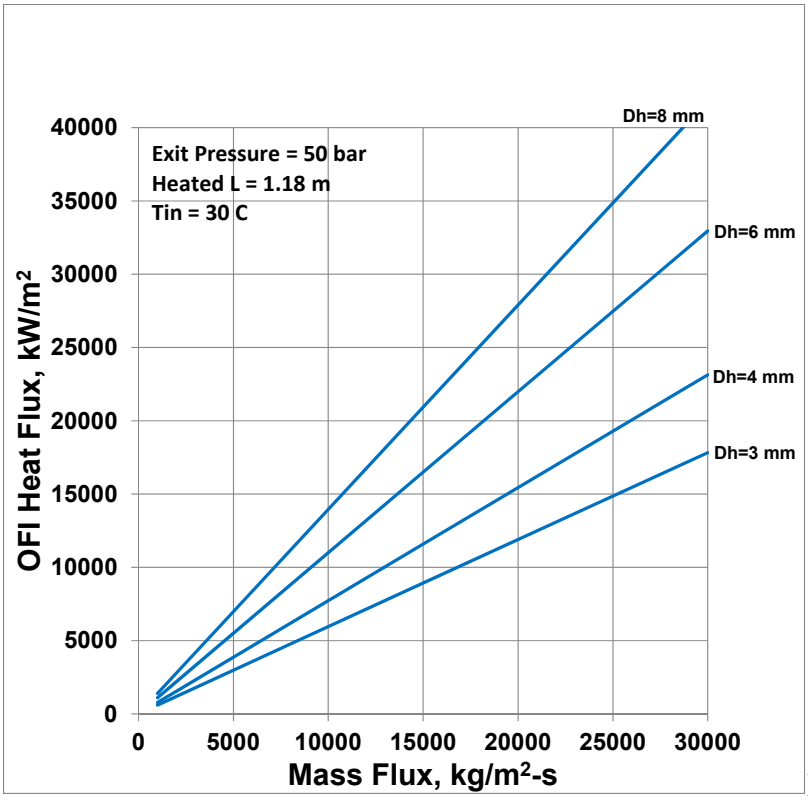

Fig. 11, Part 13 of 15

Fig. 11. Continued

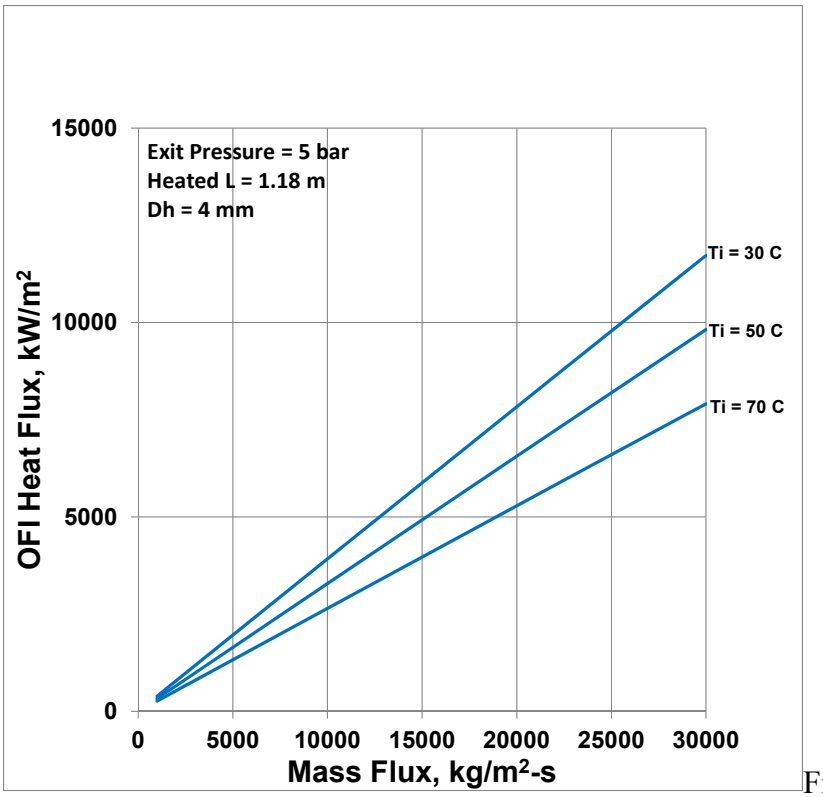

Fig. 11, Part 14 of 15

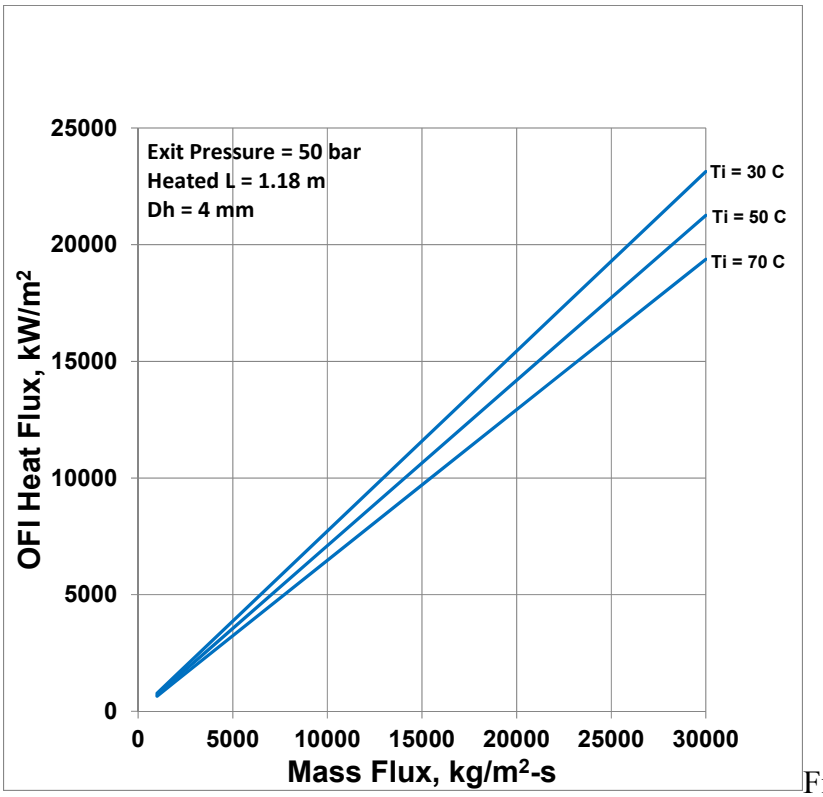

Fig. 11, Part 15 of 15

Fig. 11. Continued

APPENDIX E. PARAMETRIC VARIATION OF BERGLES-ROHSENOW ONB HEAT FLUX

The heat flux at the onset of nucleate boiling (ONB) obtained by the Bergles-Rohsenow correlation (calculated iteratively as described in Appendix A) was used in making the comparison plots given in Appendix B.

The ONB heat flux is a function of five independent parameters: P, L_h , D_h , G, and T_i . The effect of exit pressure P, heated diameter D_h or inlet temperature T_i on the ONB obtained by the Bergles-Rohsenow correlation is shown in Fig. 12 (having 15 parts). In these separate-effect plots, only one parameter is changed at a time, holding the other four parameters constant. The parts 1 to 5 of Fig. 12 are for L_h=0.28 m, the parts 6 to 10 for L_h=0.61 m, and the parts 11 to 15 for L_h=1.18 m. At each heated length, the ONB heat flux increases with increasing exit pressure at constant D_h , L_h , T_{in} , and G (see Fig. 12 part 1). The ONB increases with increasing heated diameter at constant P, L_h , T_{in} , and G (see Fig. 12 parts 2 and 3). The ONB decreases with increasing inlet temperature at constant P, L_h , D_h , and G (see Fig. 12 parts 4 and 5). In short, the variation trend of ONB heat flux is qualitatively similar to that of the OFI heat flux.

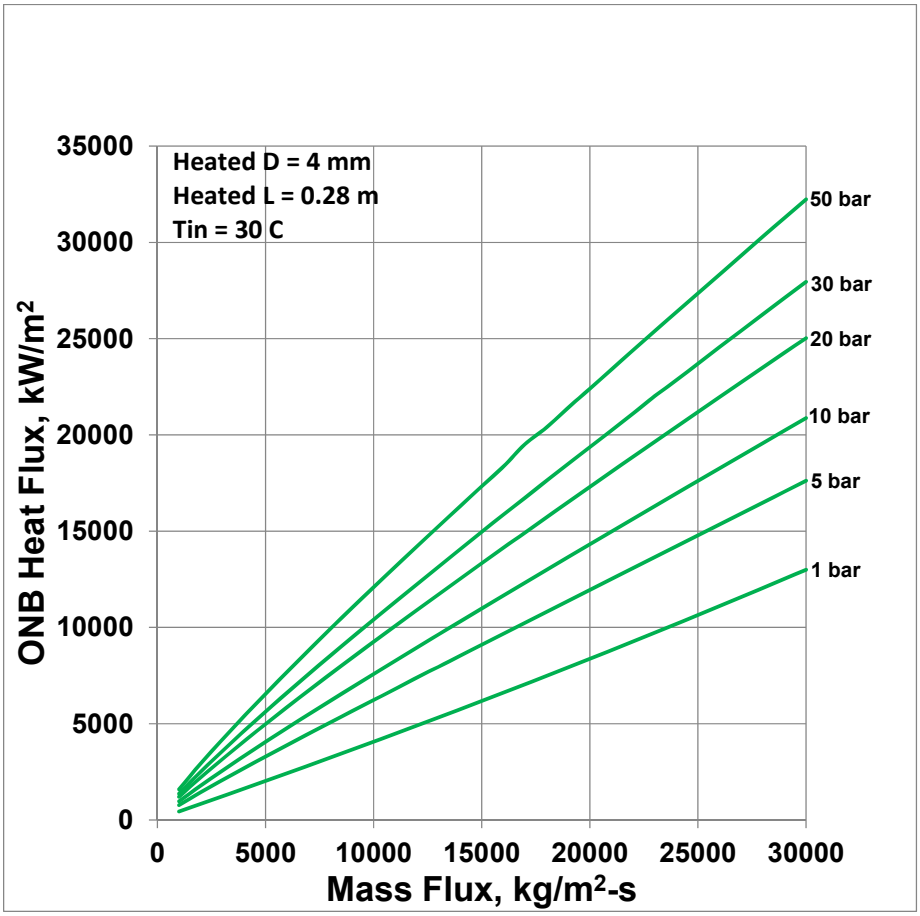

Fig. 12, Part 1 of 15

Fig. 12. Parametric Variation of Bergles-Rohsenow ONB Heat Flux

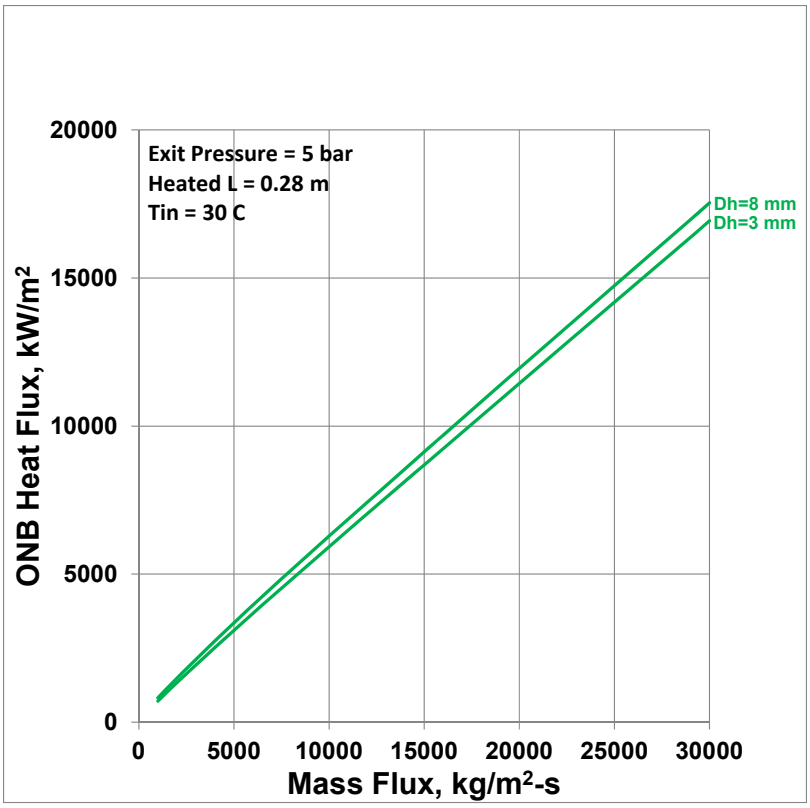

Fig. 12, Part 2 of 15

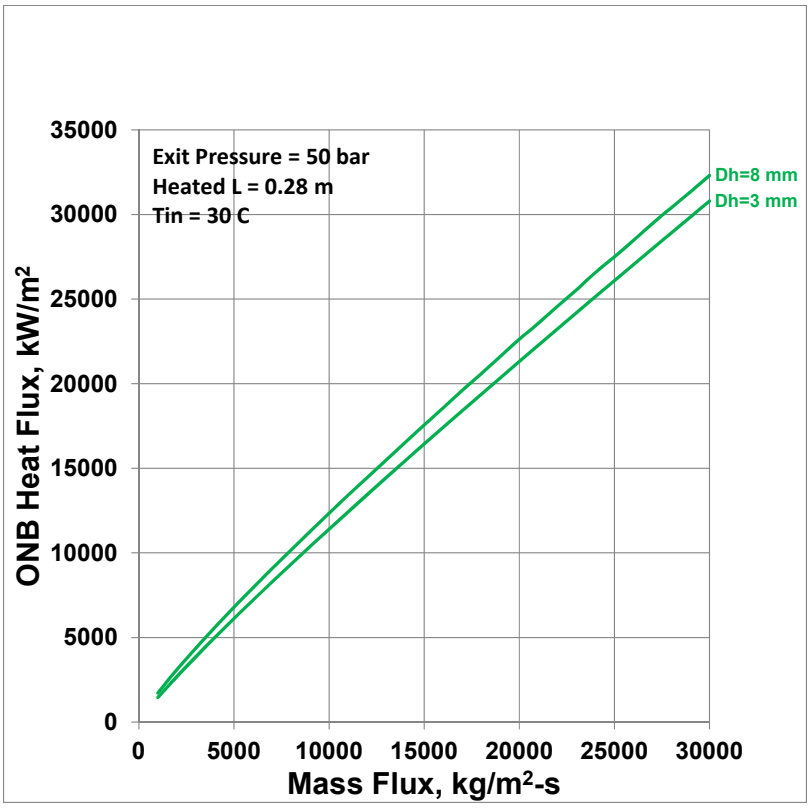

Fig. 12, Part 3 of 15

Fig. 12. Continued

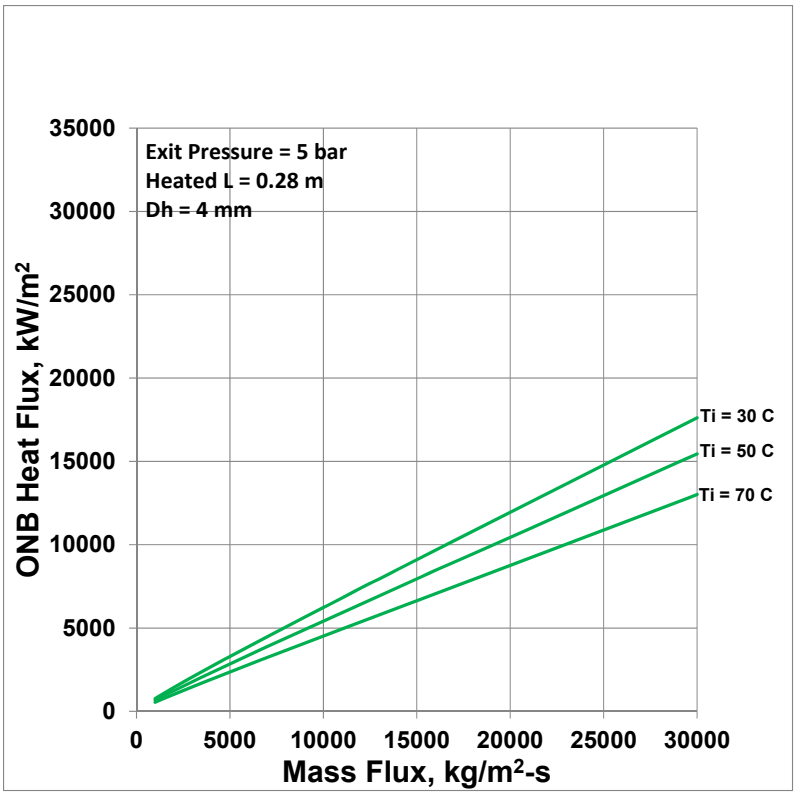

Fig. 12, Part 4 of 15

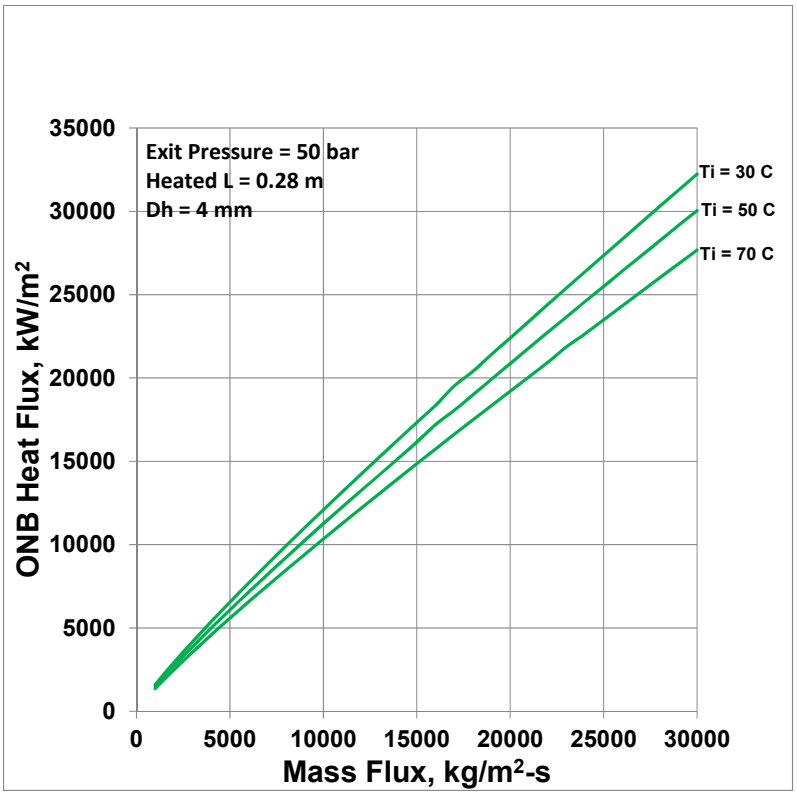

Fig. 12, Part 5 of 15

Fig. 12. Continued

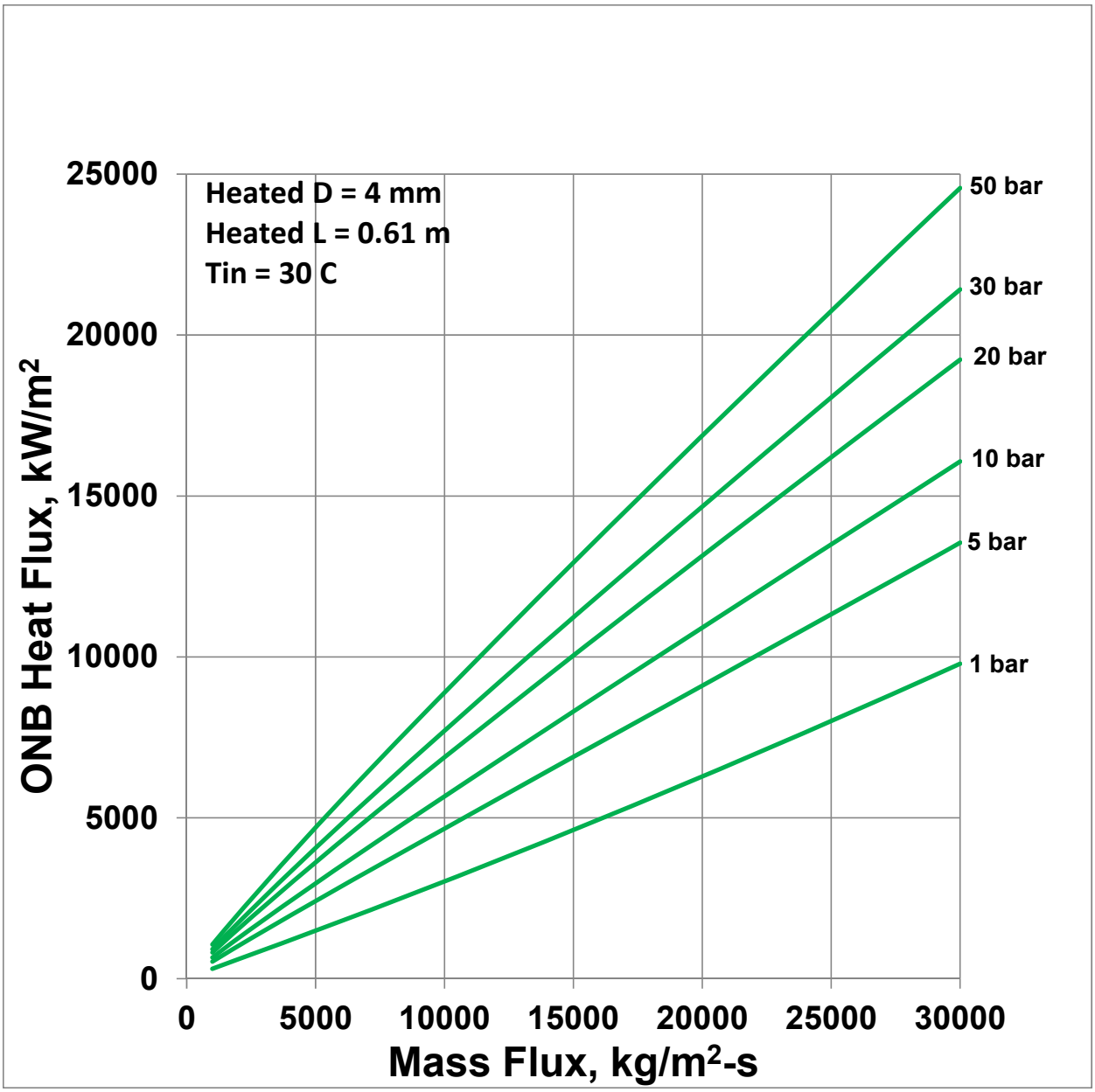

Fig. 12, Part 6 of 15

Fig. 12. Continued

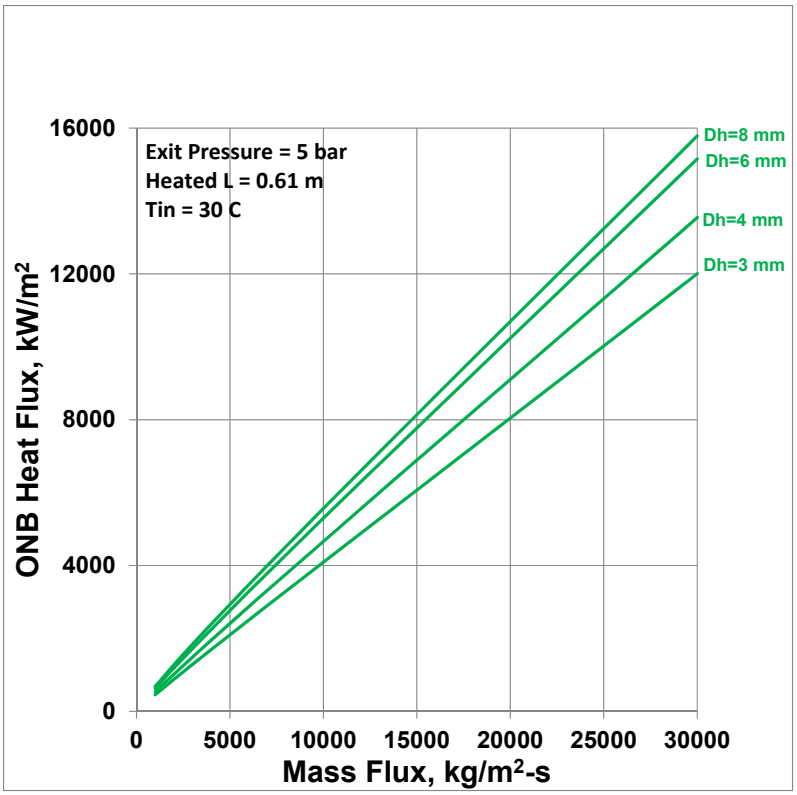

Fig. 12, Part 7 of 15

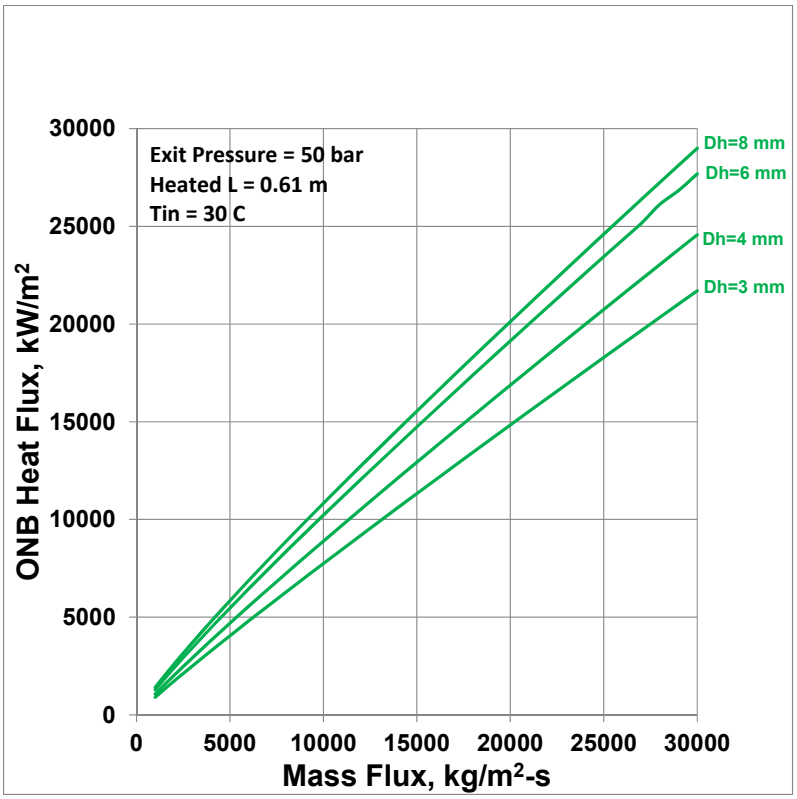

Fig. 12, Part 8 of 15

Fig. 12. Continued

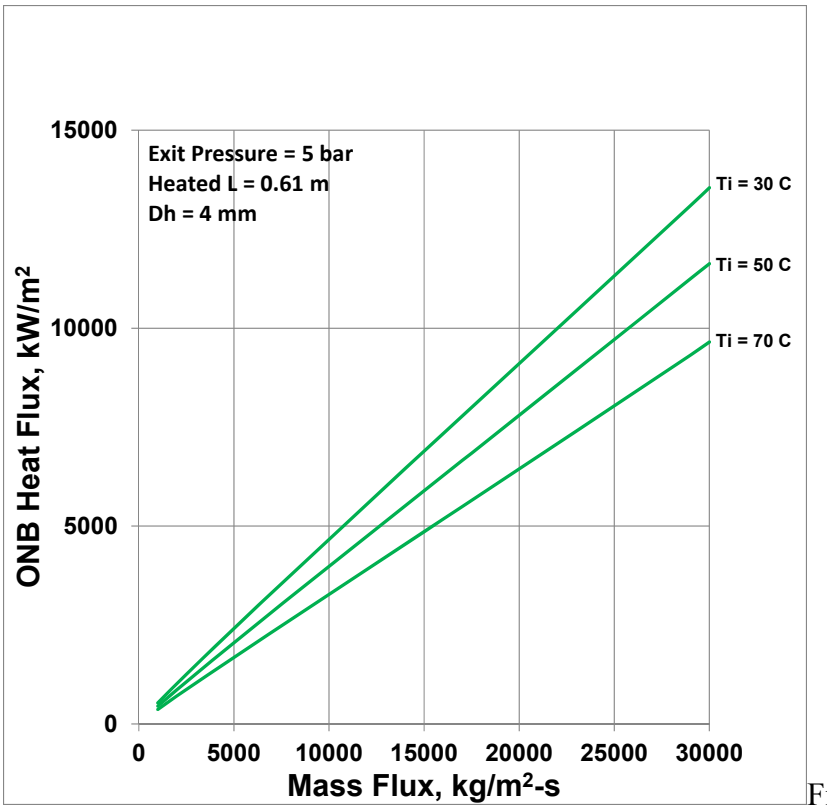

Fig. 12, Part 9 of 15

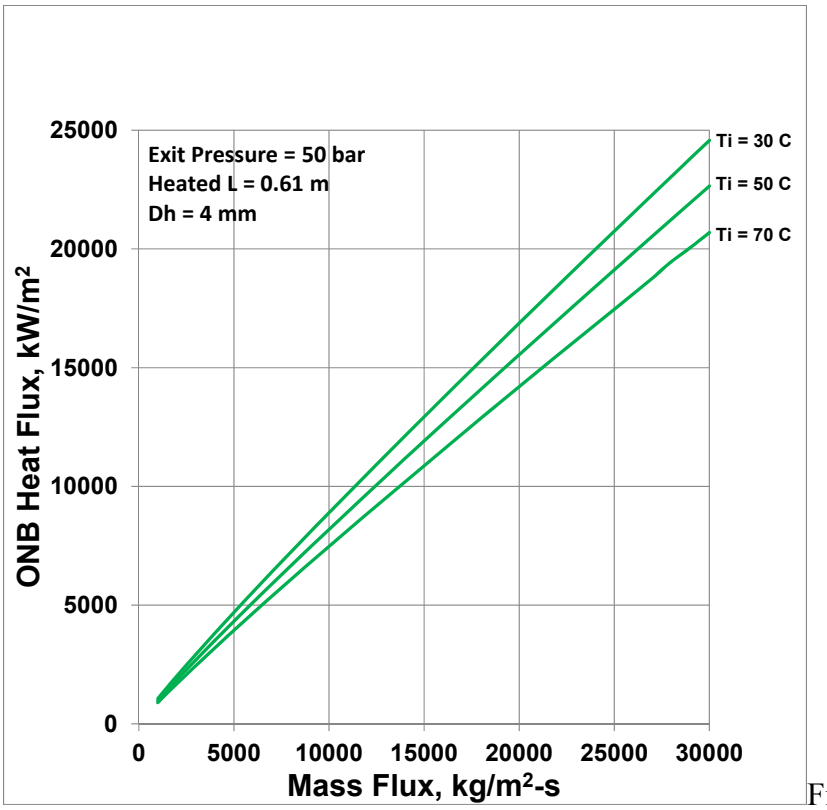

Fig. 12, Part 10 of 15

Fig. 12. Continued

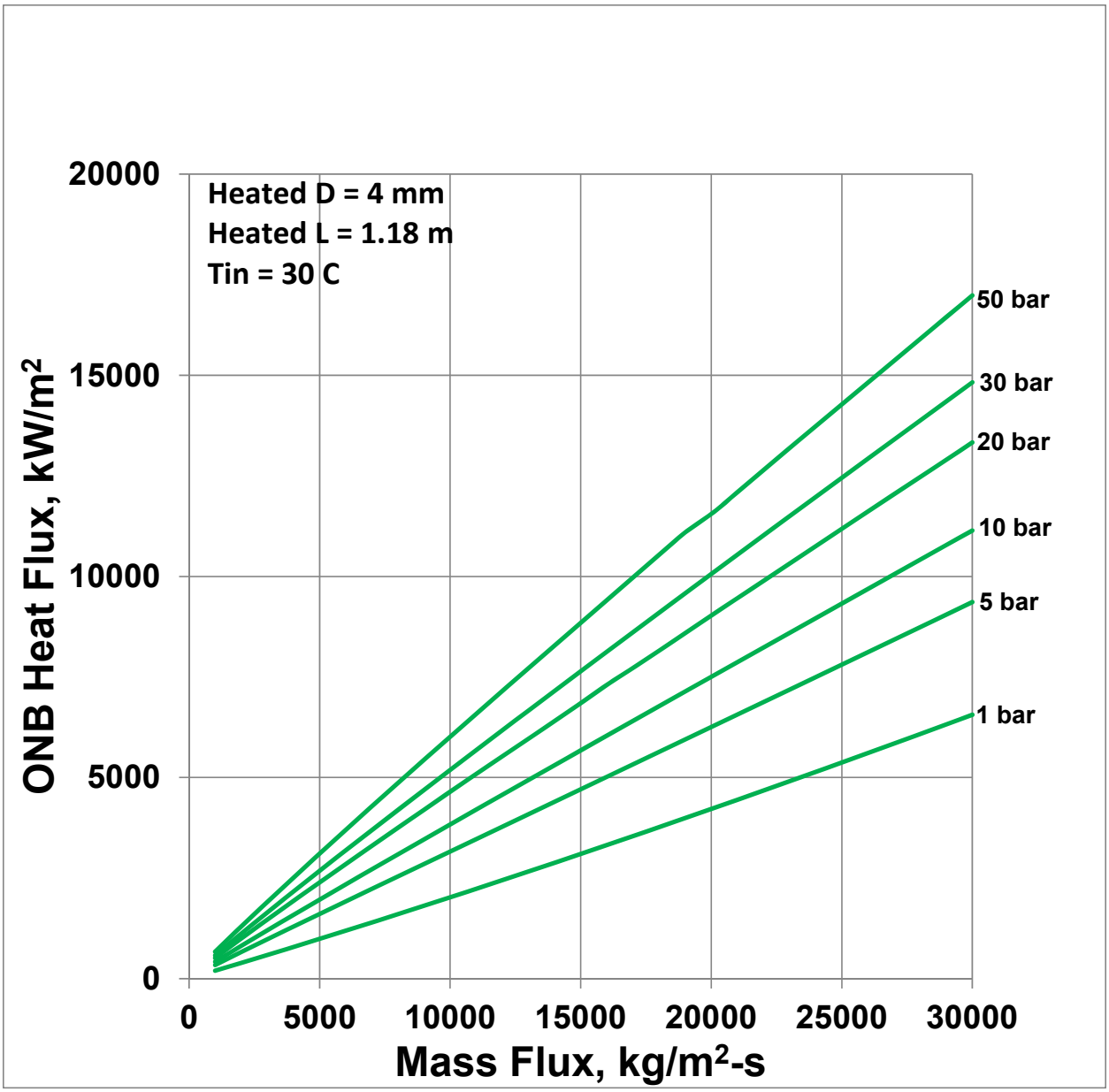

Fig. 12, Part 11 of 15

Fig. 12. Continued

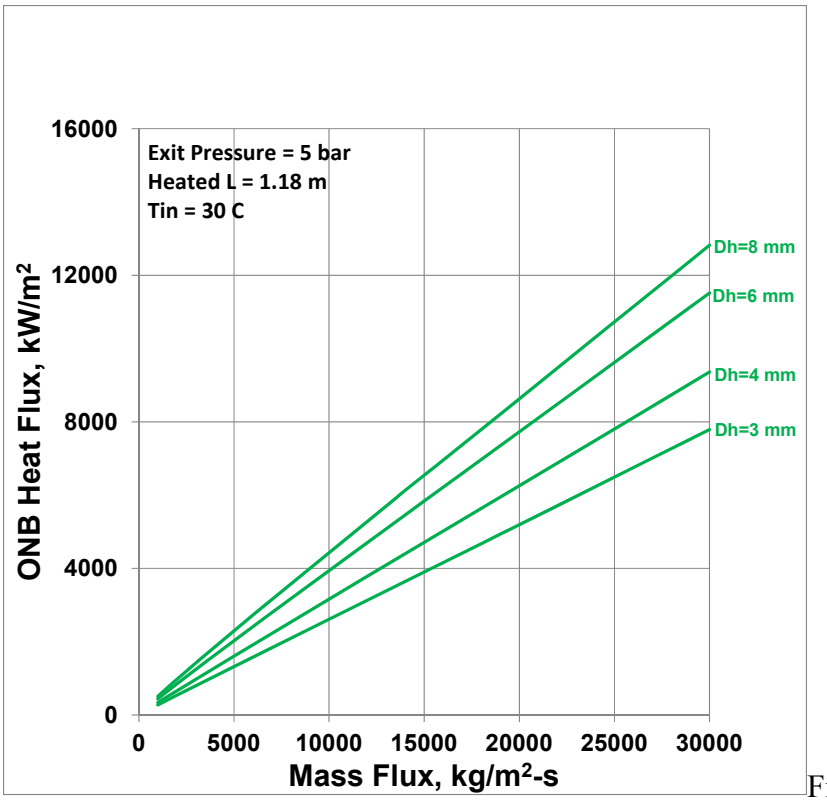

Fig. 12, Part 12 of 15

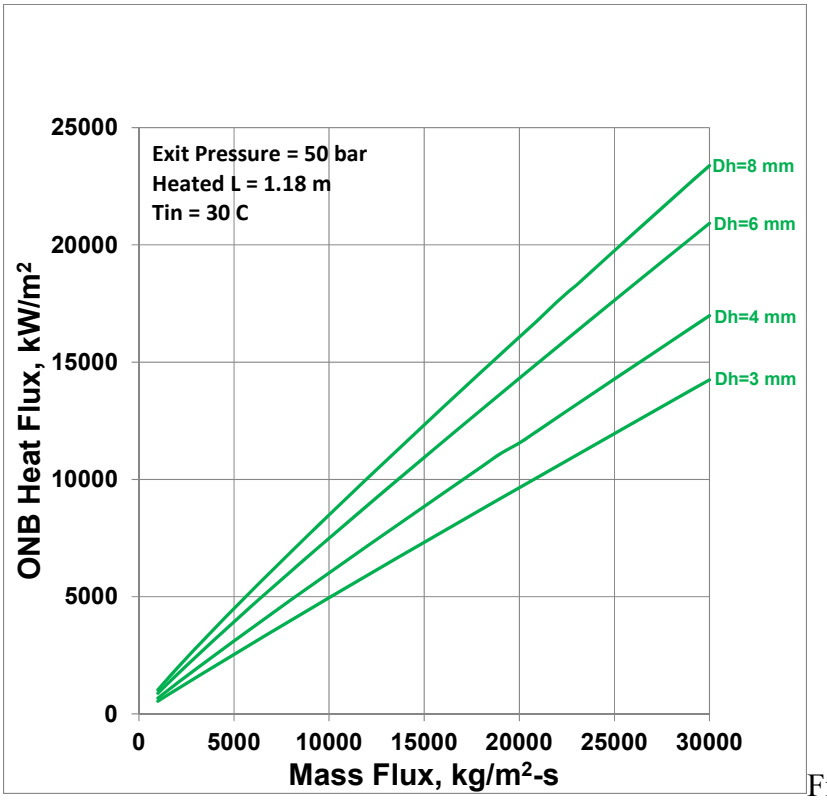

Fig. 12, Part 13 of 15

Fig. 12. Continued

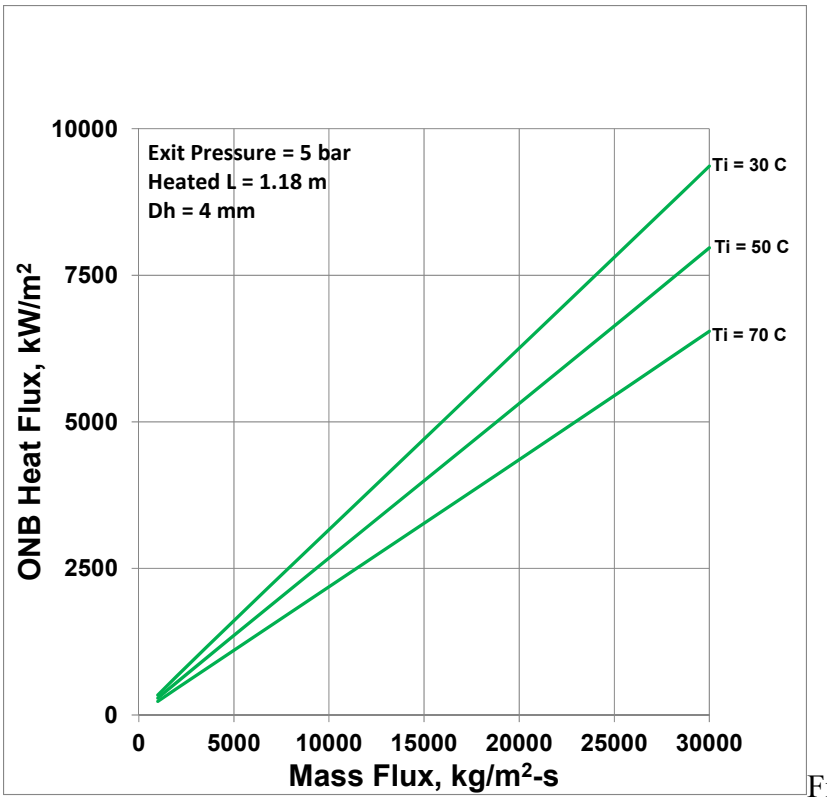

Fig. 12, Part 14 of 15

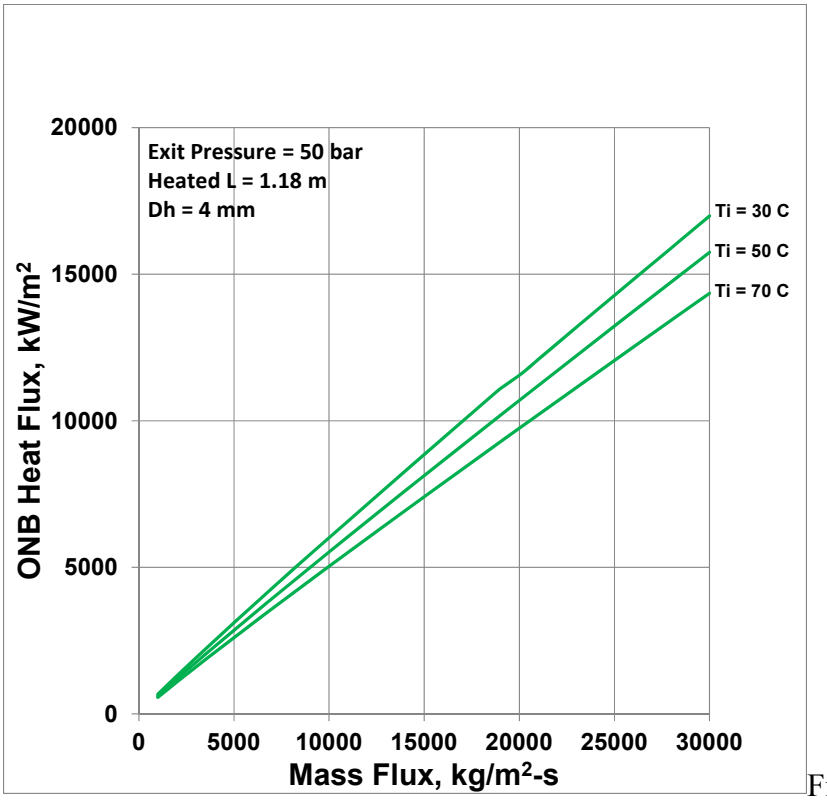

Fig. 12, Part 15 of 15

Fig. 12. Continued

APPENDIX F. COMPUTER PROGRAM USED FOR CALCULATING ONB, OFI, AND CHF

```
C     Reversal of CHF and OFI.
C23456789012345678901234567890123456789012345678901234567890123456789012345678901234567890
C     Compare CHF (Extended Groeneveld 2006 Table, and Hall-Mudawar ICC),
C     OFI Heat Flux (Whittle-Forgan, and Saha-Zuber), and ONB Heat Flux
C     (Bergles-Rohsenow).
C
      COMMON/NO1/GG(50) ,HTFLX_ONB_BR(50),
     1 HTFLX_OFI_WF1(50),HTFLX_OFI_WF2(50),
     2 HTFLX_OFI_SZ1(50),HTFLX_OFI_SZ2(50),
     3 HTFLX_CHF_GR(50) ,HTFLX_CHF_HM(50),
     4 QUAL_OUT_GR(50)  ,QUAL_OUT_HM(50),
     5 POUTA(300),DDHA(300),TINA(300)
      REAL LENGTH
      DIMENSION ONB_OFI_CHF(9000,50),GG_REV(300),HTFLX_REV(300)
C
      NQ=6
      NGG=30
C     NQ    = Number of quantities (CHF, OFI, etc) to be calculated and tabulated.
C             NQ is internally set to 6, and these quantities are listed below.
C     NCASE = Number of cases to be tabulated. A case is a set of input data
C             (exit pressure, heated dia, etc.) in the input file on UNIT=5.
C             For each case, NQ quantities will be tabulated at several (NGG)
C             mass flux values.
C             NCASE is the first input data on UNIT=5, followed by the data for
C             each case on a separate line.
C     IP    = Case number index
C     NGG   = Number of mass flux values at which the quantities (CHF, OFI, etc)
C             will be tabulated. NGG is internally set to 30, and the values are
C             1000, 2000, ... 30000 kg/m^2-s.
C
C  The following NQ quantities are written on UNIT=10.
C  ONB_OFI_CHF(1+(IP-1)*NQ,I) = ONB ht flux for case IP at mass flux GG(I)
C  ONB_OFI_CHF(2+(IP-1)*NQ,I) = W & F OFI ht flux for case IP at mass flux GG(I)
C  ONB_OFI_CHF(3+(IP-1)*NQ,I) = S & Z OFI ht flux for case IP at mass flux GG(I)
C  ONB_OFI_CHF(4+(IP-1)*NQ,I) = Extended Gro CHF for case IP at mass flux GG(I)
C  ONB_OFI_CHF(5+(IP-1)*NQ,I) = Exit quality at Extended Gro CHF
C  ONB_OFI_CHF(6+(IP-1)*NQ,I) = Hall-Mud ICC CHF for case IP at mass flux GG(I)
C  GG_REV(IP)    = Mass flux at OFI-CHF reversal for case IP
C  HTFLX_REV(IP) = Heat flux at OFI-CHF reversal for case IP
C
C     INPUT DATA READ ON UNIT 5
C     POUT    = Exit pressure, Pa
C     DDH     = Heated diameter    = 4 * (Flow area)/ (Heated perimeter)
C     LENGTH  = Heated length, m
C     TIN     = Inlet temperature, C
C     PPH_PPW = Heated perimeter/Wetted perimeter ratio
C     ETA     = A parameter in the Whittle and Forgan OFI criterion.
C               Its value recommended by IAEA and ANL is 32.5 .
C     IFLOW   = 0 implies downflow, and IFLOW = 1 implies upflow.
C     IPIN    = (0, -1) Flag to indicate whether the inlet pressure will be
C               calculated or not. If not calculated, it is set equal to the
C               input exit pressure POUT.
C
C     UNIT=5  is the input data file.
C     UNIT=6  is the main output file.
C     UNIT=9  is a debug file.
C     UNIT=10 is the output file for plotting on spreadsheet.
      OPEN(UNIT=5,FILE='onb.ofi.chf.input',
```

```
     1 STATUS='OLD',FORM='FORMATTED')
       OPEN(UNIT=6,FILE='onb.ofi.chf.output',
     1 STATUS='UNKNOWN',FORM='FORMATTED')
       OPEN(UNIT=10,FILE='onb.ofi.chf.for_spreadsheet',
     1 STATUS='UNKNOWN',FORM='FORMATTED')
C
       READ(5,1) NCASE
   1   FORMAT(I6)
       WRITE(10,4)
C
       DO 20 IP=1,NCASE
       READ(5,2) POUT,DDH,LENGTH,TIN,PPH_PPW,ETA,IFLOW,IPIN
       POUTA(IP)=POUT
       DDHA(IP)=DDH
       TINA(IP)=TIN
C      WRITE(10,28) IP,POUT*1.0E-5,DDH,LENGTH,TIN,PPH_PPW,ETA,IFLOW,IPIN
C      Read Groeneveld 2006 CHF Table, and display it at pressure POUT.
       IF(IP .EQ. 1) CALL GETGRO(POUT)
       CALL REVERSAL(POUT,DDH,LENGTH,TIN,PPH_PPW,ETA,IFLOW,IPIN,IP)
       IZ=(IP-1)*NQ
       DO 9 I=1,NGG
       ONB_OFI_CHF(IZ+1,I)=HTFLX_ONB_BR(I)*0.001
       ONB_OFI_CHF(IZ+2,I)=HTFLX_OFI_WF1(I)*0.001
       ONB_OFI_CHF(IZ+3,I)=HTFLX_OFI_SZ1(I)*0.001
       ONB_OFI_CHF(IZ+4,I)=HTFLX_CHF_GR(I)*0.001
       ONB_OFI_CHF(IZ+5,I)=QUAL_OUT_GR(I)
       ONB_OFI_CHF(IZ+6,I)=HTFLX_CHF_HM(I)*0.001
   9   CONTINUE
C
C      INTERPOLATE MASS FLUX & HEAT FLUX AT OFI-CHF REVERSAL.
C
C      Initialize them to 0.0 first. So GG_REV(IP)=0.0 will imply that
C      it is out of range, i.e., GG_REV(IP) > 30,000 kg/m^2-s
       GG_REV(IP)=0.0
       HTFLX_REV(IP)=0.0
       DO 10 I=1,NGG
       IF(HTFLX_OFI_WF1(I) .LT. HTFLX_CHF_GR(I)) THEN
       GO TO 10
       ELSE
       SLOPE_OFI=(HTFLX_OFI_WF1(I)-HTFLX_OFI_WF1(I-1))/(GG(I)-GG(I-1))
       SLOPE_CHF=(HTFLX_CHF_GR(I) -HTFLX_CHF_GR(I-1))/(GG(I)-GG(I-1))
       GG_REV(IP)=GG(I-1)+(HTFLX_CHF_GR(I-1)-HTFLX_OFI_WF1(I-1))/
     1 (SLOPE_OFI-SLOPE_CHF)
       HTFLX_REV(IP)=HTFLX_OFI_WF1(I-1)+SLOPE_OFI*(GG_REV(IP)-GG(I-1))
       HTFLX_REV2   =HTFLX_CHF_GR(I-1) +SLOPE_CHF*(GG_REV(IP)-GG(I-1))
       IF(ABS(HTFLX_REV(IP)-HTFLX_REV2) .GT. 1.0E-8)
     1 WRITE(10,*) 'ERROR in Reversal Ht flux for Case ',IP,
     2 HTFLX_REV(IP),HTFLX_REV2
C      WRITE(10,29) IP,GG_REV(IP),HTFLX_REV(IP)*0.001,HTFLX_REV2*0.001
       GO TO 19
       ENDIF
  10   CONTINUE
  19   WRITE(10,28) IP,POUT*1.0E-5,DDH,LENGTH,TIN,PPH_PPW,ETA,IFLOW,
     1 IPIN,GG_REV(IP),HTFLX_REV(IP)*0.001
  20   CONTINUE
C
C      WRITE OUTPUT ON UNIT=10, NC heat fluxes per line.
       NC=18
C      NC = Number of heat fluxes printed per line on UNIT=10
       NA=(NCASE*NQ)/NC
       IF(NCASE*NQ .GT. NA*NC) NA=NA+1
       DO 30 NB=1,NA
       IZ1=(NB-1)*NC+1
```

```
      IZ2=NB*NC
      IF(IZ2 .GT. NCASE*NQ) IZ2=NCASE*NQ
      IP1=IZ1/NQ+1
      IP2=MIN(IP1+NC/NQ-1,NCASE)
      WRITE(10,*)
      WRITE(10,31) 'P(bar) =',((POUTA(IP)*1.0E-5,IZ=1,NQ),IP=IP1,IP2)
      WRITE(10,31) 'Dh(mm) =',((DDHA(IP)*1.0E+3,IZ=1,NQ),IP=IP1,IP2)
      WRITE(10,31) 'Ti (C) =',((TINA(IP),IZ=1,NQ),IP=IP1,IP2)
      WRITE(10,27)
      DO 15 I=1,NGG
      WRITE(10,26) GG(I),(ONB_OFI_CHF(IZ,I),IZ=IZ1,IZ2)
   15 CONTINUE
   30 CONTINUE
C
      DIFMEAN1=0.0
      DIFMAXA1=0.0
      DIFRMS_1=0.0
      MAXCASE1=0
      MAXMFLX1=0
      DIFMEAN2=0.0
      DIFMAXA2=0.0
      DIFRMS_2=0.0
      MAXCASE2=0
      MAXMFLX2=0
      DIFMEAN3=0.0
      DIFMAXA3=0.0
      DIFRMS_3=0.0
      MAXCASE3=0
      MAXMFLX3=0
      DIFMEAN4=0.0
      DIFMAXA4=0.0
      DIFRMS_4=0.0
      MAXCASE4=0
      MAXMFLX4=0
      DIFMEAN5=0.0
      DIFMAXA5=0.0
      DIFRMS_5=0.0
      MAXCASE5=0
      MAXMFLX5=0
      DIFMEAN6=0.0
      DIFMAXA6=0.0
      DIFRMS_6=0.0
      MAXCASE6=0
      MAXMFLX6=0
      DIFMEAN7=0.0
      DIFMAXA7=0.0
      DIFRMS_7=0.0
      MAXCASE7=0
      MAXMFLX7=0
      NCOUNT1=0
      NCOUNT2=0
      NCOUNT3=0
      NCOUNT4=0
      NCOUNT5=0
      NCOUNT6=0
      NCOUNT7=0
C
C     CALCULATE MEAN DIFF, MAXIMUM ABSOLUTE DIFF, RMS DIFF OVER FIRST HALF
C     OF THE INPUT CASES
C     (1) Between CHFs from Groeneveld table and Hall-Mudawar ICC
C     (2) Between OFI heat fluxes from W & F and Saha-Zuber
C     (3) Between ONB obtd using PIN=POUT and that obtd using actual PIN.
C     (4) Between W&F OFI obtd using PIN=POUT and that obtd using actual PIN.
```

```
C     (5) Between S&Z OFI obtd using PIN=POUT and that obtd using actual PIN.
C     (6) Between Gro CHF obtd using PIN=POUT and that obtd using actual PIN.
C     (7) Between H-M CHF obtd using PIN=POUT and that obtd using actual PIN.
      NCASE1=NCASE/2
C     Loop over half of the input cases.
      DO 40 IP=1,NCASE1
      IP2=NCASE1+IP
C     Cases IP and IP2 must have identical input data except for option IPIN.
      IZ=(IP-1)*NQ
      IZ2=(IP2-1)*NQ
      DO 40 I=1,NGG
C
C     (1) Between CHFs from Groeneveld table and Hall-Mudawar ICC
C     Note: H-M ICC is good only if the Groeneveld exit quality is negative.
      IF(ONB_OFI_CHF(IZ+5,I) .LE. 0.0) THEN
      DIFMEAN1=DIFMEAN1+
     1    (ONB_OFI_CHF(IZ+6,I)/ONB_OFI_CHF(IZ+4,I)-1.0)
      DIFABS=ABS(ONB_OFI_CHF(IZ+6,I)/ONB_OFI_CHF(IZ+4,I)-1.0)
      IF(DIFABS .GT. DIFMAXA1) THEN
      DIFMAXA1=DIFABS
      MAXCASE1=IP
      MAXMFLX1=I
      ENDIF
      DIFRMS_1=DIFRMS_1+
     1    (ONB_OFI_CHF(IZ+6,I)/ONB_OFI_CHF(IZ+4,I)-1.0)**2
      NCOUNT1=NCOUNT1+1
      ENDIF
C     WRITE(*,39) GG(I),ONB_OFI_CHF(IZ+4,I),ONB_OFI_CHF(IZ+6,I),
C    1 ONB_OFI_CHF(IZ+5,I)
C
C     (2) Between OFI heat fluxes from W & F and Saha-Zuber
      IF(GG(I) .GT. 1000) THEN
      DIFMEAN2=DIFMEAN2+
     1    (ONB_OFI_CHF(IZ+3,I)/ONB_OFI_CHF(IZ+2,I)-1.0)
      DIFABS=ABS(ONB_OFI_CHF(IZ+3,I)/ONB_OFI_CHF(IZ+2,I)-1.0)
      IF(DIFABS .GT. DIFMAXA2) THEN
      DIFMAXA2=DIFABS
      MAXCASE2=IP
      MAXMFLX2=I
      ENDIF
      DIFRMS_2=DIFRMS_2+
     1    (ONB_OFI_CHF(IZ+3,I)/ONB_OFI_CHF(IZ+2,I)-1.0)**2
      NCOUNT2=NCOUNT2+1
      ENDIF
C     WRITE(*,39) GG(I),ONB_OFI_CHF(IZ+2,I),ONB_OFI_CHF(IZ+3,I)
C
C     (3) Between ONB obtd using PIN=POUT and that obtd using actual PIN.
      DIFMEAN3=DIFMEAN3+
     1    (ONB_OFI_CHF(IZ2+1,I)/ONB_OFI_CHF(IZ+1,I)-1.0)
      DIFABS=ABS(ONB_OFI_CHF(IZ2+1,I)/ONB_OFI_CHF(IZ+1,I)-1.0)
      IF(DIFABS .GT. DIFMAXA3) THEN
      DIFMAXA3=DIFABS
      MAXCASE3=IP
      MAXMFLX3=I
      ENDIF
      DIFRMS_3=DIFRMS_3+
     1    (ONB_OFI_CHF(IZ2+1,I)/ONB_OFI_CHF(IZ+1,I)-1.0)**2
      NCOUNT3=NCOUNT3+1
C     WRITE(*,39) GG(I),ONB_OFI_CHF(IZ+1,I),ONB_OFI_CHF(IZ2+1,I)
C
C     (4) Between W&F OFI obtd using PIN=POUT and that obtd using actual PIN.
      DIFMEAN4=DIFMEAN4+
     1    (ONB_OFI_CHF(IZ2+2,I)/ONB_OFI_CHF(IZ+2,I)-1.0)
```

```
      DIFABS=ABS(ONB_OFI_CHF(IZ2+2,I)/ONB_OFI_CHF(IZ+2,I)-1.0)
      IF(DIFABS .GT. DIFMAXA4) THEN
      DIFMAXA4=DIFABS
      MAXCASE4=IP
      MAXMFLX4=I
      ENDIF
      DIFRMS_4=DIFRMS_4+
     1    (ONB_OFI_CHF(IZ2+2,I)/ONB_OFI_CHF(IZ+2,I)-1.0)**2
      NCOUNT4=NCOUNT4+1
C     WRITE(*,39) GG(I),ONB_OFI_CHF(IZ+2,I),ONB_OFI_CHF(IZ2+2,I)
C
C     (5) Between S&Z OFI obtd using PIN=POUT and that obtd using actual PIN.
      DIFMEAN5=DIFMEAN5+
     1    (ONB_OFI_CHF(IZ2+3,I)/ONB_OFI_CHF(IZ+3,I)-1.0)
      DIFABS=ABS(ONB_OFI_CHF(IZ2+3,I)/ONB_OFI_CHF(IZ+3,I)-1.0)
      IF(DIFABS .GT. DIFMAXA5) THEN
      DIFMAXA5=DIFABS
      MAXCASE5=IP
      MAXMFLX5=I
      ENDIF
      DIFRMS_5=DIFRMS_5+
     1    (ONB_OFI_CHF(IZ2+3,I)/ONB_OFI_CHF(IZ+3,I)-1.0)**2
      NCOUNT5=NCOUNT5+1
C     WRITE(*,39) GG(I),ONB_OFI_CHF(IZ+3,I),ONB_OFI_CHF(IZ2+3,I)
C
C     (6) Between Gro CHF obtd using PIN=POUT and that obtd using actual PIN.
      DIFMEAN6=DIFMEAN6+
     1    (ONB_OFI_CHF(IZ2+4,I)/ONB_OFI_CHF(IZ+4,I)-1.0)
      DIFABS=ABS(ONB_OFI_CHF(IZ2+4,I)/ONB_OFI_CHF(IZ+4,I)-1.0)
      IF(DIFABS .GT. DIFMAXA6) THEN
      DIFMAXA6=DIFABS
      MAXCASE6=IP
      MAXMFLX6=I
      ENDIF
      DIFRMS_6=DIFRMS_6+
     1    (ONB_OFI_CHF(IZ2+4,I)/ONB_OFI_CHF(IZ+4,I)-1.0)**2
      NCOUNT6=NCOUNT6+1
C     WRITE(*,39) GG(I),ONB_OFI_CHF(IZ+4,I),ONB_OFI_CHF(IZ2+4,I),
C    1 ONB_OFI_CHF(IZ+5,I),ONB_OFI_CHF(IZ2+5,I)
C
C     (7) Between H-M CHF obtd using PIN=POUT and that obtd using actual PIN.
      IF(ONB_OFI_CHF(IZ+5,I) .LE. 0.0 .AND.
     1   ONB_OFI_CHF(IZ2+5,I) .LE. 0.0) THEN
      DIFMEAN7=DIFMEAN7+
     1    (ONB_OFI_CHF(IZ2+6,I)/ONB_OFI_CHF(IZ+6,I)-1.0)
      DIFABS=ABS(ONB_OFI_CHF(IZ2+6,I)/ONB_OFI_CHF(IZ+6,I)-1.0)
      IF(DIFABS .GT. DIFMAXA7) THEN
      DIFMAXA7=DIFABS
      MAXCASE7=IP
      MAXMFLX7=I
      ENDIF
      DIFRMS_7=DIFRMS_7+
     1    (ONB_OFI_CHF(IZ2+6,I)/ONB_OFI_CHF(IZ+6,I)-1.0)**2
      NCOUNT7=NCOUNT7+1
      ENDIF
C     WRITE(*,39) GG(I),ONB_OFI_CHF(IZ+6,I),ONB_OFI_CHF(IZ2+6,I),
C    1 ONB_OFI_CHF(IZ+5,I),ONB_OFI_CHF(IZ2+5,I)
  40  CONTINUE
      IF(NCOUNT1.GT.0) DIFMEAN1=(DIFMEAN1/NCOUNT1)*100.0
      IF(NCOUNT2.GT.0) DIFMEAN2=(DIFMEAN2/NCOUNT2)*100.0
      IF(NCOUNT3.GT.0) DIFMEAN3=(DIFMEAN3/NCOUNT3)*100.0
      IF(NCOUNT4.GT.0) DIFMEAN4=(DIFMEAN4/NCOUNT4)*100.0
      IF(NCOUNT5.GT.0) DIFMEAN5=(DIFMEAN5/NCOUNT5)*100.0
```

```
      IF(NCOUNT6.GT.0) DIFMEAN6=(DIFMEAN6/NCOUNT6)*100.0
      IF(NCOUNT7.GT.0) DIFMEAN7=(DIFMEAN7/NCOUNT7)*100.0
C
      DIFMAXA1=DIFMAXA1*100.0
      DIFMAXA2=DIFMAXA2*100.0
      DIFMAXA3=DIFMAXA3*100.0
      DIFMAXA4=DIFMAXA4*100.0
      DIFMAXA5=DIFMAXA5*100.0
      DIFMAXA6=DIFMAXA6*100.0
      DIFMAXA7=DIFMAXA7*100.0
C
      IF(NCOUNT1.GT.0) DIFRMS_1=SQRT(DIFRMS_1/NCOUNT1)*100.0
      IF(NCOUNT2.GT.0) DIFRMS_2=SQRT(DIFRMS_2/NCOUNT2)*100.0
      IF(NCOUNT3.GT.0) DIFRMS_3=SQRT(DIFRMS_3/NCOUNT3)*100.0
      IF(NCOUNT4.GT.0) DIFRMS_4=SQRT(DIFRMS_4/NCOUNT4)*100.0
      IF(NCOUNT5.GT.0) DIFRMS_5=SQRT(DIFRMS_5/NCOUNT5)*100.0
      IF(NCOUNT6.GT.0) DIFRMS_6=SQRT(DIFRMS_6/NCOUNT6)*100.0
      IF(NCOUNT7.GT.0) DIFRMS_7=SQRT(DIFRMS_7/NCOUNT7)*100.0
      WRITE(*,*)
      WRITE(*,34)
      WRITE(*,35) NCOUNT1,NCOUNT2,NCOUNT3,
     1    NCOUNT4,NCOUNT5,NCOUNT6,NCOUNT7
      WRITE(*,36) DIFMEAN1,DIFMEAN2,DIFMEAN3,
     1   DIFMEAN4,DIFMEAN5,DIFMEAN6,DIFMEAN7
      WRITE(*,37) DIFMAXA1,DIFMAXA2,DIFMAXA3,
     1   DIFMAXA4,DIFMAXA5,DIFMAXA6,DIFMAXA7
      WRITE(*,33) MAXCASE1,MAXMFLX1,MAXCASE2,MAXMFLX2,MAXCASE3,MAXMFLX3,
     1 MAXCASE4,MAXMFLX4,MAXCASE5,MAXMFLX5,MAXCASE6,MAXMFLX6,
     2 MAXCASE7,MAXMFLX7
      WRITE(*,38) DIFRMS_1,DIFRMS_2,DIFRMS_3,
     1   DIFRMS_4,DIFRMS_5,DIFRMS_6,DIFRMS_7
      WRITE(6,*)
      WRITE(6,34)
      WRITE(6,35) NCOUNT1,NCOUNT2,NCOUNT3,
     1    NCOUNT4,NCOUNT5,NCOUNT6,NCOUNT7
      WRITE(6,36) DIFMEAN1,DIFMEAN2,DIFMEAN3,
     1   DIFMEAN4,DIFMEAN5,DIFMEAN6,DIFMEAN7
      WRITE(6,37) DIFMAXA1,DIFMAXA2,DIFMAXA3,
     1   DIFMAXA4,DIFMAXA5,DIFMAXA6,DIFMAXA7
      WRITE(6,33) MAXCASE1,MAXMFLX1,MAXCASE2,MAXMFLX2,MAXCASE3,MAXMFLX3,
     1 MAXCASE4,MAXMFLX4,MAXCASE5,MAXMFLX5,MAXCASE6,MAXMFLX6,
     2 MAXCASE7,MAXMFLX7
      WRITE(6,38) DIFRMS_1,DIFRMS_2,DIFRMS_3,
     1   DIFRMS_4,DIFRMS_5,DIFRMS_6,DIFRMS_7
C
   2  FORMAT(6F12.4,2I3)
   4  FORMAT(8X,'       P(bar)    Htd.D(m)    Htd.L(m)      Tin(C)',
     1 '       Ph/Pw     ETA-W&F IFLOW Grev,kg/m2-s  q_rev,kW/m2')
  28  FORMAT('Case =',I3,F12.1,5F12.4,2I3,2F12.1)
  29  FORMAT('Case =',I3,3F12.1)
  25  FORMAT('    G      ONB     OFI   CHF-Gr  CHF-HM   X-Gr  ',
     1              '   ONB     OFI   CHF-Gr  CHF-HM   X-Gr  ',
     2              '   ONB     OFI   CHF-Gr  CHF-HM   X-Gr  ',
     3              '   ONB     OFI   CHF-Gr  CHF-HM   X-Gr')
  26  FORMAT(F8.0,3(4F8.0,F8.4,F8.0))
  31  FORMAT(A,3(6F8.0))
  27  FORMAT('    G      ONB   OFI-WF  OFI-SZ  CHF-Gr   X-Gr   CHF-HM ',
     1              '   ONB   OFI-WF  OFI-SZ  CHF-Gr   X-Gr   CHF-HM ',
     2              '   ONB   OFI-WF  OFI-SZ  CHF-Gr   X-Gr   CHF-HM ')
  34  FORMAT(T23,'Gro CHF',T35,'WF OFI',T47,'ONB Pi',T57,'WF OFI Pi',
     1 T69,'SZ OFI Pi',T81,'Gro CHF Pi',T93,'HM CHF Pi',/,
     1       T23,'HM CHF',T35,'SZ OFI',T47,'ONB Po',T57,'WF OFI Po',
     1 T69,'SZ OFI Po',T81,'Gro CHF Po',T93,'HM CHF Po')
```

```
   33  FORMAT('Case / Mass Flux Row ',7(I3,'/',I3,5X))
   35  FORMAT('Number of data  ',7(3X,I6,3X))
   36  FORMAT('Mean Diff. %    ',7F12.3)
   37  FORMAT('Max Abs Diff. % ',7F12.3)
   38  FORMAT('RMS  Diff. %    ',7F12.3)
   39  FORMAT(F12.0,2F12.1,2F12.5)
       END
C
       SUBROUTINE REVERSAL(POUT,DDH,LENGTH,TIN,PPH_PPW,ETA,IFLOW,IPIN,IP)
C      Reversal of CHF and OFI.
C      Compare CHF (Extended Groeneveld 2006 Table, and Hall-Mudawar ICC),
C      OFI Heat Flux (Whittle-Forgan, and Saha-Zuber), and ONB Heat Flux
C      (Bergles-Rohsebow).
C      M. Kalimullah, A. P. Olson, and E. E. Feldman, June 27, 2012
C      References:
C      (1) M. Kalimullah, E. E. Feldman, and A. P. Olson, "Review of Subcooled
C          CHF Correlations and Databases,"Intra-Laboratory Memorandum to
C          J. E. Matos and J. G. Stevens, GTRI - Conversion Program, Nuclear
C          Engineering Division, Argonne National Laboratory, Argonne, IL, USA
C          (April 30, 2012).
C      (2) Whittle and Forgan, Nuclear Eng & Design, Vol. 6, pp. 89-99 (1967).
C      (3) M. Kalimullah and A. P. Olson, "A User's Guide to the PLTEMP/ANL
C          Code," ANL/RERTR/TM-11-22, Version 4.11,GTRI - Conversion Program,
C          Nuclear Engineering Division, Argonne National Laboratory, Argonne,
C          IL, USA (November 15, 2011).
C
C      Friction Factor     =GETF(RE,ROUGH)
C      Tsat                =FUNCTION ZTSAT(P,IFLUID)
C      Liquid
C      Enthalpy            =FUNCTION ZHLIQ(P,T,IFLUID)
C      Density             =FUNCTION ZROLIQ(H,P,T,IFLUID)
C      Kinematic Viscosity =FUNCTION ZVISLIQ(H,P,T,RHO,IFLUID)
C      Cp                  =FUNCTION ZCPLIQ(H,P,T,IFLUID)
C      Thermal Conductivity=FUNCTION ZTHCL(H,P,T,IFLUID)
C      Temperature         =FUNCTION ZTLIQ(P,H,IFLUID,HFUNCL)
C      Vapor
C      Enthalpy            =FUNCTION ZHVAP(P,T,IFLUID)
C      Density             =FUNCTION ZROVAP(H,P,T,IFLUID)
       PARAMETER(NN1=25,NN2=25,NN3=25,JW=30)
       REAL LENGTH,KORIF,NUSSLT,NSUB,NZUB
       CHARACTER*8 STABLE,ICALLER
       EXTERNAL HFUNCL
C
       COMMON/GRODAT/GR(NN1,NN2), FLUXM(NN2), PKPA(NN3), QUAL(NN1),
      1 GRALL(NN1,NN2,NN3),CHFFG(JW),N1,N2,N3
       COMMON/NO1/GG(50) ,HTFLX_ONB_BR(50),
      1 HTFLX_OFI_WF1(50),HTFLX_OFI_WF2(50),
      2 HTFLX_OFI_SZ1(50),HTFLX_OFI_SZ2(50),
      3 HTFLX_CHF_GR(50) ,HTFLX_CHF_HM(50),
      4 QUAL_OUT_GR(50)  ,QUAL_OUT_HM(50),
      5 POUTA(300),DDHA(300),TINA(300)
C
C      KORIF   = Minor loss coefficient (if any)
C      HTFLX   = Uniform heat flux, W/m**2
C      HTFLX_ONB_BR  = Heat flux at ONB, Bergles-Rohsenow, W/m**2
C      HTFLX_OFI_WF1 = Heat flux at OFI, Whittle-Forgan using Eta=32.5, W/m**2
C      HTFLX_OFI_WF2 = Heat flux at OFI, Whittle-Forgan using R from Eq. (1)
C                      of Ref. 3, W/m**2
C      HTFLX_OFI_SZ1 = Heat flux ao OFI, Saha-Zuber, W/m**2
C      HTFLX_OFI_SZ2 = Heat flux ao OFI, Improved Saha-Zuber, W/m**2
C      HTFLX_CHF_GR  = Critical heat flux, Extended Groeneveld 2006 table, W/m**2
C      HTFLX_CHF_HM  = Critical heat flux, Hall-Mudawar ICC W/m**2
C      LENGTH  = Heated length, m
```

```
C     POUT    = Exit pressure, Pa
C     IFLUID  = 0 implies light water, IFLUID = 1 implies heavy water.
C     IFLOW   = 0 implies downflow, and IFLOW = 1 implies upflow.
C     IPIN    = 0 implies calculate inlet pressure, amd IPIN = -1 implies do not
C               calculate inlet pressure.
C     LLP     = Number of iterations done to find the inlet pressure.
C     PPH     = Heated perimeter, m
C     PPW     = Wetted perimeter, m
C     PPH_PPW = PPH/PPW ratio
C     QQ      = Power input per channel, W
C     TIN     = Inlet temperature, C
C     TOUT    = Exit temperature, C
C     TSATOUT = Saturation temperature at the exit pressure, C
C     HIN     = Inlet enthalpy, J/kg
C     HOUT    = Exit enthalpy, J/kg
C     HFOUT   = Saturated liquid enthalpy at the exit pressure, J/kg
C     PPH_PPW = Heated perimeter/Wetted perimeter ratio
C     DDH     = Heated diameter    = 4 * (Flow area)/ (Heated perimeter)
C     DDE     = Hydraulic diameter = 4 * (Flow area)/ (Wetted perimeter)
C
C     INPUT DATA (Six parameters: Exit pressure, Heated dia, Heated length,
C                 Inlet temp, Mass flux, Heated/Wetted perimeter ratio)
C
      GG(1)=1000.0
      DO 4 I=2,30
      GG(I)=GG(I-1)+1000.0
   4  CONTINUE
      LLP=3
      IFLUID=0
      GRAV=9.8
      ROUGH=0.0
      KORIF=0.0
      PBAR=POUT/1.0E5
      DDE=DDH * PPH_PPW
      TSATOUT=ZTSAT(POUT,IFLUID)
      HFOUT=ZHLIQ(POUT,TSATOUT,IFLUID)
      HGOUT=ZHVAP(POUT,TSATOUT,IFLUID)
      HFG_OUT=HGOUT-HFOUT
      OPEN(UNIT=9,FILE='onb.ofi.chf.debug',
     1 STATUS='UNKNOWN',FORM='FORMATTED')
C
C     HEAT FLUX AT ONB BERGLES-ROHSENOW
C
C     Loop over mass velocities.
      WRITE(6,3)
      WRITE(6,28) IP,POUT*1.0E-5,DDH,LENGTH,TIN,PPH_PPW,ETA,IFLOW,IPIN
      DO 10 I=1,30
C     Guess exit temperature at ONB. Find heat flux at ONB in two ways.
C     One by heat balance, and the other by Bergles-Rohsenow correlation.
C     Adjust TOUT to make the two heat fluxes equal.
      EPS=0.00001
      TSTEP =0.1
      TOUT=TIN+0.1*(TSATOUT-TIN)
      TOUT=TIN+1.0
      ITERN=0
      ERROR=1.0
   1  CONTINUE
      ITERN=ITERN+1
      TOUT=TOUT+TSTEP
      HOUT=ZHLIQ(POUT,TOUT,IFLUID)
C
C     Calculate inlet pressure PIN using an average fric factor
C     and an orifice coeff KORIF.
```

```
C     Guess PIN = POUT.
      PIN=POUT
      IF(IPIN .EQ. -1) GO TO 32
      LOOP=0
   6  CONTINUE
      LOOP=LOOP+1
      PAVE=0.5*(PIN+POUT)
      TAVE=0.5*(TIN+TOUT)
      HAVE=ZHLIQ(PAVE,TAVE,IFLUID)
      RHO_AVE=ZROLIQ(HAVE,PAVE,TAVE,IFLUID)
      VISC_AVE=ZVISLIQ(HAVE,PAVE,TAVE,RHO_AVE,IFLUID)
      AVISC_AVE=VISC_AVE*RHO_AVE
      REAVE=GG(I)*DDE/AVISC_AVE
      FRICF=GETF(REAVE,ROUGH)
      DELP=(KORIF+FRICF*LENGTH/DDE)*0.5*GG(I)**2/RHO_AVE
      DELP_GRAV=RHO_AVE*GRAV*LENGTH
      IF(IFLOW .EQ. 0) DELP=DELP - DELP_GRAV
      IF(IFLOW .EQ. 1) DELP=DELP + DELP_GRAV
      PIN1=PIN
      PIN=POUT+DELP
      ERR_PIN=PIN1/PIN-1.0
      IF(LOOP.LT.LLP) GO TO 6
C     WRITE(9,3) 'ONB_BR ',GG(I),PIN1,PAVE,TOUT,TAVE,
C    1 RHO_AVE,AVISC_AVE,REAVE,FRICF,DELP,PIN,ERR_PIN
C
C     Find inlet enthalpy at TIN and PIN.
  32  HIN=ZHLIQ(PIN,TIN,IFLUID)
      HTFLX_ONB_GUESS=DDH*GG(I)*(HOUT-HIN)/(4.0*LENGTH)
      RHO_OUT=ZROLIQ(HOUT,POUT,TOUT,IFLUID)
      VISC_OUT=ZVISLIQ(HOUT,POUT,TOUT,RHO_OUT,IFLUID)
C     VISC_OUT = Kinematic viscosity at exit
      AVISC_OUT=VISC_OUT*RHO_OUT
C     AVISC_OUT = Absolute viscosity at exit, Pa-s
      CP_OUT=ZCPLIQ(HOUT,POUT,TOUT,IFLUID)
      THC_OUT=ZTHCL(HOUT,POUT,TOUT,IFLUID)
      RE=GG(I)*DDE/AVISC_OUT
      PR=AVISC_OUT*CP_OUT/THC_OUT
      IF(ITERN.EQ.1) TWALL=TOUT+5.0
C     This guess of the wall temp at the heated length exit is used in the
C     first iteration. In later iterations, the wall temp is calculated
C     using a correlation for the single-phase heat transfer coeff.
      HWALL=ZHLIQ(POUT,TWALL,IFLUID)
      RHO_WALL=ZROLIQ(HWALL,POUT,TWALL,IFLUID)
      VISC_WALL=ZVISLIQ(HWALL,POUT,TWALL,RHO_WALL,IFLUID)
      AVISC_WALL=VISC_WALL*RHO_WALL
C     Improved Dittus-Boelter Nu correlation for single-phase
C     forced convection
      NUSSLT_DB=0.023*RE**0.8 *PR**0.4 *(AVISC_OUT/AVISC_WALL)**0.11
C     Petukhov-Popov Nu correlation for single-phase forced convection
      FRIC_OUT=GETF(RE,ROUGH)
      1=0.125*FRIC_OUT*RE * PR * (AVISC_OUT/AVISC_WALL)**0.11
      2=PR**(1.0/3.0)
      3=1.0+3.4*FRIC_OUT + (11.7+1.8/2)*(0.125*FRIC_OUT)**0.5
     1 *(PR/2-1.0)
      NUSSLT_PP=1/3
C     Sieder-Tate Nu correlation for single-phase forced convection
      NUSSLT_ST=0.027*RE**0.8 *PR**(1./3.) *(AVISC_OUT/AVISC_WALL)**0.14
      NUSSLT=NUSSLT_PP
      HCOEF_OUT=NUSSLT*THC_OUT/DDE
      DTWALL_TB=HTFLX_ONB_GUESS/HCOEF_OUT
C     DTWALL_TB = Wall temp - Coolant bulk temp at exit.
      TWALL= DTWALL_TB + TOUT
      DTSAT=MAX(0.0, DTWALL_TB+TOUT-TSATOUT)
```

```
      XX=2.16/(PBAR)**0.0234
      HTFLX_ONB_BR(I)=1082.9*(PBAR)**1.156 * (1.8*DTSAT)**XX
      ERRORX=ERROR
      ERROR=ABS(HTFLX_ONB_BR(I)/HTFLX_ONB_GUESS-1.0)
C     WRITE(9,5) 'ONB_BR ',ITERN,TOUT,TSTEP,HOUT,AVISC_OUT,
C    1 CP_OUT,THC_OUT,RE,PR,NUSSLT
C     WRITE(9,5) 'ONB_BR ',ITERN,GG(I),HCOEF_OUT,DTWALL_TB,DTSAT,
C    2 HTFLX_ONB_GUESS,HTFLX_ONB_BR(I),
C    3 HTFLX_ONB_BR(I)/HTFLX_ONB_GUESS,ERROR
      IF(ERROR .LT. EPS) GO TO 2
      IF(ITERN .GT. 2000) THEN
      WRITE(6,*) 'Maximum number of iteratins (2000) exceeded.'
      GO TO 2
      ENDIF
      IF(HTFLX_ONB_BR(I) .LT. HTFLX_ONB_GUESS) GO TO 1
      IF(HTFLX_ONB_BR(I) .GT. HTFLX_ONB_GUESS) THEN
      IF(TSTEP .LE. 1.0E-5) GO TO 2
      TOUT=TOUT-TSTEP
      TSTEP=TSTEP/10.0
      GO TO 1
      ENDIF
   2  CONTINUE
      WRITE(6,3) 'ONB_BR ',GG(I),PIN,TOUT,HOUT,RE,PR,NUSSLT,
     1 HCOEF_OUT,DTWALL_TB,DTSAT,HTFLX_ONB_BR(I),ERROR
  10  CONTINUE
      WRITE(6,*)
C
C     HEAT FLUX AT OFI WHITTLE-FORGAN USING ETA = 32.5
C
C     Get RR from Eta. Get exit temp from RR. Get exit enthalpy
C     from exit temp. Calculate inlet pressure PIN. Get inlet enthalpy
C     from TIN and PIN. Get the heat flux at OFI by heat balance, using
C     the inlet and exit enthalpies.
      RR=1.0/(1.0 + ETA*DDH/LENGTH)
      TOUT=TIN+RR*(TSATOUT-TIN)
      HOUT=ZHLIQ(POUT,TOUT,IFLUID)
C
C     Loop over mass velocities.
      DO 20 I=1,30
C     Calculate inlet pressure PIN using an average fric factor
C     and an orifice coeff KORIF.
C     Guess PIN = POUT.
      PIN=POUT
      IF(IPIN .EQ. -1) GO TO 33
      LOOP=0
   7  CONTINUE
      LOOP=LOOP+1
      PAVE=0.5*(PIN+POUT)
      TAVE=0.5*(TIN+TOUT)
      HAVE=ZHLIQ(PAVE,TAVE,IFLUID)
      RHO_AVE=ZROLIQ(HAVE,PAVE,TAVE,IFLUID)
      VISC_AVE=ZVISLIQ(HAVE,PAVE,TAVE,RHO_AVE,IFLUID)
      AVISC_AVE=VISC_AVE*RHO_AVE
      REAVE=GG(I)*DDE/AVISC_AVE
      FRICF_AVE=GETF(REAVE,ROUGH)
      DELP=(KORIF+FRICF_AVE*LENGTH/DDE)*0.5*GG(I)**2/RHO_AVE
      DELP_GRAV=RHO_AVE*GRAV*LENGTH
      IF(IFLOW .EQ. 0) DELP=DELP - DELP_GRAV
      IF(IFLOW .EQ. 1) DELP=DELP + DELP_GRAV
      PIN1=PIN
      PIN=POUT+DELP
      ERR_PIN=PIN1/PIN-1.0
      IF(LOOP.LT.LLP) GO TO 7
```

```
C     WRITE(9,3) 'OFI_WF1',GG(I),PIN1,PAVE,TOUT,TAVE,
C    1 RHO_AVE,AVISC_AVE,REAVE,FRICF_AVE,DELP,PIN,ERR_PIN
C
C     Find inlet enthalpy at TIN and PIN.
  33  HIN=ZHLIQ(PIN,TIN,IFLUID)
      HTFLX_OFI_WF1(I)=DDH*GG(I)*(HOUT-HIN)/(4.0*LENGTH)
      WRITE(6,3) 'OFI_WF1',GG(I),PIN,TOUT,HOUT,HTFLX_OFI_WF1(I)
  20  CONTINUE
      WRITE(6,*)
C
C     HEAT FLUX AT OFI WHITTLE-FORGAN USING R FROM EQ. (1) OF REF. 3,
C     APPLICABLE IF 100 < LENGTH/DDH < 200
C
C     Get RR from Eq. (1). Get exit temp from RR. Get exit enthalpy
C     from exit temp. Calculate inlet pressure PIN. Get inlet enthalpy
C     from TIN and PIN. Get the heat flux at OFI by heat balance, using
C     the inlet and exit enthalpies.
      RR=0.697+0.00063*LENGTH/DDH
      IF(LENGTH/DDH .LT. 100.0 .OR. LENGTH/DDH .GT. 200.0)
     1 WRITE(6,8) LENGTH/DDH
   8  FORMAT('WARNING: (Heated length)/(Heated diameter) ratio is out of
     1 the application range',/,
     2 9X,'of Eq. (1) for R in Whittle-Forgan OFI criterion. Lh/Dh =',
     3 F8.3)
      TOUT=TIN+RR*(TSATOUT-TIN)
      HOUT=ZHLIQ(POUT,TOUT,IFLUID)
C
C     Loop over mass velocities.
      DO 30 I=1,30
C     Calculate inlet pressure PIN using an average fric factor
C     and an orifice coeff KORIF.
C     Guess PIN = POUT.
      PIN=POUT
      IF(IPIN .EQ. -1) GO TO 34
      LOOP=0
   9  CONTINUE
      LOOP=LOOP+1
      PAVE=0.5*(PIN+POUT)
      TAVE=0.5*(TIN+TOUT)
      HAVE=ZHLIQ(PAVE,TAVE,IFLUID)
      RHO_AVE=ZROLIQ(HAVE,PAVE,TAVE,IFLUID)
      VISC_AVE=ZVISLIQ(HAVE,PAVE,TAVE,RHO_AVE,IFLUID)
      AVISC_AVE=VISC_AVE*RHO_AVE
      REAVE=GG(I)*DDE/AVISC_AVE
      FRICF_AVE=GETF(REAVE,ROUGH)
      DELP=(KORIF+FRICF_AVE*LENGTH/DDE)*0.5*GG(I)**2/RHO_AVE
      DELP_GRAV=RHO_AVE*GRAV*LENGTH
      IF(IFLOW .EQ. 0) DELP=DELP - DELP_GRAV
      IF(IFLOW .EQ. 1) DELP=DELP + DELP_GRAV
      PIN1=PIN
      PIN=POUT+DELP
      ERR_PIN=PIN1/PIN-1.0
      IF(LOOP.LT.LLP) GO TO 9
C     WRITE(9,3) 'OFI_WF2',GG(I),PIN1,PAVE,TOUT,TAVE,
C    1 RHO_AVE,AVISC_AVE,REAVE,FRICF_AVE,DELP,PIN,ERR_PIN
C
C     Find inlet enthalpy at TIN and PIN.
  34  HIN=ZHLIQ(PIN,TIN,IFLUID)
      HTFLX_OFI_WF2(I)=DDH*GG(I)*(HOUT-HIN)/(4.0*LENGTH)
      WRITE(6,3) 'OFI_WF2',GG(I),PIN,TOUT,HOUT,HTFLX_OFI_WF2(I)
  30  CONTINUE
      WRITE(6,*)
C
```

```
C     HEAT FLUX AT OFI BY SAHA-ZUBER OSV CORRELATION
C
C     Loop over mass velocities.
      DO 40 I=1,30
C     Guess a value of coolant exit temp TOUT, and find exit enthalpy
C     and exit quality Xo from TOUT and POUT. Find inlet pressure PIN.
C     Get inlet enthalpy from TIN and PIN. Calculate the heat flux by
C     heat balance, using the inlet and exit enthalpies. This a guess
C     value of the OFI heat flux.
C     Calculate Peclet number and Stanton number. Using the guess value
C     of the OFI heat flux, find Xosv using Saha-Zuber correlation.
C     Adjust TOUT so that Xosv = Xo. The converged exit temp gives the
C     OFI heat flux based on Saha-Zuber correlation.
      EPS=0.00001
      TSTEP =0.1
      TOUT=TIN+0.1*(TSATOUT-TIN)
      TOUT=TIN+1.0
      ITERN=0
      ERROR=1.0
  11  CONTINUE
      ITERN=ITERN+1
      TOUT=TOUT+TSTEP
      HOUT=ZHLIQ(POUT,TOUT,IFLUID)
C
C     Calculate inlet pressure PIN using an average fric factor
C     and an orifice coeff KORIF.
C     Guess PIN = POUT.
      PIN=POUT
      IF(IPIN .EQ. -1) GO TO 35
      LOOP=0
  12  CONTINUE
      LOOP=LOOP+1
      PAVE=0.5*(PIN+POUT)
      TAVE=0.5*(TIN+TOUT)
      HAVE=ZHLIQ(PAVE,TAVE,IFLUID)
      RHO_AVE=ZROLIQ(HAVE,PAVE,TAVE,IFLUID)
      VISC_AVE=ZVISLIQ(HAVE,PAVE,TAVE,RHO_AVE,IFLUID)
      AVISC_AVE=VISC_AVE*RHO_AVE
      REAVE=GG(I)*DDE/AVISC_AVE
      FRICF=GETF(REAVE,ROUGH)
      DELP=(KORIF+FRICF*LENGTH/DDE)*0.5*GG(I)**2/RHO_AVE
      DELP_GRAV=RHO_AVE*GRAV*LENGTH
      IF(IFLOW .EQ. 0) DELP=DELP - DELP_GRAV
      IF(IFLOW .EQ. 1) DELP=DELP + DELP_GRAV
      PIN1=PIN
      PIN=POUT+DELP
      ERR_PIN=PIN1/PIN-1.0
      IF(LOOP.LT.LLP) GO TO 12
C     WRITE(9,3) 'OFI_SZ1',GG(I),PIN1,PAVE,TOUT,TAVE,
C    1 RHO_AVE,AVISC_AVE,REAVE,FRICF,DELP,PIN,ERR_PIN
C
C     Find inlet enthalpy at TIN and PIN.
  35  HIN=ZHLIQ(PIN,TIN,IFLUID)
      HTFLX_OFI_GUESS=DDH*GG(I)*(HOUT-HIN)/(4.0*LENGTH)
      CP_FOUT=ZCPLIQ(HFOUT,POUT,TSATOUT,IFLUID)
      THC_FOUT=ZTHCL(HFOUT,POUT,TSATOUT,IFLUID)
      PE_FOUT=GG(I)*DDH*CP_FOUT/THC_FOUT
      ST_FOUT=MAX(455.0/PE_FOUT, 0.0065)
      QUAL_OUT=(HOUT-HFOUT)/HFG_OUT
      HTFLX_OFI_SZ1(I)=-QUAL_OUT*ST_FOUT*GG(I)*HFG_OUT
      ERRORX=ERROR
      ERROR=ABS(HTFLX_OFI_SZ1(I)/HTFLX_OFI_GUESS-1.0)
C     WRITE(9,5) 'OFI_SZ1',ITERN,TOUT,TSTEP,HOUT,HFOUT,HFG_OUT,
```

```
C    1 CP_FOUT,THC_FOUT
C     WRITE(9,5) 'OFI_ZS1',ITERN,GG(I),PE_FOUT,ST_FOUT,QUAL_OUT,
C    2 HTFLX_OFI_GUESS,HTFLX_OFI_SZ1(I),
C    3 HTFLX_OFI_SZ1(I)/HTFLX_OFI_GUESS,ERROR
      IF(ERROR .LT. EPS) GO TO 13
      IF(ITERN .GT. 2500) THEN
      WRITE(6,*) 'Maximum number of iteratins (2500) exceeded.'
      GO TO 13
      ENDIF
      IF(HTFLX_OFI_SZ1(I) .GT. HTFLX_OFI_GUESS) GO TO 11
      IF(HTFLX_OFI_SZ1(I) .LT. HTFLX_OFI_GUESS) THEN
      IF(TSTEP .LE. 1.0E-5) GO TO 13
      TOUT=TOUT-TSTEP
      TSTEP=TSTEP/10.0
      GO TO 11
      ENDIF
  13  CONTINUE
      WRITE(6,3) 'OFI_SZ1',GG(I),PIN,TOUT,HOUT,HTFLX_OFI_GUESS,
     1 THC_FOUT,PE_FOUT,ST_FOUT,QUAL_OUT,HTFLX_OFI_SZ1(I),ERROR
  40  CONTINUE
      WRITE(6,*)
C
C     HEAT FLUX AT OFI BY MODIFIED SAHA-ZUBER CORRELATION,
C     (Siman-Tov, ORNL, 1995)
C
C     Loop over mass velocities.
      DO 50 I=1,30
C     Guess a value of coolant exit temp TOUT, and find exit enthalpy
C     and exit quality Xo from TOUT and POUT. Find inlet pressure PIN.
C     Get inlet enthalpy from TIN and PIN. Calculate the heat flux by
C     heat balance, using the inlet and exit enthalpies. This a guess
C     value of the OFI heat flux.
C     Get Peclet number. Calculate Stanton number using improved
C     Saha-Zuber correlation (Siman-Tov, 1995). Using the guess value
C     of the OFI heat flux, find Xosv using Saha-Zuber correlation.
C     Adjust TOUT so that Xosv = Xo. The converged exit temp gives the
C     OFI heat flux based on Saha-Zuber correlation.
      EPS=0.00001
      TSTEP =0.1
      TOUT=TIN+0.1*(TSATOUT-TIN)
      TOUT=TIN+1.0
      ITERN=0
      ERROR=1.0
  14  CONTINUE
      ITERN=ITERN+1
      TOUT=TOUT+TSTEP
      HOUT=ZHLIQ(POUT,TOUT,IFLUID)
C
C     Calculate inlet pressure PIN using an average fric factor
C     and an orifice coeff KORIF.
C     Guess PIN = POUT.
      PIN=POUT
      IF(IPIN .EQ. -1) GO TO 36
      LOOP=0
  15  CONTINUE
      LOOP=LOOP+1
      PAVE=0.5*(PIN+POUT)
      TAVE=0.5*(TIN+TOUT)
      HAVE=ZHLIQ(PAVE,TAVE,IFLUID)
      RHO_AVE=ZROLIQ(HAVE,PAVE,TAVE,IFLUID)
      VISC_AVE=ZVISLIQ(HAVE,PAVE,TAVE,RHO_AVE,IFLUID)
      AVISC_AVE=VISC_AVE*RHO_AVE
      REAVE=GG(I)*DDE/AVISC_AVE
```

```
      FRICF=GETF(REAVE,ROUGH)
      DELP=(KORIF+FRICF*LENGTH/DDE)*0.5*GG(I)**2/RHO_AVE
      DELP_GRAV=RHO_AVE*GRAV*LENGTH
      IF(IFLOW .EQ. 0) DELP=DELP - DELP_GRAV
      IF(IFLOW .EQ. 1) DELP=DELP + DELP_GRAV
      PIN1=PIN
      PIN=POUT+DELP
      ERR_PIN=PIN1/PIN-1.0
      IF(LOOP.LT.LLP) GO TO 15
C     WRITE(9,3) 'OFI_SZ2',GG(I),PIN1,PAVE,TOUT,TAVE,
C    1 RHO_AVE,AVISC_AVE,REAVE,FRICF,DELP,PIN,ERR_PIN
C
C     Find inlet enthalpy at TIN and PIN.
  36  HIN=ZHLIQ(PIN,TIN,IFLUID)
      HTFLX_OFI_GUESS=DDH*GG(I)*(HOUT-HIN)/(4.0*LENGTH)
      CP_FOUT=ZCPLIQ(HFOUT,POUT,TSATOUT,IFLUID)
      THC_FOUT=ZTHCL(HFOUT,POUT,TSATOUT,IFLUID)
      PE_FOUT=GG(I)*DDH*CP_FOUT/THC_FOUT
C     ETASUB = Siman-Tov's correction factor for Stanton number
      ETASUB=0.55+11.21/(TSATOUT-TOUT)
      ST_FOUT=MAX(455.0/PE_FOUT, 0.0065)*ETASUB
      QUAL_OUT=(HOUT-HFOUT)/HFG_OUT
      HTFLX_OFI_SZ2(I)=-QUAL_OUT*ST_FOUT*GG(I)*HFG_OUT
      ERRORX=ERROR
      ERROR=ABS(HTFLX_OFI_SZ2(I)/HTFLX_OFI_GUESS-1.0)
C     WRITE(9,5) 'OFI_SZ2',ITERN,TOUT,TSTEP,HOUT,HFOUT,HFG_OUT,
C    1 CP_FOUT,THC_FOUT
C     WRITE(9,5) 'OFI_ZS2',ITERN,GG(I),PE_FOUT,ST_FOUT,QUAL_OUT,
C    2 HTFLX_OFI_GUESS,HTFLX_OFI_SZ2(I),
C    3 HTFLX_OFI_SZ2(I)/HTFLX_OFI_GUESS,ERROR
      IF(ERROR .LT. EPS) GO TO 16
      IF(ITERN .GT. 2500) THEN
      WRITE(6,*) 'Maximum number of iteratins (2500) exceeded.'
      GO TO 16
      ENDIF
      IF(HTFLX_OFI_SZ2(I) .GT. HTFLX_OFI_GUESS) GO TO 14
      IF(HTFLX_OFI_SZ2(I) .LT. HTFLX_OFI_GUESS) THEN
      IF(TSTEP .LE. 1.0E-5) GO TO 16
      TOUT=TOUT-TSTEP
      TSTEP=TSTEP/10.0
      GO TO 14
      ENDIF
  16  CONTINUE
      WRITE(6,3) 'OFI_SZ2',GG(I),PIN,TOUT,HOUT,HTFLX_OFI_GUESS,
     1 THC_FOUT,PE_FOUT,ST_FOUT,QUAL_OUT,ETASUB,HTFLX_OFI_SZ2(I),ERROR
  50  CONTINUE
      WRITE(6,*)
C
C EXTENDED GROENEVELD 2006 CHF TABLE (Ref. 43)
C
      TSATOUT=ZTSAT(POUT,IFLUID)
      HFOUT=ZHLIQ(POUT,TSATOUT,IFLUID)
      HGOUT=ZHVAP(POUT,TSATOUT,IFLUID)
C     HFOUT, HGOUT = Enthalpy of saturated liquid and vapor, J/kg
      HFG_OUT=HGOUT-HFOUT
C
C     Loop over mass velocities.
      DO 60 I=1,30
C     Guess a heat flux HTFLX_CHF_GUESS. Assuming PIN=POUT, find the exit
C     coolant temp TOUT. Iterate to calculate the inlet pressure PIN. Using
C     the converged PIN, find the inlet enthalpy HIN at (PIN,TIN). Find HOUT,
C     TOUT, exit quality QUAL_OUT_GR(I), and the critical heat flux HTFLX_CHF_GR(I).
C     Iterate on the heat flux to make HTFLX_CHF_GR(I) equal to the guess
```

```
C     heat flux HTFLX_CHF_GUESS.
      EPS=0.00001
      ITERN=0
      ERROR=1.0
      HTFLX_CHF_GUESS=0.0
      HTFLX_STEP=5.0E+5
  17  CONTINUE
      ITERN=ITERN+1
      HTFLX_CHF_GUESS=HTFLX_CHF_GUESS+HTFLX_STEP
C
C     Iterate on inlet pressure PIN to calculate it using an average fric
C     factor and an orifice coeff KORIF. Start with guess PIN = POUT.
      PIN=POUT
      IF(IPIN .EQ. -1) GO TO 37
      LOOP=0
  18  CONTINUE
      LOOP=LOOP+1
      HIN=ZHLIQ(PIN,TIN,IFLUID)
      HOUT=HIN+4.0*LENGTH*HTFLX_CHF_GUESS/(DDH*GG(I))
      TOUT=ZTLIQ(POUT,HOUT,IFLUID,HFUNCL)
      PAVE=0.5*(PIN+POUT)
      TAVE=0.5*(TIN+TOUT)
      HAVE=ZHLIQ(PAVE,TAVE,IFLUID)
      RHO_AVE=ZROLIQ(HAVE,PAVE,TAVE,IFLUID)
      VISC_AVE=ZVISLIQ(HAVE,PAVE,TAVE,RHO_AVE,IFLUID)
      AVISC_AVE=VISC_AVE*RHO_AVE
      REAVE=GG(I)*DDE/AVISC_AVE
      FRICF=GETF(REAVE,ROUGH)
      DELP=(KORIF+FRICF*LENGTH/DDE)*0.5*GG(I)**2/RHO_AVE
      DELP_GRAV=RHO_AVE*GRAV*LENGTH
      IF(IFLOW .EQ. 0) DELP=DELP - DELP_GRAV
      IF(IFLOW .EQ. 1) DELP=DELP + DELP_GRAV
      PIN1=PIN
      PIN=POUT+DELP
      ERR_PIN=PIN1/PIN-1.0
      IF(LOOP.LT.LLP) GO TO 18
C     WRITE(9,3) 'CHF_GR ',GG(I),HTFLX_CHF_GUESS,PAVE,TOUT,
C    1 TAVE,RHO_AVE,AVISC_AVE,REAVE,FRICF,DELP,PIN,ERR_PIN
C
C     Find inlet enthalpy at TIN and calculated PIN.
  37  HIN=ZHLIQ(PIN,TIN,IFLUID)
      HOUT=HIN+4.0*LENGTH*HTFLX_CHF_GUESS/(DDH*GG(I))
      QUAL_OUT_GR(I)=(HOUT-HFOUT)/HFG_OUT
C     QUAL_OUT_GR(I) = Exit quality in the channel
C     Find diameter correction factor FK1
      IF(DDH .LT. 0.003) THEN
      FK1=(0.008/0.003)**0.312
      ELSE IF(DDH .LT. 0.025) THEN
      FK1=(0.008/DDH)**0.312
      ELSE
      FK1=(0.008/0.025)**0.312
      ENDIF
C     Find mass flux correction factor FG1
      IF(GG(I) .LE. 8000.0) THEN
      FG1=1.0
      ELSE IF(GG(I) .LE. 30000.0) THEN
      FG1=(GG(I)/8000.0)**0.376
      ELSE
      FG1=(30000.0/8000.0)**0.376
      ENDIF
C     3-D interpolation
      POUTKPA=POUT*1.0E-3
      FLXM=GG(I)
```

```
      QUAL_OUT=QUAL_OUT_GR(I)
      CALL INTERP3D(GRALL,QUAL,FLUXM,PKPA,QUAL_OUT,FLXM,POUTKPA,CFLX,
     1 N1,N2,N3)
      HTFLX_CHF_GR(I)=FK1*CFLX*FG1*1.0E3
      ERROR=ABS(HTFLX_CHF_GR(I)/HTFLX_CHF_GUESS-1.0)
C     WRITE(9,5) 'CHF_GR ',I,POUT,DDH,GG(I),QUAL_OUT_GR(I),TIN,LENGTH,
C    1 HTFLX_CHF_GR(I),CFLX,FK1,FG1
C     WRITE(9,5) 'CHF_GR ',I,TSATOUT,TOUT,HOUT,HGOUT,HFOUT,ERROR
      IF(ERROR .LT. EPS) GO TO 19
      IF(ITERN .GT. 2000) THEN
      WRITE(6,*) 'Maximum number of iteratins (2000) exceeded.'
      GO TO 19
      ENDIF
      IF(HTFLX_CHF_GR(I) .GT. HTFLX_CHF_GUESS) GO TO 17
      IF(HTFLX_CHF_GR(I) .LT. HTFLX_CHF_GUESS) THEN
      IF(HTFLX_STEP .LE. 1.0E+2) GO TO 19
      HTFLX_CHF_GUESS=HTFLX_CHF_GUESS - HTFLX_STEP
      HTFLX_STEP=HTFLX_STEP/10.0
      GO TO 17
      ENDIF
  19  CONTINUE
      WRITE(6,3) 'CHF_GR ',GG(I),PIN,TOUT,HOUT,HTFLX_CHF_GUESS,
     1 FK1,FG1,QUAL_OUT_GR(I),HTFLX_CHF_GR(I),ERROR
  60  CONTINUE
      WRITE(6,*)
C
C HALL-MUDAWAR SUBCOOLED CHF INLET CONDITIONS CORRELATION (ref. 44)
C
      CC1=0.0722
      CC2=-0.312
      CC3=-0.644
      CC4=0.900
      CC5=0.724
      TSATOUT=ZTSAT(POUT,IFLUID)
      HFOUT=ZHLIQ(POUT,TSATOUT,IFLUID)
      HGOUT=ZHVAP(POUT,TSATOUT,IFLUID)
      HFG_OUT=HGOUT-HFOUT
      RHOF_OUT=ZROLIQ(HFOUT,POUT,TSATOUT,IFLUID)
      RHOG_OUT=ZROVAP(HGOUT,POUT,TSATOUT,IFLUID)
      SIGMAO=TENSION(TSATOUT,IFLUID,ICALLER)
C HFOUT, HGOUT = Saturated liquid and vapor enthalpy at exit, J/kg
C HFG_OUT      = Latent heat of vaporization at exit, J/kg
C HFIN, HGIN   = Saturated liquid and vapor enthalpy at inlet, J/kg
C HFGIN        = Latent heat of vaporization at inlet, J/kg
C RHOF_OUT     = Saturated liquid density at exit, kg/m^3
C RHOG_OUT     = Saturated vapor density at exit, kg/m^3
C
C     Loop over mass velocities.
      DO 70 I=1,30
C     Guess a heat flux HTFLX_CHF_GUESS. Assuming PIN=POUT, find the exit
C     coolant temp TOUT. Iterate to calculate the inlet pressure PIN.
C     Using the converged PIN, find the inlet enthalpy HIN at (PIN,TIN).
C     Find HOUT, TOUT, exit quality XXOUT, and the critical heat flux
C     HTFLX_CHF_HM(I). Iterate on the heat flux to make HTFLX_CHF_HM(I)
C     equal to the guess heat flux HTFLX_CHF_GUESS.
      EPS=0.00001
      ITERN=0
      ERROR=1.0
      HTFLX_CHF_GUESS=0.0
      HTFLX_STEP=5.0E+5
  23  CONTINUE
      ITERN=ITERN+1
      HTFLX_CHF_GUESS=HTFLX_CHF_GUESS+HTFLX_STEP
```

```
C
C     Iterate on inlet pressure PIN to calculate it using an average fric
C     factor and an orifice coeff KORIF. Start with guess PIN = POUT.
      PIN=POUT
      IF(IPIN .EQ. -1) GO TO 38
      LOOP=0
  24  CONTINUE
      LOOP=LOOP+1
      HIN=ZHLIQ(PIN,TIN,IFLUID)
      HOUT=HIN+4.0*LENGTH*HTFLX_CHF_GUESS/(DDH*GG(I))
      TOUT=ZTLIQ(POUT,HOUT,IFLUID,HFUNCL)
      PAVE=0.5*(PIN+POUT)
      TAVE=0.5*(TIN+TOUT)
      HAVE=ZHLIQ(PAVE,TAVE,IFLUID)
      RHO_AVE=ZROLIQ(HAVE,PAVE,TAVE,IFLUID)
      VISC_AVE=ZVISLIQ(HAVE,PAVE,TAVE,RHO_AVE,IFLUID)
      AVISC_AVE=VISC_AVE*RHO_AVE
      REAVE=GG(I)*DDE/AVISC_AVE
      FRICF=GETF(REAVE,ROUGH)
      DELP=(KORIF+FRICF*LENGTH/DDE)*0.5*GG(I)**2/RHO_AVE
      DELP_GRAV=RHO_AVE*GRAV*LENGTH
      IF(IFLOW .EQ. 0) DELP=DELP - DELP_GRAV
      IF(IFLOW .EQ. 1) DELP=DELP + DELP_GRAV
      PIN1=PIN
      PIN=POUT+DELP
      ERR_PIN=PIN1/PIN-1.0
      IF(LOOP.LT.LLP) GO TO 24
C     WRITE(9,3) 'CHF_HM ',GG(I),HTFLX_CHF_GUESS,PAVE,TOUT,
C    1 TAVE,RHO_AVE,AVISC_AVE,REAVE,FRICF,DELP,PIN,ERR_PIN
C
C     Find inlet enthalpy at TIN and calculated PIN.
C     Assuming PIN=POUT makes a small/negligible difference in CHF.
  38  HIN=ZHLIQ(PIN,TIN,IFLUID)
C     Find pseudo quality at inlet
      XXINS=(HIN-HFOUT)/HFG_OUT
      WEBER=GG(I)**2 *DDH/(RHOF_OUT*SIGMAO)
      RHOFG=RHOF_OUT/RHOG_OUT
      WEBER2=WEBER**CC2
      RHOFG3=RHOFG**CC3
      RHOFG5=RHOFG**CC5
      BOILN=CC1*WEBER2 *RHOFG3 *(1.0 - CC4*XXINS*RHOFG5)
      BOILD=1.0 + 4.0*CC1*CC4*WEBER2 * RHOFG3*RHOFG5 * LENGTH/DDH
      HTFLX_CHF_HM(I)=BOILN/BOILD * GG(I)*HFG_OUT
      HOUT=HIN+4.0*LENGTH*HTFLX_CHF_HM(I)/(DDH*GG(I))
      XXOUT=(HOUT-HFOUT)/HFG_OUT
      QUAL_OUT_HM(I)=XXOUT
      ERROR=ABS(HTFLX_CHF_HM(I)/HTFLX_CHF_GUESS-1.0)
C     WRITE(9,5) 'CHF_HM ',I,POUT,DDH,GG(I),XXOUT,SIGMAO,
C    1 LENGTH,HTFLX_CHF_HM(I),WEBER,BOILN,BOILD
C     WRITE(9,5) 'CHF_HM ',I,PIN,TSATOUT,HOUT,HGOUT,HFOUT,
C    1 HFG_OUT,RHOF_OUT,RHOG_OUT,XXIN,XXINS,ERROR
      IF(ERROR .LT. EPS) GO TO 25
      IF(ITERN .GT. 2000) THEN
      WRITE(6,*) 'Maximum number of iteratins (2000) exceeded.'
      GO TO 25
      ENDIF
      IF(HTFLX_CHF_HM(I) .GT. HTFLX_CHF_GUESS) GO TO 23
      IF(HTFLX_CHF_HM(I) .LT. HTFLX_CHF_GUESS) THEN
      IF(HTFLX_STEP .LE. 1.0E+2) GO TO 25
      HTFLX_CHF_GUESS=HTFLX_CHF_GUESS - HTFLX_STEP
      HTFLX_STEP=HTFLX_STEP/10.0
      GO TO 23
      ENDIF
```

```
  25  CONTINUE
      WRITE(6,3) 'CHF_HM ',GG(I),PIN,TOUT,HOUT,HTFLX_CHF_GUESS,
     1 XXOUT,HTFLX_CHF_HM(I),ERROR
  70  CONTINUE
C
C     PRINT ALL RESULTS TOGETHER, in kW/m^2
C
      WRITE(6,*)
      WRITE(6,28) IP,POUT*1.0E-5,DDH,LENGTH,TIN,PPH_PPW,ETA,IFLOW,IPIN
      WRITE(6,27)
      WRITE(*,*)
      WRITE(*,28) IP,POUT*1.0E-5,DDH,LENGTH,TIN,PPH_PPW,ETA,IFLOW,IPIN
      WRITE(*,27)
      DO 80 I=1,30
      WRITE(6,26) 'ONB_OFI_CHF',GG(I),HTFLX_ONB_BR(I)*0.001,
     1 HTFLX_OFI_WF1(I)*0.001,HTFLX_OFI_WF2(I)*0.001,
     2 HTFLX_OFI_SZ1(I)*0.001,HTFLX_OFI_SZ2(I)*0.001,
     3 HTFLX_CHF_GR(I)*0.001 ,HTFLX_CHF_HM(I)*0.001,
     4 QUAL_OUT_GR(I),QUAL_OUT_HM(I)
      WRITE(*,26) 'ONB_OFI_CHF',GG(I),HTFLX_ONB_BR(I)*0.001,
     1 HTFLX_OFI_WF1(I)*0.001,HTFLX_OFI_WF2(I)*0.001,
     2 HTFLX_OFI_SZ1(I)*0.001,HTFLX_OFI_SZ2(I)*0.001,
     3 HTFLX_CHF_GR(I)*0.001 ,HTFLX_CHF_HM(I)*0.001,
     4 QUAL_OUT_GR(I),QUAL_OUT_HM(I)
  80  CONTINUE
   3  FORMAT(A,   5X,1P,12E12.4)
   5  FORMAT(A,I4,1X,1P,12E12.4)
  26  FORMAT(A,1X,8F12.1,2F12.5)
C 27  FORMAT(T16,'Mass flux',T28,'ONB Htflx',T40,'OFI W&F-R',
C    1 T50,'OFI W&F-Eta',T66,'OFI S&Z',T76,'OFI S&Z-M',T88,
  27  FORMAT(T16,'Mass flux',T28,'ONB Htflx',T38,'OFI W&F-Eta',
     1 T52,'OFI W&F-R',T66,'OFI S&Z',T76,'OFI S&Z-M',T88,
     2 'CHF GR_Ex',T99,'CHF HM-ICC',T112,'Exit Qual',
     3 T124,'Exit Qual',/,T17,'kg/m^2-s',
     3 T31,'kW/m^2',T43,'kW/m^2',T55,'kW/m^2',T67,'kW/m^2',
     4 T79,'kW/m^2',T91,'kW/m^2',T103,'kW/m^2',T111,'Groeneveld',
     5 T126,'H-M ICC')
  28  FORMAT('Case =',I3,F12.1,5F12.4,2I3)
      RETURN
      END
```

Nuclear Engineering Division
Argonne National Laboratory
9700 South Cass Avenue, Bldg. #208
Argonne, IL 60439

www.anl.gov